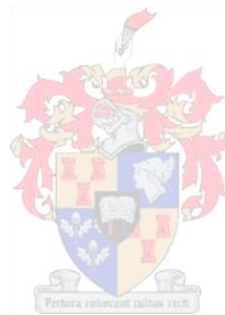


Functional characterization of a putative signalling peptide TAXIMIN in the model plant *Arabidopsis thaliana* and a medicinal plant *Sutherlandia frutescens* L. R. Br.

Janine Colling



Thesis submitted in fulfilment of the requirements for the degree of Doctor (PhD) in Sciences (Plant Biotechnology) at Stellenbosch University and Doctor (PhD) in Sciences (Biochemistry and Biotechnology) at Ghent University

Stellenbosch University – Faculty of Sciences
Department of Genetics

Ghent University – Faculty of Sciences
Department of Plant Biotechnology and Bioinformatics

Promoters

Prof. Dr. NP Makunga (Stellenbosch University)

Prof. Dr. A Goossens (Ghent University)

Declaration

By submitting this dissertation electronically, I declare that the entirety of the work contained therein is my own original work, that I am the sole author thereof (save to the extent explicitly stated otherwise), that reproduction and publication thereof by Stellenbosch and Ghent University will not infringe any third party rights and that I have not previously in its entirety or in part submitted it for obtaining any qualification.

This dissertation has also been presented at (Ghent University) in terms of a joint-/double-degree agreement.

Date.....

(Student) Janine Colling.....

(Promoter Ghent University) Alain Goossens.....

(Promoter Stellenbosch University) Nokwanda P Makunga.....

Copyright © 2016

Stellenbosch and Ghent University

All rights reserved

List of Outputs from the study

Chapter

Colling J, Pollier J, Makunga NP, Goossens (2013). cDNA-AFLP-based transcript profiling for genome-wide expression analysis of jasmonate-treated plants and plant cultures. In: Goossens A, Pauwels L (eds). *Jasmonate Signalling. Methods in Molecular Biology*. Springer, New York. Pg. 287 – 303.

Publication

Colling J, Tohge T, De Clercq R, Brunoud G, Vernoux T, Fernie AR, Makunga NP, Goossens A, Pauwels L (2015). Overexpression of the *Arabidopsis thaliana* signalling peptide TAXIMIN1 affects lateral organ development. *Journal of Experimental Botany* 66: 5337 – 5349 (doi: 10.1093/jxb/erv291).

Table of Contents

Declaration	II
List of Outputs from this study	III
List of Figures	V
List of Tables	VII
List of Abbreviations	VIII
Abstract	XIII
Samevatting	XV
Chapter 1	1
Introduction and Literature review	
Chapter 2:	50
cDNA-AFLP-based transcript profiling for genome-wide expression analysis of jasmonate-treated plants and plant cultures	
Chapter 3:	67
Functional characterization of the TAXIMIN orthologs of <i>Arabidopsis thaliana</i>	
Chapter 4:	113
Taximin results in changes in the light response in <i>Arabidopsis thaliana</i>	
Chapter 5:	124
Engineering of <i>Sutherlandia frutescens</i> L. R. Br. metabolism	
Chapter 6:	160
Conclusion and future prospects	
Acknowledgements	164
Annex	166

List of Figures

Chapter 1:

Figure 1. Classification of small signalling peptides in plants.

Figure 2. Peptide receptor complexes mediate various responses in plants.

Figure 3. Examples of the function of various signalling peptides in *Arabidopsis thaliana*

Figure 4. Chemical structure of secondary metabolites in *Sutherlandia frutescens*.

Figure 5. Chemical structure of flavonoid and partial representation of the flavonoid biosynthesis pathway.

Figure 6. Partial representation of the terpenoid biosynthesis pathway in plants.

Figure 7. Partial representation of polyamine and ethylene biosynthesis in plants.

Chapter 2:

Figure 1. Overview of the cDNA-AFLP procedure.

Chapter 3:

Figure 1. Distribution of the TAXIMIN peptide family in the plant kingdom.

Figure 2. The TAXIMIN peptides in *Arabidopsis*.

Figure 3. Localization of TAX1 in root cells of *Arabidopsis thaliana*.

Figure 4. Effects of constitutive overexpression of *TAX2* and *TbTAX.6xHis* in *Arabidopsis thaliana*.

Figure 5. Phenotypes of *TAX1* overexpressing seedlings and flowering plants.

Figure 6. *TAX1* overexpression in Col-0 background results in an alteration of fruit morphology.

Figure 7. *TAX1* overexpression in Ler background results in a changes of fruit morphology.

Figure 8. Constitutive *TAX1* overexpression results in lateral organ fusion with reduced penetrance.

Figure 9. Paraclade junction phenotypes in line OE-2 and Ler background with reduced penetrance.

Figure 10. Constitutive expression of *TAX1ΔSP*.

Figure 11. T-DNA insertion lines for *TAX* genes in *Arabidopsis thaliana*.

Figure 12. *TAX1* and *TAX2* have distinct promoter activities.

Figure 13. Reduced accessory shoot number is not due to the absence of meristem outgrowth.

Figure 14. Transient expression assay to test if TAX1 interferes with the regulatory activity of the LOF1 splice variants.

Figure 15. Expression of lateral organ boundary genes does not change in *TAX1* overexpressing lines.

Figure 16. RT-PCR of *TAX1* expression and RT-qPCR quantification of boundary genes in Col-0 and inducible line treated with DEX or EtOH.

Figure 17. Quantification of the expression of boundary genes in the SAM of 6-week old DEX treated plants of the *TAX1* inducible line.

Figure 18. GUS staining of 10-day old *in vitro* germinated seeds for *LOF1* (gene trap) and p*LOF2*::GUS and the cross with 35S::*TAX1*.

Figure 19. Transient expression assay testing if LOF1 can regulate *TAX1* expression.

Figure 20. Quantification of *TAX* and other boundary genes in nodes of 5 week old *lof1lof2* mutants.

Figure 21. Quantification of the expression of boundary genes in Col-0, *Ler*, *ctf* and 35S::*LOF1* lines.

Figure 22. *TAX1* overexpression results in minor alterations of primary metabolites in leaf and root.

Chapter 4

Figure 1. Fusion phenotypes induced by short day conditions in the *lof1lof2* mutant.

Figure 2. Cefotaxime alters the light stress response of *Arabidopsis thaliana* *TAX1* OE lines.

Figure 3. *tax* and *lof* mutants cultivated in continuous or long day conditions.

Figure 4. Analysis of the metabolic differences between Wt and *TAX1* OE line.

Figure 5. IT-MS analysis of *Arabidopsis* wild type (Col-0) and *TAX1* OE lines on Basal MS or MS supplemented with cefotaxime in continuous or 16-h light growth room.

Chapter 5

Figure 1. Examples of Transcriptionally differentially expressed fragments (TDF) of *in vitro* stressed *Sutherlandia frutescens* shoots identified with cDNA-AFLP.

Figure 2. Effect of salt stress on the physiological parameters of *in vitro* *S. frutescens* shoots.

Figure 3. ¹⁵N/¹⁴N and ¹³C/¹²C abundance and C:N ratio in salt treated *Sutherlandia frutescens* shoots.

Figure 4. Amino-acid and polyamine levels represented as relative percentage (%) or as biplots and SUB content of salt treated shoots.

Figure 5. PCR amplification of T-DNA in hairy roots of *Sutherlandia frutescens*.

Figure 6. FT-MS analysis of MeJA or untreated *S. frutescens* hairy roots.

Annex

Figure S1. Gus expression patterns driven by p*TAX1* and p*TAX2*.

List of Tables

Chapter 1

Table 1: Examples of post translationally modified and Cysteine -rich peptides.

Chapter 5

Table 1: Amino-acid concentrations (mg/ μ l) in control and salt treated *in vitro* *Sutherlandia frutescens* shoots.

Table 2: Sequences and BLASTx results of transcriptionally differentially expressed fragments (TDF) of *in vitro* stress treated *Sutherlandia frutescens* shoots.

Table 3: Full length gene sequences for *TbTAX* gene and homologs in *Medicago truncatula*.

Annex

Supplementary Table S1. Sequences of primers used in this study.

Supplementary Table S2. Reporting metabolite data presented in this study.

Supplementary Table S3. Primary metabolite profiling of Col-0 and *TAX1* overexpressing lines in leaf.

Supplementary Table S4. Primary metabolite profiling of Col-0 and *TAX1* overexpressing lines in root.

List of Abbreviations

<i>a/a</i>	Amino acids
aAS	α -Amyrin synthase
ABA	Abscisic acid
ABCB	ATP-binding cassette transporter
ACC	1-Aminocyclopropane-1-carboxylic acid oxidase
ADC	Arginine decarboxylase
AFP	Antifungal proteins
AIH	Agmatine iminohydrolase
ANOVA	Analysis of variance
bAS	β -Amyrin synthase
BAK	BRI1-ASSOCIATED RECEPTOR KINASE1
bHLH	Basic-Helix-Loop-Helix
BOP	BLADE ON PETIOLE
Bp	Base pairs
BR	Brassinosteroid
BRI1	BRASSINOSTEROID INDEPENDENT1
BY-2	Bright yellow 2
4CL	4-Coumarate: coenzyme A ligase
C4H	Cinnamate-4-hydroxylase
CaMV	Cauliflower Mosaic Virus
CAS	Cycloartenol synthase
cDNA-AFLP	cDNA Amplified Fragment Length Polymorphism
CDS	Coding sequence
Cef	Cefotaxime
CEP1	C-terminally encoded peptide 1
CHAL	CHALLAH
CHI	Chalcone isomerase
CHS	Chalcone synthase
CI	Chalcone isomerase
C:N	Carbon:nitrogen ratio
CLV3	CLAVATA3
CLE	CLAVATA3/ENDOSPERM SURROUNDING REGION
CoA	Coenzyme A
Col-0	Columbia-0 ecotype
CPA	Carbamoylputrescine aminohydrolase
CRP	CYSTEINE RICH PEPTIDES
CS	Chalcone synthase
<i>ctf</i>	CONSTRICTED FRUIT

CTR	Control
CUC	CUP SHAPED COTYLEDONS
Cys	Cysteine
D7OMT	Daidzein 7-O-methyltransferase
DD	Differential display
DBD	DNA binding domain
DFR	Dihydroflavonol 4-reductase
DEPC	Diethylpyrocarbonate
DEX	Dexamethasone
DFR	Dihydroflavonol-reductase
DMAPP	Dimethylallyl pyrophosphate
DTT	Dithiothreitol
DVL	DEVIL
E	Transpiration rate
ECD	Extracellular domain
EDTA	Ethylenediaminetetra-acetic acid
ENOD	EARLY NODULIN
<i>er</i>	ERECTA
EPF	EPIDERMAL PATTERNING FACTOR
ESI	Electron spray ionization
EST	Expressed sequence tag
F3H	Flavanone-3-hydroxylase
FDA	Food and drug administration
FLS	Flavonol synthase
fLUC	Firefly luciferase
FNS	Flavone synthase
FPP	Farnesyl pyrophosphate
FPS	Farnesyl pyrophosphate synthase
FT-ICR MS	Fourier transform ion cyclotron resonance mass spectrometry
FUL	FRUITFUL
gDNA	Genomic DNA
GABA	Gamma-aminobutyric acid
GC-MS	Gas chromatography mass spectrometry
GFP	Green fluorescent protein
GGPPS	Geranyl geranyl pyrophosphate synthase
GLV	GOLVEN
GOGAT	Glutamine synthetase/glutamate synthase
GPD	Glyceraldehyde-3-phosphate dehydrogenase
GPP	Geranyl pyrophosphate
GR	Glucocorticoid receptor

Gs	Stomatal conductance
GUS	β -Glucuronidase
HI4'OMT	2,7,4'-Trihydroxyisoflavanone-4'-O-methyl transferase
HMG CoA	3-Hydroxy-3-methylglutaryl coenzyme A
HMGR	HMG CoA reductase
HSD	Honestly significant difference
Hyp	Hydroxyproline
IDA	INFLORESCENCE DEFICIENT IN ABSCISSION
IDL	IDA-LIKE
IFS	2-Hydroxyisoflavanone synthase
IPP	3-Isopentenyl pyrophosphate
JAZ	Jasmonate Zim domain
KAPP	Kinase associated protein phosphatase
LAS	Lanosterol synthase
LC-MS	Liquid chromatography mass spectrometry
Ler	Landsberg <i>erecta</i>
LOB	LATERAL ORGAN BOUNDARIES
LOF	LATERAL ORGAN FUSION
LRR RLK	Leucine-rich repeat receptor-like kinases
MAP	Mitogen-activated protein
MeJA	Methyl Jasmonate
MEP	Methyl erythritol phosphate
MS	Murashige and Skoog
MVA	Mevalonate pathway
NAA	Naphthalene acetic acid
ns	No significant difference
OAT	Ornithine aminotransferase
OC	Organizing centre
ODC	Ornithine decarboxylase
OE	Overexpression
OMT	O-Methyl transferase
ORCA	Octadecanoid-derivative responsive <i>Catharanthus</i> AP2 domain
ORF	Open reading frame
OSC	Oxidosqualene cyclases
PCA	Principal component analysis
PCR	Polymerase chain reaction
PDA	Photo diode array
P5C	Δ 1-Pyrrolidine 5-carboxylate
P5CS	Δ -1-Pyrroline-5-carboxylate synthetase
P5CR	Δ -1-Pyrroline-5-carboxylate reductase

PAL	Phenylalanine ammonia lyase
PCR	Polymerase chain reaction
PI	Propidium iodide
Pn	Net rate of photosynthesis
PP2A	PROTEIN PHOSPHATASE 2A
PP2C	PROTEIN PHOSPHATASE type 2C
PPFD	Photosynthetic photon flux density
PSK	PHYTOSULFOKINE
PSY	PLANT PEPTIDE CONTAINING SULFATED TYROSINE
RT-qPCR	Quantitative real time polymerase chain reaction
RALF	Rapid alkalization factor
RAP-PCR	RNA fingerprinting by arbitrary primer PCR
RDA	Representational difference analysis
RGF	ROOT GROWTH FACTOR
RK	Receptor kinase
RLK	Receptor-like kinase
rLUC	Renilla luciferase
RNAseq	RNA sequencing
Rop	Rho-GTPase
ROS	Reactive oxygen species
ROT	ROTUNDIFOLIA
RGF	ROOT GROWTH FACTOR
RT-PCR	Real time polymerase chain reaction
Δ SP	Without signal peptide
SAGE	Serial analysis of gene expression
SAM	Shoot apical meristem
SAMDC	S-adenosyl methionine decarboxylase
SCR/SP11	S-locus Cys-Rich/S-locus Protein11
SE	Standard error
SEM	Scanning electron microscopy
SEp	Squalene epoxidase
SHP	SHATTERPROOF
SI	Self incompatibility
SLG	S-locus glycoprotein
SPCH	SPEECHLESS
SPDS	Spermidine synthase
SPMS/TSPMS	Spermine/thermospermine synthase
SRK	S-Locus receptor kinase
SS	Squalene synthase
STM	SHOOT MERISTEMLESS

SUB	Sutherlandioside B
TAX	TAXIMIN
TDF	Transcriptionally differentially expressed fragments
TDIF	Tracheary element differentiation inhibitory factor
TDR	TDIF RECEPTOR
TEA	Transient expression assay
TF	Transcription factor
TIA	Terpenoid indole alkaloid
TMM	TOO MANY MOUTHS
TPD	TAPETUM DETERMINANT
UAS	Upstream activator sequence
UGT	UDP-glucosyl transferase
UPLC	Ultraperformance liquid chromatograph
UTR	Untranslated region
Wt	Wild type
WUE	Water use efficiency
WUS	WUSCHEL

Abstract

Secondary metabolite production in plants assists with protection against predators and attraction of pollinators. Manipulation of secondary metabolite pathways towards increased production of compounds of interest has become a target. The techniques to assist with understanding regulation of these pathways are therefore important. Several factors influence metabolite synthesis in plants including age, developmental stage, tissue type and environmental factors. In this study we describe a technique, cDNA-AFLP, which can be applied to study changes in whole genome expression to identify genes which are differentially expressed during stress conditions. We also describe the study of the function of a novel signalling peptide TAXIMIN in the model plant *Arabidopsis thaliana*. This peptide was discovered by cDNA-AFLP analysis of Methyl Jasmonate (MeJA) elicited *Taxus baccata* cell suspension cultures.

TAXIMIN represents a novel signalling peptide which belongs to the cysteine rich peptides and has an N-terminal signal peptide and a C-terminal peptide with six conserved cysteines and three conserved prolines. Two *TbTAX* homologs (*TAX1* and *TAX2*) were discovered in *A. thaliana*. Fusion of the full length peptide to the Venus fluorescent protein targeted the peptide to the plasma membrane-cell wall interface and this movement was abolished when the N-terminal signal was removed. Single and double mutants lacked a visible phenotype which can be related to functional redundancy with other genes or lack of environmental factors to induce a phenotypic response. Fusion of the *TAX* promoters to the GUS reporter gene revealed that *TAX2* was expressed in vasculature tissue, whilst *TAX1* expression was found in anthers, nectaries, roots and the base of the organs of the paraclade junctions indicating the neo-functionalization of the two peptides. Constitutive expression of *TAX1* resulted in a fusion phenotype in the paraclade junctions and a fruit phenotype. Fruits were shorter and wider at the tip which co-incided with a wider replum as well as seed-stacking in this region. The fusion phenotype was similar to the phenotype observed for a mutant of the MYB transcription factor *LATERAL ORGAN FUSION (LOF1)* which plays a role in boundary formation. However, *TAX1* overexpression (*TAX1 OE*) did not result in reduced *LOF* expression in paraclade junctions and *TAX1* expression was similar to wild type plants in the *lof1lof2* mutant paraclade junctions. Dexamethasone induction of *TAX1* overexpression also did not result in changes in *LOF1* expression in seedling or in the shoot apical meristem. No changes in *LOF2* driven GUS expression level or pattern was observed when crossing to the *TAX1* overexpression background. *TAX1* therefore appears to regulate boundary formation independently from *LOF1*. However, these pathways may converge later in development. Metabolite analysis of the primary metabolite profiles of the leaf and roots of *TAX1 OE* lines

indicated increases in phosphate (leaves) and serine (root and leaves) levels which were observed in all lines. *TAX1* OE lines also appeared to be sensitive to the length of the photoperiod and this may be related to a reduced abundance of sinapoyl malate in leaves.

cDNA-AFLP was applied to study changes in genome expression of nitrogen, salinity or MeJA-stressed *Sutherlandia frutescens* shoots cultivated *in vitro*. Results indicated that pathways involved in polyamine biosynthesis or regulated by plant hormones such as ethylene or abscisic acid are differentially expressed. Salinity stress caused a reduction in nitrogen uptake, but did not affect photosynthesis or the carbon: nitrogen ratio. On the metabolite level an increase in arginine and proline content was observed. This might be related to the reduction of ammonium toxicity effects or the osmotic response to reduce the damage due to accumulating ions. Plants were generally tolerant to low levels of salinity and no significant changes in sutherlandioside B abundance were observed. Constitutive expression of TAXIMIN genes from *T. baccata* and *Medicago truncatula* did not alter the abundance of sutherlandins, sutherlandiosides or soyasaponins in *S. frutescens* hairy roots. This suggests that these peptides do not directly affect the biosynthesis pathways of these compounds in *S. frutescens*. Application of MeJA enhanced soyasaponin production confirming previous reports on induction of these pathways by MeJA elicitation. This study describes the establishment of a platform which can be used to study changes in the transcriptome in response to the application of stress in non-model plants and includes the use of tools to study the function of uncharacterized genes in the model plant *A. thaliana*. This study also describes the transformation of a non-model medicinal plant (*S. frutescens*) which could be used to study the effects of 'novel' heterologous genes on the metabolism of these plants.

Samevatting

Plante produseer sekondêre metaboliete vir beskerming teen herbivore en om insekte vir bestuiwing te lok. Die manipulasie van sekondêre metaboliet produksie, ten einde verhoogde produksie van die metaboliete van belang mee te bring, het 'n teiken geword. Tegnieke wat tot ons kennis van die regulasie van die produksie paaie kan lei is van belang. Verskeie faktore soos bv. ouderdom, ontwikkelingsfase, tipe weefsel en omgewingsfaktore beïnvloed die produksie van metaboliete in plante. In hierdie studie beskryf ons 'n tegniek, cDNA-AFLP, wat toegepas kan word om die verandering in genoom wye geen uitdrukking te bestudeer en dus veranderinge in geen uitdrukking tydens verskillend stress kondisies te identifiseer. In hierdie studie, is die funksie van 'n nuwe sein-peptied, TAXIMIN ondersoek in die model plant *Arabidopsis thaliana* ondersoek. Hierdie peptide is tydens die analise van Metiel Jasmonaat behandelde *Taxus baccata* sel suspensie kultuur m.b.v cDNA-AFLP ontdek.

TAXIMIN verteenwoordig 'n nuwe sein peptide wat aan die cysteine ryke peptied groep behoort. Dit besit 'n N-terminale sein-peptied en 'n C-terminale peptied wat gekonserveerde cysteine en proliene bevat. Twee *TbTAX* homoloë (*TAX1* en *TAX2*) is in die model plant *A. thaliana* ontdek. Fusie van die vol-lengte peptied aan 'n Venus fluoreserende proteïen het die proteïen na die die plasmamembraan-selwand skeiding geteiken. Die beweging is vernietig indien die N-terminal sein peptied verwyder is. Plante met 'n enkele of dubbel *TAX* mutasie het geen sigbare fenotipe getoon. Die afwesigheid van 'n fenotipe mag weens die teenwoordigheid van funksionele ressesiewe gene wees of weens die vereiste van die teenwoordigheid van spesifieke omgewingsfaktore wat 'n fenotipe kan induseer. Die fusie van die *TAX* promoters aan die GUS verklikker geen het aangedui dat *TAX2* hoofsaaklik in die vaskulêre weefsel uitgedruk word. Terwyl *TAX1* geen uitdrukking in die helmknoppie, nektarkliere, wortels en die basis van die organe van die nodes uitgedruk word. Die resultaat kan dui op die ontwikkeling van afsonderlike regulering van geen uitdrukkingpatrone of selfs spesialisering van die funksie van die twee peptiede. Aaneenhoudende uitdrukking van *TAX1* het tot 'n fusie fenotipe in die nodes asook 'n vrug fenotipe gelei. In vergelyking met die wilde tipe vrugte, het die vrugte van *TAX1* ooruitdrukking (OU) korter en wyer by die punt vertoon. Dit het terselfdertyd met 'n breër replum asook met saad-stapeling in hierdie area gepaard gegaan het. Die fusie fenotipe was soortgelyk aan die fenotipe wat in plante met 'n mutasie in die MYB transkripsie faktor *LATERAL ORGAN FUSION (LOF1)* waargeneem is. *LOF1* speel 'n rol in die skeiding van organe. Analises het getoon dat die *TAX1* OU nie tot 'n vermindering in *LOF1* geen uitdrukking in die nodes van die plante gelei nie. Die vlak van geen uitdrukking van die *TAX1* geen in die *lof1lof2* mutante plante was ook soortelyk aan die geen uitdrukking in wilde tipe plante. Die toediening van dexametasoon het tot die induksie van ooruitdrukking

van *TAX1* geen gelei. Dit het egter nie *LOF1* geen uitdrukking in saailinge of in die stingel apikale meristem verander nie. 'n Kruising tussen 'n lyn wat *TAX1* ooruitdruk en 'n lyn waar die uitdrukking van GUS deur die promoter van *LOF2* gedrewe word, het geen verandering in die patroon of vlak van *LOF2* geen uitdrukking getoon nie. Dit wil dus voorkom asof *TAX1* die skeiding tussen organe op 'n onafhanklike wyse van *LOF1* reguleer. Dit is wel moontlik dat die twee gene ontwikkeling in plante op 'n latere wyse tesame beheer. Analise van die primêre metaboliet samestelling van die blare en wortels van al die *TAX1* OU plante het 'n toename in fosfaat (blare) en serien (wortels en blare) vlakke getoon. Die *TAX1* OU plante was ook sensitief vir die periode van ligblootstelling en hierdie effek mag verwant wees aan die vermindering in sinapoyl malaat produksie in blare.

Die cDNA-AFLP tegniek is toegepas om die verandering in genoom-wye geen uitdrukking van *in vitro Sutherlandia frutescens* plante wat met stikstof, sout of Metiel Jasmonaat behandel is te bestudeer. Die resultate het aangedui dat reaksies wat tot poli-amien produksie of die produksie van plant hormone soos etileen of absisiensuur lei, verandering toon. Sout stress het 'n verlaging in stikstof opname veroorsaak, maar het geen effek op fotosintese of die koolstof tot stikstof verhouding veroorsaak nie. 'n Toename in die arginien en prolien vlakke is waargeneem en die verandering mag verwantskap hou met vermindering van ammonium toksisiteit. 'n Alternatiewe opsie is dat die produksie van die metaboliete tydens die osmotiese reaksie toeneem om die akkumulasie van ione wat skade aanbring, te verminder. Die plante was in die algemeen verdraagsaam vir lae vlakke van sout en geen aansienlike verandering in die sutherlandioside B vlakke is waargeneem nie. Aaneenhoudende uitdrukking van die TAXIMIN gene van *T. baccata* en *Medicago truncatula* het nie die vlakke van die sutherlandins, sutherlandiosides of saponiene in die *S. frutescens* harige wortels geaffekteer nie. Hierdie resultaat dui daarop dat die gene nie direk die produksie van die metaboliete in *S. frutescens* reguleer nie. Toediening van Metiel Jasmonaat het die produksie van sojasaponiene verhoog en dit bevestig vorige bevindings dat Metiel Jasmonaat behandeling hierdie metaboliese paaie kan induseer. Hierdie studie beskryf die ontwikkeling van 'n platform wat gebruik kan word om die veranderinge in die transkriptoom weens die toediening van stress op nie-model plante te ondersoek. Dit platform sluit die beskrywing van tegnieke om die funksie van gene wat nie voorheen gekarakteriseer is nie in die model plant *A. thaliana* te ondersoek. Die studie beskryf ook die transformasie van 'n nie-model medisinale plant (*S. frutescens*) wat gebruik kan word om die effek van 'n nuwe heteroloë geen op metabolisme van die plante te bestudeer.

Chapter 1

INTRODUCTION AND LITERATURE REVIEW

Plant secondary metabolites

Since the discovery of secondary metabolites, people have been interested in exploiting it for various purposes. Plants synthesize many different classes of secondary metabolites which include the phenolics, terpenes, steroids and alkaloids (Bourgau *et al.*, 2001). These metabolites can function as flavour additives, they can enhance the aromatic fragrances of perfumes, they are used in cosmetics and their application as dyes is useful for the food and the textile industry. Secondary metabolites also have health benefitting properties and large pharmaceutical industries have exploited and profited from the bio-activity of these compounds which can be used to combat diseases. However, secondary metabolite production is not one of the essential processes for survival in plants, and they are mainly activated for specific functions such as allowing interaction with the environment (Oksman-Caldentey and Inzé, 2004). Plants generally synthesize secondary metabolites to attract pollinators or for seed dispersal by animals which eat the fruit; it provides UV protection and acts as a deterrent for herbivores or pathogens (Aharoni and Galili, 2011). As a result, secondary metabolite levels are often low and vary with season and geographical location (Lambert *et al.*, 2011). Due to the low bio-availability, metabolites are not produced in quantities sufficient for industrial requirements, which can also make drugs containing these compounds expensive.

Alternative production techniques such as chemical synthesis of metabolites have been considered, but secondary metabolites are structurally complex making this process expensive and time consuming. Research efforts have focussed on engineering these biosynthetic pathways in plants and harnessing alternative organisms (microbes) through synthetic biological techniques to ensure ample supply of these compounds (Mora-Pale *et al.*, 2013). Furthermore, *in vitro* cultivation of (bio-engineered) plants and organisms provide several advantages for example, cultivation conditions (pH, temperature, light) can be optimized to increase the yield (Mora-Pale *et al.*, 2013). Metabolite production by cell suspension cultures is also more sustainable and eco-friendly (Ramirez-Estrada *et al.*, 2015). Cultivated cell suspension cultures are also genetically identical; therefore selection of lines producing high metabolite yields can be clonally propagated (Lambert *et al.*, 2011). One well known example of using *in vitro* plant culture systems for the manufacture of a pharmaceutical product is the synthesis of the diterpenoid taxol[®] (generic name paclitaxel). These compounds were first discovered in the medicinal tree *Taxus brevifolia* (Mora-Pale *et al.*, 2013) and they are highly effective anti-cancer drugs. Application of pharmaceuticals containing taxol has been approved by the Food and Drug Administration (FDA) for the treatment of ovarian and breast cancer (Angelova *et al.*, 2006).

Optimizing taxol synthesis in cell suspension cultures of *Taxus baccata*

Taxol is isolated from the bark of the European yew tree; however this method of bark removal is unsustainable and also hampered due to low concentrations. It is estimated that production of 1 kg of taxol requires 10 000 kg of *Taxus* bark or an equivalent of 3 000 yew trees (Malik *et al.*, 2011). Therefore, focus was placed on generating alternative production techniques and establishing a successful platform for cultivation of cell suspension cultures. Since the *T. baccata* species is more widespread than *T. brevifolia*, cell cultures of this species have been used for commercial taxol production (Mora-Pale *et al.*, 2013). However, the yield of secondary metabolites in the undifferentiated cell suspension cultures could be low since some compounds are produced in specialized plant tissues (Bourgaud *et al.*, 2001; Pavarini *et al.*, 2012) and this system may therefore require further optimization. Currently, *in vitro* production of taxol involves a two-stage system; cell suspension cultures are first cultivated in a growth medium containing Gamborg B5 which provides macro and micro nutrients, supplemented with plant growth hormones (NAA and BAP) and a carbon source (sucrose and fructose). Cells are maintained in this medium until it reaches the optimum density at the end of the exponential phase. Once the cells enter the stationary phase they are subcultured onto a production medium (Malik *et al.*, 2011) containing Gamborg B5, the plant growth regulators picloram and kinetin and only sucrose as a carbon source. Modification of various factors (eg. carbohydrate source, plant growth hormones and other medium additives) has been investigated for their effect on taxol yield and these conditions have already been amended. To further enhance metabolite levels a classical biotechnology approach targeting and manipulating the genes and enzymes involved in the metabolic pathway have been attempted. This includes genetic engineering to reduce catabolism of the metabolite of interest; increasing expression of the rate limiting enzyme, preventing feed-back inhibition of key enzymes, reducing flux of precursors to competing pathways and compartmentalization of the compound to name a few examples (Oksman-Caldentey and Inzé, 2004).

In vitro cultures also provide a good platform to study the genes and enzymes involved in the production pathway. However, targeting of the biosynthetic enzymes can increase production to a certain extent; therefore, novel regulators (transcription factors, sRNA etc) are currently of interest. One approach to identify new mechanisms is to trigger the defence pathways in which the secondary metabolites are synthesized through the application of elicitors (Angelova *et al.*, 2006). Investigation of changes in gene expression at different time points can be used to understand regulation of the defence responses and allow for its manipulation. Several different types of elicitors exist and include abiotic elicitors such as presence of heavy metal salts or changes in pH and temperature (Bourgaud *et al.*, 2001). Exogenous biotic elicitors include oligosaccharides such as chitosan and glycoproteins which

are produced by pathogens. Endogenous elicitors are produced by enzymes from the pathogen which digest certain plant components (Angelova *et al.*, 2006). Methyl Jasmonate (MeJA) and other jasmonate derived compounds are oxylipin-type molecules which function as endogenous elicitors in plants (Dar *et al.*, 2015). These compounds are produced by oxidative metabolism of polyunsaturated fatty acids starting from α -linolenic acid derived from membrane lipids and is known as the octadecanoid pathway (Dar *et al.*, 2015). Since its discovery, jasmonate has also been classified as a phytohormone (Dar *et al.*, 2015). Jasmonate plays a role in various developmental processes such as seed germination, fertility, embryo development, leaf movement and senescence, fruit ripening and gravitropism amongst others (de Smet *et al.*, 2015). Other plant growth hormones such as salicylic acid and ethylene also play a role in the defence against pathogens (Dar *et al.*, 2015). Whereas salicylic acid functions against biotrophic pathogens which live and feed on living tissue, the other two hormones Jasmonate and ethylene act against necrotrophs which feed on dead tissue (Dar *et al.*, 2015). Additionally, it has been shown that Jasmonate and Salicylic acid function antagonistically (Dong, 1998). Whereas Salicylic acid can inhibit proteinase inhibitor genes, Jasmonate and ethylene can partly overcome this inhibitory effect (Dong, 1998).

Production of volatile MeJA also results in the activation of the defence response, this involves induction of a signalling cascade resulting in transcriptional changes and ultimately leading to altered plant secondary metabolism (Mora-Pale *et al.*, 2013). The advantage of applying MeJA is that it can activate several different branches of secondary metabolite synthesis (Pauwels *et al.*, 2009). It is therefore useful to elicit the defence response in different species belonging to both the angiosperms and gymnosperms (De Geyter *et al.*, 2012). Since MeJA application can induce changes in gene expression, analysis of these transcripts can reveal novel regulators.

In one such experiment, cDNA-AFLP was used to discover unique genes which regulate taxol biosynthesis. This involved studying the gene expression profile of MeJA elicited cell suspension cultures of *T. baccata* along various time frames to identify potential novel target genes involved in the defence response which may regulate secondary metabolite production (Onrubia, 2012). This knowledge may also contribute to our understanding of the ability of some plants to be resistant to specific pathogens and could assist with transferring tolerance to susceptible plants.

Application of cDNA-AFLP to identify changes in gene expression profile of MeJA elicited plants

Several tools to study changes in gene expression exist such as microarray analysis, cDNA libraries, suppressive subtractive hybridization, sequencing of expressed sequence tags (EST), differential display (DD), sequencing of serial analysis of gene expression (SAGE), RNA fingerprinting by arbitrary primer polymerase chain reaction (RAP-PCR), Representational Difference Analysis (RDA) and RNA sequencing (RNA-seq) (Casassola *et al.*, 2013). Each of these techniques has certain advantages and disadvantages.

Microarrays consist of specific gene probes which are linked to a glass, plastic or a nylon matrix. The target nucleic acid which is labelled with a fluorescent probe interacts with the probes on the microarray and depending on the expression of a gene can result in low or high fluorescence intensity (Casassola *et al.*, 2013). The advantage of this technique is that it is fast and allows for screening of a large number of genes (Casassola *et al.*, 2013). It is also semi-quantitative and sensitive to transcripts which are present in low levels (Alba *et al.*, 2004). The disadvantages of microarrays are that not all genes are necessarily represented on the microarray and difficulties may occur to distinguish between homologous genes (Breyne *et al.*, 2003)

Differential display and RAP-PCR involves cDNA synthesis from RNA using 5'- arbitrary or 3'-oligo dT primers to amplify transcripts (Casassola *et al.*, 2013). This is followed by a second amplification using arbitrary primers or the 3'-oligo dT primers. The PCR products are then separated on a gel and differentially amplified genes can be isolated and sequenced for identification. The disadvantages of DD are that it can be laborious, the banding pattern can be difficult to analyse and one band can consist of more than one cDNA (Kok *et al.*, 2007).

SAGE uses 3'oligo dT primers to convert RNA to cDNA. After restriction digestion, adapters are ligated to the products which are linked and amplified by PCR (Casassola *et al.*, 2013). Since several fragments are linked together they form concatamers and these are cloned and sequenced. This technique has the advantage that it can be used to quantify differences in expression (Alba *et al.*, 2004). However the disadvantage is, that it can also be laborious and time consuming due to the requirement of large scale sequencing to compare different conditions (Kok *et al.*, 2007).

RNA sequencing studies the whole transcriptome of a species using bioinformatics and deep-sequencing tools. This technique involves conversion of RNA to a cDNA library and attaching adapters at both ends followed by sequencing each molecule (Wang *et al.*, 2009). In single end sequencing short sequences from one end is produced whilst in pair-end

sequencing sequences of both ends are produced (Wang *et al.*, 2009). The reads which can be typically 30 – 400 bp long can either be aligned to a reference genome or it can be assembled *de novo* (Wang *et al.*, 2009). RNAseq has several advantages; it can measure transcript levels and different isoforms more accurately and results are also highly reproducible (Wang *et al.*, 2009). No prior sequence information of the organism is needed and this technique also requires less RNA for analysis (Wang *et al.*, 2009). The drawback of this technique is that production of cDNA libraries requires that larger RNA molecules have to be fragmented using RNA or cDNA fragmentation to generate smaller (200 – 500 bp) reads (Wang *et al.*, 2009). This can be problematic because different fragmentation methods generate a difference in bias of the product (Wang *et al.*, 2009). RNA fragmentation causes transcripts which are incomplete at the ends, whilst cDNA fragmentation creates bias towards the 3' end of the transcripts (Wang *et al.*, 2009). Additionally, challenges exist with the analysis of the results which requires bioinformatics and large datasets which have to be stored and processed (Wang *et al.*, 2009). Each of these techniques therefore has their advantages and disadvantages and is more suitable for specific types of studies.

In this study we describe the application of cDNA Amplified Fragment Length Polymorphism (cDNA-AFLP), a genome wide expression analysis technique to study changes in gene expression. This technique involves synthesis of cDNA followed by digestion with different restriction enzymes to generate unique fragments. These fragments are subjected to selective PCR amplifications and products are separated on a high resolution gel (Breyne *et al.*, 2003). This technique has the advantage that it does not require any prior sequence information for the organism being used. It also allows for the comparison of different tissue types or stages of development and can be used for time scale experiments (Alba *et al.*, 2004). Application of cDNA-AFLP to study changes in gene expression in the MeJA elicited *T. baccata* cell cultures identified several novel regulators.

cDNA-AFLP lead to discovery of a novel signalling peptide TAXIMIN in MeJA elicited *Taxus baccata* cell suspension cultures

Screening of the transcriptome data, led to identification of several tags which correlated with known genes regulating this pathway. For example taxadiene synthase expression was increased 12-hours after MeJA elicitation and peaked at one to four days (Onrubia, 2012; Onrubia *et al.*, 2014). Some of the tags encoded novel genes which could be potential regulators of this pathway. A tag called TB595 with a unique sequence displaying a transient increase in expression after transfer from the growth medium to the production medium, appeared to correlate with increased taxol biosynthesis (Onrubia *et al.*, 2014). Cluster

Chapter 1

analysis indicated that this gene was co-regulated with putative proteins with a Jasmonate ZIM domain (characteristic of JAZ proteins) or which had a TIFY domain. However, expression of these tags was similar between elicited and non-elicited cultures (Onrubia, 2012).

JAZ proteins function as repressors of jasmonate signalling and bind to the transcription factor MYC2 to inactivate it (Chini *et al.*, 2007). Upon jasmonates perception, JAZ proteins are targeted for proteasome degradation by the SCF^{COI1} (Skp1, Cullin and F-box) E3 ubiquitin ligase. This degradation releases MYC2 and allows for transcriptional activation of several jasmonate targets (Chini *et al.*, 2007). Quantification of *TbTAX* expression using RT-qPCR indicated that the *TbTAX* gene was upregulated during the first two hours after transfer to the production medium in both the control and MeJA treated samples, but *TbTAX* expression persisted longer in the MeJA treated samples (Onrubia, 2012). Various *T. baccata* tissue types also displayed different *TbTAX* expression levels with the young cortex and wooden branch exhibiting the highest *TbTAX* expression (unpublished). The full length gene sequence of the TB595 tag was amplified and the gene (*TbTAX*) and peptide (TAXIMIN) was used for further investigation. To assess if *TbTAX* could induce expression of secondary metabolite biosynthesis genes, Onrubia (2012) performed transient expression assays (TEA). This comprised using tobacco (*Nicotiana tabacum*) Bright Yellow-2 (BY-2) protoplast cultures and constitutively expressing *TbTAX* with promoters of various secondary metabolite genes. Overexpression of *TbTAX* could induce expression of taxol (taxadiene synthase), nicotine (putrescine N-methyltransferase), anatabine (quinolinate phosphoribosyltransferase) and terpenoid indole alkaloid (strictosidine synthase) biosynthesis promoters to varying levels (Onrubia, 2012). Additionally, TAXIMIN had a synergistic effect with MeJA to induce expression of these secondary metabolite producing genes (Onrubia, 2012).

Next, hairy root lines of *Nicotiana tabacum* overexpressing *TbTAX* (*TbTAX*-OE) or GUS (control) were generated to test if *TbTAX* was functional *in vivo* and could induce secondary metabolism in plant organs. No difference in total alkaloid production in *TbTAX*-OE or control hairy root lines in standard growth conditions were observed (Onrubia, 2012; Onrubia *et al.*, 2014). Addition of MeJA significantly increased levels of the main alkaloid nicotine and anatabine in the *TbTAX* overexpressing hairy root lines (Onrubia, 2012). Changes in these metabolites were however not correlated to variation in the transcript levels of enzymes involved in their biosynthesis pathway. This suggests that the induction effect of TAXIMIN operates through a different mechanism (Onrubia *et al.*, 2014).

Application of a chemically synthesized TAXIMIN peptide of which the prolines were hydroxylated (HyproTAXIMIN), also resulted in increased production of paclitaxel and the taxol

precursor baccatin III in *T. baccata* cell suspension cultures (Onrubia *et al.*, 2014). Simultaneous application of HyproTAXIMIN with MeJA had a synergistic effect and caused further increase in paclitaxel and baccatin III production up to seven days (Onrubia *et al.*, 2014). However, no significant changes in production of the most abundant saponins in the presence or absence of MeJA were detected in *Medicago truncatula* hairy roots which overexpress *TbTAX* (Onrubia *et al.*, 2014). These results pointed to the possible role of this peptide in regulating secondary metabolic pathways, but this effect might be species specific and it is possible that homologs of *TbTAX* may perform different functions in other plants.

To further characterize the TAXIMIN peptide, *in silico* analysis was performed to identify typical properties of this peptide. Analysis using SignalP 4.0 (Peterson *et al.*, 2011) indicated that there was a signal peptide cleavage site in the amino acid (a/a) sequence (Onrubia, 2012) indicating that it has an N-terminal secretion peptide. The C-terminal of the peptide contained several cysteines and prolines that were highly conserved between species (Onrubia *et al.*, 2014). Results also showed that the TAXIMIN a/a sequence is highly conserved across the entire plant kingdom. However, due to the absence of a known protein domain, no function could be assigned for the peptide (Onrubia *et al.*, 2014). Since *in silico* analysis predicted that the peptide was transported to the plasmamembrane, vacuole, chloroplast and endoplasmic reticulum this required further investigation (Onrubia, 2012; Onrubia *et al.*, 2014). Expression of a TAXIMIN-Venus fusion in *Nicotiana benthamiana* leaves indicated that the peptide was located in the plasmamembrane suggesting that this peptide is secreted (Onrubia *et al.*, 2014). Collectively, these characteristics suggest that TAXIMIN is a putative novel signalling peptide.

Discovery of signalling peptides

Signalling peptides are present in both monocot and dicotyledonous plants and they can be highly variable since the different classes are not phylogenetically related (Wheeler and Irving, 2012). Some peptides are present in several species for example AtPEP1 (*Arabidopsis thaliana*) and ZmPROPEP1 (Maize); both function to induce genes involved in defence responses (Marmioli and Maestri, 2014). Other peptides developed or function exclusively in one species for example the LURE peptides in *Torenia fournieri* (Wheeler and Irving, 2012) are released by the synergid cells. These peptides are responsible for attracting and guiding the pollen tube as it grows through the pistil tissue towards the ovary (Okuda *et al.*, 2009). This attracting effect was found to be species specific as LURE peptides from *Arabidopsis* were unable to bind to the pollen tip of *T. fournieri* (Okuda *et al.*, 2009). Peptide families can consist of several genes and a study using one representative of different peptide groups revealed that genes for a peptide family could be spread out over the chromosomes or they

Chapter 1

could occur in clusters (Wheeler and Irving, 2012). Some genes for a peptide family may be functionally redundant such as the CLAVATA/CLE (CLV3/EMBRYO SURROUNDING REGION RELATED) peptides which are involved in meristem maintenance (Czyzewicz *et al.*, 2013). CLV3 regulates stem cell differentiation in the shoot apical meristem (SAM), whilst CLE40 and CLE19 play a role in differentiation of stem cells in the root meristem (Fiers *et al.*, 2007). In some instances genes from the same family may also have opposite effects for example CLE41, CLE44 and CLE42 were found to suppress xylem development in *Zinnia* cultures whilst CLV3 promotes xylem differentiation (Fiers *et al.*, 2007). Peptide functions may therefore vary and is highly dependent on their expression patterns in different tissue and time points of development or in response to environmental factors (Wheeler and Irving, 2012).

The discovery of signalling peptides eluded researchers for many years and currently bio-informatics tools still experience difficulties to identify peptides and to predict their specific functions. The reason for this is because the genes for the peptides are small in size. This makes it difficult to use gene prediction algorithms to identify the short open reading frames (ORF) in the genome (Lindsey *et al.*, 2002; Murphy *et al.*, 2012). Additionally, genes for peptides are also not well represented on microarrays (Lindsey *et al.*, 2002; Murphy *et al.*, 2012). Peptides may also be easily missed, since some peptides require processing (post-translational modifications) to render the peptide biologically active. These modifications are not represented on the transcriptional level (Murphy *et al.*, 2012). Peptide transcripts are also not present in high levels (Lindsey *et al.*, 2002; Murphy *et al.*, 2012) and peptides may occur in low physiological concentrations (nanomolar range) (Murphy *et al.*, 2012). Techniques for peptide discovery have since been modified and now include screening methods using their specific properties. For example, systemin (18 a/a) is a peptide discovered in tomato (*Solanum lycopersicum*) after wounding of leaves and it causes the production of proteinase inhibitors (Murphy *et al.*, 2012). Bioassays discovered two peptides (TobHypSysI and TobHypSYSII) through using the property of these peptides to induce proteinase inhibitors; although homologous sequences for systemin was absent in tobacco plants (Murphy *et al.*, 2012). These TobHypSys peptides also cause the rapid alkalinization of the growth substrate. Using this property, a new 49 a/a peptide called RAPID ALKALINIZATION FACTOR (RALF) was discovered using a medium alkalinization assay (Murphy *et al.*, 2012). The PHYTOSULFOKINE (PSK- α) peptide was discovered when investigating why conditioned medium of *Asparagus officinalis* mesophyll cells could enhance the growth of low density cell suspension cultures (Murphy *et al.*, 2012). Although useful, one limiting factor with the application of bioassays to discover novel peptides is that peptides which are present in low concentrations could easily be missed. An alternative solution is to use peptidomics to identify peptides. This procedure takes into consideration the unique properties of a peptide

such as the post-translational modifications to increase their concentration in the screening extracts (Murphy *et al.*, 2012).

Except for identification of peptides in the genome, determining their functions can also be challenging as there is a shortage in the number of loss-of-function mutants. The small size of peptide genes reduces the prospect of having T-DNA insertion lines for these genes (Lindsey *et al.*, 2002; Murphy *et al.*, 2012). Additionally, the use of mutants to determine a peptides' function is also complicated due to functional redundancy which result in absence of 'mutant' phenotypes (Murphy *et al.*, 2012). However, the fact that peptides form families have enabled *in silico* analysis to discover and putative annotate homologous genes. In some instances peptides were also discovered due to mutations in enzymes involved in post-translational modification. These mutations can result in specific phenotypes, which assist with prediction of a peptides' function which might be related to the observed phenotype (Murphy *et al.*, 2012). Since their original discovery, the identification of typical properties of peptides has simplified their detection in the genome sequence and in extracts.

Typical characteristics of signalling peptides

A bio-informatics search indicated that there are about 1 000 putative peptide ligands in the *Arabidopsis* genome (Lease and Walker, 2006). Some peptides can be derived from a precursor, whilst others are directly produced from the 5' region of the mRNA, pri-miRNA or from sORFs (Tavormina *et al.*, 2015). The precursor derived peptides can be subdivided into peptides derived from a non-functional precursor or those derived from a functional precursor with a different function also known as cryptides (Tavormina *et al.*, 2015). The peptides derived from a non-functional precursor can be classified into two groups as indicated in Figure 1. The first group is the small post-translationally modified peptides which are characterized by post-translational modifications and processing. Then there are the Cysteine-rich peptides (CRP) which form disulphide bridges (Murphy *et al.*, 2012). The cysteine rich peptides can be further subdivided into two groups which include Cys-rich peptides which are processed (intermediate type) and Cys-rich peptides which are not processed (Matsubayashi, 2011; 2012; Tabata and Sawa, 2014). Recently, a third group the non-cysteine-rich peptides without post translational modifications have been defined (Tavormina *et al.*, 2015).

Chapter 1

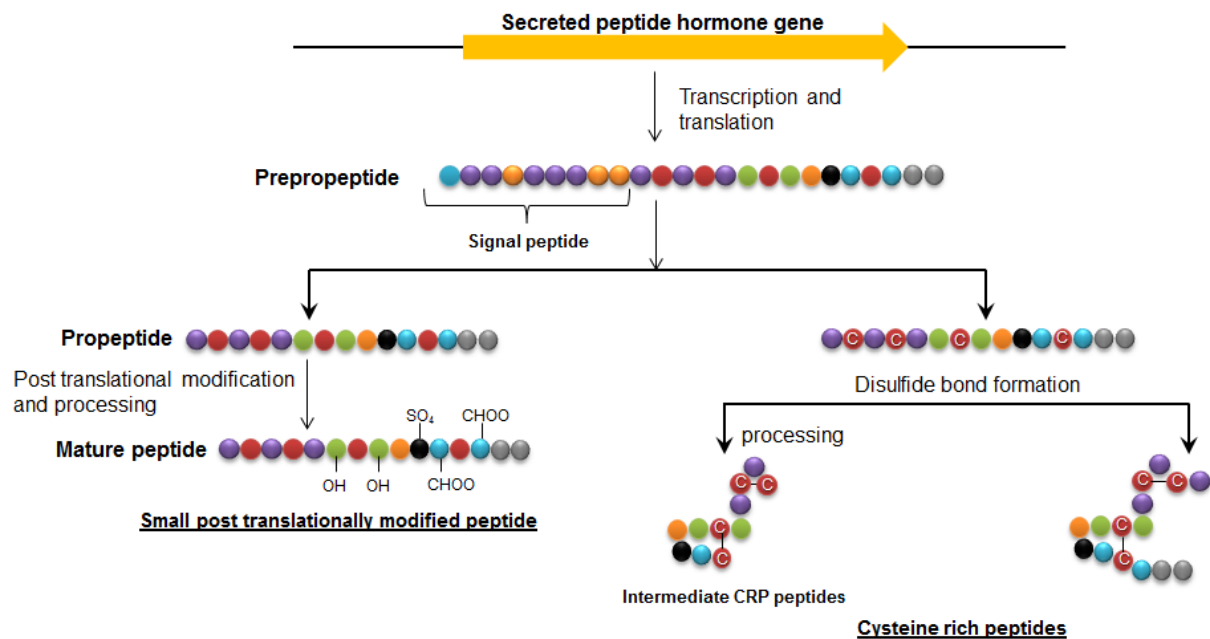


Figure 1. Classification of small signalling peptides in plants. Transcription and translation of a signalling peptide gene produces a prepropeptide which is processed to remove the N-terminal signal peptide producing the propeptide. Peptides can be divided into two groups; the small post translationally modified peptides are produced when the propeptide undergoes post-translational modification (sulfation (SO_4), hydroxylation (OH) or glycosylation ($-\text{CHOO}$)) and processing to form the mature peptide. The second group is the cysteine rich peptides (CRP) which can be subdivided into the intermediate peptides which are processed and involves the formation of disulphide bridges whereas the second group of CRP only forms disulphide bridges (Figure adapted and modified from Matsubayashi, 2011).

Post-translationally modified peptides

The first group, namely the post-translationally modified peptides are synthesized as a larger nonfunctional precursor (prepropeptide) with variable size, but usually less than 100 a/a (Aalen, 2013) or between 5 – 75 a/a (Czyzewicz *et al.*, 2013) with few or no cysteine residues (Tabata and Sawa, 2014). This prepropeptide contains an N-terminal sequence which generally directs it to the secretory pathway via the endoplasmic reticulum (Murphy *et al.*, 2012; Tavormina *et al.*, 2015). It also has a C-terminally encoded propeptide (Matsubayashi, 2011) which contains the biologically active mature peptide (<20 a/a). The mature peptide is released from the precursor after processing and post-translational modifications which occur in the Golgi network (Murphy *et al.*, 2012; Wheeler and Irving, 2012). The mature peptide often contains conserved domains/motifs which are responsible for the biological activity (Somssich and Simon, 2012). Some peptides (eg. tobacco systemin) can have more than

one motif/domain (Franssen and Bisseling, 2001) within a peptide which is suggested to allow a faster or amplified response (Wheeler and Irving, 2012). The mature peptide also requires post-translational modification to be functionally active in the cell. Three types of post translation modifications exist and include tyrosine sulfation, proline hydroxylation (Hyp) and Hyp arabinosylation (Farroki *et al.*, 2008, Matsubayashi, 2011, Murphy *et al.*, 2012). Modifications of peptides may be critical as it affects the solubility, correct folding, stability and activity of the peptides (Somssich and Simon, 2012) as well as their affinity for their target receptors (Matsubayashi, 2011).

In Table 1 several examples of post translationally modified peptides are listed and includes a description of the size of the mature peptide as well as the post-translational modifications to the peptides. These peptides also play various functions in the plant which will be discussed in another section. Some examples include roles in development such as the CLE peptide CLV3 which functions in maintenance of the stem cell population in the SAM (Fiers *et al.*, 2007). CLE peptides have a 14 a/a CLE motif which is processed to a 12-13 a/a active mature peptide (Murphy *et al.*, 2012). The mature peptide has three conserved prolines and those at position 4 and 9 are hydroxylated, whilst Pro7 is arabinosylated (Murphy *et al.*, 2012). These modifications (especially the arabinosylated Pro7) are important for binding of the CLV3 peptide to the CLV1 receptor (Katsir *et al.*, 2011). A second example is PSK (PHYTOSULFOKINE) which plays a role in stimulating cell division; promoting tracheary element differentiation, root and hypocotyl elongation, it plays a role in plant innate immunity response and can influence somatic embryogenesis (Matsubayashi, 2014). The mature PSK peptide constitutes out of five a/a and post-translational modifications include tyrosine sulfation (Matsubayashi, 2014). After post-translational modification, the propeptide is processed by proteolytic cleavage to release the mature active peptide. The enzymes for processing are not yet known for all peptides (Wheeler and Irving, 2012), but more than 500 putative protease encoding genes have been identified in the *A. thaliana* genome (Butenko *et al.*, 2009).

Chapter 1

Table 1: Examples of post translationally modified and Cysteine -rich peptides

Peptide		Mature size	Secreted or non-secreted	Functions	Function(s)	Modifications
Post translational modified peptides						
PSK	PHYTOSULFOKINE	5 a/a ⁺	Secreted ^{**}	Extracellularly	Cellular proliferation ^{**} and expansion [*]	Tyr-SO ₄ [^]
PSY1	PLANT PEPTIDE CONTAINING SULFATED TYROSINE1	18 a/a ⁺	Secreted ⁺		Promotes cellular proliferation ^{**} and expansion [*]	Tyr-SO ₄ [^] , Hyp-Ara [^] , Pro-OH [^]
CLE or CLE-LIKE	Eg. CLAVATA3 (CLV3)	12 ⁺ - 13 a/a [^]	Secreted ^{**}	Extracellularly [*]	Meristem maintenance in the shoot apical meristem [*]	Pro-OH [^] , Hyp-Ara [^]
RGF/GVL	ROOT GROWTH FACTOR/ GOLVEN	13 a/a [^]	Secreted [*]	Extracellularly [*]	Maintenance of stem cells in root meristem ^{**}	Tyr-SO ₄ [^] , Pro-OH [^]
TDIF	TRACHEARY ELEMENT DIFFERENTIATION INHIBITORY FACTOR	12 a/a [^]	Secreted [*]	Extracellularly [*]	Prevents tracheary differentiation, Determines cell fate in anthers ⁺	Pro-OH [^]
IDA and IDA-LIKE	INFLORESCENCE DEFICIENT IN ABSCISSION	- +	Secreted ^{**}	Extracellularly [*]	Floral abscission ^{**} and lateral root emergence [*]	Pro-OH
CEP1	C-TERMINALLY ENCODED PEPTIDE1	15 a/a ⁺	Secreted ^{**}		Possible role in lateral root development ^{**}	Pro-OH [^]
Cysteine-rich peptides						
RALF	RAPID ALKALINIZATION FACTOR	49 a/a ⁺	Secreted ^{**}	Extracellularly [*]	Innate immune response ⁺	4 cysteines [^]

EPF	EPIDERMAL PATTERNING FACTOR		Secreted*	Extracellularly*	Stomatal density (Katsir <i>et al.</i> , 2011)	6-8 [#] cysteines (Katsir <i>et al.</i> , 2011)
STOMAGEN	(EPFL9)	43 a/a [#]	Secreted*	Extracellularly*	Regulates stomatal density [#]	6 cysteines [#]
CHAL	CHALLAH				Regulates epidermal stomata patterning [#]	8 cysteines [#]
ENOD	EARLY NODULIN	12 and 24 a/a ⁺	Not secreted*		Root nodule initiation in legumes ⁺	4 cysteines [#]
LURE	Discovered in <i>Torenia fournieri</i> (Okuda <i>et al.</i> , 2009)	60 – 70 a/a ^{\$}	Secreted*	Extracellularly*	Secreted by synergid cell to attract the pollen tube (Okuda <i>et al.</i> , 2009)	6 cysteines (Okuda <i>et al.</i> , 2009)
SP11/SCR	S-locus Cys-Rich/S-locus Protein11	- ⁺	Secreted ^{**}	Extracellularly*	Self incompatibility ⁺	8 cysteines ⁺
Other						
Systemin		18 a/a ⁺	Not secreted ^{**}	Extracellularly*	Systemic defense response ⁺	
ROT4/DVL	ROT FOUR LIKE/ DEVIL	- ⁺	Not secreted ^{**}	Intracellularly*	Cell proliferation, morphogenesis of leaves ^{+\$}	
PLS	POLARIS	36 a/a ^{\$}	Not secreted ^{**}	Intracellularly*	Root growth and development ⁺	

Table collated from data from (*) Matusbayashi (2014); (+) Butenko *et al.*, (2009); (#) Marshall *et al.*, (2011); (^) Murphy *et al.*, (2012) (\$); Tavormina *et al.*, (2015) (unless stated differently).

Cysteine rich peptides

The second group of peptides are the cysteine-rich peptides (CRP) which are larger (<160 a/a), than the small post-translationally modified peptides and cationic in nature (Marshall *et al.*, 2011; Murphy *et al.*, 2012). More than 800 *Arabidopsis* genes encoding putatively secreted CRP have been identified during a bio-informatics analysis, whilst the rice genome contained almost ~600 CRP (Silverstein *et al.*, 2007). These peptides have a conserved N-terminal signal peptide (Marshall *et al.*, 2011; Murphy *et al.*, 2012) which targets the peptide for export in the secretory pathway (Wheeler and Irving, 2012). Once the N-terminal is cleaved off the mature peptide is produced by the C-terminal Cys-rich domain (Wheeler and Irving, 2012) which can contain between four to 16 Cysteine residues (Marshall *et al.*, 2011). These cysteine residues associate to form disulfide bridges which are important for the biological activity of the peptide (Murphy *et al.*, 2012). Peptides often do not require proteolytical cleavage once they are synthesized, as the formation of Cys bonds renders them functionally active (Murphy *et al.*, 2012).

Cysteine rich peptides play various functions in plants, some represent peptides which play a role in defence and may be important for protection of nutrient rich tissue (eg. flowers, seeds, leaves and tubers) in the plant (Broekaert *et al.*, 1995; Silverstein *et al.*, 2007). Radish (*Raphanus sativus*) seeds for example have abundant cysteine rich antifungal proteins (AFPs) in the outer cell walls of the endosperm, cotyledon and hypocotyl tissue which first become hydrated upon germination (Broekaert *et al.*, 1995). Another example is the PLANT DEFENSINS (PDFs) which also have antifungal activity (Tavormina *et al.*, 2015). Production of CRPs may also be induced by pathways involved in mediating stress responses such as the jasmonate or the ethylene pathway (Silverstein *et al.*, 2007; Marmioli and Maestri, 2014). Examples of other CRP (Table 1) include the RAPID ALKALINIZATION FACTOR (RALF) which has four cysteines. This peptide plays several roles in plant growth and development (Silverstein *et al.*, 2007) including causing a reduction in root elongation in tomato and *Arabidopsis* seedlings amongst others (Murphy and de Smet, 2014). Another example is the LURE peptides which have six cysteines and are involved in pollen tube guidance (Wheeler and Irving, 2012).

The third group, the non-cysteine rich/non post translationally modified peptides are between 8 to 36 amino acids long and their functions mainly include defence responses (Tavormina *et al.*, 2015). Examples of these peptides include Systemin and PLANT ELICITOR PEPTIDES (PEP) which are involved in the systemic defence responses in plants (Tavormina *et al.*, 2015). Using the criteria described above, the TAXIMIN peptide is most likely a Cys-

Chapter 1

rich peptide, because it contains six cysteines which is highly conserved across the plant kingdom.

Once produced, these peptides can act either on the cell which produced it (autonomously) or it can be transported or secreted after production, modification and processing to act on surrounding cells (Fukuda and Higashiyama, 2011). Tomato systemin (produced from a 200 a/a precursor prosystemin) is synthesized in phloem parenchyma cells and translocates to the apoplast of the vascular bundles (Naváez-Vásquez and Ryan, 2004). Here, it is detected by the systemin receptor and results in the activation of the genes involved in the octadecanoid pathway (Naváez-Vásquez and Ryan, 2004). Activation of the jasmonate signalling pathway then functions as the long distance signal to activate defence responses in distal cells leading to the systemic response (Sun *et al.*, 2011). Some peptides can therefore activate responses and mediate signalling across larger distances in the plant. Other peptides have specific functions and may only act across a few cell layers for example CLV3 is produced in layer L1 and L2 in the SAM and diffuses to layer L3 where the receptor (CLV1/CLV2) is located (Farroki *et al.*, 2008). Once peptides reach their target cells, the domains are recognized and bind to specific receptors in the plasmamembrane to mediate their response (Somssich and Simon, 2012; Tabata and Sawa, 2014).

Receptor like kinases recognize signalling peptides and initiate a downstream signalling cascade

The *Arabidopsis* genome encodes for almost 600 receptor kinase (RK) genes (Czyzewicz *et al.*, 2013) whilst there are about 1100 genes in the rice genome (Walker and Lease, 2010). Receptor kinases can be found in both animals and plants suggesting that the plant RK developed from a common ancestor as the animal receptor tyrosine/serine kinases and RAF protein kinases (Walker and Lease, 2010). Two types of RK exist; the first is the Receptor like kinase (RLK) which has a tripartite structure consisting out of an (N-terminally encoded) extracellular domain (ECD), a transmembrane segment and a (C-terminally encoded) conserved intracellular kinase domain (Butenko *et al.*, 2009; Han *et al.*, 2014). The extracellular domain is highly diverse which allows them to detect a large variety of signals. This facilitates co-ordination of growth and development, to mediate defence responses or to establishing symbiotic relationships amongst others (Han *et al.*, 2014). Based on the extracellular domain the RLK are subdivided into 21 structural classes (Shiu and Bleeker, 2001). The largest group (216 genes) has a leucine rich repeat (LRR) domain containing between 1-32 LRR (Shiu and Bleeker, 2001; Walker and Lease, 2010). Receptor like kinases can also be classified according to its catalytic domain (Butenko *et al.*, 2009) and phylogenetic

analysis of the kinase domain revealed that there are at least 44 different subfamilies (Shiu and Bleecker, 2001). At least 13 of these subfamilies contained members of the LRR receptor like kinases (Shiu and Bleecker, 2001). The extracellular LRR domain has a specific peptide recognition region (Wheeler and Irving, 2012) and is responsible for recognizing and binding of target molecules.

The second type of receptor kinases lack the extracellular domain and only consists of a cytoplasmic kinase. To participate in signalling, they form complexes with other receptors. Once the ligand binds to the receptors it can result in conformational changes of the receptor (Czyzewicz *et al.*, 2013). This allows association with other members of the complex leading to the production of homomeric or heteromeric dimers (Wheeler and Irving, 2012) which is important for signalling. For example the CLV1 receptor is a serine/threonine kinase and is formed by two complexes of 185 kDa and 450 kDa (Lindsey *et al.*, 2002). The 185 kDa complex is a heterodimer formed by CLV1 and CLV2 which are bound by disulfide bonds (Takayama and Sakagami, 2002). The 450 kDa complex consists out of the 185 kDa complex plus a Rho-GTPase (Rop) and a kinase associated protein phosphatase (KAPP) protein (Lindsey *et al.*, 2002; Takayama and Sakagami, 2002). Upon ligand binding and activation these receptors are predicted to phosphorylate serine and threonine residues to mediate the signalling response (Butenko *et al.*, 2009). Interestingly, a higher number of peptides exist than the number of genes for receptor kinases.

Several of the genes for RLK families were derived from gene duplication. However, over time these duplicated genes may have become non-functional or developed specific functions. Alternatively, they were only expressed in specific tissue (spatial expression) or at specific stages (temporal expression) of development (Morillo *et al.*, 2006; Walker and Lease, 2010; Aalen, 2013). This could account for the redundancy observed for some receptors and unique expression or functions for other RLK of the same family. Peptides belonging to the same family are also able to bind to the same family of RLK (Katsir *et al.*, 2011) implying that different peptides can activate the same signalling cascade.

It is therefore possible that a peptide can bind to a receptor and activate one developmental response (Fig. 2). The peptide can also bind to different receptors and activate individual or overlapping responses (Fig. 2). Alternatively, different peptides can bind the same receptor and result in different responses (Fig. 2) (Endo *et al.*, 2014). The use of peptide mutants to predict a function of a gene based on observed phenotypes can therefore be complicated, since peptides and receptors can have unique expression patterns. Mutations in peptide or receptor genes would therefore only result in the observation of phenotypes in specific tissue or at time points when these genes are normally expressed. The use of tools

Chapter 1

such as reporter lines would therefore be useful to obtain an indication of the spatio-temporal expression of these peptide and/or receptor genes. Additionally, since peptide families can interact with receptor families, the constitutive expression of peptide genes (gain-of-function) can initiate ectopic phenotypes. Care should therefore be taken when interpreting results from these gain-of-function lines.

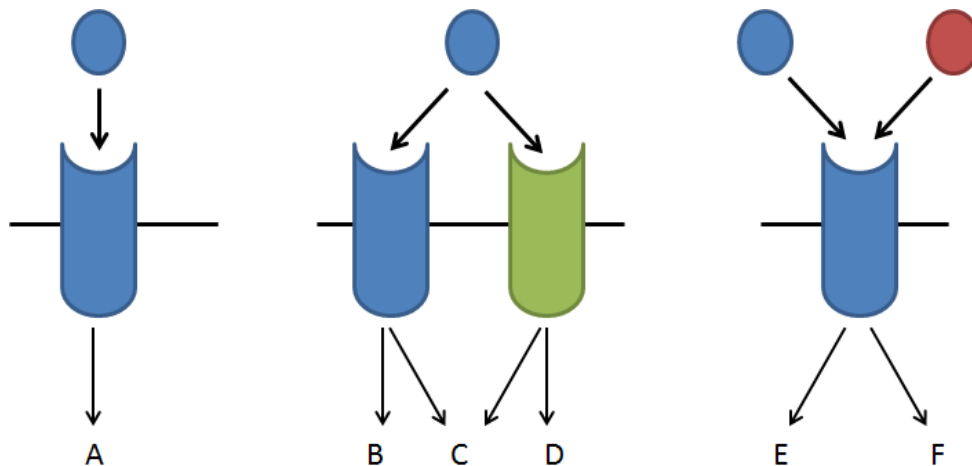


Figure 2. Peptide receptor complexes mediate various responses in plants. Specific binding of a peptide to a receptor can initiate a unique response. However a peptide can bind to more than one receptor and initiate multiple responses. A receptor can also bind to more than one peptide and activate different responses (Figure adapted from Endo *et al.*, 2014).

Except for binding to signalling peptides, the RLK may also be involved in mediating other responses. This includes binding to other components such as lipochitin oligosaccharides from pathogens during pathogen attack (Tichtinsky *et al.*, 2003) or plant hormones to regulate growth and development. For example, the steroid hormone brassinosteroid (BR) is involved in multiple developmental processes in plants such as induction of ethylene synthesis, xylem differentiation, regulation of pollen tube growth and leaf bending amongst others (Li and Chory, 1999). When BR binds to the receptor BRASSINOSTEROID INDEPENDENT1 (BRI1) it causes it to homodimerize and subsequently phosphorylates another receptor BRI1-ASSOCIATED RECEPTOR KINASE1 (BAK1) (Morillo *et al.*, 2006). However, the BRI1 receptor in tomato is also responsible for binding to systemin (Morillo *et al.*, 2006). Signalling peptides therefore mediate their response by using existing pathways. Binding of the peptide to the receptor initiates a down-stream signalling cascade which can result in the transcriptional activation/repression of several genes. For example the post-translationally modified peptides may activate the MITOGEN-ACTIVATED PROTEIN KINASE (MAPK) cascade which regulates the activity of certain transcriptional factors (Tavormina *et al.*, 2015). These signalling pathways can result in changes in expression patterns of other transcription

factors or changes in the apoplastic pH through its effect on proton transporters (Tavormina *et al.*, 2015). The presence of peptide families and receptors which can associate with multitude of components therefore increases the number of signalling pathways allowing plants to regulate and fine tune a variety of responses. These responses include roles in growth and development, stress responses, interaction with micro-organisms and reproduction amongst others (Tavormina *et al.*, 2015).

Peptides can regulate the growth and development of plants

Several peptides play an active role in regulating developmental processes of plants (Fig. 3). Some peptides are involved in determining cell fate for eg. the CLE peptides (Murphy *et al.*, 2012). Upon expression of the CLV3 peptide in the L1 and L2 layer of the SAM, this peptide functions in a regulatory feedback mechanism to restrict expression of the WUSCHEL (*WUS*) transcription factor (TF) (Fiers *et al.*, 2007). *WUS* is mainly expressed in the L3 layer of the central zone in the organizing centre (OC) and restricts expression of CLV3 (Fiers *et al.*, 2007; Katsir *et al.*, 2011). *WUS* expression in the OC is important to maintain the undifferentiated stem cell identity of these cells (Fiers *et al.*, 2007; Katsir *et al.*, 2011) whilst CLV3 signalling promotes stem cell differentiation (Katsir *et al.*, 2011). Once synthesized the CLV3 peptide most likely binds to CLV1-CLV2 receptor complex in the L3 layer which suppresses *WUS* expression (Fiers *et al.*, 2007). Although these peptides play an important role in the meristem activity, plant hormones such as auxin also play a key role (Fiers *et al.*, 2007). In the root apical meristem, stem cell maintenance is mediated by the ROOT GROWTH FACTOR or GOLVEN (RGF/GLV) and CLE-Like (CLEL) peptides (Murphy *et al.*, 2012). Other peptides are also involved in cell differentiation for example TDIF (TRACHEARY ELEMENT DIFFERENTIATION INHIBITORY FACTOR) which binds to the TDIF RECEPTOR (TDR) and some CLE peptides function in vasculature development (Murphy *et al.*, 2012) and maintenance of the vascular stem cells (Endo *et al.*, 2014).

Some peptides regulate specific functions for example stomatal development in plants is regulated by the EPIDERMAL PATTERNING FACTOR (EPF) family of peptides (Torii, 2012) which also include STOMAGEN and CHALLAH (CHAL) peptides (Katsir *et al.*, 2011). These peptides function to ensure that the stomata are correctly positioned and are at least separated from each other by one epidermal cell (Katsir *et al.*, 2011; Torii, 2012). During stomatal development a meristemoid mother cell undergoes asymmetric cell division to produce a stomatal precursor stem cell known as the meristemoid (Torii, 2012). This cell undergoes several more asymmetric divisions to produce surrounding non-stomatal ground cells and finally differentiates into the guard mother cell. The guard mother cell divides

Chapter 1

symmetrically to produce the paired guard cells (Torii, 2012). The EPF signalling peptide mediates its response by binding to the ERECTA LRR receptor kinase family of receptors (Katsir *et al.*, 2011) or to the receptor TOO MANY MOUTHS (TMM) which lacks a cytoplasmic domain to regulate stomatal development (Katsir *et al.*, 2011; Torii, 2012). This signalling mechanism also involves the activity of the basic-helix-loop-helix (bHLH) transcription factor SPEECHLESS (SPCH) which is responsible for inducing the stomatal cell lineage (Torii, 2012).

Certain developmental processes are also regulated by peptides such as the INFLORESCENCE DEFICIENT IN ABSCISSION (IDA) or IDA-LIKE (IDL) peptides which mediate floral abscission (Farroki *et al.*, 2008). The IDA peptides are specifically expressed in the abscission zone at the base of floral organs (Kumpf *et al.*, 2013). These peptides bind to the LRR-RLK HAESA or HAESA-LIKE family of receptor kinases expressed specifically in the cells of the abscission zone (Murphy *et al.*, 2012; Aalen *et al.*, 2013). This may influence expression of enzymes involved in cell wall remodelling such as xyloglucan endotransglucosylase/hydrolases and expansins, resulting in cell wall loosening (Kumpf *et al.*, 2013). Activation of cell wall degradation enzymes such as polygalacturonases may cause separation of the cells in the abscission zone (Kumpf *et al.*, 2013; Aalen *et al.*, 2013). Recently an additional role for IDA peptides in lateral root emergence was also demonstrated (Kumpf *et al.*, 2013).

Plants have also evolved mechanisms to recognize its own pollen which terminates fertilization and therefore increases genetic diversity (Lindsey *et al.*, 2002). This feature is known as the SELF INCOMPATIBILITY (SI) trait and was identified in the *Brassica* family (Marshall *et al.*, 2011). Plants have a single polymorphic locus (S-locus) which generates SCR/SP11 (S-locus cysteine-rich protein/S-locus protein 11) proteins on the surface of the pollen. In the stigmatic papillae cells, two proteins, S-locus glycoprotein (SLG) and S-locus receptor kinase (SRK) are expressed which recognizes the male derived SCR/SP11 peptide and prevents pollen germination (Lindsey *et al.*, 2002). Other examples of peptides with a role in development can be obtained in Table 1 and in Fig. 3.

Some peptides can also play more than one function for example the highly conserved peptide PSK plays a role in cell proliferation and differentiation into tracheary elements (Takayama and Sakagami, 2002; Farroki *et al.*, 2008) and also plays a role in pattern triggered immunity (Igarashi *et al.*, 2012). Several different peptides (Fig. 3) such as PSK have therefore enabled plants to interact with its environment to allow defence against pathogens or for initiating beneficial plant-bacterial interactions (Marshall *et al.*, 2011).

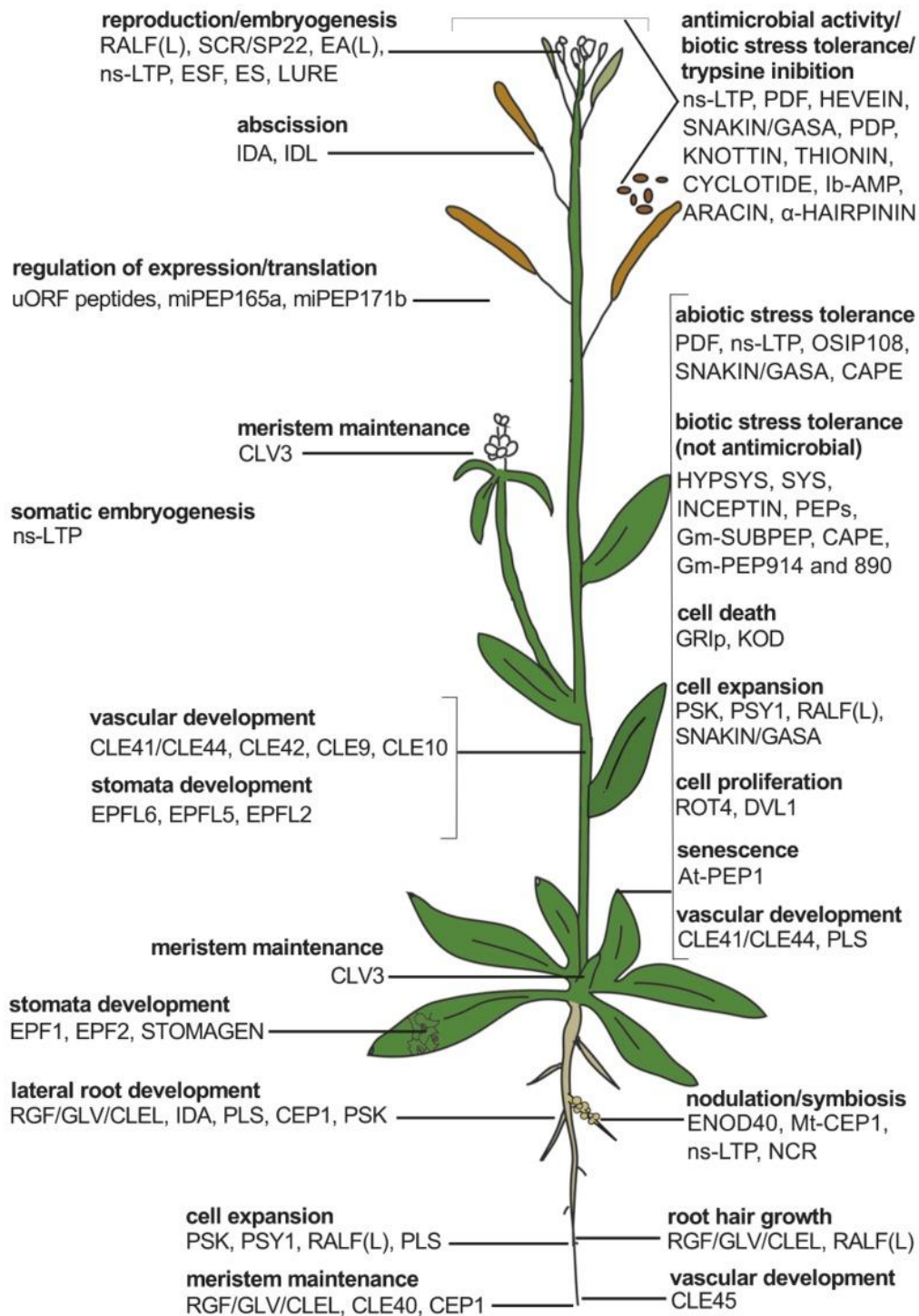


Figure 3: Examples of the various signalling peptides' functions in *Arabidopsis thaliana* (figure from Tavormina *et al.*, 2015). Peptides perform various functions in plants growth and development including preventing self-fertilization (SCR/SP22), regulating meristem development (CLV3) and allowing interaction with the environment (eg. ENOD40 during nodulation).

Peptides can initiate symbiotic relationships or have a defence function

Legumes have developed the ability to fix atmospheric nitrogen by forming symbiotic relationships with endophytic bacteria or fungi (Morillo *et al.*, 2006). Nodule formation involves the peptide ENOD40, but may also involve the plant hormone ethylene (Lindsey *et al.*, 2002). During nodulation, the root cortical cells next to the root xylem poles start to divide. Synthesis of ethylene by the enzyme 1-aminocyclopropane-1-carboxylic acid (ACC) oxidase typically blocks cortical cell divisions and may assist with controlling the position of nodule formation (Lindsey *et al.*, 2002). ENOD40 is found to be expressed in the pericycle cells next to the protoxylem poles prior to the division of cortical cells (Lindsey *et al.*, 2002). This implies a role in counteracting the effects of ethylene and promoting nodule formation (Lindsey *et al.*, 2002). It remains unclear whether ENOD40 functions as an RNA molecule since the peptide form only appears in some plant families (Farroki *et al.*, 2008), but this may also be due to the instability of peptides which are so small (Tavormina *et al.*, 2015). Interestingly, some non-leguminous plants also have the ENOD40 orthologs, suggesting that this gene may have other functional roles (Farroki *et al.*, 2008). Whilst some interactions with micro-organisms are beneficial, plants are also continuously under attack either by herbivores or pathogens which want to feed on it.

Plants synthesize defensins which display diverse activities ranging from inhibiting fungal growth, anti-bacterial activity, inhibition of trypsin and α -amylase and roles in development amongst others (Van der Weerden and Anderson, 2013). Systemin was the first signalling peptide discovered in tomato plants which were being eaten or in response to mechanical damage (Franssen and Bisseling, 2001; Lindsey *et al.*, 2002). At low (femtomolar) concentrations systemin resulted in a mitogen-activated protein (MAP) kinase activation (Lindsey *et al.*, 2002). This led to induction of expression of genes encoding for proteinase-inhibitors such as serine protease inhibitors which interfere with feeding of insects (Franssen and Bisseling, 2001; Lindsey *et al.*, 2002). Systemin can also activate other pathways such as the octadecanoid pathway which produces Jasmonic acid resulting in the transcription of genes involved in defence (Lindsey *et al.*, 2002). These defence genes include activation of secondary metabolism and application of systemin can therefore indirectly lead to the activation of secondary metabolite synthesis through the Jasmonate signalling response. As an example tomato plants which constitutively expressed prosystemin displayed increased Jasmonate synthesis and this was correlated to higher levels of the hydroxycinnamic acid caffeoylputrescine (Chen *et al.*, 2006). This metabolite is suggested to play a putative role in reproductive development and its synthesis in tomato plants was increased by mechanical wounding, feeding of insects or infection by pathogens (Chen *et al.*, 2006). Jasmonate biosynthesis is therefore a prime target for the manipulation of secondary metabolism since

activation of jasmonate signalling pathways can result in the increased biosynthesis of phenylpropanoids, glucosinolates, antioxidants, alkaloids, terpenoids, quinones and also polyamines, (Chen *et al.*, 2006).

One reason why the jasmonate biosynthesis enzymes are not directly targeted for increased metabolite synthesis, is because they appear to be regulated by the availability of their substrates (Chen *et al.*, 2006). Since application or constitutive expression of a signalling peptide such as systemin can result in enhanced or constitutive expression of the jasmonate pathway, this provides an alternative strategy to (indirectly) increase metabolite production. We were therefore interested if TAXIMIN which has properties of a CRP and may play a role in activation of defence mechanisms, could result in a similar effect as systemin.

Can TAXIMIN function as a ‘universal regulator or master switch’ of secondary metabolism?

The cDNA-AFLP data indicated that *TbTAX* expression was co-regulated with genes of the Jasmonate pathway and TAXIMIN appeared to induce activation of the promoters involved in secondary metabolism (Onrubia, 2012). To functionally characterize the TAXIMIN peptide and assess its role in the plant we used the model plant *Arabidopsis thaliana*. Additionally, to determine if this peptide could also result in changes in secondary metabolism in other plants we used the medicinal plant *Sutherlandia frutescens*.

Sutherlandia frutescens, is a legume indigenous to southern Africa. Six *Sutherlandia* species namely, *S. frutescens*, *S. microphylla*, *S. montana*, *S. speciosa*, *S. tomentosa* and *S. humilis* can be found growing in various regions of southern Africa (Mosche *et al.*, 1998; Van Wyk and Albrecht, 2008). Due to the popularity of this herb, numerous types of pharmaceutical products (tablets, gels, tinctures and tea) are also commercially available. Several *in vitro* studies to confirm the efficacy of this herb and to unravel the role of *Sutherlandia* extracts on cancerous cell lines (Chinkwo, 2005; Stander *et al.*, 2009; Vorster *et al.*, 2012; Mqoco *et al.*, 2014) and diabetes (Chadwick *et al.*, 2007; Williams *et al.*, 2013) can be found. Studies have indicated that *Sutherlandia* extracts possess anti-oxidant (Fernandes *et al.*, 2004), anti-bacterial (Katerere and Eloff, 2005), anti-inflammatory (Kundu *et al.*, 2005), anti-mutagenic (Reid *et al.*, 2006) and immune modulating activities (Faleschini *et al.*, 2013) to list a few examples. These biological activities can be ascribed to the presence of several secondary metabolites which are present in these plants.

Chapter 1

Currently, the metabolite data of *Sutherlandia* plants are incomplete. Chemical profiling of *Sutherlandia* extracts indicated the presence of free amino acids (arginine, asparagine) and non-amino acid compounds (L-Canavanine, gamma aminobutyric acid (GABA)), pinitol and secondary metabolites such as sutherlandioside A-D (triperpenoid glycosides; Fig. 4), γ -sitosterol (phytosterols), stigmast-4-en-3-one (steroid/ triterpenoid ketones) and sutherlandin A-D (flavonoids, Fig. 4) (Van Wyk and Albrecht, 2008). At least 56 additional triterpene glycosides were detected in *Sutherlandia* and several more compounds remain to be elucidated (Van Wyk and Albrecht, 2008). GC-MS analysis also revealed the presence of squalene, Vitamin E, β -amyrin and α -amyrin (triterpene) in plant extracts (unpublished). Due to the lack of information on all compounds present, the four metabolites arginine, asparagine, canavanine and GABA were quantified in herbal products for standardization purposes. Since the discovery of sutherlandins and sutherlandiosides these compounds are being developed for this purpose, however commercial standards of these metabolites are still lacking. The level of these compounds in plants and commercial products can be rather low and we were interested if TAXIMIN could affect their synthesis. Legumes such as *Medicago* and *S. frutescens* typically produce secondary metabolites belonging to the (iso)flavonoid (Jaganath and Crozier, 2011) and triterpene saponins (Broeckling *et al.*, 2005). Flavonoids display various pharmacological benefits such as anti-cancer activity or it can reduce the risk of cardiovascular diseases (Schijlen *et al.*, 2004). Consumption of fruits (citrus, berries and apples) and vegetables (onions), legumes (soybean) and tea (Schijlen *et al.*, 2012), which contain high levels of flavonoids are highly beneficial to the health of humans. Terpenoids such as the red pigment lycopene in tomato fruit are also beneficial to human health and these compounds display activity against chronic diseases such as cardiovascular diseases and cancer and they are also used in cosmetic products to protect against skin aging (Putignani *et al.*, 2013). Some of the terpenoids also display antimalarial (artemisinin), anti-microbial and diuretic activity (Aharoni *et al.*, 2005). Great interest exists in manipulation of these two biosynthetic pathways not only to increase secondary metabolite production but also for the identification of the enzymes which are responsible for the synthesis of novel flavonoids and terpenoids in legumes.

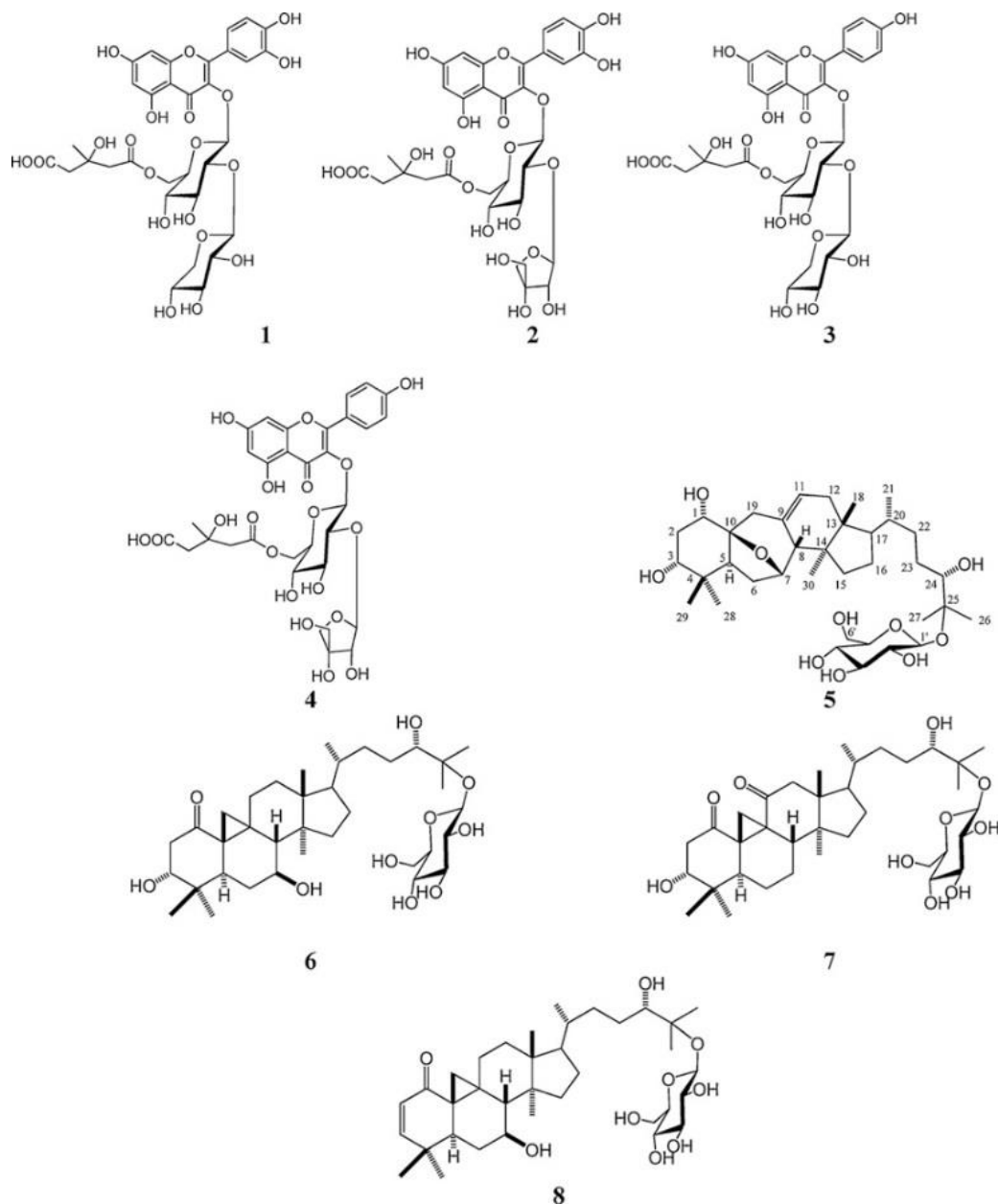


Figure 4. Chemical structure of secondary metabolites in *Sutherlandia frutescens*. The sutherlandin A-D (1-4) flavonoids and sutherlandiosides A-D (5-8) saponins produced by *S. frutescens* is of interest to pharmaceutical companies for their potential health benefiting properties (Figure obtained from Avula *et al.*, 2010).

Flavonoid diversity in plants

Plants synthesize flavonoids for various purposes including to protect against UV light (Broeckling *et al.*, 2005), to defend against pathogens (Lillo *et al.*, 2008) and to attract pollinators or herbivores for seed dispersal (Winkel-Shirley, 2002). Some flavonoids can protect plants against the presence of certain toxic elements (aluminium) in the soil, others

Chapter 1

can play a role in the transport of plant hormones (eg. auxin) (Winkel-Shirley, 2002; Falcone *et al.*, 2012). In some species these compounds play a role in attracting beneficial microorganisms such as rhizobacteria for nodule formation (Falcone *et al.*, 2012). They can also scavenge reactive oxygen species (ROS) and they can influence male fertility or influence pollen germination (Schiljen *et al.*, 2004). Plants synthesize several different types of flavonoids which can be divided into groups such as the flavones (luteolin, apigenin), flavonols (quercetin, kaempferol, myricetin), flavanones (naringenin), aurones and the anthocyanins (cyanidin and pelargonidin) (Schiljen *et al.*, 2004; Putignani *et al.*, 2013). To enable manipulation of flavonoid biosynthesis the enzymes in the pathway have been elucidated.

Flavonoid biosynthesis

The basic flavonoid structure consist of a 15-C skeleton (flavan nucleus) forming two aromatic benzene (6-C) rings (A and B; Fig. 5) which is linked via a heterocyclic pyrane ring (C) (Schiljen *et al.*, 2004). The different classes of flavonoids are distinguished based on their level of oxidation and the pattern of substitution on the C-ring (Kumar and Pandey, 2013). Flavonoid biosynthesis starts with the precursor phenylalanine produced by the shikimate pathway which is located in the chloroplast (Lillo *et al.*, 2008). This pathway is also responsible for the synthesis of aromatic amino acids (phenylalanine, tyrosine and tryptophan) (Tzin and Galili, 2010).

During the first part of this pathway phenylalanine is converted to cinnamate by the enzyme phenylalanine ammonia lyase (PAL) (Fig. 5). Next cinnamate 4-hydroxylase (C4H) converts cinnamate to 4-coumarate by attaching a 4'-OH group. This product is converted to 4-coumaroyl-Coenzyme A (CoA) by 4-coumarate: coenzyme A ligase (4CL) (Davies, 2000). Conversion of phenylalanine to 4-coumaroyl-CoA is known as the phenylpropanoid pathway (Schiljen *et al.*, 2004). This pathway also provides the precursors used for lignin biosynthesis (Lillo *et al.*, 2008). Next, 4-coumaroyl-CoA reacts with three units of malonyl-CoA derived from the malonic acid pathway (Jaganath and Crozier, 2011) and is converted to the yellow coloured 2',4',6',4-tetrahydroxychalcone (naringenin chalcone) by chalcone synthase (CHS) (Davies, 2000). Chalcone isomerase (CI) converts naringenin chalcone to naringenin (flavanone) (Schiljen *et al.*, 2004) which is a common precursor for production of most flavonoids. Flavanone 3-hydroxylase (F3H) converts naringenin to dihydrokaempferol a dihydroflavonols (Schiljen *et al.*, 2004). The flavanone and dihydroflavonols can be converted to flavone and flavonols (kaempferol, quercetin and myricetin) by flavone synthase (FNS) and

flavonol synthase (FLS) respectively (Davies, 2000). Alternatively, the dihydroflavonols can also be reduced at position 4 by dihydroflavonol 4-reductase (DFR) to produce leucoanthocyanidins which can be used for anthocyanidin production. Once produced, the flavanoids are mostly soluble in water and they are stored in the vacuole (Davies, 2000).

The large variety (more than 7000) of flavonoids that exist in nature can be ascribed to enzymes which modify the basic flavonoid structures. These modifications are important as they influence the chemical properties of the molecules and therefore affect the functional role of these compounds. For example flavonoid hydroxylases attach OH groups to the 3' or both 3' and 5'- of the B-ring (Schijlen *et al.*, 2004). This hydroxylation pattern influences the colour properties of the compounds since the addition of OH groups increases the visible absorption maximum for each compound thereby affecting the colour of flowers (Schijlen *et al.*, 2004). A flower containing mainly pelargonidin which has one OH group appears orange, pink or red, whilst cyanidin pigments with two OH groups appear red or magenta. The delphinidin pigments which have three OH groups have a purple or blue appearance (Zucker *et al.*, 2002). However, flower colour is also affected by other factors such as vacuolar pH and metal complexation which contribute to creating the wide diversity of colours (Tanaka *et al.*, 1998). Other modifications of flavonoids include glycosylation by UDP-glucosyl transferase (UGT) which usually adds sugar residues at position 3 of the C-ring (Schijlen *et al.*, 2004), acylation, methylation and sulphation (Davies, 2000). Addition of –OH and sugars also increase the water solubility and is important for storage (Jaganath and Crozier, 2011), whilst addition of methyl and isopentenyl groups makes them more lipophilic (Jaganath and Crozier, 2011). Although many different classes of flavonoids can be produced some flavonoids such as the isoflavonoids are only synthesized by the *Leguminosae* family (Schijlen *et al.*, 2004; Putignani *et al.*, 2013).

Isoflavonoids are produced exclusively in legumes

Production of isoflavonoids by legumes is important for developing symbiotic relationships with *Rhizobium* bacteria as these isoflavonoids can bind to NodD proteins. This induces the expression of nodulation (*nod*) genes of the bacteria to initiate nodule formation in plants (Schijlen *et al.*, 2004; Cooper, 2007). Isoflavonoids differ from the other flavonoids as the B ring is attached to the C3 position of the C ring (Putignani *et al.*, 2013). Isoflavonoid synthesis can start from the precursor naringenin chalcone which is converted to 2',4',4'-trihydroxychalcone (Isoliquiritigenin) by the enzyme Chalcone Reductase (Schijlen *et al.*, 2004).

Chapter 1

Next, Chalcone Isomerase (CHI) converts Isoliquiritigenin to liquiritigenin (Schijlen *et al.*, 2004). A cytochrome P450 enzyme, 2-hydroxyisoflavanone synthase (IFS) can convert Liquiritigenin and Naringenin to the isoflavones daidzein and genistein respectively (Akashi *et al.*, 2003; Schijlen *et al.*, 2004). This step involves migration of the B-ring from C-2 to C-3 and subsequent hydroxylation of the C-2 radical (Akashi *et al.*, 2003) followed by dehydration (Schijlen *et al.*, 2004). Production of daidzein and genistein is used to induce nodule formation by *B. japonicum* and *Rhizobium* sp. NGR234 (Cooper, 2007). Additionally, daidzein can also undergo a further 7-O-methylation by the enzyme daidzein 7-O-methyltransferase (D7OMT) producing isoformononetin (Akashi *et al.*, 2006). Alternatively, the enzyme 2,7,4'-trihydroxyisoflavanone-4'-O-methyl transferase (HI4'OMT) can convert liquiritigenin to 2,7-dihydroxy-4'-methoxyisoflavanone which is further dehydrated to formononetin (7-hydroxy-4'-methoxyisoflavone) (Jaganath and Crozier, 2011). Formononetin is the precursor for the production of the pterocarpan phytoalexins such as medicarpin (alfalfa and liquorice), pisatin (pea) and vestitol (*Lotus japonicas*) (Akashi *et al.*, 2003; 2006). Some of these isoflavonoids such as genistein (Shao *et al.*, 1998) and daidzein (Choi and Kim, 2008) have been found to display *in vitro* anticancer properties. In plants, phytoalexins are involved in defence responses against pathogens and their synthesis is stimulated by biotic and abiotic stress (Jaganath and Crozier, 2011). These biosynthetic pathways may be good targets for increasing the health promoting activity of plants and to make them more resistant against pathogen attack. Although many different types of flavonoids exist, the second group of metabolites, the terpenoids are even more variable.

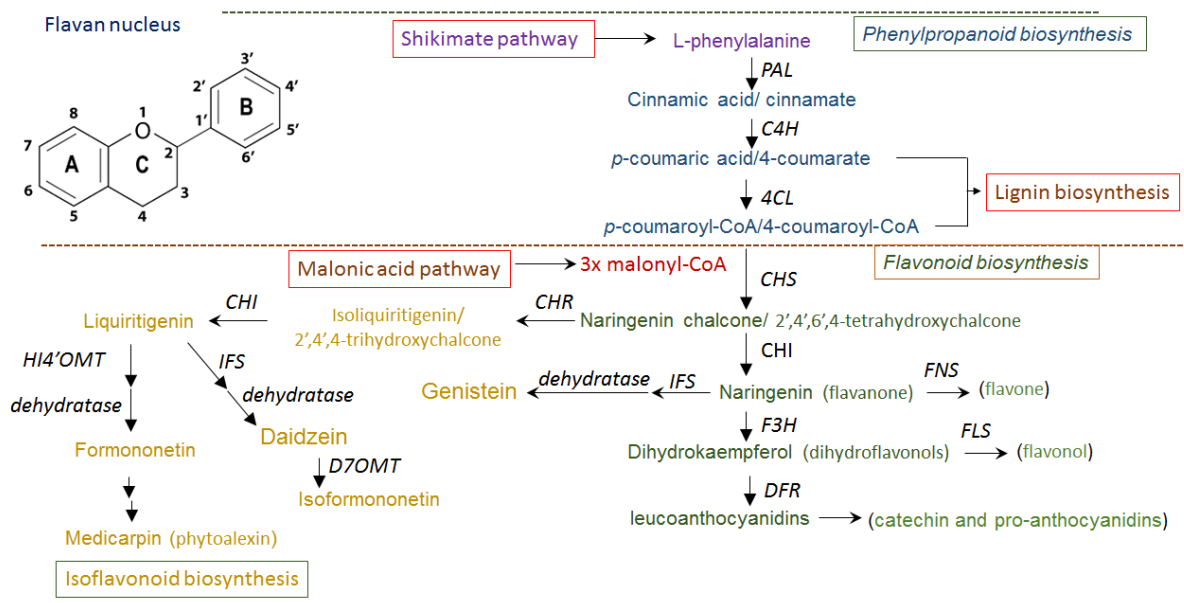


Figure 5. Chemical structure of flavonoid and partial representation of the flavonoid biosynthesis pathway. The Shikimate pathway produces the precursor phenylalanine which is converted to *p*-coumaroyl-CoA during the phenylpropanoid biosynthesis pathway. This provides the precursor for synthesis of different flavonoid groups such as the flavone, flavonol, anthocyanins and in legumes specifically to the production of isoflavonoids. Abbreviations are as follows: *C4H* cinnamate 4-hydroxylase; *4CL* 4-coumarate:coenzyme A ligase; *CHI* chalcone isomerase; *CHR* chalcone reductase *CHS* chalcone synthase; *D7OMT* daidzein 7-O-methyltransferase; *DFR* dihydroflavonol 4-reductase; *F3H* flavanone-3-hydroxylase; *FLS* flavonol synthase; *FNS* flavone synthase; *HI4'OMT* 2,7,4'-trihydroxyisoflavanone-4'-O-methyltransferase; *IFS* isoflavanone synthase; *PAL* phenylalanine ammonium lyase. Structure of flavonoid nucleus was obtained from Lillo *et al.*, (2008). Biosynthesis pathway collated from various sources (Winkel-Shirley, 2002; Akashi *et al.*, 2006; Lillo *et al.*, 2008; Davies, 2010; Jaganath and Crozier, 2011)

Terpenoids diversity in plants

Terpenoids are the largest group of secondary metabolites with more than 30 000 (Ro, 2011) – 50 000 known terpenoids (Mora-Pale *et al.*, 2013). Plants synthesize terpenoids to defend them against predators and to allow for interaction between plants (Aharoni *et al.*, 2005). Terpenoids are synthesized from isoprene (5-C) units and depending on the number of units, they can produce hemiterpenoids (one isoprene unit), monoterpenoids (two isoprene units eg limonene), sesquiterpenoids (three isoprene units), diterpenoids (four isoprene units), sesterterpenoids (five isoprene units), triterpenoids (six isoprene units eg cholesterol), tetraterpenoids (eight isoprene units eg. carotenoids) and polyterpenoids (multiple isoprene units) (Putignani *et al.*, 2013). In plants, terpenoid biosynthesis provides the precursors for

Chapter 1

the synthesis of other compounds such as the phytohormones (gibberellic acid, abscisic acid and cytokines), carotenoids, chlorophylls and plastoquinones and secondary metabolites (Aharoni *et al.*, 2005). Attempts to modify terpenoid biosynthesis in plants have also resulted in elucidation of the enzymes involved in this pathway.

Terpenoid biosynthesis

Terpenoids are synthesized from isopentenyl pyrophosphate (IPP) (Sawai and Saito, 2011) and dimethylallyl pyrophosphate (DMAPP) which is produced by two pathways (Fig. 6) (Augustin *et al.*, 2011). In the cytosolic mevalonate pathway (MVA) they are produced from three acetyl-CoA which are first converted to 3-hydroxy-3-methylglutaryl coenzyme A (HMG CoA). This product is then reduced to mevalonate by 3-hydroxy-3-methylglutaryl coenzyme A reductase (HMGR) which is located in the endoplasmic reticulum (Reddy and Couvreur, 2009). HMGR is a rate limiting step in the MVA pathway (Ro, 2011). Next, mevalonate is phosphorylated and decarboxylated to form IPP. The triterpenoids and sesquiterpenoids are synthesized using precursors from the MVA pathway (Sawai and Saito, 2011). In the second plastidial Methyl Erythritol Phosphate (MEP) pathway, IPP is derived from pyruvate and phosphoglyceraldehyde (Augustin *et al.*, 2011). This pathway mainly results in the production of the monoterpenoids, diterpenoids and tetraterpenoids (Sawai and Saito, 2011). The pathway starts when an IPP unit is linked to the DMAPP allylic isomer resulting in production of the 10-C monoterpene geranyl pyrophosphate (GPP) (Fig. 6) (Augustijn *et al.*, 2011). Addition of a second IPP unit by farnesyl pyrophosphate synthase (FPS) leads to production of 15-C sesquiterpene farnesyl diphosphate (FPP) (Yendo *et al.*, 2010; Augustin *et al.*, 2011). Addition of another IPP to FPP by the enzyme geranyl geranyl pyrophosphate synthetase (GGPPS) produces the 20-C geranyl geranyl diphosphate (GGPP) which is the precursor for the synthesis of the polyterpenes and diterpenes which includes the gibberellins, carotenoids and chlorophyll (Fig. 6).

Alternatively, two FPP molecules are joined by squalene synthase (SS) generating 30-C triterpene squalene (Yendo *et al.*, 2010). Squalene is then oxidized by squalene epoxidase (SEp) to generate 2,3-oxidosqualene which is in turn cyclized. This results in the production of different types of triterpenoid skeletons (Sawai and Saito, 2011) which include the sterols, steroids and saponins (Xu *et al.*, 2004). Cyclization of the 2,3-oxidosqualene by oxidosqualene cyclases (OSC) forms a branch point between the sterol and triterpene saponin pathways (Gholami, 2009). A large number of OSCs exist in plants and contribute to create

a great variety of terpenoids (Sawai and Saito, 2011). The sterol pathway which also leads to the production of the plant growth hormone brassinosteroid, starts with cyclization of 2,3-oxidosqualene by either cycloartenol synthase (CAS) which produces cycloartenol (Gholami *et al.*, 2014) or lanosterol synthase (LAS) which produces lanosterol (Sawai and Saito, 2011). There has been a lot of interest in the production of saponins which can be found in plants belonging to the family *Liliaceae*, *Dioscoreaceae*, *Solanaceae*, *Sapindaceae* and *Agavaceae* (Negi *et al.*, 2013).

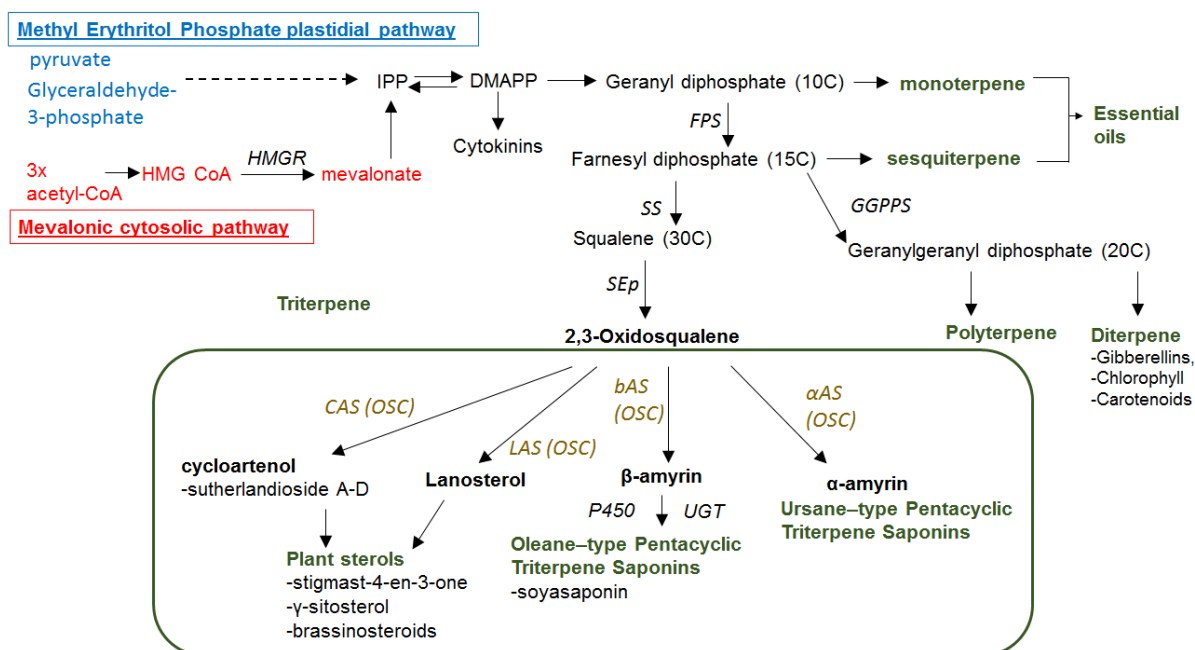


Figure 6. Partial representation of the terpenoid biosynthesis pathway in plants. The precursors IPP and DMAPP are derived from the Methyl Erythritol Phosphate (MEP) and Mevalonate pathway (MEV) and are used for the synthesis of monoterpene, sesquiterpene, polyterpene and diterpenes. The triterpenes consist of production of the plant sterols and the saponins by various Oxidosqualene synthases. Abbreviations are as follow: *aAS* α -amyrin synthase; *bAS* β -amyrin synthase; *CAS* cycloartenol synthase *DMAPP* dimethylallyl diphosphate; *FPP* farnesyl diphosphate; *FPS* farnesyl pyrophosphate synthase; *GPP* geranyl pyrophosphate; *GGPPS* geranyl geranyl pyrophosphate synthase; *HMG CoA* -hydroxy-3-methylglutaryl coenzyme A; *HMGR* 3-hydroxy-3-methylglutaryl coenzyme A reductase; *IPP* isopentenyl diphosphate; *OSC* Oxidosqualene synthase; *P450* cytochrome P450; *SEp* squalene epoxidase; *SS* squalene synthase; *UGT* UDP glucosyl transferase (Figure adapted from Aharoni *et al.*, 2005 and Augustin *et al.*, 2011).

Saponins

Saponins are of great industrial value due to their pharmacological activity which include anti-platelet, anti-HIV, anti-tumor, immunoadjuvant, anti-inflammatory, anti-bacterial, anti-viral, insecticidal, fungicidal, anti-leishmanial and allelopathic properties (Yendo *et al.*, 2010, Augustin *et al.*, 2011). Additionally, saponins can be used for their flavour, foaming, emulsifying and haemolytic properties (Vincken *et al.*, 2007). These triterpenoid saponins are produced when the 2,3-oxidosqualene precursor is converted to β -amyrin by the OSC β -amyrin synthase (bAS) which is converted to a lipid soluble aglycone nucleus known as the sapogenin (Yendo *et al.*, 2010). This non-polar nucleus (Vincken *et al.*, 2007) is attached to a water soluble glycone (sugar) causing them to be amphiphilic (Negi *et al.*, 2013). When in contact with water, saponins form colloidal solutions which allows for foaming (Sparg *et al.*, 2004; Yendo *et al.*, 2010). There are several different saponin skeleton structures eg dammaranes, tirucallanes, lupanes, hopanes, oleananes, taraxasteranes, ursanes, cucurbitanes, cycolartanes, lanostanes and steroids (Vincken *et al.*, 2007). The basic sapogenin structures are modified by addition of small functional groups which include hydroxyl-, keto-, aldehyde- and carboxyl moieties at different positions of the backbone (Augustin *et al.*, 2011). Enzymes of the class cytochrome P450 which are heme-thiolate mono-oxygenases are also involved in the modifications (Augustin *et al.*, 2011). Glycosylations of the saponin backbone by various UDP-glycosyl transferases which involve the addition of monosaccharide moieties (Yendo *et al.*, 2010; Negi *et al.*, 2013) is important for the stability, solubility, biological activity, signalling and storage or transport of these metabolites (Augustin *et al.*, 2011; Sawai and Saito, 2011). Since saponins cause membrane disruption, plants have developed mechanisms to limit the negative effects on cells for example saponins are stored in vacuoles, or are only released by enzymatic activity (Augustin *et al.*, 2011). Saponin biosynthesis and accumulation can also occur tissue specifically and this is influenced by certain regulators (Sawai and Saito, 2011; Gholami *et al.*, 2014). Synthesis of these secondary metabolites are also increased during the defence response and their production is also strongly influenced by several environmental factors (Gholami *et al.*, 2014). At the same time flavonoids can also be produced tissue specifically and its synthesis can also be influenced by plant hormones or in response to environmental factors (Schijlen *et al.*, 2004). Studies on the regulation of flavonoid and terpenoid biosynthesis have revealed some regulatory elements.

Transcriptional regulation of plant secondary metabolism

The production of various secondary metabolites are regulated spatio-temporally by a network of transcription factors (Patra *et al.*, 2013) and production of these compounds can occur in specific tissue or it can be associated with a certain developmental stage (Yang *et al.*, 2012). Various biotic and abiotic factors also influence secondary metabolite production through their effect on expression of the transcription factors regulating these pathways (Patra *et al.*, 2013).

These transcription factors can either bind directly to the promoters of genes to activate or repress their expression or they can form complexes with other proteins to regulate expression (Patra *et al.*, 2013). Several transcription factor families such as MYB, bHLH, AP2/ERF, WRKY, Zinc fingers, DOF and NAC have been identified which can regulate secondary metabolism (Yang *et al.*, 2012). Flavonoid biosynthesis is typically regulated by transcription factors belonging either to the R2R3 MYB, basic-Helix-Loop-Helix (bHLH) families (Schijlen *et al.*, 2004) as well as WD-repeat (WDR) proteins (Patra *et al.*, 2013). In contrast, the transcription factors which regulate terpenoid biosynthesis were not as well known and there has been a lot of effort to elucidate these regulators. Alkaloid and terpenoid biosynthesis is thought to be regulated by two families of transcription factors, the AP2/ERF and WRKY family transcription factors (Patra *et al.*, 2013). For example a WRKY transcription factor has been identified in cotton (*Gossypium arboreum*) which regulates sesquiterpene biosynthesis (Aharoni *et al.*, 2005). Studies using MeJA elicitation in *Taxus sp.* led to the identification of two transcription factors TcWRKY1 in *Taxus chinensis* and TcAP2 in *T. cuspidate* which are involved in terpenoid biosynthesis and their expression is regulated by MeJA (Onrubia *et al.*, 2014).

Experiments have also shown that the various branches/steps of the secondary metabolic pathway can be regulated by different transcription factors (Patra *et al.*, 2013). For example, the OCTADECANOID-DERIVATIVE RESPONSIVE CATHARANTHUS AP2-DOMAIN 2 and 3 (ORCA2 and ORCA3) transcription factors regulate some of the genes for the terpenoid indole alkaloid (TIA) production pathway in *Catharanthus roseus* (Madagascar periwinkle) (De Geyter *et al.*, 2012). However, the ORCA3 transcription factor was found to only regulate a branch of indole alkaloid biosynthesis and recently a novel transcription factor called BIS1 (bHLH Iridoid Synthesis 1) was shown to regulate the pathway upstream of loganic acid methyltransferase (LAMT) in this species (Van Moerkercke *et al.*, 2015).

The expression of some transcription factors can also be induced by Methyl Jasmonate, ethylene and gibberellic acid or by abiotic and biotic stress factors which are important for mounting a defence response (Patra *et al.*, 2015). Some transcription factors are also post-

Chapter 1

translationally regulated by the ubiquitin/26S proteasome system (Patra *et al.*, 2013). The production of certain secondary metabolites are regulated by Jasmonate through the activity of proteins with a Jasmonate ZIM domain (JAZ) and an F-Box protein, CORONATINE INSENSITIVE 1 (COI1)-based SCF^{COI} complex (Patra *et al.*, 2013). These JAZ proteins can interact with some of the transcription factors (bHLH, R2R3 MYB) which prevents them from forming complexes. Upon detection of Jasmonate, the ubiquitin/26S proteasome system targets these JAZ proteins for degradation by the SCF^{COI} complex (Patra *et al.*, 2013). The transcription factors (such as MYC2) are released and can form the necessary complexes to regulate expression of their target genes (Patra *et al.*, 2013). Insight into these regulatory elements or the conditions which influence these pathways would be helpful for construction of these biosynthetic pathways in other organisms towards increasing resistance or for changing the flower colour of ornamentals for example (Schijlen *et al.*, 2004). Since the signalling mechanisms involved in secondary metabolite synthesis are complex and incomplete the application of abiotic and biotic stress which activates these pathways, can assist with elucidation of these mechanisms.

Environmental factors influencing secondary metabolite production

Plants are sessile and therefore they developed several mechanisms to adapt to changes in the environment (eg. abiotic stress) or to fend off other biological organisms (biotic stress induced by eg. predators, herbivores and micro-organisms). These abiotic and biotic stresses induce both primary and secondary metabolite responses which can contribute to the survival of the plant. Metabolite analysis of the flavonoid content of the legume *Lathyrus japonicus* which grows in both coastal and inland regions were performed to assess the impact of geographical and climatic separation on the chemical profile of the plants (Ohtsuki *et al.*, 2013). Extracts displayed changes in the flavonoid glycosylation pattern with flavonols in extracts from inland plants displaying glycosylation at both position 3' and 7'. The flavonoids from extracts prepared from plants growing in the coastal regions were only glycosylated at position 3' (Ohtsuki *et al.*, 2013). Although not investigated in that study, it would have been interesting to determine if changes in gene expression patterns which could account for changes in the modification pattern occurred. This approach could assist with the identification of genes which regulate these pathways or to the discovery of novel genes responsible for performing modifications of these flavonoids. The changes which occur in chemical profile of plants growing in different environmental conditions can also alter the bio-activity of herbal products which are produced from these plants.

In a study investigating extracts which were prepared from *Sutherlandia* plants growing in different geographical locations, these extracts displayed differences in biological activity against cancerous cells (Chinkwo, 2005). Several studies have followed to discern if chemical differences between these populations exists. Both amino acid analysis (Mncwangani and Viljoen, 2012) and secondary metabolite (Albrecht *et al.*, 2012; Acharya *et al.*, 2014) profiling of extracts from different locations indicated that there was intra- and inter- population variation. Populations derived from the Karoo region for example contain the sutherlandioside B (SUB) triterpenoid whilst SUB was not detected in populations from the Gansbaai region (Albrecht *et al.*, 2012). Little information regarding genetic differences or variance in their growth conditions which can cause these observed chemotypic patterns was available. Changes in environmental factors such as temperature, drought, alkalinity, salinity, nutrient deficiency (Ramakrishna and Ravishankar, 2011), light, UV radiation and soil composition (Pavarini *et al.*, 2012) can influence metabolite production.

Therefore to study the impact of different types of stress; a system for the *in vitro* manipulation of the salt-, water- and nutrient content of the *in vitro* growth medium for *S. frutescens* was set up (Colling, 2009). The impact on the production of the four routinely quantified compounds (canavanine, arginine, GABA and asparagine) in *Sutherlandia* shoots was determined. These stress conditions were chosen as plants in coastal regions experience limited water access, high salinity and high light conditions (Ohtsuki *et al.*, 2013). Additionally, the impact of nutrient availability on the growth, development and metabolism of *S. frutescens* shoots were included as these plants are also commercially cultivated and in some instances may receive fertilization. To test nutrient availability, nitrogen supply was chosen as it is one of the important macronutrients required by plants (Taiz and Zeiger, 2010).

Nitrogen metabolism in plants

Briefly indicated in Figure 6, nitrogen metabolism involves uptake of inorganic nitrogen from soil in the form of nitrate (NO_3^-) and ammonium (NH_4^+) (Masclaux-Daubresse *et al.*, 2010). When nitrate is absorbed, it is first converted to nitrite (NO_2^-) which is reduced to ammonium (Masclaux-Daubresse *et al.*, 2010). Ammonium is assimilated by the glutamine synthetase-glutamate synthase (GOGAT) pathway into glutamate to produce glutamine (Serapiglia *et al.*, 2008; Masclaux-Daubresse *et al.*, 2010). This step is important as it prevents ammonium accumulation in the plant (Kováčik and Klejdus, 2014). Glutamine can react with 2-oxoglutarate and produce two molecules of glutamate (Masclaux-Daubresse *et al.*, 2010). Glutamate is used for synthesis of proline, putrescine and GABA and the level of these compounds can increase during various stress conditions (Serapiglia *et al.*, 2008). The

Chapter 1

carbohydrates (sucrose and glucose) which are generated during photosynthesis provide the carbon skeletons which are used during nitrogen metabolism to assimilate ammonium, producing the amino acids (Zheng, 2009). These two pathways (carbon and nitrogen metabolism) are therefore connected and also tightly regulated (Zheng, 2009). During limited nitrogen availability the organic nitrogen-containing metabolites (free amino acids, proteins and polyamines) tend to become limited (Kováčik and Klejdus, 2014). Therefore the metabolism shifts from producing nitrogen based compounds to carbon based compounds (phenolics, phenolic acids, flavonoids, anthocyanins and coumarin) (Kováčik and Klejdus, 2014).

In conditions where plants are provided with high levels of nitrogen, the plants' response depends on the glutamate synthase activity which can be inhibited by excess nitrogen causing an increase of ammonium accumulation (Serapiglia *et al.*, 2008). Ammonium accumulation is problematic as it is toxic to the plant (Kováčik and Klejdus, 2014) and several processes in the plant produce ammonium and contribute to its accumulation. During phenylpropanoid biosynthesis, phenylalanine ammonia-lyase (PAL) converts phenylalanine to trans-cinnamic acid releasing ammonium (Dunn *et al.*, 1998; Kováčik and Klejdus, 2014). It is also produced during photorespiration and the degradation of proteins. To limit the toxic effects, the excess ammonium can be removed by the GOGAT system (Kováčik and Klejdus, 2014) or plants increase the synthesis of the polyamines (putrescine, spermidine, spermine and proline) and the amino acid arginine (Serapiglia *et al.*, 2008). Production of polyamines and amino acids (arginine, proline and asparagine) may also be important during limited nitrogen conditions as they function as nitrogen and carbon storage compounds (Asraf and Bashir, 2003; Serapiglia *et al.*, 2008).

Proline is often produced during stress conditions and it functions to assist with water uptake, restoring osmotic balance and reducing the damage induced by ROS (Iqbal *et al.*, 2015). Proline can be produced from glutamate by two enzymes (Fig. 7). First glutamate is converted to Δ^1 -pyrroline-5-carboxylate (P5C) by the enzyme P5C synthetase (P5CS). Next, P5C reductase (P5CR) converts P5C to proline (Iqbal *et al.*, 2015; Khan *et al.*, 2015). Alternatively, ornithine can also be converted to P5C by the enzyme ornithine Δ -aminotransferase (OAT) which can be used for proline biosynthesis (Verslues and Sharma, 2010; Iqbal *et al.*, 2015). In some instances proline synthesis can also occur from arginine which is first converted to ornithine by the enzyme arginase (Verslues and Sharma, 2010). Although the accumulation of proline is often used as a marker of stress responses in some species, it may not necessarily be a stress tolerance response. In these instances, proline accumulation may be an indication of the damage induced by the accumulation of salts in

plant tissue (Asraf and Foolad, 2007). Increased polyamines synthesis is also a characteristic of plants which are subjected to other stress conditions.

The function of polyamines in the plants' stress response

Polyamines are low molecular weight aliphatic compounds which are cationic in nature at physiological pH. This enables reversible binding to negatively charged molecules such as proteins and chromatin or membrane structures (López-Gómez *et al.*, 2014). Binding to these molecules assists with stabilization of their structure and also influences DNA and RNA synthesis (Pál *et al.*, 2015). Additionally, these compounds can also function to scavenge accumulating ROS to limit damage induced by these oxidative radicals (Bouchereau *et al.*, 1999; Khan *et al.*, 2015). Polyamines can also influence photosynthesis by binding to the photosynthetic complexes to increase photosynthesis during stress (Pál *et al.*, 2015). Due the important role of these compounds in stress responses, the biosynthetic pathway for their production have been elucidated to attempt increasing the tolerance of various plants to abiotic stress conditions.

Elucidating the polyamine biosynthesis pathway

The polyamines of interest are putrescine, spermidine and spermine and their synthesis is also increased during osmotic adjustment which allows plants to lower the osmotic potential of cells to allow for water uptake. During polyamine biosynthesis ornithine is converted to putrescine by the enzymes ornithine decarboxylase (ODC) as indicated in Fig. 7 (Chen *et al.*, 2006; Serapiglia *et al.*, 2008). Putrescine can also be synthesized from arginine which is first converted to agmatine by arginine decarboxylase (ADC) and then two enzymes agmatine iminohydrolase (AIH) and N-carbamoylputrescine aminohydrolase (CPA) converts it to putrescine (Chen *et al.*, 2006). Sequential addition of aminopropyl moieties to the putrescine basic skeleton by two enzymes spermidine synthase (SPDS) and spermine/thermospermine synthases (SPMS/TSPMS) produces spermidine and spermine respectively (Pál *et al.*, 2015). The aminopropyl moieties are obtained from decarboxylated S-adenosylmethionine (S-AdoMet) which is produced from methionine by S-AdoMet synthetase (SAMS). Next, S-AdoMet is decarboxylated to S-adenosyl-5'-3-methyl thiopropylamine (dcSAM) by the enzyme S-adenosylmethionine decarboxylase (SAMDC) (Pál *et al.*, 2015). Synthesis of spermidine and spermine competes with production of the gaseous plant hormone ethylene (Bassard *et al.*, 2010). Production of this hormone is also activated in plants during abiotic stress since it

Chapter 1

plays an important function in salinity tolerance (Iqbal *et al.*, 2015). During ethylene biosynthesis S-adenosyl methionine is converted to 1-aminocyclopropane-1-carboxylic acid (ACC) by the enzyme ACC synthase (Serrano and Martínez-Madrid, 1999). Next ACC oxidase converts ACC to ethylene (Serrano and Martínez-Madrid, 1999). Ethylene production can in turn regulate production of spermidine and putrescine since it can inhibit ADC and SAMDC activity

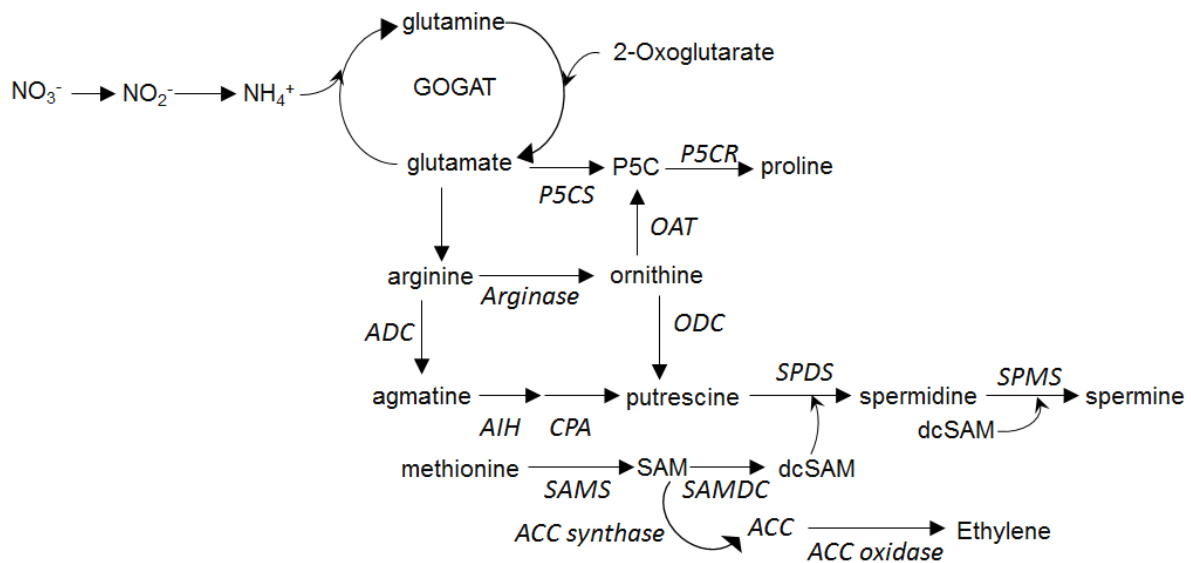


Figure 7. Partial representation of nitrogen metabolism leading to polyamine and ethylene biosynthesis in plants. Nitrate is taken up and converted to glutamate by the GOGAT pathway. Glutamate functions as a precursor for the synthesis of other amino acids which in turn lead to the production of plant hormones such as ethylene and polyamines which are involved in stress responses. Abbreviations are as follows: ACC 1-aminocyclopropane-1-carboxylic acid; ADC arginine decarboxylase; AIH agmatine iminohydrolase; CPA N-carbamoylputrescine aminohydrolase; dcSAM S-adenosyl-5'-3-methylthiopropylamine; OAT ornithine amino transferase; ODC ornithine decarboxylase; P5C Δ 1-pyrroline-5-carboxylate; P5CR P5C reductase; P5CS P5C synthase; SAM S-adenosylmethionine; SAMDC S-adenosylmethionine decarboxylase; SAMS S-adenosylmethionine synthetase; SPDS spermidine synthase; SPMS spermine synthase; SAMDC S-adenosylmethionine decarboxylase (Figure adapted from Chen *et al.*, 2006 and Bassard *et al.*, 2010).

Some of the polyamines are also used for secondary metabolite synthesis for example in some Solanaceae species the polyamines are converted to secondary metabolites such as nicotine or tropane alkaloids (Bassard *et al.*, 2010).

A role for polyamines in secondary metabolite synthesis

Stress can also impact secondary metabolite synthesis and plants may alter their metabolism and divert the production of carbohydrates to the production of secondary metabolites to assist with ROS scavenging (Salem *et al.*, 2014; Gengmao *et al.*, 2015). During this process polyamines can become conjugated with phenolic acids such as coumaric, caffeic and ferulic acid producing phenolamides or hydroxycinnamic acid amides (Bassard *et al.*, 2010). Phenolamides play a role in development and the class of phenolamide produced depends on the species (Bassard *et al.*, 2010). Polyamines therefore play various roles in plants and except for nitrogen stress, polyamine synthesis is also activated during other stress conditions for example low temperature or pH, nutrient imbalances and ionic stress (Serapiglia *et al.*, 2008).

Salinity stress

To study the impact of salinity stress, *Sutherlandia* shoots were cultivated in medium containing different levels of sodium chloride. Application of salt stress however is complex as it causes both water and ionic stress. High levels of salt in the growth medium or soil causes a reduction in the water potential of the medium which can result in a drought effect. The presence of high levels of Na⁺ and Cl⁻ ions in the medium, also results in accumulation of these ions in plant tissue (Gengmao *et al.*, 2015). This causes interference with metabolic reactions such as photosynthesis and result in ion toxicity and increased production of ROS (Taiz and Zeiger, 2010). On the physiological level, plants display a reduction in cell growth, leaf area and biomass accumulation (Rai *et al.*, 2011) due to its effect on photosynthesis (Gengmao *et al.*, 2015). Prolonged exposure to salt can impair Rubisco (ribulose-1,5-bisphosphate carboxylase/oxygenase) enzyme activity (Silva *et al.*, 2010) and cause a reduction in chlorophyll content (Rai *et al.*, 2011).

Plants respond to salt stress in several ways. Salt stress can impact phytohormone production especially abscisic acid (ABA) and ethylene synthesis which play important roles in stress responses (Amjad *et al.*, 2014). Ethylene production can increase proline biosynthesis and activate the antioxidant system to scavenge ROS (Iqbal *et al.*, 2015). ABA is involved in regulation of stomata opening and can reduce water loss by closing stomata (Amjad *et al.*, 2014). To reduce the effects of Na⁺ and Cl⁻ ion accumulation which affects the ion balance (K⁺/Na⁺ ratio), mechanisms such as active extrusion is used to maintain a high K⁺/Na⁺ in the cytosol (Rai *et al.*, 2011). Similar to nitrogen stress plants activate osmotic adjustment (Taiz and Zeiger, 2010) to lower the osmotic potential of cells and allow for water

Chapter 1

uptake (Gengmao *et al.*, 2015; Khan *et al.*, 2015) which also assists with restoring ion homeostasis (Rai *et al.*, 2011). Plants therefore increase synthesis of compatible organic compounds such as sugars/polyols (sucrose, mannitol, trehalose), quaternary amines (glycine betaine, polyamines) and proline which can be detected and quantified in plants.

Metabolite and physiological responses of *in vitro* stressed *S. frutescens* plants

Cultivation of *Sutherlandia* shoots in a medium with reduced or increased nitrogen content affected production of the amino acid content (asparagine, arginine, canavanine). The level of these a/a appeared to be correlated with the amount of available nitrogen in the medium, increasing as the nitrogen level became higher (Colling, 2009). GABA levels were negatively correlated with the nitrogen level, decreasing with increasing nitrogen content (Colling, 2009). Physiological responses of the shoots included higher fresh mass and reduced rooting capacity with increasing nitrogen levels (Colling, 2009). Application of salt stress to *in vitro* *S. frutescens* shoots resulted in increased arginine levels and a reduction in the rooting frequency and shoot length with increasing salt concentration in the medium (Colling, 2009). Changes in certain physiological parameters such as rooting ability can be related to the role of plant hormones which are also involved in various stress responses. In this initial study we only investigated production of four compounds of primary metabolism. To gain a better understanding of these responses, it would be beneficial to expand this study to include a metabolic, transcriptomic and physiological assessment of these responses in this controlled environment.

Rationale for this study

At the beginning of this chapter we discussed the importance of secondary metabolites and described our interest in the manipulation of these biosynthetic pathways to ensure optimal yield and to discover novel regulators of these pathways. Manipulation of these pathways includes the application of stress conditions (biotic or abiotic) which can also result in other metabolic and physiological responses. Elucidation of these stress responses can contribute to our understanding of the ability of plants to adapt to these adverse growth conditions and could indicate why some plants are resistant whilst other plants are tolerant or susceptible to specific stress conditions. We describe how the application of the biotic stress Methyl Jasmonate elicitation resulted in the identification of a cysteine rich novel signalling peptide (TAXIMIN) using cDNA-AFLP analysis of the transcriptome of *Taxus baccata* cell cultures.

Our interest in this peptide is to discover its function using the model plant *Arabidopsis thaliana* and to elucidate whether it can alter the secondary metabolism of the medicinal plant *Sutherlandia frutescens*. This medicinal plant of southern Africa displays *in vitro* anti-proliferating activities which might be related to the presence of certain flavonoids and terpenoids. Studies have been investigating the role of geographical differences on the production of the secondary metabolites in this plant and our studies have investigated the role of water, salt and nitrogen availability or presence on production of some (non)amino acids. Now, our interest has shifted to understand how plants respond to the stress conditions (nitrogen and salt and MeJA elicitation) on the transcriptome level. Since the genome sequence of *S. frutescens* is not available we decided to investigate this through the application of cDNA-AFLP. These approaches were aimed at providing new insights into the growth, development and regulation of secondary metabolism in plants

AIMS of this study

The focus in this study was to first describe the technique cDNA-AFLP (**Chapter 2**) that was used to identify a gene which was differentially expressed after application of an elicitor (MeJA) and could be used to identify novel genes in other species such as *Sutherlandia frutescens* after application of stress conditions.

Secondly, in **Chapter 3-4**, we aimed to functionally characterize the novel signalling peptide TAXIMIN discovered in *T. baccata* using the model plant *Arabidopsis thaliana* using available T-DNA mutant lines and other tools to study the function of these genes.

Next, in **Chapter 5**, we describe the application of cDNA-AFLP towards investigating the differential gene expression in the medicinal plant *S. frutescens* treated with different abiotic (salt and nutrient stress) and biotic (MeJA) stresses towards understanding mechanisms involved in these stress responses. We also describe the induction of hairy roots of *S. frutescens* which constitutively express two TAXIMIN homologs from *Medicago truncatula* towards elucidating the role of TAXIMIN in regulating secondary metabolism in this plant.

In the final chapter, **Chapter 6**, we summarize all the results discussed in the thesis and give an overview of future work and question which arose from this study.

REFERENCES

Aalen RB (2013). Maturing peptides open for communication. *Journal of Experimental Botany* **64**: 5231 – 5235.

Aalen RB, Wildhagen M, Stø IM, Butenko MA (2013). IDA: a peptide ligand regulating cell separation processes in *Arabidopsis*. *Journal of Experimental Botany* **64**: 5253 – 5261.

Acharya D, Enslin G, Chen W, Sandasi M, Mavimbela T, Viljoen A (2014). A chemometric approach to the quality control of *Sutherlandia* (cancer bush). *Biochemical Systematics and Ecology* **56**: 221 – 230.

Aharoni A, Jongsma MA, Bouwmeester HJ (2005). Volatile science? Metabolic engineering of terpenoids in plants. *Trends in Plant Science* **10**: 594 – 602.

Akashi T, Sawada Y, Shimada N, Sakurai N, Aoki T, Ayabe S-I (2003). cDNA Cloning and Biochemical Characterization of S-Adenosyl-L-Methionine:2,7,4-Trihydroxyisoflavanone 4-O-Methyltransferase, a Critical Enzyme of the Legume Isoflavonoid Phytoalexin Pathway. *Plant Cell Physiology* **44**: 103 – 112.

Akashi T, Van Etten HD, Sawada Y, Wasmann CC, Uchiyama H, Ayabe S-I (2006). Catalytic specificity of pea O-methyltransferases suggests gene duplication for (+)-pisatin biosynthesis. *Phytochemistry* **67**: 2525 – 2530.

Alba R, Fei Z, Payton P, Liu Y, Moore SL, Debbie P, Cohn J, D'Ascenzo M, Gordon JS, Rose JKC, Martin G, Tanksley SD, Bouzayen M, Jahn MM, Giovannoni J (2004). ESTs, cDNA microarrays, and gene expression profiling: tools for dissecting plant physiology and development. *The Plant Journal* **39**: 697 – 714.

Albrecht CF, Stander MA, Grobbelaar MC, Colling J, Kossmann J, Hills PN, Makunga NP (2012). LC–MS-based metabolomics assists with quality assessment and traceability of wild and cultivated plants of *Sutherlandia frutescens* (Fabaceae). *South African Journal of Botany* **82**: 33 – 45.

Amjad M, Akhtar J, Anwar-ul-Haq M, Yang A, Akhtar SS, Jacobsen S-E (2014). Integrating role of ethylene and ABA in tomato plants adaptation to salt stress. *Scientia Horticulturae* **172**: 109 – 116.

Angelova Z, Georgiev S, Roos W (2006). Elicitation of plants. *Biotechnology & Biotechnological Equipment* **20**: 72 – 83.

Asraf M, Foolad MR (2007). Roles of glycine betaine and proline in improving plant abiotic stress resistance. *Environmental and Experimental Botany* **59**: 206 – 216.

Augustin JM, Kuzina V, Andersen SB, Bak S (2011). Molecular activities, biosynthesis and evolution of triterpenoid saponins. *Phytochemistry* **72**: 435 – 457.

Avula B, Wang Y-H, Smillie TJ, Fu X, Li XC, Mabusela W, Syce J, Johnson Q, Folk W, Khan IA (2010). Quantitative determination of flavonoids and cycloartenol glycosides from aerial parts of *Sutherlandia frutescens* (L.) R. Br. by using LC-UV/ELSD methods and confirmation by using LC-MS method. *Journal of Pharmaceutical and Biomedical Analysis* **52**: 173 – 180.

Bassard J-E, Ullmann P, Bernier F, Werck-Reichert D (2010). Phenolamides: Bridging polyamines to the phenolic metabolism. *Phytochemistry* **71**: 1808 – 1824.

Bourgaud F, Gravot A, Milesi S, Gontier E (2001). Production of plant secondary metabolites: a historical perspective. *Plant Science* **161**: 839 – 851.

Breyne P, Dreesen R, Cannoot B, Rombaut D, Vandepoele K, Rombauts S, Vanderhaeghe R, Inzé D, Zabeau M (2003). Quantitative cDNA-AFLP analysis for genome-wide expression studies. *Molecular Genetics and Genomics* **269**: 173 – 179.

Broeckling CD, Huhman D, Farag MA, Smith JT, May GD, Mendes P, Dixon RA, Summer LW (2005). Metabolic profiling of *Medicago truncatula* cell cultures reveals the effects of biotic and abiotic elicitors on metabolism. *Journal of Experimental Botany* **56**: 323 – 336

Broekaert WF, Terras FRG, Cammue BPA, Osborn RW (1995). Plant Defensins: Novel antimicrobial peptides as components of the host defense system. *Plant Physiology* **108**: 1353 – 1358.

Butenko MA, Vie AK, Brembu T, Aalen RB, Bones AM (2009). Plant peptides in signalling: looking for new partners. *Trends in Plant Science* **14**: 255 – 263.

Casassola A, Brammer SP, Chave MS, Martinelli JA, Grando MF, Denardin ND (2013). Gene expression: A review on methods for the study of defense-related gene differential expression in Plants. *American Journal of Plant Science* **4**: 64 – 73.

Chadwick WA, Roux S, van de Venter M, Louw J, Oelofsen W (2007). Anti-diabetic effects *Sutherlandia frutescens* in Wistar rats fed a diabetogenic diet. *Journal of Ethnopharmacology* **109**: 121 – 127.

Chen H, Jones AD, Howe GA (2006). Constitutive activation of the jasmonate signalling pathway enhances the production of secondary metabolites in tomato. *FEBS Letters* **580**: 2540 – 2546.

Chini A, Fonseca S, Fernández G, Adie B, Chico JM, Lorenzo O, García-Casado G, López-Vidriero I, Lozano FM, Ponce MR, Micol JL, Solano R (2007). The JAZ family of repressors is the missing link in jasmonate signalling. *Nature* **448**: 666 – 671.

Chinkwo KA (2005). *Sutherlandia frutescens* extracts can induce apoptosis in cultured carcinoma cells. *Journal of Ethnopharmacology* **98**: 163 – 170.

Choi EJ, Kim GH (2008). Daidzein causes cell cycle arrest at the G1 and G2/M phases in human breast cancer MCF-7 and MDA-MB-453 cells. *Phytomedicine* **15**: 683 – 690.

Colling J (2009). Towards understanding the metabolism of *in vitro* *Sutherlandia frutescens* (L.) R. Br. cultures. Stellenbosch University. Faculty of Sciences. <http://scholar.sun.ac.za/handle/10019.1/4601>

Cooper JE (2007). Early interactions between legumes and rhizobia: disclosing complexity in a molecular dialogue. *Journal of Applied Microbiology* **103**: 1355 – 1365.

Czyzewicz N, Yue K, Beeckman T, de Smet I (2013). Message in a bottle: small signalling peptide outputs during growth and development. *Journal of Experimental Botany* **64**: 5281 – 5296.

Dar TA, Uddin M, Khan MMA, Hakeem KR, Jaleel H (2015). Jasmonates counter plant stress: A Review. *Environmental and Experimental Botany* **115**: 49 – 57.

Davies KM (2010). Plant colour and fragrance. In: Verpoorte R, Alfermann AW (eds.). *Metabolic engineering of plant secondary metabolism*. Kluwer academic publishers, Dordrecht, Netherlands, pg. 127 – 145.

De Geyter N, Gholami A, Goormachtig S, Goossens (2012). Transcriptional machineries in jasmonate-elicited plant secondary metabolism. *Trends in Plant Science* **17**: 349 – 359.

De Smet S, Cuypers A, Vangronsveld J, Remans T (2015). Gene Networks involved in hormonal control of root development in *Arabidopsis thaliana*: A framework for studying its disturbance by metal stress. *International journal of Molecular Science* **16**: 19195 – 19224.

Chapter 1

Dong X (1998). SA, JA, ethylene, and disease resistance in plants. *Current Opinion in Plant Biology* **1**: 316 – 323.

Endo S, Betsuyaku S, Fukuda H (2014). Endogenous peptide ligand-receptor systems for diverse signaling networks in plants. *Current Opinion in Plant Biology* **21**: 140 – 146.

Falcone Ferreyra ML, Rius SP, Casati P (2012). Flavonoids: biosynthesis, biological functions, and biotechnological applications. *Frontiers in Plant Science* **28**: 1 – 15.

Faleschini MT, Myer MS, Harding N, Fouchè G (2013). Chemical profiling with cytokine stimulating investigations of *Sutherlandia frutescens* L. R. (Br.) (Fabaceae). *South African Journal of Botany* **85**: 48 – 55.

Farroki N, Whitelegge JP, Brusslan JA (2008). Plant peptides and peptidomics. *Plant Biotechnology Journal* **6**: 105 – 134.

Fernandes AC, Cromarty AD, Albrecht C, van Rensburg CE (2004). The antioxidant potential of *Sutherlandia frutescens*. *Journal of Ethnopharmacology* **95**: 1 – 5.

Fiers M, Ku KL, Liu C-M (2007). CLE peptide ligands and their roles in establishing meristems. *Current Opinion in Plant Biology* **10**: 39 – 43.

Franssen HJ, Bisseling T (2001). Peptide signaling in plants. *Proceedings of the National Academy of Science of the USA* **98**: 12855 – 12856.

Fukuda H, Higashiyama T (2011). Diverse functions of plant peptides: Entering a new phase. *Plant Cell Physiology* **52**: 1 – 4.

Gengmao Z, Yu H, Xing S, Shihui L, Quanmei S, Changhai W (2015). Salinity stress increases secondary metabolites and enzyme activity in safflower. *Industrial Crops and Products* **64**: 175 – 181.

Gholami A (2013). Identification of Potential Regulators of Jasmonate-modulated Secondary Metabolism in *Medicago truncatula*. Ghent University. Faculty of Sciences.

Gholami A, De Geyter N, Pollier J, Goormachtig S, Goossens A (2014). Natural product biosynthesis in *Medicago* species. *Natural Products Report* **31**: 356 – 380.

Han Z, Sun Y, Chai J (2014). Structural insight into the activation of plant receptor kinases. *Current Opinion in Plant Biology* **20**: 55 – 63.

Igarashi D, Tsuda K, Katagiri F (2012). The peptide growth factor, phytosulfokine, attenuates pattern-triggered immunity. *The Plant Journal* **71**: 194 – 204.

Iqbal N, Umar S, Khan NA (2015). Nitrogen availability regulates proline and ethylene production and alleviates salinity stress in mustard (*Brassica juncea*). *Journal of Plant Physiology* **178**: 84 – 91.

Jaganath IB, Crozier A (2011). Flavonoid biosynthesis. In: *Plant Metabolism and Biotechnology*. Ashihara H, Crozier A, Komamine A (eds.). John Wiley & Sons, Ltd. West Sussex, United Kingdom pg. 293 – 320.

Katerere DR, Eloff JN (2005). Antibacterial and antioxidant activity of *Sutherlandia frutescens* (Fabaceae), a reputed anti-HIV/AIDS phytomedicine. *Phytotherapy Research* **19**: 779 – 781.

Katsir L, Davies KA, Bergmann DC, Laux T (2011). Peptide signaling in plant development. *Current Biology* **21**: R356 – R364.

Khan MS, Ahmad D, Khan MA (2015). Utilization of genes encoding osmoprotectants in transgenic plants for enhanced abiotic stress tolerance. *Electronic Journal of Biotechnology* **18**: 257 – 266.

Kok EJ, Franssen-van Hal NLW, Winnubst LNW, Kramer EHM, Dijksma WTP, Kuiper HA, Keijer J (2007). Assessment of representational difference analysis (RDA) to construct informative cDNA microarrays for gene expression analysis of species with limited transcriptome information, using red and green tomatoes as a model. *Journal of Plant Physiology* **164**: 337 – 349.

Kováčik J, Klejdus B (2014). Induction of phenolic metabolites and physiological changes in chamomile plants in relation to nitrogen nutrition. *Food Chemistry* **142**: 334 – 341.

Kumar S, Pandey AK (2013). Chemistry and biological activities of flavonoids: An overview. *The Scientific World Journal* **2013**: 1 – 17.

Kumpf RP, Shi C-L, Larrieu A, Stø IM, Butenko MA, Péret B, Riiser ES, Bennett MJ, Aalen RB (2013). Floral organ abscission peptide IDA and its HAE/HSL2 receptors control cell separation during lateral root emergence. *Proceedings of the National Academy of Science of the USA* **110**: 5235 – 5240.

Kundu JK, Mossanda KS, Na HK, Surh YJ (2005). Inhibitory effects of the extracts of *Sutherlandia frutescens* (L.) R. Br. and *Harpagophytum procumbens* DC. On phorbol ester-induced COX-2 expression in mouse skin: AP-1 and CREB as potential upstream targets. *Cancer Letters* **31**: 21 – 31.

Lambert E, Faizal A, Geelen D (2011). Modulation of triterpene saponin production: *In vitro* cultures, elicitation and metabolic engineering. *Applied Biochemistry and Biotechnology* **164**: 220 – 237.

Lease KA, Walker JC (2006). The *Arabidopsis* unannotated secreted peptide database, a resource for plant peptidomics. *Plant Physiology* **142**: 831 – 838.

Li J, Chory J (1999). Brassinosteroid actions in plants. *Journal of Experimental Botany* **50**: 275 – 282.

Lillo C, Lea US, Ruoff P (2008). Nutrient depletion as a key factor for manipulating gene expression and product formation in different branches of the flavonoid pathway. *Plant Cell and Environment* **31**: 587 – 601.

Lindsey K, Casson S, Chilley P (2002). Peptides: new signalling molecules in plants. *Trends in Plant Science* **7**: 78 – 83.

López-Gómez M, Cobos-Porras L, Hidalgo-Castellanos J, Lluch C (2014). Occurrence of polyamines in root nodules of *Phaseolus vulgaris* in symbiosis with *Rhizobium tropici* in response to salt stress. *Phytochemistry* **107**: 32 – 41.

Malik S, Cusidó RM, Mirjalili MH, Moyano E, Palazón J, Bonfill M (2011). Production of the anticancer drug taxol in *Taxus baccata* suspension cultures: A review. *Process Biochemistry* **46**: 23 – 34.

Marmioli N, Maestri E (2014). Plant peptides in defense and signaling. *Peptides* **56**: 30 – 44.

Marshall E, Costa LM, Gutierrez-Marcos J (2011). Cysteine-rich peptides (CRPs) mediate diverse aspects of cell-cell communication in plant reproduction and development. *Journal of Experimental Botany* **52**: 1677 – 1686.

- Masclaux-Daubresse C, Daniel-Vedele F, Dechorgnat J, Chardon F, Gaufichon L, Suzuki A** (2010). Nitrogen uptake, assimilation and remobilization in plants: challenges for sustainable and productive agriculture. *Annals of Botany* **105**: 1141 – 1157.
- Matsubayashi Y** (2011). Post-translational modifications in secreted peptide hormones in plants. *Plant and Cell Physiology* **52**: 5 – 13.
- Matsubayashi Y** (2012). Recent progress in research on small post-translationally modified peptide signals in plants. *Genes to Cells* **17**: 1 – 10.
- Matsubayashi Y** (2014). Post translationally modified small-peptide signals in plants. *Annual Review of Plant Biology* **65**: 385 – 413.
- Mncwangi NP, Viljoen AM** (2012). Qualitative variation of amino acids in *Sutherlandia frutescens* (Cancer bush) – towards setting parameters for quality control. *South African Journal of Botany* **82**: 46 – 52.
- Mora-Pale M, Sanchez-Rodriguez SP, Linhardt RJ, Dordick JS, Koffas MAG** (2013). Metabolic engineering and *in vitro* biosynthesis of phytochemicals and non-natural analogues. *Plant Science* **210**: 10 – 24.
- Morillo SA, Tax FE** (2006). Functional analysis of receptor-like kinases in monocots and dicots. *Current Opinion in Plant Biology* **9**: 460 – 469.
- Mqoco TV, Visagie MH, Albrecht C, Joubert AM** (2014). Differential cellular interaction of *Sutherlandia frutescens* extracts on tumorigenic and non-tumorigenic breast cells. *South African Journal of Botany* **90**: 59 – 67.
- Murphy E, Smith S, De Smet I** (2012). Small signalling peptides in *Arabidopsis* development: How cells communicate over a short distance. *The Plant Cell* **24**: 3198 – 3217.
- Murphy E, de Smet I** (2014). Understanding the RALF family: a tale of many species. *Trends in Plant Science* **19**: 664 – 671.
- Narváez-Vásquez J, Ryan CA** (2004). The cellular localization of prosystemin: a functional role for phloem parenchyma in systemic wound signalling. *Planta* **218**: 360 – 369.
- Negi JS, Negi PS, Pant GJ, Rawat MSM, Negi SK** (2013). Naturally occurring saponins: *Chemistry and Biology* **1**: 001 – 006.
- Ohtsuki T, Murai Y, Iwashina T, Setoguchi H** (2013). Geographical differentiation inferred from flavonoid content between coastal and freshwater populations of the coastal plant *Lathyrus japonicus* (Fabaceae). *Biochemical Systematics and Ecology* **51**: 243 – 250.
- Oksman-Caldentey K-M, Inzé D** (2004). Plant cell factories in the post-genomic era: new ways to produce designer secondary metabolites. *Trends in Plant Science* **9**: 1360 – 1385.
- Okuda S, Tsutsui H, Shiina K, Sprunck S, Takeuchi H, Yui R, Kasahara RD, Hamamura Y, Mizukami A, Susaki D, Kawano N, Sakakibara T, Namiki S, Itoh k, Otsuka K, Matsuzaki M, Nozaki H, Kuroiwa T, Nakano A, Kanaoka MM, Dresselhaus T, Sasaki N, Higashiyama T** (2009). Defensin-like polypeptide LUREs are pollen tube attractants secreted from synergid cells. *Nature* **458**: 357 – 362.
- Onrubia Ibáñez M** (2012). A Molecular approach to Taxol Biosynthesis. PhD thesis. Universitat Pompeu Fabra. Department of Experimental and Health Sciences. <http://www.tesisenred.net/bitstream/handle/10803/83344/tmoi.pdf?sequence=1>

Onrubia M, Pollier J, Van den Bossche R, Goethals M, Gevaert K, Moyano E, Vidal-Limon H, Cusidó RM, Palazón J, Goossens A (2014). Taximin, a conserved plant-specific peptide is involved in the modulation of plant-specialized metabolism. *Plant Biotechnology Journal* **12**: 971 – 983.

Patra B, Schluttenhofer C, Wu Y, Pattanaik S, Yuan L (2013). Transcriptional regulation of secondary metabolite biosynthesis in plants. *Biochimica et Biophysica Acta (BBA) – Gene Regulatory Mechanisms* **1829**: 1236 – 1247.

Pál M, Szalai G, Janda T (2015). Speculation: Polyamines are important in abiotic stress signaling. *Plant Science* **237**: 16 – 23.

Pauwels P, Inzé D, Goossens A (2009). Jasmonate-inducible gene: what does it mean? *Trends in Plant Science* **14**: 87 – 91.

Pavarini DP, Pavarini SP, Niehues M, Lopes NP (2012). Exogenous influences on plant secondary metabolite levels. *Animal Feed Science and Technology* **176**: 5 – 16.

Petersen TN, Brunak S, von Heijne G, Nielsen H (2011). SignalP 4.0: discriminating signal peptides from transmembrane regions. *Nature Methods* **8**: 785 – 786.

Putignani L, Massa O, Alisi A (2013). Engineered *Escherichia coli* as new source of flavonoids and terpenoids. *Food Research International* **54**: 1084 – 1095.

Rai MK, Kalia RK, Singh R, Gangola MP, Dhawan AK (2011). Developing stress tolerant plants through *in vitro* selection – An overview of the recent progress. *Environmental and Experimental Botany* **71**: 89 – 98.

Ramakrishna A, Ravishankar GA (2011). Influence of abiotic stress signals on secondary metabolites in plants. *Plant Signaling & Behavior* **6**: 1720 – 1731.

Ramirez-Estrada K, Osuda L, Moyano E, Bonfill M, Tapia N, Cusido RM, Palazon J (2015). Changes in gene transcription and taxane production in elicited cell cultures of *Taxus x media* and *Taxus globosa*. *Phytochemistry* **117**: 174 – 184.

Reddy LH, Couvreur P (2009). Squalene: A natural triterpene for use in disease management and therapy. *Advanced Drug Delivery Reviews* **61**: 1412 – 1426.

Reid KA, Maes J, van Staden J, De Kimpe N, Mulholland DA, Verschaeve L (2006). Evaluation of the mutagenic and antimutagenic effects of South African plants. *Journal of Ethnopharmacology* **106**: 44 – 50.

Ro D-K (2011). Terpenoid biosynthesis. In: Ashihara H, Crozier A, Komamine A (eds.). *Plant Metabolism and Biotechnology*. John Wiley & Sons, Ltd. West Sussex, United Kingdom. pp. 217 – 240.

Salem N, Msaada K, Dhifi W, Limam F, Marzouk B (2014). Effect of salinity on plant growth and biological activities of *Carthamus tinctorius* L. extracts at two flowering stages. *Acta Physiologiae Plantarum* **36**: 433 – 445.

Sawai S, Saito K (2011). Triterpenoid biosynthesis and engineering in plants. *Frontiers in Plant Science* **2**: 1 – 8.

Schijlen EGWM, de Vos CHR, van Tunen AJ, Bovy AG (2004). Modification of flavonoid biosynthesis in crop plants. *Phytochemistry* **65**: 2631 – 2648.

Chapter 1

Serapiglia MJ, Minocha R, Minocha SC (2008). Changes in polyamines, inorganic ions and glutamine synthetase activity in response to nitrogen availability and form in red spruce (*Picea rubens*). *Tree Physiology* **28**: 1793 – 1803.

Serrano M, Martínez-Madrid MC (1999). Ethylene biosynthesis and polyamine and ABA levels in cut carnations treated with Aminotriazole. *Journal of the American Society for Horticultural Science* **124**: 81 – 85.

Shao Z-M, Wu J, Shen Z-Z, Barsky SH (1998). Genistein exerts multiple suppressive effects on human breast carcinoma cells. *Cancer Research* **58**: 4851 – 4857.

Shiu S-H, Bleecker AB (2001). Receptor-like kinases from *Arabidopsis* form a monophyletic gene family related to animal receptor kinases. *Proceedings of the National Academy of Science of the USA* **98**: 10763 – 10768.

Silva EN, Ribeiro RV, Ferreira-Silva SL, Viégas RA, Silveira JAG (2010). Comparative effects of salinity and water stress on photosynthesis, water relations and growth of *Jatropha curcas* plants. *Journal of Arid Environments* **74**: 1130 – 1137.

Silverstein KAT, Moskal WA Jr, Wu HC, Underwood BA, Graham MA, Town CD, VandenBosch KA (2007). Small cysteine-rich peptides resembling antimicrobial peptides have been under-predicted in plants. *The Plant Journal* **51**: 262 – 280.

Somssich M, Simon R (2012). Peptides regulating apical meristem development. In: Irving HR, Gehring C (eds.). *Plant signaling peptides*. Springer-Verlag, Heidelberg, Berlin, pg. 25 – 40.

Sparg SG, Light ME, van Staden J (2004). Biological activities and distribution of plant saponins. *Journal of Ethnopharmacology* **94**: 219 – 243.

Sun J-Q, Jiang H-L, Li C-Y (2011). Systemin/Jasmonate-mediated systemic defense signalling in Tomato. *Molecular Plant* **4**: 607 – 615.

Tabata R, Sawa S (2014). Maturation processes and structures of small secreted peptides in plants. *Frontiers in Plant Science* **5**: 1 – 6.

Taiz L, Zeiger E (2010). *Plant physiology* 5th edition. Sinauer Associates Inc. Massachusetts, USA. pg109, 114.

Takayama S, Sakagami Y (2002). Peptide signaling in plants. *Current Opinion in Plant Biology* **5**: 382 – 387.

Tanaka Y, Tsuda S, Kusumi T (1998). Metabolic engineering to modify flower color. *Plant Cell Physiology* **39**: 1119 – 1126.

Tavormina P, De Coninck B, Nikonorova N, De Smet I, Cammue BPA (2015). The plant peptidome: An expanding repertoire of structural features and biological functions. *The Plant Cell* **8**: 2095 – 2118.

Tichtinsky G, Vanoosthuysse V, Cock JM, Gaude T (2003). Making inroads into plant receptor kinase signalling pathways. *Trends in Plant Science* **8**: 231 – 237.

Torii KU (2012). Leucine-rich repeat receptor kinases in plants: Structure, function and signal transduction pathways. *International Review of Cytology* **234**: 1 – 46.

Tzin V, Galili G (2010). New insights into the Shikimate and aromatic amino acids biosynthesis pathways in Plants. *Molecular Plant* **3**: 956 – 972.

- Van der Weerden NL, Anderson MA** (2013). Plant defensins: Common fold, multiple functions. *Fungal Biology Reviews* **26**: 121 – 131.
- Van Moerkercke A, Steensma P, Schweizer F, Pollier J, Gariboldi I, Payne R, Vanden Bossche R, Miettinen K, Espoz J, Purnama PC, Kellner F, Seppänen-Laakso T, O'Connor SE, Rischer H, Memelink J** (2015). The bHLH transcription factor BIS1 controls the iridoid branch of the monoterpene indole alkaloid pathway in *Catharanthus roseus*. *Proceedings of the National Academy of Sciences of the United States of America* **112**: 8130 – 8135.
- Van Wyk B-E, Albrecht C** (2008). A review of the taxonomy, ethnobotany, chemistry and pharmacology of *Sutherlandia frutescens* (Fabaceae). *Journal of Ethnopharmacology* **119**: 620 – 629.
- Verslues PE, Sharma S** (2010). Proline metabolism and its implications for plant-environment interaction. *The Arabidopsis Book* **8**: e0140.
- Vincken J-P, Heng L, de Groot A, Gruppen H** (2007). Saponins, classification and occurrence in the plant kingdom. *Phytochemistry* **68**: 275 – 297.
- Vorster C, Stander A, Joubert A** (2012). Differential signalling involved in *Sutherlandia frutescens*-induced cell death in MCF-7 and MCF-12A cells. *Journal of Ethnopharmacology* **140**: 123 – 130.
- Walker JC, Lease KA** (2010). The leucine-rich repeat receptor protein kinases of *Arabidopsis thaliana* – a Paradigm for plant LRR receptors. In: Bradshaw RA, Dennis EA, (eds.). *Handbook of Cell Signaling* 2nd edition, Academic Press, USA, pg. 601 – 608.
- Wang Z, Gerstein M, Snyder M** (2009). RNA-Seq: a revolutionary tool for transcriptomics. *Nature Reviews Genetics* **10**: 57 – 63.
- Wheeler JI, Irving HR** (2012). Plant peptide signaling: An evolutionary adaptation. In: Irving HR, Gehring C (eds.). *Plant signaling peptides*. Springer-Verlag, Heidelberg, Berlin, pg. 1 – 19.
- Williams S, Roux S, Koekemoer T, van de Venter M, Dealtry G** (2013). *Sutherlandia frutescens* prevents changes in diabetes-related gene expression in a fructose-induced insulin resistant cell model. *Journal of Ethnopharmacology* **146**: 482 – 489.
- Winkel-Shirley B** (2002). Biosynthesis of flavonoids and effects of stress. *Current Opinion in Plant Biology* **5**: 218 – 223.
- Xu R, Faxio GC, Matsuda SPT** (2004). On the origins of triterpenoid skeletal diversity. *Phytochemistry* **65**: 261 – 291.
- Yang C-Q, Fang X, Wu X-M, Mao Y-B, Wang L-J** (2012). Transcriptional regulation of plant secondary metabolism. *Journal of Integrative Plant Biology* **54**: 703 – 712.
- Yendo ACA, de Costa F, Gosmann G, Fett-Neto AG** (2010). Production of plant bioactive triterpenoid saponins elicitation strategies and target genes to improve yields. *Molecular Biotechnology* **46**: 94 – 104.
- Zheng Z-L** (2009). Carbon and nitrogen nutrient balance signalling in plants. *Plant Signaling & Behavior* **4**: 584 – 591.
- Zuker A, Tzfira T, Ben-Meir H, Ovadis M, Shklarman E, Itzhaki H, Forkmann G, Martens S, Neta-Sharir I, Weiss D, Vainstein A** (2002). Modification of flower color and fragrance by antisense suppression of the flavanone 3-hydroxylase gene. *Molecular Breeding* **9**: 33 – 41.

Chapter 2

cDNA-AFLP-based transcript profiling for genome-wide expression analysis of jasmonate-treated plants and plant cultures

Manuscript: “cDNA-AFLP--based transcript profiling for genome-wide expression analysis of jasmonate-treated plants and plant cultures”

Janine Colling^{1,2,3*}, Jacob Pollier^{1,2}, Nokwanda P. Makunga^{3,4} and Alain Goossens^{1,2}

¹Department of Plant Systems Biology, Flanders Institute for Biotechnology (VIB), Technologiepark 927, B-9052 Gent, Belgium

²Department of Plant Biotechnology and Bioinformatics, Ghent University, Technologiepark 927, B-9052 Gent, Belgium

³Institute for Plant Biotechnology, Department of Genetics, Stellenbosch University, Stellenbosch, 7602, South Africa

⁴Department of Botany and Zoology, Stellenbosch University, Stellenbosch, 7602, South Africa

In: Jasmonate Signalling. Methods in Molecular Biology. Springer, New York.

***Author contributions:** writing of the manuscript.

SUMMARY

cDNA-AFLP is a commonly used, robust, and reproducible tool for genome-wide expression analysis in any species, without requirement of prior sequence knowledge. Quantitative expression data are generated by gel-based visualization of cDNA-AFLP fingerprints obtained by selective PCR amplification of subsets of restriction fragments from a double-stranded cDNA template. Differences in gene expression levels across the samples are reflected in different band intensities on the high-resolution polyacrylamide gels. The differentially expressed genes can be identified by direct sequencing of re-amplified cDNA-AFLP tags purified from the gels. The cDNA-AFLP technique is especially useful for profiling of transcriptional responses of jasmonate-treated plants or plant (tissue) cultures and the discovery of jasmonate-responsive genes.

Key Words: cDNA-AFLP, transcript profiling, jasmonate, gene expression, transcriptome, elicitation

1. INTRODUCTION

Amplified Fragment Length Polymorphism (AFLP) is a robust and reliable DNA-fingerprinting technique based on the polymerase chain reaction (PCR) amplification of restriction fragments of genomic DNA (Vos *et al.*, 1995, Zabeau *et al.*, 1993). Practically, the AFLP protocol can be divided into three distinct steps: (i) digestion of the DNA template with two restriction enzymes, followed by ligation of specific oligonucleotide adapters to the sticky ends of the digested DNA; (ii) selective PCR amplification of a subset of the restriction fragments by means of AFLP primers with a few extra selective nucleotides besides the adapter and restriction site-specific sequences; and (iii) visualization of the amplified DNA fragments on high-resolution polyacrylamide gels (Vos *et al.*, 1995).

The cDNA-AFLP technique is derived from the AFLP protocol and has become a widely used, robust, and reproducible tool for genome-wide expression analysis in any organism, without the need for prior sequence knowledge (Breyne *et al.*, 2003, Pollier *et al.*, 2011, Vuylsteke *et al.*, 2007). Similar to AFLP, the original cDNA-AFLP method (Bachem *et al.*, 1996) starts with a DNA template (double-stranded cDNA) that is digested with two restriction enzymes. After ligation of adapters to the restriction fragments, a subset of the restriction fragments is amplified by selective PCR. Finally, the amplified fragments are visualized on high-resolution polyacrylamide gels, with fragment intensities reflecting the relative abundance (copy number) of the corresponding genes across the samples (Bachem

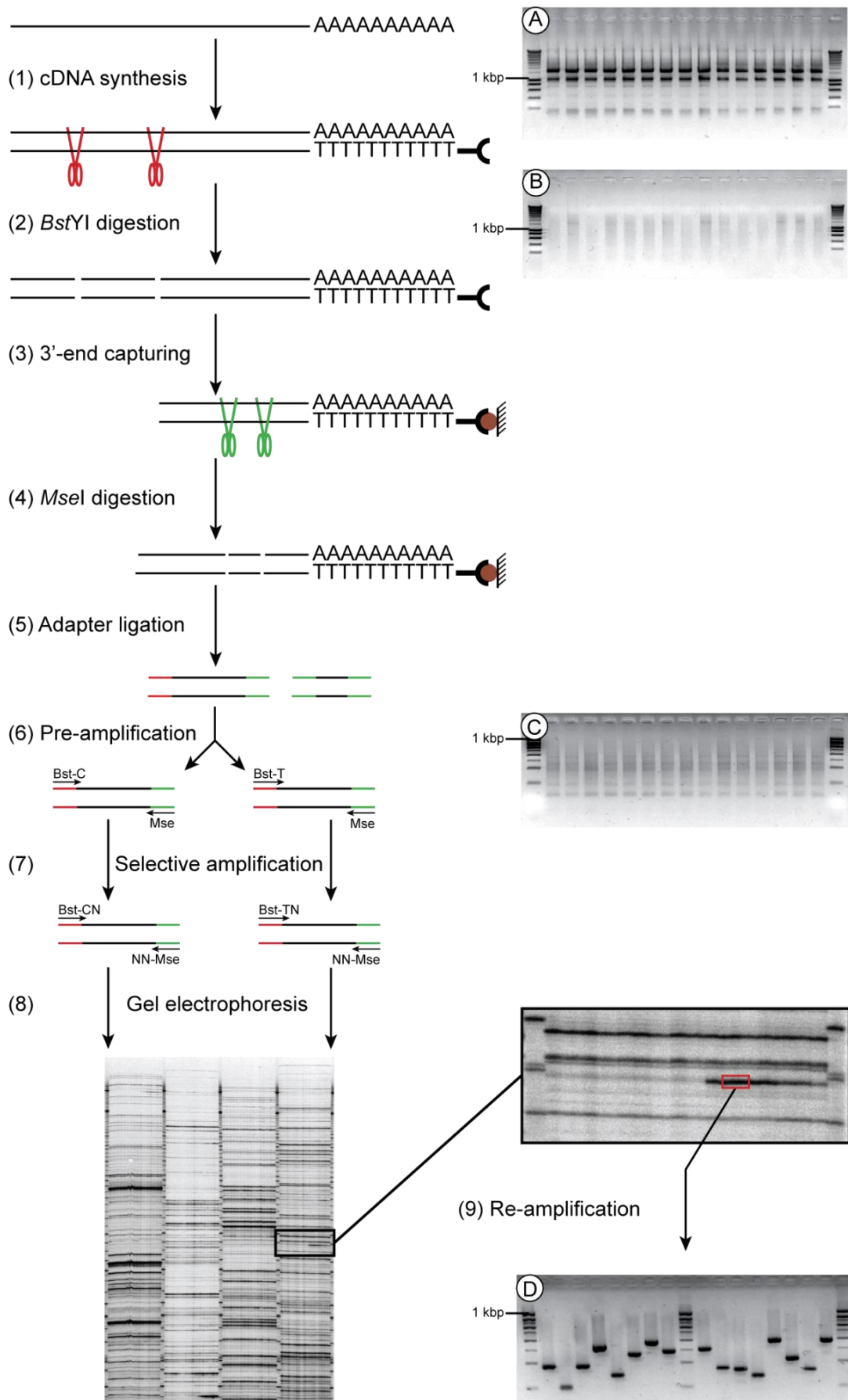
et al., 1996). To identify the differentially expressed genes, the corresponding cDNA-AFLP tags are purified from the polyacrylamide gel, re-amplified and sequenced.

Since its development, several modifications of the original cDNA-AFLP protocol have been published (Bachem *et al.*, 1998, Breyne and Zabeau, 2001, Breyne *et al.*, 2003, Vuylsteke *et al.*, 2007). Here, we focus on the one-gene-one-tag variant of the original cDNA-AFLP method (Breyne and Zabeau, 2001, Breyne *et al.*, 2003, Vuylsteke *et al.*, 2007). In contrast to the original method, in which multiple sequence tags can be obtained for a single gene (one-gene-multiple-tag), the one-gene-one-tag method includes the selection of the 3' end restriction fragments of the transcripts prior to the selective PCR amplification, leading to a single diagnostic sequence tag per transcript (Vuylsteke *et al.*, 2007). This significantly reduces the total number of tags to be screened and, hence, the workload, but might lead to reduced transcriptome coverage or in sequence tags that do not cover the coding sequence, thereby hindering the functional annotation of the fragments (Breyne *et al.*, 2003, Vuylsteke *et al.*, 2007). In addition, the one-gene-one-tag variant makes use of the *Bst*YI/*Mse*I restriction enzyme combination, instead of a combination of two tetracutters in the original cDNA-AFLP protocol. This results in a higher average fragment length that facilitates the functional annotation of the transcripts and the full-length cDNA cloning (Vuylsteke *et al.*, 2007) (see Fig. 1). This method has proven successful for transcriptome analysis of several jasmonate-elicited medicinal plant species (Goossens *et al.*, 2003, Pollier *et al.*, 2011, Rischer *et al.*, 2006). It is also useful to carry out pilot studies in model species, such as *Arabidopsis thaliana*, to screen large sample sets (e.g. time series) for the most relevant samples for full-transcriptome analysis by other methods, such as microarray analysis or RNA-sequencing (Pauwels *et al.*, 2008).

Figure 1. Overview of the cDNA-AFLP procedure.

The left panel shows the different steps in the procedure that include (1) synthesis of double-stranded cDNA from an RNA template with a biotinylated oligo-dT primer; (2) digestion of the cDNA with the restriction enzyme *Bst*YI; (3) 3' end capturing of the digested cDNA by binding of the biotin to streptavidin-coated beads to isolate a single-sequence tag per transcript; (4) digestion of the captured cDNA fragments with the restriction enzyme *Mse*I; (5) ligation of specific *Bst*YI and *Mse*I adapters to the sticky ends of the digested DNA; (6) preamplification with the *Bst*YI + C or *Bst*YI + T primer in combination with the *Mse*I primer to reduce the complexity of the template mixture; (7) selective amplification of a subset of the transcript fragments by using *Bst*YI and *Mse*I primers with a few extra selective nucleotides; (8) visualization of the amplified DNA fragments on high-resolution polyacrylamide gels; and (9) purification, re-amplification, and sequencing of DNA fragments for identification of the differentially expressed genes. The right panel gives examples of good-quality RNA (a), cDNA (b), preamplifications (c), and re-amplification of 16 cDNA-AFLP tags (d)

Chapter 2



2. MATERIALS

2.1. Equipment

1. Magnetic stirrer.
2. Microwave oven.
3. Autoclave.
4. Dynabeads M-2800 Streptavidin (Invitrogen, Carlsbad, CA, USA).
4. Magnetic stands for isolation of Dynabeads (Invitrogen).
5. Power supply (PowerPac 3000; Bio-Rad Laboratories, Hercules, CA, USA).
6. Vacuum gel drier GD-1 (Heto-Holten Lab Equipments, Allerød, Denmark).
7. PhosphorImager scanning instrument and imaging plates (GE-Healthcare, Little Chalfont, UK).
8. Kodak BioMax MR film, 35 × 43 cm (Sigma-Aldrich, St. Louis, MO, USA).
9. Water repellent (Rain-X; Shell Car Care International Ltd., Manchester, UK).
11. Sequi-Gen GT electrophoresis system (38 × 50 cm) (Bio-Rad Laboratories).
10. Whatman pure cellulose blotting paper (3MM Chr, 35 × 43 cm) (GE-Healthcare).
11. Adhesive PCR foil seals (ABgene Ltd., Epsom, UK).
12. Nanodrop.

2.2. Buffers, media, solutions and reagents

Use ultrapure water (resistivity of 18 MΩ cm at 25°C) and analytical grade reagents to prepare all solutions. Prepare and store all reagents at room temperature, unless stated otherwise. Products and buffers may be used for multiple steps in the protocol, but will only be described the first time they are needed.

2.2.1. Double-stranded cDNA synthesis

1. Diethylpyrocarbonate (DEPC)-treated water: Add 100 µL of DEPC to 100 mL of water and incubate for at least 1 h at 37°C. Autoclave for at least 15 min to decompose the remaining traces of DEPC.
2. SuperScript™ II Reverse Transcriptase, supplied with 5× first-strand buffer and 100 mM dithiothreitol (DTT) (Invitrogen).
3. 10 mM dNTP mix.
4. Biotin-labeled oligo-dT25 primer (see Note 1).
5. *Escherichia coli* DNA Ligase, supplied with 10× *E. coli* DNA Ligase reaction buffer.
6. DNA Polymerase I.

Chapter 2

7. Ribonuclease H (RNase H).
8. cDNA purification kit.
9. 0.5 M ethylenediaminetetraacetic acid (EDTA) (pH 8.0): Add 18.61 g of EDTA to 80 mL of water and mix with a magnetic stirrer. Add NaOH pellets to adjust the pH to 8.0. Make up with water to 100 mL and autoclave (see Note 2).
10. 10× TAE buffer: Dissolve 48.4 g of Tris in 500 mL of water. Add 11.44 mL of acetic acid (glacial) and 20 mL of 0.5 M EDTA (pH 8.0). Make up to 1 L with water.
11. 1.2% (w/v) agarose gel: Add 3.6 g of agarose to 300 mL of 0.5× TAE buffer (see Note 3). Heat the solution to boiling in a microwave to dissolve the agarose. Cool the solution to approximately 60°C and add a nucleic acid stain to allow visualization of the DNA after electrophoresis. Pour the gel solution in a casting tray containing a sample comb and allow the gel to harden at room temperature. The remaining gel solution can be stored for up to 1 month at 60°C.

2.2.2. PCR template preparation

1. 1 M tris(hydroxymethyl)aminomethane-acetic acid (Tris–HAc) (pH 7.5): Dissolve 12.1 g of Tris in approximately 80 mL of water. Mix well and adjust the pH to 7.5 with acetic acid. Make up to 100 mL with water and autoclave.
2. 1 M magnesium acetate (MgAc): Dissolve 2.145 g of MgAc tetrahydrate in water. Make up to 10 mL with water and filter sterilize.
3. 4 M potassium acetate (KAc): Dissolve 3.926 g of KAc in water. Make up to 10 mL with water and filter sterilize. Store at -20°C.
4. 1 M Tris–HCl (pH 8.0): Dissolve 12.1 g of Tris in approximately 80 mL of water. Mix well and adjust the pH to 8.0 with hydrochloric acid. Make up to 100 mL with water and autoclave.
5. 5 M sodium chloride (NaCl): Dissolve 29.22 g of NaCl in approximately 80 mL of water. Make up to 100 mL with water and autoclave.
6. 10× RL buffer: Mix 1 mL of 1 M Tris–HAc, pH 7.5 with 1 mL of 1 M MgAc, 1.25 mL of 4 M KAc, and 10 µL of 50 mg/mL bovine serum albumin. Add 0.077 g of DTT and make up to 10 mL with water. Store in 1-mL aliquots at -20°C (see Note 4).
7. 2× STEX buffer: Mix 40 mL of 5 M NaCl with 2 mL of Tris–HCl, (pH 8.0), 400 µL of 0.5 M EDTA (pH 8.0), and 2 mL of Triton X-100. Make up to 100 mL with water.
8. T₁₀E_{0.1} buffer: Add 1 mL of 1 M Tris–HCl (pH 8.0) and 20 µL of 0.5 M EDTA (pH 8.0) to 80 mL of water. Make up to 100 mL with water and autoclave.
9. 10 mM ATP solution.
10. T4 DNA Ligase (Invitrogen).

2.2.3. Pre-amplification and re-amplification

1. AmpliTaq DNA polymerase, supplied with 10× PCR buffer and 25 mM MgCl₂ solution (Applied Biosystems, Foster City, CA, USA).
2. SilverStar™ DNA polymerase, supplied with 10× PCR buffer and 50 mM MgCl₂ solution (Eurogentec, Seraing, Belgium).

2.2.4. Selective amplification

1. 1 M Tris–HCl (pH 7.5): Dissolve 12.1 g of Tris in approximately 80 mL of water. Mix well and adjust the pH to 7.5 with hydrochloric acid. Make up to 100 mL with water and autoclave.
2. 1 M MgCl₂: Dissolve 2.033 g of magnesium chloride hexahydrate in water. Make up to 10 mL with water.
3. 10× T4 buffer: Mix 2.5 mL of 1 M Tris–HCl, pH 7.5 with 1 mL of 1 M MgCl₂. Add 0.077 g of DTT and 0.013 g of spermidine trihydrochloride. Make up to 10 mL with water. Store in 1-mL aliquots at -20°C (see Note 4).
4. T4 Polynucleotide Kinase (New England BioLabs).
5. ATP, [γ -³³P] 3000 Ci/mmol (Perkin Elmer, Waltham, MA, USA).
6. AmpliTaq Gold DNA polymerase, supplied with 10× PCR buffer and 25 mM MgCl₂ solution (Applied Biosystems, Foster City, CA, USA).
7. Formamide loading dye: in a 50-mL Falcon tube, mix 49 mL of formamide with 1 mL of 0.5 M EDTA (pH 8.0) and add 0.03 g of bromophenol blue and 0.03 g of xylene cyanol. Store this solution at 4°C.

2.2.5. SequaMark™ 10 base ladder

1. SequaMark™ DNA template (Research Genetics, Huntsville, AL, USA).
2. PCR cleanup kit.
3. Vent_R™ (exo-) DNA polymerase, supplied with 10× ThermoPol reaction buffer (New England Biolabs).
4. dNTP/ddTTP mix: Mix 0.6 μ L of 10 mM dATP, 2 μ L of 10 mM dCTP, 2 μ L of 10 mM dGTP, 0.66 μ L of 10 mM dTTP, and 14.4 μ L of 10 mM ddTTP. Make up to 200 μ L with water.

2.2.6. Gel electrophoresis and detection

1. 10× Maxam buffer: Dissolve 121 g of Tris and 61.8 g of boric acid in water and make up to 1 L with water.
2. 4.5% (w/v) denaturing polyacrylamide gel solution: Add 450 g of urea and 112.5 mL of acrylamide/bis-acrylamide (19:1, 40% stock solution) to a 2 L beaker. Add water to 700

Chapter 2

mL and stir for 1 h while heating at 60°C. When the urea is dissolved, add 100 mL of 10× Maxam buffer and 4 mL of 0.5 M EDTA, (pH 8.0). Filter the resulting solution through a 0.45-µm filter with a vacuum pump, and make up to 1 L with water. Store the gel solution at 4°C in the dark for up to 1 month.

3. 10% ammonium persulfate (APS): dissolve 1 g of APS in water and add up to 10 mL with water. Store this solution at 4°C in the dark for up to 1 month.
4. *N,N,N',N'*-Tetramethylethylenediamine (TEMED). Store this product at 4°C in the dark.
5. Sodium acetate (NaAc).

2.3. Restriction enzymes and primers

2.3.1. PCR template preparation

1. *Bst*YI restriction enzyme (New England BioLabs, Ipswich, MA, USA).
2. *Mse*I restriction enzyme (New England Biolabs).
3. Oligonucleotide *Mse*I-Forward: 5'-GACGATGAGTCCTGAG-3'.
4. Oligonucleotide *Mse*I-Reverse: 5'-TACTCAGGACTCAT-3'.
5. Oligonucleotide *Bst*YI-Forward: 5'-CTCGTAGACTGCGTAGT-3'.
6. Oligonucleotide *Bst*YI-Reverse: 5'-GATCACTACGCAGTCTAC-3'.
7. *Bst*YI adapter (5 µM): Add 5 µL *Bst*YI-Forward (100 µM) and 5 µL *Bst*YI-Reverse (100 µM) to 90 µL of water.
8. *Mse*I adapter (50 µM): Mix 50 µL *Mse*I-Forward (100 µM) and 50 µL *Mse*I-Reverse (100 µM).

2.3.2. Pre-amplification, selective amplification, SequaMark 10 base ladder and re-amplification

1. Pre-amplification primers: *Bst*YI-T+0 or *Bst*YI-C+0 primer (5'-GACTGCGTAGTGATC(C/T)-3') and *Mse*I+0 primer (5'-GATGAGTCCTGAGTAA-3').
2. Selective amplification primers: *Bst*YI-T/C+N primers (5'-GACTGCGTAGTGATC(C/T)N-3') and *Mse*I+NN primers (5'-GATGAGTCCTGAGTAANN-3'). N represents the selective nucleotides.
3. SequaMark™ primers: Forward: 5'-ACCAGAAGCTGGACGCAG-3'; Reverse: 5'-ACACAGGAAACAGCTATGACCA-3'.
4. Re-amplification primers: Forward 1: 5'-AAAAGCAGGCTGACTGCGTAGTG-3'; Reverse 1: 5'-AGAAAGCTGGGTGATGAGTCCTGA-3'; Forward 2: 5'-GGGACAAGTTTGTACAAAAAAGCAGGCT-3'; Reverse 2: 5'-GGGACCACTTTGTACAAGAAAGCTGGGT-3'.

3. METHODS

3.1. *Double-stranded cDNA synthesis*

1. For each sample, dilute 2 µg of total RNA into a total volume of 20 µL using DEPC-treated water (see Note 5).
2. For the first-strand cDNA synthesis mix, combine 8 µL of 5× first-strand buffer, 4 µL of DEPC-treated water, 4 µL of 100 mM DTT, 2 µL of 10 mM dNTP mix, 1 µL of biotin-labeled oligo-dT25 primer (700 ng/µL), and 1 µL of SuperScript™ II Reverse Transcriptase (200 U/µL) for each sample.
3. Add 20 µL of the first-strand cDNA synthesis mix to each sample.
4. Mix well and incubate for 2 h at 42°C.
5. For the second-strand cDNA synthesis mix, combine 87.4 µL of water, 16 µL of 10× *E. coli* DNA Ligase reaction buffer, 6 µL of 100 mM DTT, 3 µL of 10 mM dNTP mix, 5.0 µL of DNA Polymerase I (10 U/µL), 1.5 µL of *E. coli* DNA Ligase (10 U/µL), and 1.1 µL RNase H (1.5 U/µL) for each sample.
6. Add 120 µL of the second-strand cDNA synthesis mix to the 40 µL of the first-strand reaction cocktail.
7. Mix well and incubate for 1 h at 12°C, followed by 1 h at 22°C.
8. Purify the double-stranded cDNA with a cDNA purification kit according to the manufacturer's instructions. Elute the cDNA in 30 µL of elution buffer.
9. Run 8 µL of each cDNA sample on a 1.2% agarose gel in 0.5× TAE running buffer at 100 V for 15-20 min (see Note 6 and Fig. 1B).

3.2. *PCR template preparation*

This section describes the first digestion, 3'-end capturing, second digestion and adapter ligation.

1. Prepare the first digestion mix by mixing 15 µL of water, 4 µL of 10× RL buffer, and 1 µL of *Bst*YI restriction enzyme (10 U/µL) for each sample.
2. Add 20 µL of the first digestion mix to 20 µL of each cDNA sample.
3. Incubate for 2 h at 60°C (see Note 7).
4. For each sample, wash 10 µL Dynabeads with 100 µL 2× STEX. Resuspend the Dynabeads in a final volume of 40 µL 2× STEX per sample (see Note 8).
5. Mix 40 µL of the resuspended Dynabeads with each digested cDNA sample to give a final volume of 80 µL.
6. Incubate the samples for 30 min at room temperature, with gentle agitation (1,000 rpm) to ensure the beads remain suspended.
7. Collect the beads with the magnet and remove the supernatants.

Chapter 2

8. Remove the tubes from the magnet.
9. Add 100 μL 1 \times STEX and resuspend the beads (see Note 9).
10. Transfer the resuspended beads to a fresh tube.
11. Repeat steps 7-10 four additional times.
12. Collect the beads with the magnet and remove the supernatants.
13. Remove the tubes from the magnet.
14. Add 30 μL of T₁₀E_{0.1} buffer and resuspend the beads.
15. Transfer the resuspended beads to a fresh tube.
16. Prepare the second digestion mix by mixing 5 μL of water, 4 μL of 10 \times RL buffer, and 1 μL of *MseI* restriction enzyme (10 U/ μL) for each sample.
17. Add 10 μL of the second digestion mix to the 30 μL of resuspended beads.
18. Incubate for 2 h at 37°C with gentle agitation (1000 rpm) to ensure the beads remain suspended.
19. Collect the beads with the magnet.
20. Transfer the supernatant containing the released fragments to a new tube.
21. Prepare the adapter ligation mix by mixing 4 μL of water, 1 μL of *Bst*YI adapter (5 μM), 1 μL of *MseI* adapter (50 μM), 1 μL of 10 mM ATP, 1 μL of 10 \times RL buffer, 1 μL of T4 DNA Ligase (1 U/ μL), and 1 μL of *Bst*YI restriction enzyme (10 U/ μL) for each sample.
22. Add 10 μL of the adapter ligation mix to the 40 μL of supernatant.
23. Incubate for 3 h at 37°C (see Note 10).
24. After adapter ligation, dilute the samples two fold by adding 50 μL of T₁₀E_{0.1} buffer to each sample (see Note 11).

3.3. Preamplification

1. Prepare the preamplification mix by mixing 30.8 μL of water, 5.0 μL of 10 \times PCR buffer, 5.0 μL of 25 mM MgCl₂, 1.5 μL of *Bst*YI-T/C+0 primer (50 ng/ μL), 1.5 μL of *MseI*+0 primer (50 ng/ μL), 1.0 μL of 10 mM dNTP mix, and 0.2 μL of AmpliTaq DNA polymerase (5 U/ μL) for each sample (see Note 12).
2. Add 45 μL of the preamplification mix to 5 μL of the PCR template.
3. Subject the samples to the following PCR program: initial denaturation for 1 min at 94°C, followed by 25 cycles of denaturation at 94°C for 30 s, annealing at 56°C for 1 min and elongation at 72°C for 1 min.
4. Analyze 10 μL of the PCR reaction on a 1.2% agarose gel in 0.5 \times TAE running buffer at 100 V for 15-20 min (see Note 13 and Fig. 1C).
5. Dilute the preamplification mix 600-fold with T₁₀E_{0.1} buffer (see Note 14).

3.5. Selective amplification

1. Prepare the primer radiolabeling mix by mixing 0.23 μL of water, 0.10 μL of *Bst*YI-T/C+N primer (50 ng/ μL), 0.10 μL of γ -³³P-ATP (3000 Ci/mmol), 0.05 μL of 10 \times T4 buffer, and 0.02 μL of T4 Polynucleotide Kinase (10 U/ μL) for each sample.
2. Incubate the reaction mixture at 37°C for 45 min.
3. Stop the reaction by incubating the mixture for 10 min at 80°C.
4. Prepare the selective amplification mix by mixing 6.0 μL of *Mse*I+NN primer (5 ng/ μL), 3.9 μL of water, 2.0 μL of 10 \times PCR buffer, 2.0 μL of 25 mM MgCl₂, 0.5 μL of γ -³³P-labeled *Bst*YI-T/C+N primer, 0.4 μL of 10 mM dNTP mix, and 0.2 μL of AmpliTaq Gold DNA polymerase (5 U/ μL) for each sample.
5. Add 15 μL of the selective amplification mix to 5 μL of the diluted preamplification mixture.
6. Subject the samples to the following PCR program: initial denaturation for 10 min at 94°C, followed by 13 cycles touchdown (denaturation at 94°C for 30 s, annealing for 30 s at an initial temperature of 65°C, reduced with 0.7°C per PCR cycle, elongation at 72°C for 1 min) and 23 additional cycles of denaturation at 94°C for 30 s, annealing at 56°C for 30 s and elongation at 72°C for 1 min.
7. Add 20 μL of formamide loading dye to each sample.
8. Incubate the samples overnight at -20°C (see Note 15).

3.6. Preparation of the SequaMark™ 10 base ladder

1. Prepare the SequaMark™ PCR mix by mixing 33.8 μL of water, 5 μL of 10 \times PCR buffer, 3 μL of 25 mM MgCl₂, 2.5 μL of 10 μM F-primer, 2.5 μL of 10 μM R-primer, 2 μL of SequaMark™ DNA template, 1 μL of 10 mM dNTP mix, and 0.2 μL of AmpliTaq DNA polymerase (5 U/ μL).
2. Subject the PCR mix to the following PCR program: 30 cycles of denaturation at 95°C for 30 s, annealing at 56°C for 30 s and elongation at 72°C for 1 min.
3. Clean the PCR reaction with a PCR cleanup kit according to the manufacturer's instructions.
4. Quantify the product on a nanodrop (see Note 16).
5. Prepare the SequaMark™ primer radiolabeling mix by mixing 0.23 μL of water, 0.1 μL of 10 μM F-primer primer, 0.1 μL of γ -³³P-ATP (3000 Ci/mmol), 0.05 μL of 10 \times T4 buffer, and 0.02 μL of T4 Polynucleotide Kinase (10 U/ μL).
6. Incubate the reaction mixture at 37°C for 45 min.
7. Stop the reaction by incubating the mixture for 10 min at 80°C.

Chapter 2

8. Prepare the radioactive SequaMark™ PCR mix by mixing 24 µL of dNTP/ddTTP mix, 14.5 µL of water, 5 µL of 10× ThermoPol reaction buffer, 2.5 µL of labeled Forward primer, 2.5 µL Vent_R™ (exo-) DNA polymerase (2 U/µL), and 1.5 µL (self-amplified) template.
9. Subject the samples to the following PCR program: initial denaturation for 5 min at 94°C, 25 cycles of denaturation at 94°C for 30 s, annealing at 56°C for 30 s, and elongation at 72°C for 1 min, followed by a final elongation step at 72°C for 7 min.
10. Add 50 µL of formamide loading dye to the PCR reaction.
11. Mix carefully and close the tubes.
12. Keep the mixture overnight at -20°C (see Note 15).

3.6. Gel electrophoresis and detection

1. Clean the glass plate and buffer tank with water and soap (see Note 17).
2. Clean the surface of the glass plate twice with ethanol and once with acetone.
3. Treat the surface of the buffer tank with Rain-X (see Note 18).
4. Assemble the gel system.
5. Prepare the gel solution by adding 500 µL of 10% APS and 100 µL of TEMED to 100 mL of 4.5% (w/v) denaturing polyacrylamide gel solution. Mix gently.
6. Immediately cast the gel by injecting the gel solution into the gel system and insert the sharktooth comb between the two glass plates with the teeth upwards. Align the holes in the comb with the edge of the glass plate of the buffer tank, and fix the comb with clamps. During this process, carefully avoid introducing air bubbles, because they will damage the front and disturb the gel image.
7. Allow the gel to polymerize for at least 1 h before use (see Note 19).
8. Prepare the running buffer by diluting 200 mL of 10× Maxam to 2 L with water.
9. Add 8 mL of 0.5 M EDTA (pH 8.0) to the 2 L of 1× Maxam.
10. Dissolve 8.8 g of NaAc in 400 mL of the prepared buffer and pour the resulting solution in the lower buffer tank (see Note 20).
11. Warm the remaining 1,600 mL of buffer to 50–55°C (6–7 min at 1,000 W in the microwave oven).
12. Fill the upper buffer tank with the warm buffer.
13. Prerun the gel for 15 min at 100 W to heat up the gel to approximately 50–55°C.
14. During the prerun, denature the samples and the SequaMark™ 10 base ladder at 95°C for 5 min.
15. After the prerun, remove the comb and clean the front with a 50-mL syringe containing the running buffer to remove all gel pieces and bubbles from the well.

cDNA-AFLP-based transcript profiling for genome-wide expression analysis

16. Insert the sharktooth comb into the well with the teeth approximately 0.5 mm into the gel (see Note 21).
17. Load 3 μL of the PCR product (or ladder) per well for a comb of 72 teeth (see Note 22).
18. Once all samples are loaded, perform the electrophoresis at a constant power of 100 W for approximately 2 h 45 min or until the dye front reaches the bottom of the gel.
19. After electrophoresis, discard the running buffer and disassemble the gel system.
20. Carefully lift the buffer tank and transfer the gel to a blotting paper.
21. Cover the gel with Saran wrap and dry at 75°C on a vacuum drier for at least 1 h.
22. To visualize the results, place the dried gel on a phosphorimager screen for 12-16 h or on an X-ray film for 2-3 days (see Note 23).

3.7. Re-amplifications

1. Place the developed X-ray film back on the gel and align correctly (see Note 23).
2. Cut the fragments of interest from the gel with a razor blade and transfer the gel pieces to Eppendorf tubes.
3. Add 100 μL of T₁₀E_{0.1} buffer to the gel pieces and crush the pieces to a fine pulp (see Note 24).
4. Incubate the samples for 1 h at room temperature to allow complete resuspension of the DNA.
5. Centrifuge for 5 min at 11,000 $\times g$ to separate the blotting paper from the DNA solution. Use the resulting supernatant as template for the re-amplification PCR.
6. Prepare the PCR 1 master mix by mixing 34.8 μL of water, 5.0 μL of 10 \times PCR buffer, 2.0 μL of 50 mM MgCl₂, 1.0 μL of Forward 1 primer (10 μM), 1.0 μL of Reverse 1 primer (10 μM), 1.0 μL of 10 mM dNTP mix, and 0.2 μL of Silverstar Taq DNA polymerase (5 U/ μL) for each sample.
7. Transfer 45 μL of the reaction mixture to 5 μL of the resuspended DNA templates.
8. Subject the samples to the following PCR program: initial denaturation for 1 min at 95°C, followed by 10 cycles of denaturation at 95°C for 30 s, annealing at 54°C for 30 s, and elongation at 72°C for 1 min. Perform a final elongation at 72°C for 2 min.
9. Prepare the PCR 2 master mix solution by mixing 28.7 μL of water, 4.0 μL of 10 \times PCR buffer, 2.0 μL of 50 mM MgCl₂, 2.4 μL of Forward 2 primer (10 μM), 1.7 μL of Reverse 2 primer (10 μM), 1.0 μL of 10 mM dNTP mix, and 0.2 μL of Silverstar Taq DNA polymerase (5 U/ μL) for each sample.
10. Transfer 40 μL of the mix to 10 μL of the first PCR reaction and mix well.
11. Subject the samples to the following PCR program: initial denaturation for 1 min at 95°C, followed by 5 cycles of denaturation at 95°C for 30 s, annealing at 45°C for 30 s and elongation at 72°C for 1 min. This is followed by 20 cycles of denaturation at 95°C

Chapter 2

for 30 s, annealing at 55°C for 30 s, and elongation at 72°C for 1 min and a final elongation step at 72°C for 2 min.

12. Analyze 5 μ L of the PCR 2 reaction on a 1.2% agarose gel in 0.5 \times TAE running buffer at 100 V for 20-25 min (see Note 25 and Fig. 1D).
13. Use the obtained re-amplified fragments for sequencing, either by direct sequencing of the PCR products, or after cloning of the fragments into a plasmid vector (see Note 26).

4. NOTES

1. The biotin-labeled oligo-dT25 primer is an oligo-dT primer consisting of a string of 25 deoxythymidine nucleotides. The primer is labeled at its 5' end with biotin. Use DEPC-treated water to dissolve the lyophilized primer, and store the resuspended primer at -20°C.
2. EDTA will not go into solution until the pH approaches 8.0. Addition of NaOH pellets will allow the EDTA to dissolve.
3. To prepare the 0.5 \times TAE buffer, dilute 50 mL of 10 \times TAE buffer to 1 L with water.
4. Because DTT may precipitate, incubate the buffer briefly at 37°C to dissolve all DTT prior to use.
5. For cDNA-AFLP analysis, it is essential to have similar quantities of pure and intact RNA for all the samples during the preparation of the total RNA. The integrity of the RNA can be determined by checking an aliquot of the RNA sample on a 1.2% agarose gel. For any eukaryotic sample, intact total RNA will show two clear bands, the 28S and 18S rRNA bands, with the intensity of the 28S band about twice that of the 18S band (see Fig. 1A). The occurrence of a low-molecular weight smear is indicative of degraded RNA. The purity of the RNA can be assessed spectrophotometrically by determining the absorbance of the samples at 230 nm (A_{230}), 260 nm (A_{260}), and 280 nm (A_{280}). The A_{260}/A_{280} ratio is indicative of the purity of the sample and should be between 1.80 and 2.00. A lower value implies contamination of the RNA sample with proteins or phenolics. The A_{260}/A_{230} ratio is a second measure of RNA purity and should be above 2.00. Lower values indicate contaminants, such as phenolics, carbohydrates and/or EDTA.
6. The cDNA should appear as a 0.1-4 kbp smear on the gel. The purified cDNA is stable and can be stored for up to 1 year at -20°C.
7. After 1 h of incubation, briefly centrifuge the tubes because water evaporates from the mixture and condensates in the tube lids.

cDNA-AFLP-based transcript profiling for genome-wide expression analysis

8. Thoroughly resuspend the Dynabeads before the washing step by pipetting until a uniform brown suspension is obtained. Wash the Dynabeads for maximum 7–8 samples in one tube.
9. The STEX buffer contains the detergent Triton X-100. Care should be taken to avoid the production of foam while washing or resuspending the Dynabeads.
10. Alternatively, the second digestion and adapter ligation can be performed simultaneously by adding the second digestion and adapter ligation mixes at the same time to the 30 μ L of resuspended beads. Incubate for 4 h at 37°C, collect the beads with the magnet, transfer the supernatant to a new tube, and proceed with step 24 of Section 3.2.
11. The diluted samples will serve as template for the preamplifications and can be stored for several years at -20°C.
12. For the preamplifications, run two separate PCRs. For the first PCR, use the *Bst*YI-C+0 primer and for the second the *Bst*YI-T+0 primer, or *vice versa*.
13. The preamplification should appear as a 50-500 bp smear on the gel.
14. To avoid large pipetting errors, prepare the 600-fold dilution in two steps. First, make a 20-fold dilution of the PCR product, and subsequently make a 30-fold dilution of the diluted PCR product. If the preamplification product on the gel has a low intensity, prepare a less diluted template for the selective amplifications (for instance, a 100-fold dilution).
15. Keeping the samples at -20°C improves the quality of the gel image after polyacrylamide gel electrophoresis.
16. The template should have a concentration of 30 ng/ μ L. To this end, several tubes with PCR product should be combined before the PCR cleanup.
17. All equipment (glass plate, buffer tank, sharktooth comb and spacers) should be thoroughly cleaned with soap and water prior to gel preparation to remove any residual gel pieces. Remaining pieces of gel or dirt will result in bubbles in the gel that will interfere with the sample running through the gel. After cleaning, rinse the equipment with purified water and dry with tissue paper.
18. Rain-X is a hydrophobic silicone polymer that will prevent the gel from sticking to the surface of the buffer tank.
19. Gels can be prepared 1 day in advance. After polymerization of the gel, remove the clamps and insert water-soaked tissue paper in the gel front. Cover with Saran Wrap and fix with the clamps to prevent the gel from drying out. Store the gel overnight at room temperature.
20. Addition of NaAc in the lower buffer tank will generate an electrolyte gradient, thereby preventing that small cDNA-AFLP fragments run off the gel.

Chapter 2

21. To prevent leaking of the sample, do not move the comb once it is pushed into the gel.
22. The volume will vary depending on the comb used for sample loading. For combs of 48 samples, load 4–5 μL ; for combs of 72 samples, load 2–3 μL ; and for combs of 96 samples, load maximum 2 μL of sample per well. Load a ladder between the different primer combinations.
23. While working in the dark room, align the X-ray film with the gel blot and staple the corners together. Punch holes through the gel blot and the attached X-ray film by using a paper puncher. Place the gel blot and the attached X-ray film in a cassette for exposure. After development of the films, re-align the film and gel blots with the paper punch-made holes. Staple the film and the gel back together. Precise alignment is very important for cutting out the correct bands.
24. The gel pieces can be crushed to pulp with a pipette tip. Alternatively, 0.1-mm Zirconia/Silica beads (Biospec Products, Bartlesville, OK, USA) can be used. Add a few mg of beads to the gel piece and add 100 μL of $\text{T}_{10}\text{E}_{0.1}$ buffer. Mix with a mixer mill for 30 s at 30 Hz.
25. The re-amplified fragments should appear as single bands on the gel.
26. The applied re-amplification method ligates an adapter to the cDNA-AFLP fragments, making the fragments 56 nucleotides longer. This enhances the sequencing quality of short fragments and results in the sequence of the complete tag in one single sequencing reaction. Furthermore, the ligated adapters (*attB1* and *attB2*) allow cloning of the re-amplified fragments in Gateway™ vectors (Invitrogen).

ACKNOWLEDGEMENTS

This work was supported by the European Framework Programme 7 project SMARTCELL (FP7-KBBE-222716). J.C. is indebted to the Ghent University for a “Bijzondere Onderzoeksfonds” predoctoral fellowship.

REFERENCES

- Bachem CWB, van der Hoeven RS, de Bruijn SM, Vreugdenhil D, Zabeau M, Visser RGF** (1996). Visualization of differential gene expression using a novel method of RNA fingerprinting based on AFLP: analysis of gene expression during potato tuber development. *The Plant Journal* **9**: 745 – 753.
- Bachem CWB, Oomen RJFJ, Visser RGF** (1998). Transcript imaging with cDNA-AFLP: a step-by-step protocol. *Plant Molecular Biology Reporter* **16**: 157 – 173.

Breyne P, Zabeau M (2001). Genome-wide expression analysis of plant cell cycle modulated genes. *Current Opinion in Plant Biology* **4**: 136 – 142.

Breyne P, Dreesen R, Cannoot B, Rombaut D, Vandepoele K, Rombauts S, Vanderhaeghen R, Inzé D, Zabeau M (2003). Quantitative cDNA-AFLP analysis for genome-wide expression studies. *Molecular Genetics and Genomics* **269**: 173 – 179.

Goossens A, Häkkinen ST, Laakso I, Seppänen-Laakso T, Biondi S, De Sutter V, Lammertyn F, Nuutila AM, Söderlund H, Zabeau M, Inzé D, Oksman-Caldentey KM (2003). A functional genomics approach toward the understanding of secondary metabolism in plant cells. *Proceedings of the National Academy of Science of the USA* **100**: 8595 – 8600.

Pauwels L, Morreel K, De Witte E, Lammertyn F, Van Montagu M, Boerjan W, Inzé D, Goossens A (2008). Mapping methyl jasmonate-mediated transcriptional reprogramming of metabolism and cell cycle progression in cultured *Arabidopsis* cells. *Proceedings of the National Academy of Science of the USA* **105**: 1380 – 1385.

Pollier J, González-Guzmán M, Ardiles-Diaz W, Geelen D, Goossens A (2011). An integrated PCR colony hybridization approach to screen cDNA libraries for full-length coding sequences. *PLoS ONE* **6**: e24978.

Rischer H, Orešič M, Seppänen-Laakso T, Katajamaa M, Lammertyn F, Ardiles-Diaz W, Van Montagu MCE, Inzé D, Oksman-Caldentey K-M, Goossens A (2006). Gene-to-metabolite networks for terpenoid indole alkaloid biosynthesis in *Catharanthus roseus* cells. *Proceedings of the National Academy of Science of the USA* **103**: 5614 – 5619.

Vos P, Hogers R, Bleeker M, Reijans M, van de Lee T, Hornes M, Frijters A, Pot J, Peleman J, Kuiper M, Zabeau M (1995). AFLP: a new technique for DNA fingerprinting. *Nucleic Acids Research* **23**: 4407 – 4414.

Vuylsteke M, Peleman JD, van Eijk MJT (2007). AFLP-based transcript profiling (cDNA-AFLP) for genome-wide expression analysis. *Nature Protocols* **2**: 1399 – 1413.

Zabeau M, Vos P (1993). Selective restriction fragment amplification: a general method for DNA fingerprinting. European Patent Application EP 534858A1

Chapter 3

Functional characterization of the TAXIMIN orthologs of *Arabidopsis thaliana*

Manuscript: “Overexpression of the *Arabidopsis thaliana* signalling peptide TAXIMIN1 affects lateral organ development”

Colling Janine^{1,2,3}, Tohge Takayuki⁴, De Clercq Rebecca^{1,2}, Brunoud Géraldine⁵, Vernoux Teva⁵, Fernie Alisdair R.⁴, Makunga Nokwanda P.^{3,6}, Goossens Alain^{1,2*} and Pauwels Laurens^{1,2}

¹Department of Plant Systems Biology, Flanders Institute for Biotechnology (VIB), Technologiepark 927, B-9052 Gent, Belgium

²Department of Plant Biotechnology and Bioinformatics, Ghent University, Technologiepark 927, B-9052 Gent, Belgium

³Institute for Plant Biotechnology, Department of Genetics, Stellenbosch University, Stellenbosch, 7602, South Africa

⁴Max-Planck-Institute of Molecular Plant Physiology, Am Mühlenberg 1, 14476, Potsdam-Golm, Germany

⁵Laboratoire de Reproduction et Développement des Plantes, CNRS, INRA, ENS Lyon, Lyon, France

⁶Department of Botany and Zoology, Stellenbosch University, Stellenbosch, 7602, South Africa

***Author contributions:** gene cloning, generation and analysis of transgenic lines, RT-qPCR, RT-PCR, GUS staining, analysis of gene expression, data interpretation and writing of the manuscript.

Part of this chapter has been reproduced as an article which was published in the Journal of Experimental Botany 66: 5337 – 5349.

SUMMARY

Lateral organ boundary formation is highly regulated by transcription factors and hormones such as auxins and brassinosteroids. However, in contrast to many other developmental processes in plants, no role for signalling peptides in the regulation of this process has been reported yet. Here, we present the first characterization of the secreted cysteine-rich TAXIMIN (TAX) signalling peptides in *Arabidopsis*. *TAX1* overexpression resulted in abnormal fruit morphology and fusion of the base of cauline leaves to both the axillary shoots and the primary stem forming a decurrent leaf attachment. The latter phenotype was associated with a reduced formation of accessory shoots possibly due to the developmental lag observed in *TAX1* overexpression lines. The phenotypes at the paraclade junction match *TAX1* promoter activity in this region and are similar to loss of LATERAL ORGAN FUSION (LOF) transcription factor function. Nevertheless, *TAX1* expression was unchanged in *lof1/lof2* paraclade junctions and, conversely, *LOF* gene expression was unchanged in *TAX1* overexpressing plants, suggesting *TAX1* may act independently. *LOF1* splice variants display opposite regulatory activity and did not exhibit *in vitro* regulation of *TAX1* expression. *TAX1* also did not appear to influence *LOF1* regulatory activity *in vitro*. This study identifies *TAX1* as the first plant signalling peptide influencing lateral organ separation and implicates the existence of a peptide signal cascade regulating this process in *Arabidopsis*.

INTRODUCTION

Development of multicellular organisms requires tight spatiotemporal control of cell differentiation. In plants, this is established by gradients of morphogens, such as hormones or noncoding RNAs and polypeptides, such as secreted peptides or mobile transcription factors (Vernoux *et al.*, 2010; Van Norman *et al.*, 2011; Skopelitis *et al.*, 2012; Long *et al.*, 2015). Two distinct classes of secreted peptides can be distinguished in plants: small post-translationally modified peptides such as the CLAVATA3/ENDOSPERM SURROUNDING REGION (CLE) family, and cysteine-rich peptides (CRPs), exemplified by the EPIDERMAL PATTERNING FACTOR (EPF) family (Murphy *et al.*, 2012). Although over 1,000 secreted peptides have been predicted based on the *Arabidopsis* genome, only a handful have been characterized so far (Czyzewicz *et al.*, 2013).

CRPs are characterized by an N-terminal secretion signal and six or eight cysteines in the mature peptide, which are responsible for internal disulfide bond formation required for the establishment of the tertiary structure of the secreted molecule (Torii, 2012). Although other roles of secreted CRPs can be envisioned, it is assumed that most CRPs are involved in cell-

to-cell signaling and are recognized by a receptor on a target cell membrane (Czyzewicz *et al.*, 2013). The best-studied ligand-receptor pathway for CRPs is the recognition of members of the EPF family by the membrane-localized ERECTA family of leucine-rich repeat receptor-like kinases. The ERECTA kinase can perceive multiple EPF family members that control distinct developmental pathways. In the epidermis, it perceives EPF1/EPF2 to restrict stomatal density (Hara *et al.*, 2007; Hara *et al.*, 2009), whereas in the phloem, it binds EPFL4/EPFL5/EPFL6 to determine inflorescence stem and pedicel length (Uchida *et al.*, 2012).

Other *Arabidopsis* CRPs that have been characterized include the AtLURE1 pollen tube attractant (Takeuchi and Higashiyama, 2012) and the S-locus Cys-Rich/S-locus Protein11 (SCR/SP11) self-incompatibility ligand (Indriolo *et al.*, 2012). Recently, a new CRP, TAXIMIN (TAX), from the yew tree, *Taxus baccata* was described (Onrubia *et al.*, 2014). The *TbTAX* gene was identified to be co-regulated with paclitaxel biosynthesis genes in elicited cell cultures, and codes for a secreted CRP that could modulate specialized metabolism in both *T. baccata* and *Nicotiana tabacum* (tobacco) (Onrubia *et al.*, 2014). However, the exact function of *TbTAX*, as well of its homologues in other plants such as *Arabidopsis*, remains unknown.

During plant growth, the shoot apical meristem (SAM) gives rise to the primary stem and all aboveground (lateral) organs. In the central zone of the SAM, slowly dividing stem cells give rise to daughter cells that will first make up the peripheral zone, then the organ primordia and finally differentiate into lateral organs, such as leaves, stems and flowers (Gaillochet *et al.*, 2015). The meristem-to-organ boundary is a group of cells of distinct identity formed between the meristem and organ primordia and is characterized by specific gene expression profiles and morphology (Aida and Tasaka, 2006; Rast and Simon, 2008). Two roles can be attributed to meristem-to-organ boundaries: (i) the initial separation of the emerging organ of the meristem; and (ii) the production of new tissues later during development, such as of axillary meristems and carpel marginal meristems (Aida and Tasaka, 2006; Khan *et al.*, 2014).

Several proteins, mostly transcriptional regulators, have been reported to regulate boundary formation (Žádníková and Simon, 2014), with the CUP-SHAPED COTYLEDON (CUC) NAC transcription factors playing an important role. *CUC* genes are expressed at the boundary regions around organ primordia and are partially redundant in ensuring maintenance of the boundary (Heisler *et al.*, 2005; Hibara *et al.*, 2006). Loss of *CUC* gene function results in organ fusion, while gain-of-function mutants show an increased size of the boundary domain (Laufs *et al.*, 2004). Loss-of-function mutants of other genes specifically expressed in boundaries (boundary genes) are also often characterized by organ fusion defects (Žádníková

Chapter 3

and Simon, 2014). These include the transcription factors LATERAL ORGAN FUSION1 (LOF1) and LOF2 (Lee *et al.*, 2009), JAGGED LATERAL ORGANS (Borghi *et al.*, 2007) and BLADE ON PETIOLE1 (BOP1) and BOP2 (Ha *et al.*, 2007; Khan *et al.*, 2012).

In participation with these transcriptional regulators, also polar auxin transport carriers play a role in boundary establishment (Žádníková and Simon, 2014). Auxin gradients originating from the meristem and organ primordia intersect at the boundary, forming a local auxin minimum. ABCB19 is an ATP-binding cassette transporter required for normal basipetal auxin transport from the meristem auxin maximum (Noh *et al.*, 2001). Loss of ABCB19 function increases auxin levels in both meristems and boundary regions, disturbs the auxin minimum and results in the fusion of cauline leaves to the primary stem and in pedicel-stem fusions, ultimately accompanied by reduced expression of boundary genes (Zhao *et al.*, 2013).

So far, no signalling peptides have been described to play a role in organ separation. Here, overexpression of the signalling peptide TAX1 in *Arabidopsis* is reported to result in fusion of the cauline leaves to stems with only minor effects on the primary metabolite of leaf and root tissue. Accordingly, *TAX1* promoter activity is higher at the base of the cauline leaf and axillary stem and in the apical meristem. Interestingly, the developmental defects caused by *TAX1* overexpression are expanded in the Landsberg *erecta* (*Ler*) background. Finally, although the *TAX1* overexpression phenotype at the paraclade junction phenocopies that of *lof1lof2* mutants, these data suggest that TAX and LOF signalling pathways converge independently.

MATERIALS AND METHODS

Plant materials and growth conditions

Plants in this study were either in Columbia (Col-0) and/or *Ler* ecotype. For *in vitro* growth, seeds were gas-sterilized, stratified and germinated on full-strength MS (Murashige and Skoog, 1962). Plants were cultivated in a growth room at 22°C with a 16-h light/8-h dark photoperiod (110 $\mu\text{Em}^{-2}\text{s}^{-1}$). For analysis of adult plants, 10-day-old *in vitro*-germinated seedlings were transferred to soil in a growth chamber at 20-22°C and a photoperiod of 16-h light/8-h darkness.

T-DNA insertion lines for *TAX1* (SALK_016616) and *TAX2* (SALK_113004C) were obtained from NASC (Alonso *et al.*, 2003). Seedlings were PCR-genotyped using a T-DNA- and gene-specific primer (Table S1; Annex). Amplicons were sequenced to confirm the location of the T-DNA.

DNA constructs

The open reading frames (ORFs) of *Arabidopsis* *TAX1* (*At2g31090*), *TAX2* (*At2g20562*) and *TAX1 Δ SP* (lacking the N-terminal signal) were amplified between *attB* sites from Col-0 cDNA using Phusion polymerase (New England Biolabs) and Gateway recombined in the Entry vector pDONR207 (Invitrogen) and then in the pFAST-G02 destination vector (Shimada *et al.*, 2010) for overexpression. The *TbTAX* ORF was amplified from *T. baccata* cDNA and fused to 6xHis by PCR and cloned into the Entry clone pDONR221 (Invitrogen) and then in the pK7WG2D (Karimi *et al.*, 2005) destination vector.

Promoter sequences of *TAX1* (1575 bp upstream of the ATG) and *TAX2* (2000 bp upstream of the ATG) were PCR amplified between *attB* sites from Col-0 gDNA, Gateway recombined in pDONRP4P1R and then in pmK7S*NFm14GW as the destination vector for promoter activity analysis (Karimi *et al.*, 2007).

For subcellular localization, the *Venus* sequence was fused to that of *TAX1* and *TAX1 Δ SP* by PCR amplification and cloned as an entry clone in pDONR207 and recombined to destination vector pFAST-R02 (Karimi *et al.*, 2005; Shimada *et al.*, 2010).

The inducible lines were generated by cloning *TAX1*, Upstream Activator Sequence (*UAS*) and the tG7 terminator in the pH7m34GW destination vector (Karimi *et al.*, 2005). The GAL4VP16GR construct was cloned in the pK2GW7 destination vector (Karimi *et al.*, 2002).

To test if *TAX1* can interfere with the regulatory activity of the LOF1 alleles, cDNA of seedlings was used to amplify the CDS for LOF1.1 and LOF1.2 using Phusion DNA polymerase to add the *attB* sites. The PCR product was first cloned into the pDONR207 entry vector. For the first transient expression assay (TEA), the LOF1 splice variants were fused to the GAL4 DNA binding domain (GAL4DBD) and cloned into the p2GW7 destination vector (Karimi *et al.*, 2002). The fLUC CDS was fused to the Upstream Activator Sequence (UAS-fLUC) and cloned into the pGWL7 Gateway vector (Karimi *et al.*, 2005). The *TAX1* CDS was transformed in the p2GW7 destination vector. For the second TEA the promoter of *TAX1* (*pTAX1*) was cloned in front of fLUC in the pGWL7 destination factor and the LOF1 splice variants were expressed in the p2GW7 destination vector.

Homozygous plant lines with one T-DNA locus were selected and used in all assays. All primers used for cloning are listed in Table S1 (Annex).

Plant transformation

All constructs were transformed into *A. tumefaciens* strain C58C1 (pMP90) for subsequent transformation of Col-0 plants by floral dip (Clough and Bent, 1998). The 35S::*TAX1* construct was used to transform both Col-0 and *Ler* plants. Plants transformed with pFAST-G02 vector were selected on MS media based on *OLE1:GFP* expression in seeds; those transformed with pmK7S*NFm14GW, pK7WG2D, pK2GW7 were selected on MS medium supplemented with kanamycin. The lines transformed with pH7m34GW were selected on MS medium supplemented with hygromycin.

Gene expression analysis

RNA was isolated from plant material using the Plant RNeasy Kit (Qiagen, Germany) following the manufacturer's instructions with the addition of a DNase (Promega) treatment step. cDNA was synthesized from 1 µg RNA using the iScript™ reverse transcriptase kit (Bio-Rad). Quantitative real-time PCR (RT-qPCR) was performed on a LightCycler 480 (Roche Applied Science, USA) using Fast Start SYBR Green I fluorescent dye (Roche). At least three biological repeats and three technical repeats were used for each analysis. Expression data were normalized through two reference genes, *UBC* (At5g25760) and *PP2A* (At1g13320). For RT-PCR, cDNA was amplified with the Go-Taq PCR mix (Promega) using different amplification cycles, and loaded on an agarose gel containing SYBR Safe (Life technologies). The cycle number showing the highest contrast without saturation was used. *ACTIN* (At3g18780) was used as the reference gene for RT-PCR experiments. Primers for expression analysis are listed in Table S1 (Annex). Paraclade junctions (one cm of nodal tissue which includes the primary stem and part of the axillary stem and cauline leaf) were collected from eight plants to form one replicate and immediately frozen in liquid nitrogen.

Transient expression assay

The protoplast assay was performed as outlined by Van den Bossche *et al.*, (2013). In the first experiment the LOF1.1 and LOF1.2 splice variants were fused to the GAL4 DNA binding domain (GAL4DBD) and co-expressed with a reporter construct in which firefly Luciferase (fLUC) is fused to an Upstream Activator Sequence (UAS-fLUC) and a construct either overexpressing *TAX1* (35S::*TAX1*) or *GUS* (35S::*GUS*) as a control. In a second experiment the LOF1.1 and LOF1.2 allele was overexpressed using the 35S promoter and co-expressed with the p*TAX1* fused to fLUC. Tobacco Bright Yellow (BY-2) protoplasts were transfected

with these constructs. A normalization construct expressing Renilla luciferase (rLUC) under the control of a 35S promoter was also included. Protoplast cells were transfected with 2 µg of each plasmid, followed by overnight incubation in the dark at room temperature with gentle agitation. Protoplasts were lysed the following day and fLUC and rLUC activities were quantified using the Dual-Luciferase reporter assay system (Promega). The variation in transfection efficiency and technical error was corrected by normalization of the fLUC values using the rLUC activities. Eight biological repeats were performed for each transcription factor being tested.

GUS expression

Plant material was harvested in 90% (v/v) acetone and kept at 4°C for one week to remove chlorophyll. For the GUS staining, plants were first rinsed in NT buffer (100 mM Tris (pH7.0)/50 mM NaCl) and incubated in ferricyanide solution (1.94 mM potassium ferricyanide ($K_3[Fe(CN)_6]$) prepared in NT buffer) for 30 min at 37°C. Next, plants were transferred to a staining solution (2.47 mM X-Gluc prepared with ferricyanide solution) and kept at 37°C for at least 8 hours. Plants were kept in 70% (v/v) ethanol prior to visualization under a Bino Leica stereomicroscope (Leica MZ16) equipped with a digital camera.

Microscopy

Imaging of living SAMs of 5-week-old plants was performed using a LSM700 laser-scanning confocal microscope (Zeiss, Jena, Germany). TAX-Venus fusions were imaged in 10-day-old seedlings with an Olympus FV10 ASW confocal microscope. For scanning electron microscopy (SEM) of gynoecia, flowers at stage 13 were collected from wild-type and *TAX1* overexpression plants cultivated in the greenhouse. Sepals, petals and stamen were removed to reveal the carpel, which was directly mounted on the steel stubs and images were collected using an Hitachi TM-1000 table-top scanning electron microscope (Hitachi High-Technologies Corporation).

Accessory shoot determination

Plants were grown in a randomized design for 6 weeks in a growth chamber with a 16-h light photoperiod. The number of axillary and accessory shoots was counted after 40 days and the

Chapter 3

axillary stem was cut to one cm above the node. The number of accessory and axillary shoots was counted and the length of accessory shoots measured again after two weeks.

DEX induction in 10-day old seedlings or the SAM of mature plants

Crosses were made between the UAS-*TAX1* and GAL4VP16GR lines and presence of at least one copy of each T-DNA insert in the cross was confirmed by PCR. Surface sterilized seeds of Col-0 and the cross were germinated on Basal MS medium and 10-days seedlings were transfer to 1 ml liquid medium containing 5 mM dexamethasone (DEX) or an equal volume of ethanol (control) and incubated in the light growth room shaking at 120 rpm. Samples were collected at time 0, 2, 4, 6-h after treatment and immediately frozen in liquid nitrogen. Quantification of *TAX1*, *LOF1*, *CUC1-3* expression was determined by RT-qPCR using primers in Table S1 (Annex). To study gene expression in the SAM, the whole inflorescence was dipped in liquid MS containing 5 mM DEX or an equal volume of EtOH and transferred back to the light growth room. The SAM was harvested after 6-h and RT-qPCR was performed to quantify expression of the boundary genes used earlier.

Metabolite profiling

Metabolite profiling was performed exactly as described by Lisec *et al.*, (2006), using the modifications for root tissue described in Joshi *et al.*, (2006). Metabolite identities were verified via comparison to spectral libraries of authentic standards housed in the Golm Metabolome Database (Kopka *et al.*, 2005). Metabolite information is provided following recent recommendation standards (Annex, Table S2; Fernie *et al.*, 2011).

RESULTS**The *TAX* genes encode putative signalling peptides**

Recently, a novel putative signalling peptide termed TAXIMIN (TAX) was identified in the medicinal tree *T. baccata*. This peptide was found to be co-regulated with taxol biosynthesis genes and overexpression of *TbTAX* in *N. tabacum* hairy roots enhanced production of alkaloids (Onrubia *et al.*, 2014). Analysis using the PLAZA comparative genomics workbench (Proost *et al.*, 2014) indicated that this peptide is highly conserved across the plant kingdom. Homologues with a remarkable sequence identity can already be found in the lower land plants

Selaginella moellendorffii and *Physcomitrella patens* (Fig. 1). In this study, the model plant *Arabidopsis thaliana* was used to further characterize the function of the TAX signalling peptides, and two homologous sequences were discovered at the loci *At2g31090* and *At2g20562*, which we renamed *TAX1* and *TAX2*, respectively.

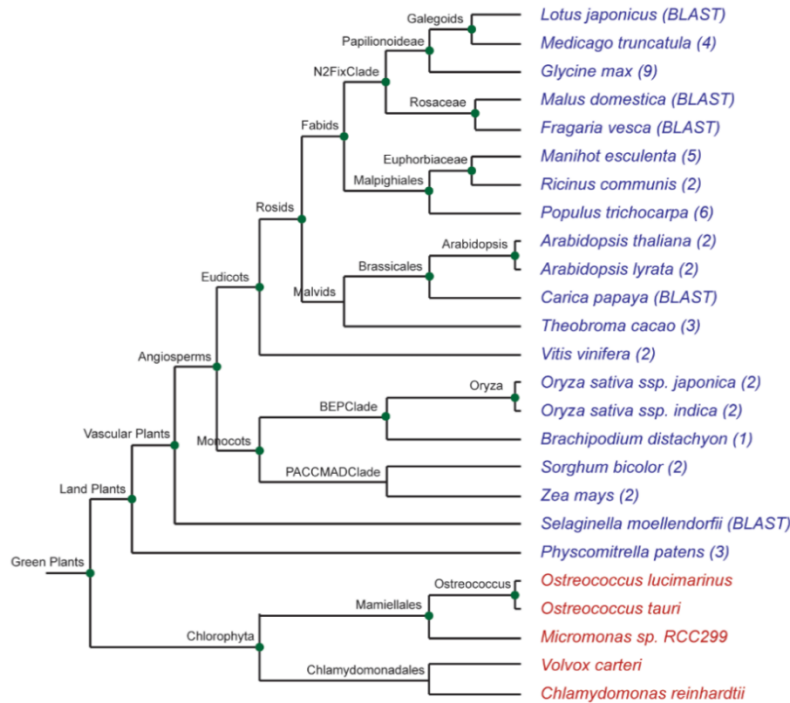


Figure 1. Distribution of the TAXIMIN peptide family in the plant kingdom.

(A) Species indicated in blue and red indicate the presence and absence, respectively, of a homologue found in the species based on data from the PLAZA3.0 comparative genomics platform. The numbers between brackets indicate the number of homologues that were detected in each species in the PLAZA3.0 platform or by BLASTp.

Both *Arabidopsis* *TAX* genes consist of two exons flanking one intron (Fig. 2B). *TbTAX* encodes a peptide of 73 amino acids (7.82 kDa), whereas *TAX1* and *TAX2* encode 75 (8.15 kDa) and 73 (7.84 kDa) amino acid peptides, respectively (Fig. 2A). The *TAX2* peptide has the highest sequence similarity to *TbTAX* with 51 amino acids identical to its gymnosperm homologue (Fig. 2A). *TAXIMIN* peptides have an *in silico*-predicted N-terminal secretion peptide (Fig. 2A, Onrubia *et al.*, 2014), generating equally sized mature peptides of 46 amino acids located at the C-terminus (Fig. 2A). The hydrophobicity of this mature peptide is striking, with up to 29 amino acid residues being hydrophobic. This hydrophobicity and equal mature peptide length is conserved in all *TAXIMIN* family members (Onrubia *et al.*, 2014). Currently, it is not known if and/or how the *TAX* peptides are post-translationally modified, but chemical synthesis of the *TbTAX* peptide was only possible when the prolines were hydroxylated (Onrubia *et al.*, 2014). The *TAX* peptides are cysteine-rich with six conserved cysteines and

Chapter 3

three conserved prolines (Fig. 2A), suggesting that this peptide belongs to the cysteine-rich family of peptides.

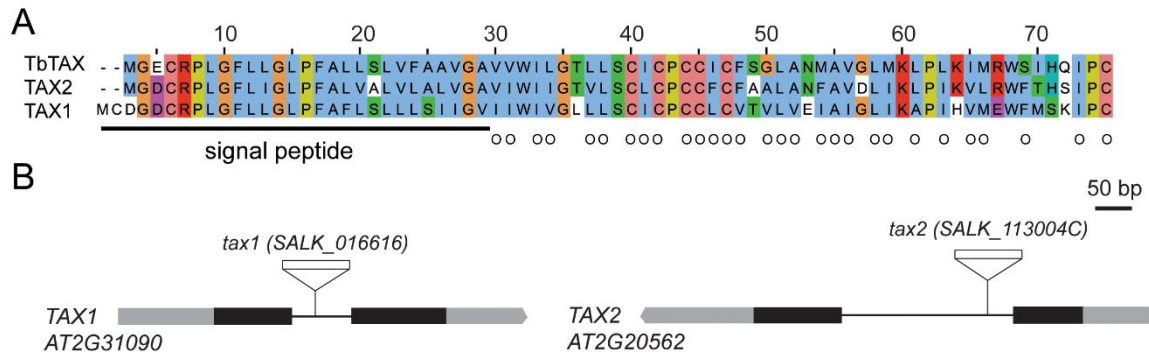


Figure 2. The TAXIMIN peptides in *Arabidopsis*.

(A) Sequence alignment of TbTAX and *Arabidopsis* homologues TAX1 and TAX2. The *in silico*-predicted TbTAX signal peptide (Onrubia *et al.*, 2014), located at the N-terminus, and hydrophobic amino acids are underlined and marked by circles, respectively. (B) Schematic diagram of the gene structure of *TAX1* and *TAX2* displaying the site of T-DNA insertion in the respective *tax* mutant lines. Black bars, grey bars and black lines represent exons, UTR regions and introns, respectively.

N-terminal signal directs the peptide to the plasmamembrane cell wall interface

To validate the functionality of the *in silico* predicted N-terminal signal peptide, fusions of TAX1 to the Venus fluorescent protein were constructed. TAX1-Venus with and without signal peptide were expressed with a 35S Cauliflower mosaic virus promoter in *Arabidopsis* seedlings and the localization of the fusion protein was determined by confocal microscopy in root cells. Similar to earlier observations of TbTAX subcellular localization (Onrubia *et al.*, 2014), TAX1-Venus was targeted to the plant cell membrane (Fig. 3A) and this was dependent on the presence of the N-terminal signal peptide (Fig. 3B). It can be concluded that, like TbTAX, TAX1 is a putative signal peptide that is likely secreted through the canonical secretion pathway.

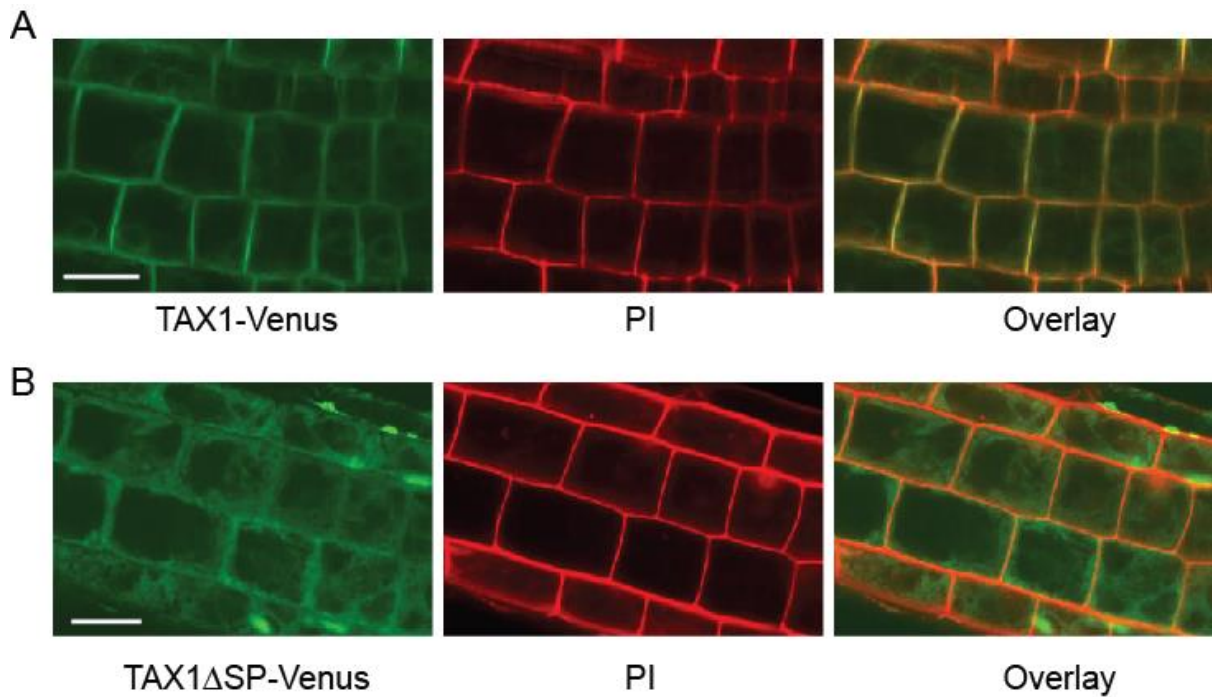


Figure 3. Localization of TAX1 in root cells of *Arabidopsis thaliana*.

(A) Localization of TAX1-Venus to the plasmamembrane, cells stained with PI and overlay of TAX1-Venus and PI to show overlap of the signals; B) Localization of TAX1 Δ SP-Venus in the cytoplasm, cells stained with PI and overlay to show reduced overlap at the plasmamembrane.

TAX1 overexpression results in developmental phenotypes

Full-length *TAX1*, *TAX2* and *TbTAX.6xHis* were constitutively expressed under control of the 35S promoter in *Arabidopsis* ecotype Col-0. For each construct, several independent lines were selected for the presence of a single T-DNA locus and showing clear overexpression in seedlings (Fig. 4A and C). The *TAX2* and *TbTAX.6xHis* OE lines did not display any observable phenotypes as seedlings or as mature plants (Fig. 4B and D-E).

Chapter 3

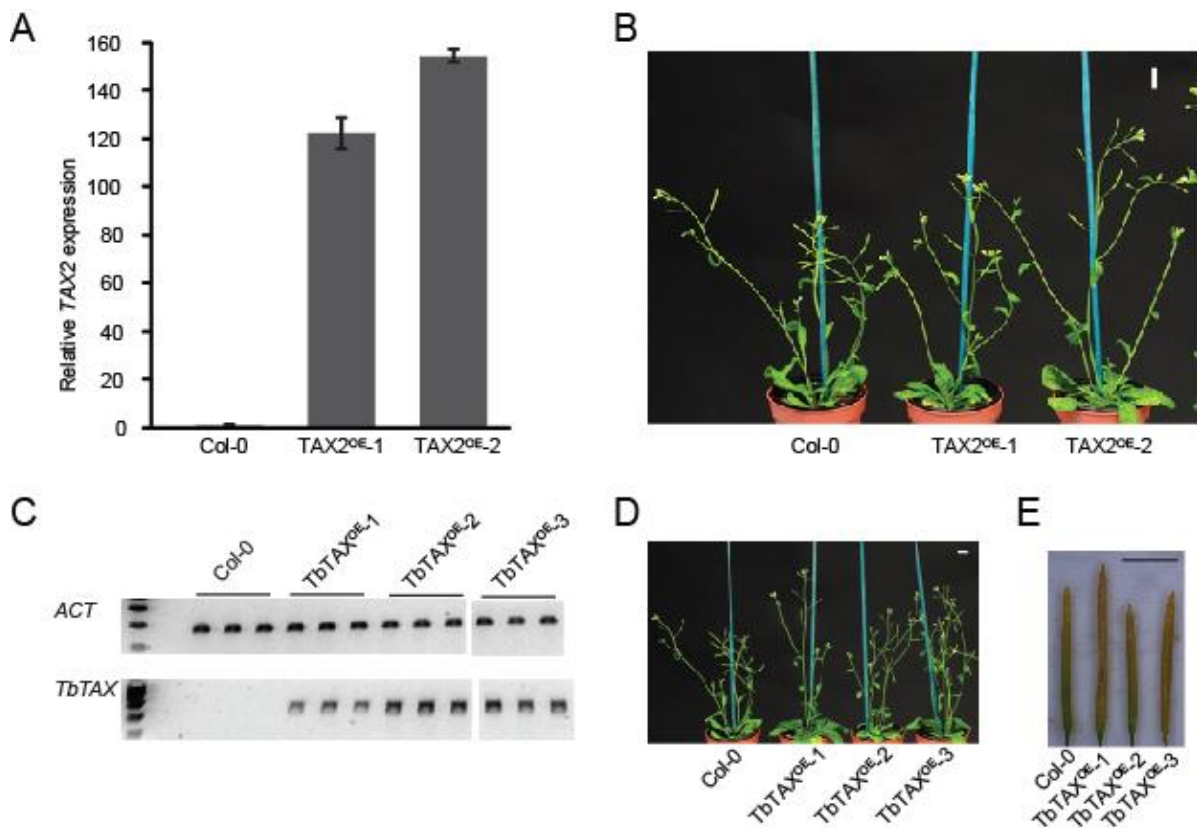


Figure 4. Effects of constitutive overexpression of *TAX2* and *TbTAX.6xHis* in *Arabidopsis thaliana*. (A) Relative expression of *TAX2* determined by RT-qPCR. The y-axis indicates fold overexpression relative to the wild type Col-0 (set to 1). (B) General morphology of *TAX2* overexpressing plants. (C) Confirmation of *TbTAX.6xHis* overexpression by RT-PCR. (D) General morphology of *TbTAX.6xHis* overexpressing plants. (E) Silique morphology of *TbTAX.6xHis* overexpressing plants. Scale bars in (B and D) are 12 mm, in (E) it is 5 mm.

For the *TAX1* OE lines, several phenotypes were observed. In seedlings, the levels of *TAX1* OE inversely correlated with the growth of the seedlings on basal MS plates and in the greenhouse (Fig. 5A-C and 6A). The highest *TAX1* overexpressing line OE-2 and OE-3 showed reduced growth of seedlings on basal MS plates (Fig. 5A). After transfer to the greenhouse, these lines were delayed in development (Fig. 5B-C). Importantly though, *TAX1* overexpressing lines OE-2 and OE-3 showed developmental defects at paraclade junctions and altered fruit morphology (Fig. 6 and 7).

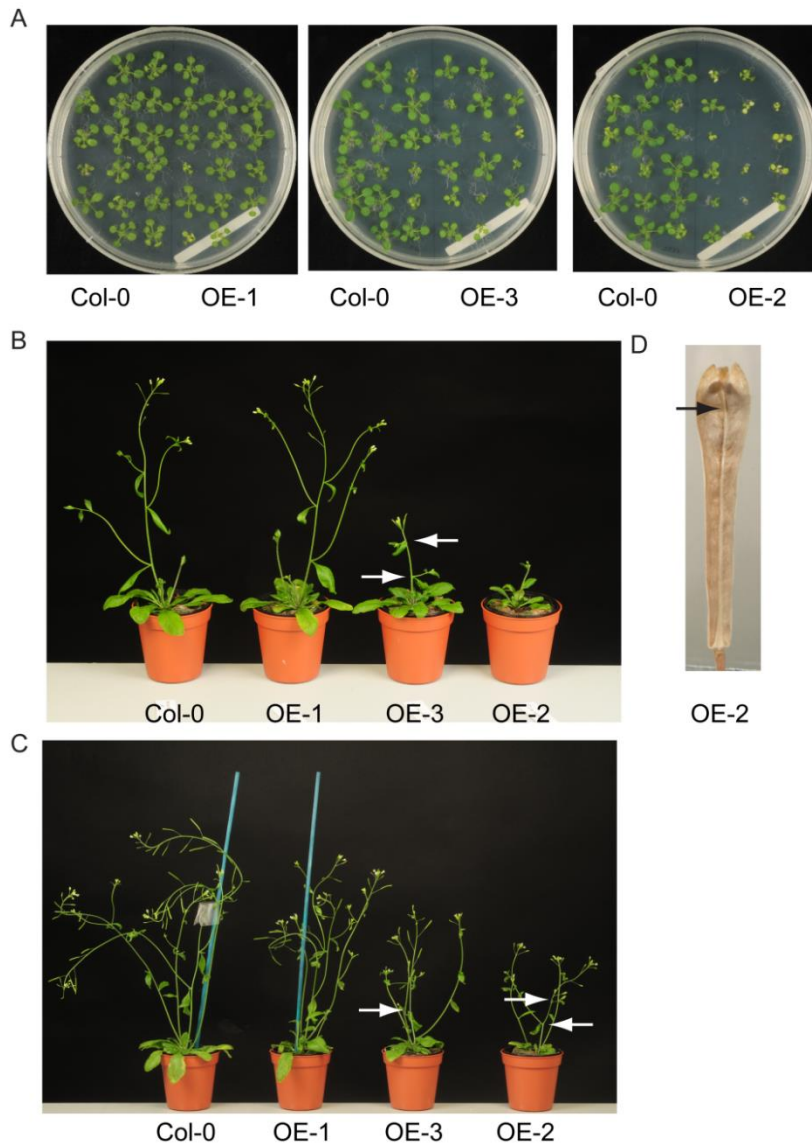


Figure 5. Phenotypes of *TAX1* overexpressing seedlings and flowering plants.

(A) Seedlings (21-days-old) germinated on basal MS. Left and right sides of each plate are wild-type Col-0 and the *TAX1* overexpressing lines, respectively. (B) Flowering plants (5-weeks-old) grown in the 16-h light growth chamber. Arrows indicate the bending of the axillary shoots in OE-3 which proceeded to grow upwards after 5 days (C, arrow in OE-3). At this age, also phenotypes in OE-2 at the inflorescence (top arrow) and the first node (bottom arrow) are visible (C). (D) Silique of *TAX1* line OE-2, arrow indicates opening site due to seed crowding in this region.

Fruits of wild-type *Arabidopsis* Col-0 were narrow, cylindrical and elongated (Fig. 6B). The siliques of the highest *TAX1* overexpressing lines OE-2 and OE-3 were shorter and wider at the tip, due to an outgrowth of both the valves (Fig. 6B) and the replum (Fig. 6C). The ovules inside the silique had a normal organization at the base of the fruit, but they were disordered at the wider tip (Fig. 6D). This was also associated with preferential opening of mature siliques at the site of seed crowding (Fig. 5D). The number of carpels in the 35S::*TAX1* siliques was

Chapter 3

unaffected. The valve outgrowths were already visible at early stages of gynoecium development (Fig. 6E) and could be followed over the course of fruit development (Fig. 6E; F).

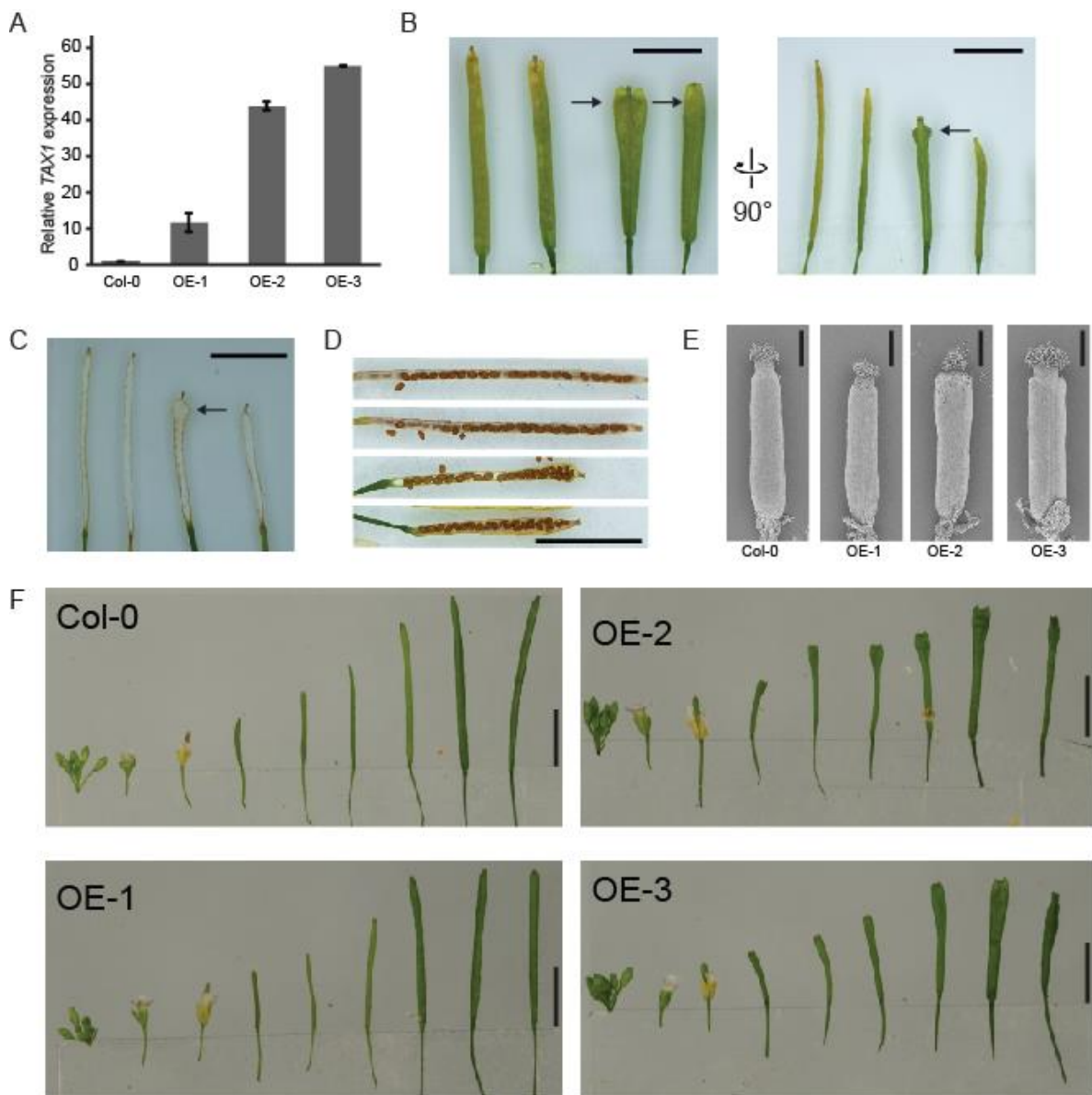


Figure 6. *TAX1* overexpression in Col-0 background results in an alteration of fruit morphology. (A) Relative expression of *TAX1* in 19-day-old seedlings compared to the Col-0 wild type for three independent 35S::*TAX1* lines. Expression values were normalized to those of the wild type (Col-0), set to 1. Values represent the average of three biological replicates \pm SE. (B) Medial and lateral view of mature siliques of *TAX1* overexpression lines. The order of the siliques in pictures (B-E) is always the same order as in (A). (C) Lateral view with seeds removed. Arrow indicates protrusion of the replum at the tip of the silique in *TAX1* overexpressing lines. (D) Lateral silique view with one valve removed. (E) SEM images of early stage gynoecia of *TAX1* OE lines. The scale bar is 400 μ m in length. (F) Development of siliques could be followed at different stages. Scale bar in B-D is 5 mm.

It is well documented that phenotypes in lateral organ development are exaggerated in the *Ler* background and more specifically by the *er* mutation in the *ERECTA* kinase gene (Mandel *et al.*, 2014). Therefore, the 35S::*TAX1* transgene was also overexpressed in this genetic background. Four lines which overexpress *TAX1* at different levels (Fig. 7A) were generated and similar fruit phenotypes in these lines compared to the Col-0 background were observed, and again the severity correlated with *TAX1* expression levels (Fig. 7A-B). The silique phenotype observed in lines OE-2 and OE-3 in Col-0 and in OE-1L, OE-3L, and OE-4L in *Ler* had complete penetrance: all siliques in all plants over several generations displayed this phenotype.



Figure 7. *TAX1* overexpression in *Ler* background results in a changes of fruit morphology.

(A) Relative expression of *TAX1* in 19-day-old seedlings compared to the *Ler* wild type for four independent 35S::*TAX1* lines. Expression values were normalized to those of the wild type (*Ler*) set to 1. Values represent the average of four biological replicates \pm SE. (B) Medial and lateral view of mature siliques of *TAX1* overexpression lines in the same order as in (A). Scale bars in B are 5 mm.

***TAX1* constitutive expression results in lateral organ fusion**

Besides the changes in fruit morphology, different types of lateral organ fusion were present in *TAX1* overexpressing lines at the paraclade junctions between the primary stem, axillary shoot and cauline leaf (Fig. 8A). These phenotypes had reduced penetrance, and occurred in most plants of line OE-3 and sporadically in OE-2 and *Ler* (Fig. 9). Of 23 OE-3 plants, 17 showed pedicel–stem fusion with outgrowths subtending some fruits, possibly corresponding to bract-like structures (Fig. 8A-B, 9A). At the first formed node on the main stem, 12 plants showed a protrusion of the main stem with the cauline leaf fused to a down- or side-wards deflected axillary shoot (Fig. 8C, 9B). At the second node, the cauline leaf had a broader leaf base and also deflected downwards (Fig. 8D, 9C). Finally, the most frequently occurring defect was a fusion of the cauline leaf to a stem together with the leaf extending down the insertion

Chapter 3

point along the stem, forming a decurrent leaf attachment. For the primary stem this was observed in 4 out of 23 plants (Fig. 8E, 9D). Interestingly, when no third node was visible, fusion occurred in 18 cases between a secondary shoot originating from the rosette, a tertiary axillary shoot, and the subtending cauline leaf (Fig. 8F).

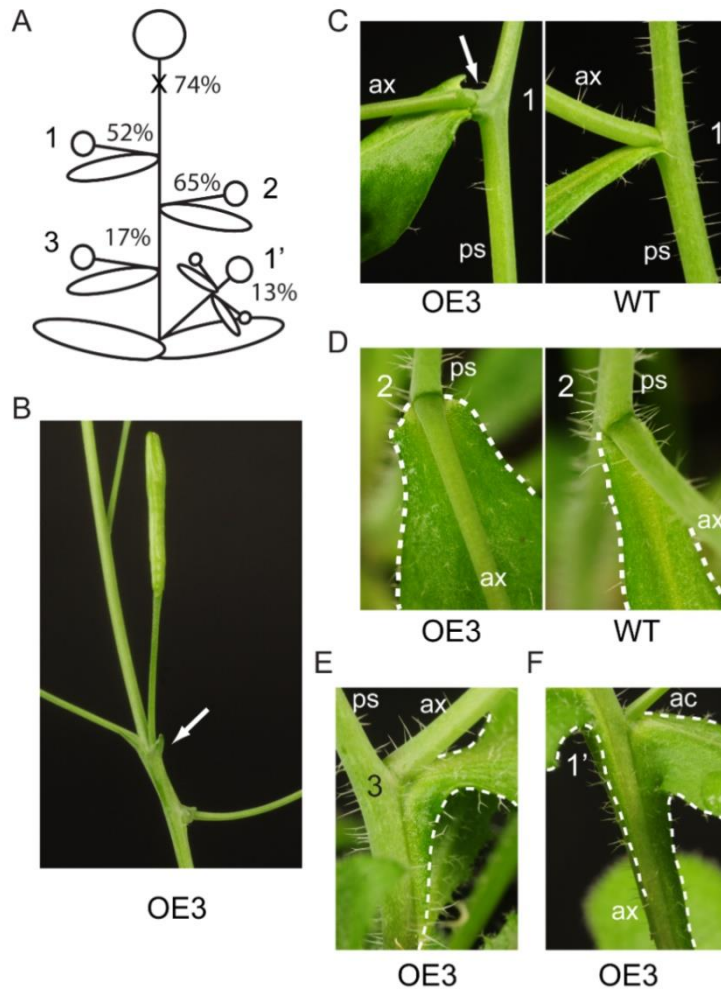


Figure 8. Constitutive *TAX1* overexpression results in lateral organ fusion with reduced penetrance. (A) Schematic overview of the location and frequency of phenotypes observed in line OE-3. (B) Undifferentiated outgrowths (indicated by arrow) at the inflorescence. (C) Side view of the protrusion (indicated by arrow) of the primary stem at the first node, accompanied with fusion of the broader cauline leaf base to the axillary stem which deflects downwards. (D) Top view of node 2 with a broader cauline leaf base. (E) Fusion of the cauline leaf to both the axillary stem and the primary stem at node 3. (F) Fusion of cauline leaves to the axillary stem that originates from the rosette and to the accessory shoot when there is no third node. Abbreviations: ax, axillary stem; ac, accessory shoot; ps, primary stem.

All these defects were associated with downward bending of the stems early during outgrowth of the axillary stem (Fig. 5B). The axillary stem bends upwards again later during development, probably due to phototropism (Fig. 5C). No fusion of pedicels to stems was observed. In the *Ler* background, additional phenotypes besides those seen in *Col-0*, were occasionally observed, such as bending of the axillary stem at tertiary branch points (Fig. 9E) and twisting of the primary stem (Fig. 9F).

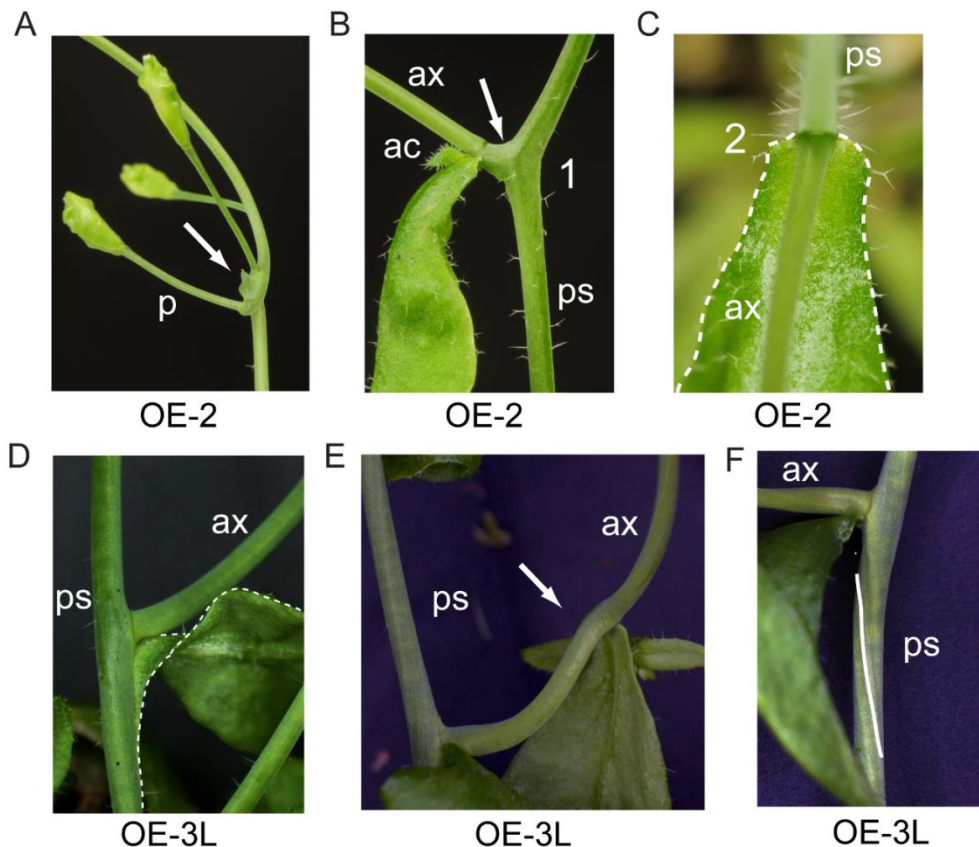


Figure 9. Paraclade junction phenotypes in line OE-2 and *Ler* background with reduced penetrance. (A) Undifferentiated outgrowths (indicated by arrow) at the inflorescence. (B) Side view of the protrusion (indicated by arrow) of the primary stem at the first node. (C) Top view of node 2 with a broader cauline leaf base. (D) Fusion of the cauline leaf to both the axillary stem and the primary stem in the *Ler* background. Dashed lines indicate contours of the cauline leaf. Additional phenotypes in the *Ler* background include bending of axillary stems at tertiary branch points (E) and twisting of the main stem (F). The white line follows the stem. Abbreviations: ax, axillary stem; ac, accessory shoot; p, pedicel; ps, primary stem.

Lateral organ phenotypes are specific for *TAX1* overexpression

Since none of the *TbTAX* and *TAX2* OE lines displayed the phenotypes observed for 35S::*TAX1*, the results for *TAX1* suggest that this peptide is specifically capable of triggering organ fusion defects. Next, whether the signal peptide of *TAX1* is essential for its activity was examined. A construct lacking the N-terminal signal, 35S::*TAX1*ΔSP was constitutively expressed, but failed to show any of the phenotypes observed for the full-length peptide (Fig. 10A-B). This result confirms that *TAX1* represents a signalling peptide that is most likely secreted through the canonical pathway and that high peptide levels inside the cell do not result in observable phenotypes. Notably, wild-type phenotypes were observed in the *TAX1*-Venus lines (data not shown), suggesting that fusion to Venus might interfere with *TAX1* processing and/or function.

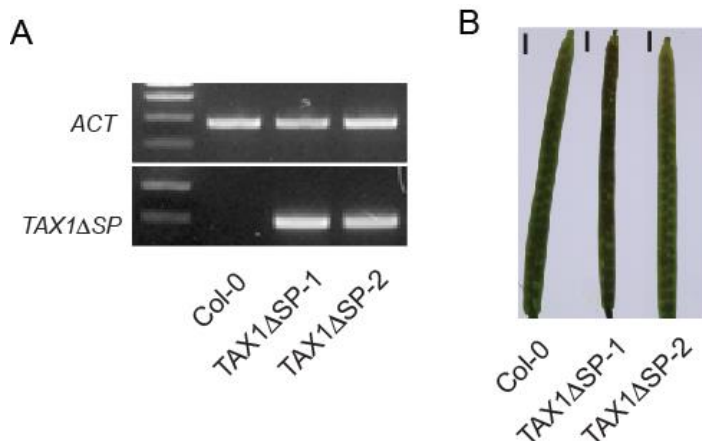


Figure 10. Constitutive expression of *TAX1*ΔSP.

(A) Confirmation of *TAX1*ΔSP overexpression by RT-PCR. (B) Silique morphology of *TAX1*ΔSP overexpressing plants. Scale bars in (B) is 1 mm.

Arabidopsis thaliana *tax* mutants lack visible morphological phenotypes

To study the loss of function mutation in the *TAX* genes, a suitable T-DNA insertion line for *TAX1* (*tax1*) and *TAX2* (*tax2*) could be obtained (Alonso *et al.*, 2003). The T-DNA was localized by sequencing to be inserted in the intron 113 bp downstream of the start codon for *tax1* and in the intron 139 bp downstream of the start codon for *tax2* (Fig. 2B).

Once it was confirmed that the T-DNA insertion lines were homozygous for the T-DNA inserts, a cross was made between *tax1* and *tax2* to exclude functional redundancy between the two genes. As the T-DNA was inserted in the intron of both genes and could be spliced

out during mRNA synthesis expression of the genes was determined by RT-PCR in seedlings and RT-qPCR in paraclade junctions. Absence or at least severe reduced expression of both *TAX* genes could be confirmed for both *TAX* genes in *tax1tax2* (Fig. 11A-C). Notwithstanding, single nor double mutant plants did not display any developmental or growth phenotypes in seedlings or in mature plants (Fig. 11D-E).

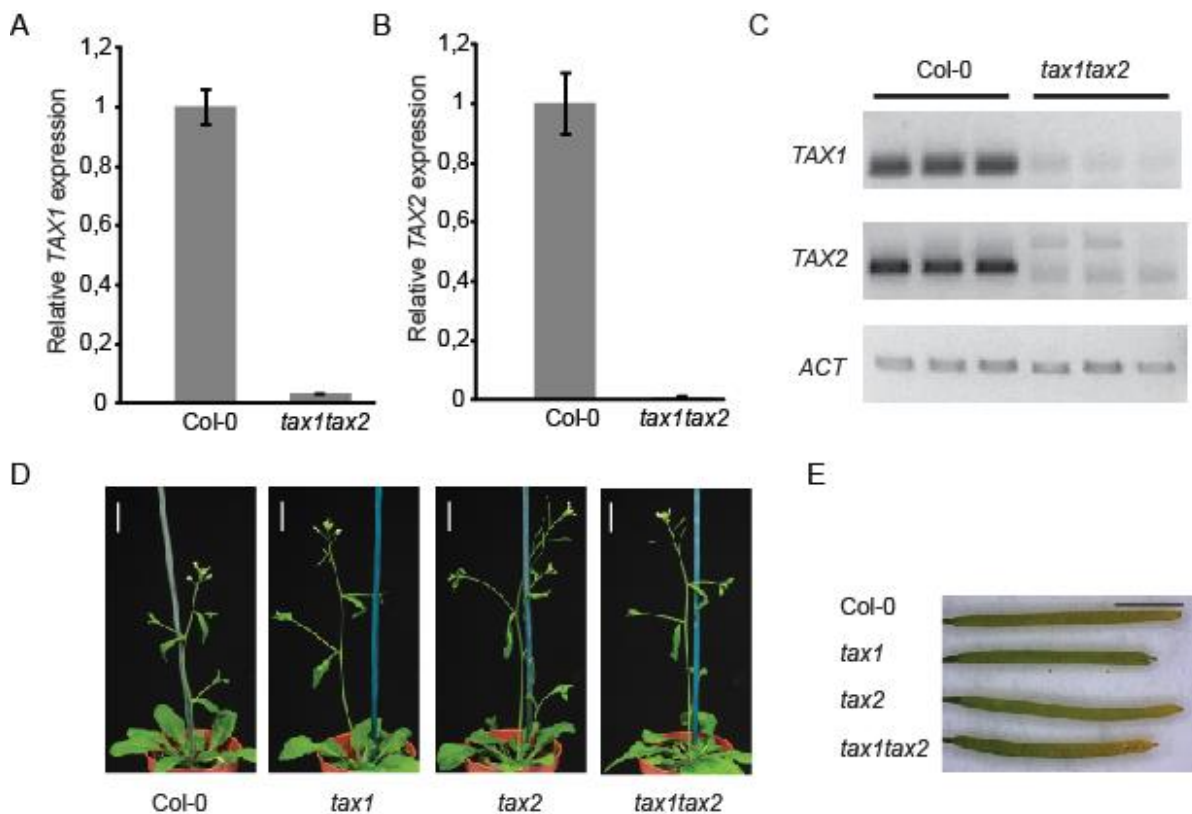


Figure 11. T-DNA insertion lines for *TAX* genes in *Arabidopsis thaliana*. Quantitative RT-PCR of (A) *TAX1* and (B) *TAX2* in the paraclade junctions of 5 week old mature plants cultivated in the greenhouse. (C) RT-PCR of *TAX1* and *TAX2* genes in the double mutant *tax1tax2*. (D) Habitat of mature *tax* mutants and (E) Siliques of Col-0, *tax1*, *tax2* and *tax1tax2* plants (top to bottom). The y-axis in A and B indicates fold reduction relative to the wild type Col-0 (set to 1). Values represent the average of four biological replicates \pm SE.

***TAX1* and *TAX2* have distinct expression patterns**

Next, the tissue-specificity of the promoter activities of *TAX1* and *TAX2* was then investigated. Promoter fragments of 1575 upstream of the start codons of *TAX1* and 2000 bp upstream of *TAX2* were cloned and used to drive a nuclear-localized GUS-GFP fusion (Karimi *et al.*, 2007).

Chapter 3

In 10-day-old *in vitro*-germinated p*TAX1*::GUS:GFP seedlings, the *GUS* expression was detected mainly in the SAM region (Fig. 12A-B, I). Using GFP, *TAX1* promoter activity was detected in the entire inflorescence meristem of 5-week-old plants, but was stronger in the organ primordia (Fig. 12C-E). *TAX1* expression was mostly specific to the L1 layer in the center of the meristem but was also detected in the L2 layer in organ primordia (Fig. 12C-E).

In mature plants cultivated for 28 days in the greenhouse, *TAX1* expression was observed in the anthers and in the nectaries in the floral tissue but no expression was visible in the gynoecium (Fig. 12F-G). The paraclade junctions between the primary stem and axillary stems showed *GUS* expression at the base of the cauline leaf and the emerging axillary shoot (Fig. 12H). The latter *TAX1* expression pattern supports a role of *TAX1* in the lateral organ fusion phenotype observed following *TAX1* overexpression. Accordingly, no expression was observed in the pedicel-stem junctions corresponding to the absence of fusion phenotypes there (Annex, Fig. S1).

In contrast, in 10-day-old p*TAX2*::GUS:GFP seedlings, *GUS* was highly expressed in the vasculature in the cotyledons, first true leaves and hypocotyl (Fig. 12J). In the floral tissue of mature plants, *GUS* was visible in the vasculature of the sepals, petals and style (Fig. 12K). Also in paraclade junctions, *GUS* was detected mainly in the vasculature of the cauline leaf (Fig. 12L). For both *TAX1* and *TAX2*, *GUS* was observed in main and lateral roots in seedlings, mainly in vasculature, but was absent from the root tip (Annex, Fig. S1). Expression in root hair cells was only observed for *TAX2* (Annex, Fig. S1B, G).

Overall, the difference in *TAX1* and *TAX2* expression patterns suggests that they play distinct roles in plant development, which is in agreement with the different effects caused by their overexpression.

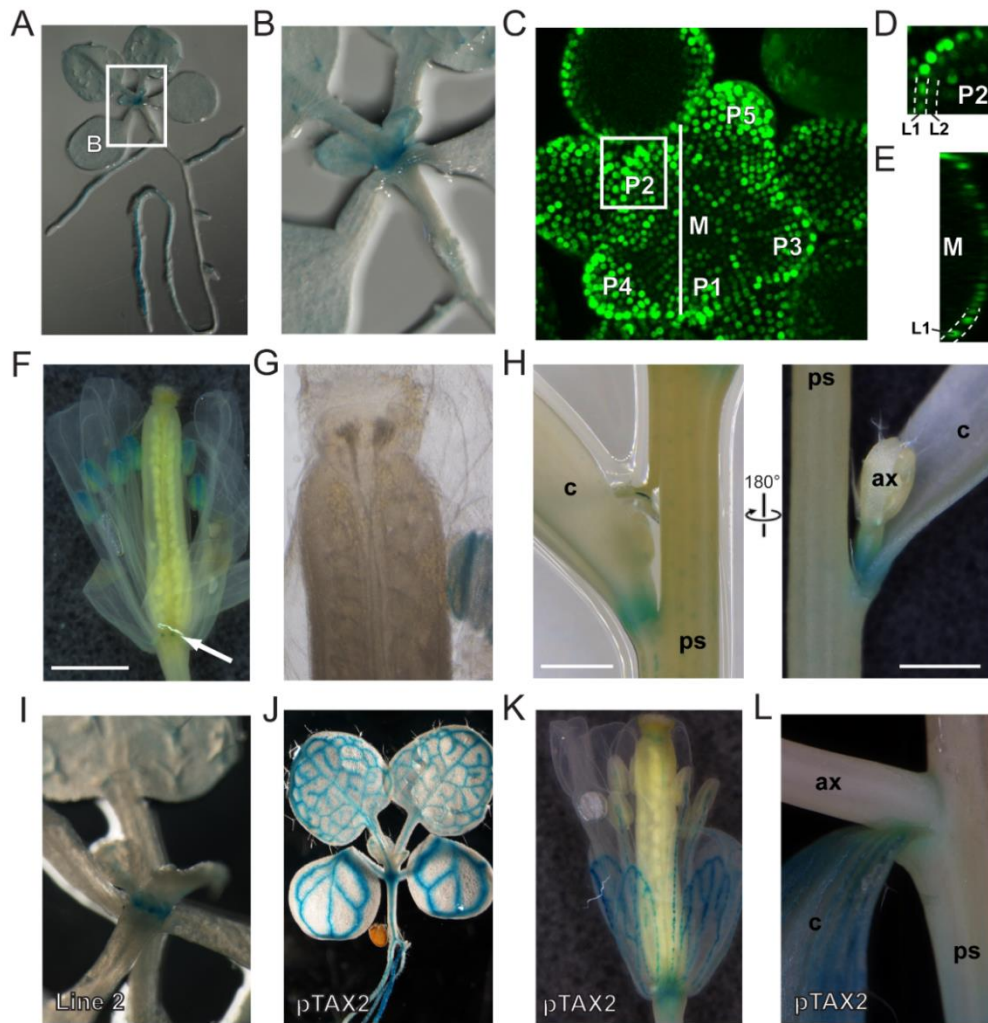


Figure 12. *TAX1* and *TAX2* have distinct promoter activities.

Plants expressing a nuclear localized GUS-GFP fusion under control of the *TAX1* (A-I) and *TAX2* (J-L) promoter were used. (A-B) GUS activity in 10-day-old seedlings. (C-E) GFP signal at the shoot apical meristem visualized by confocal microscopy. (C) Stacked image. Primordia (P) are numbered from youngest to oldest. (D) Longitudinal optical section at P2. (E) Transverse optical section of center of the meristem (M). (F-G) GUS activity in the flower (F) and in the silique (G). (H) The paraclade junction of 28-day-old mature plants. (I) GUS activity in the meristem region of 10-day-old seedlings of pTAX1::GUS-GFP for line 2. (J) GUS expression in the vasculature of a 10-day-old seedling, (K) the flower and (L) the paraclade junction of 28-day-old mature plants. ps, primary stem; ax, axillary stem; c, cauline leaf. All scale bars are 1 mm.

TAX1* overexpression lines phenocopy *lof1lof2

The results from the GUS staining experiment suggested that *TAX1* is expressed in the nodal tissue and might function in this region. Therefore, we performed a literature survey to look for mutants which display a similar phenotype as observed for the 35S::*TAX1* plants. Previously,

Chapter 3

bending was linked to loss of a MYB transcription factor called *LATERAL ORGAN FUSION* (*LOF*). The bending phenotype in the T-DNA insertion lines *lof1-1* and *lof1lof2* was the result of lack of boundary formation which resulted in fusion of the axillary stems and cauline leaf at their base (Lee *et al.*, 2009). Additionally, *lof1lof2* mutants also displayed lack of accessory shoot development in the paraclade junctions (Lee *et al.*, 2009). The presence of accessory shoots in the nodes of the *TAX1* OE lines were quantified to determine if they display a similar phenotype.

***TAX1* overexpression leads to loss of accessory shoot formation**

Accessory and axillary shoot formation was studied in the available T-DNA *tax* mutants and *TAX1* overexpressing lines in the Col-0 background (Fig. 13A). Only *TAX1* OE-3 had a significant difference (two axillary shoots instead of three) in the number of axillary shoots compare to Col-0. However, accessory shoot formation was severely reduced in all *TAX1* overexpressing lines. While on average one to two accessory shoots developed in Wt, none to one developed in the overexpression lines. This effect was independent of the level of *TAX1* overexpression or the severity of the other *TAX1* overexpression phenotypes. Similar to what was reported (Lee *et al.*, 2009), an accessory shoot nearly never developed in the *lof1lof2* mutant.

The absence of observable accessory shoots can be attributed either to the absence of a functional meristem or the absence of outgrowth. To distinguish between these two options, we removed the apical dominance of the axillary shoots and scored the outgrowth of accessory shoots. To exclude artefacts because of possible developmental lags, we used line OE-1, which most closely resembled the Wt phenotypically, but which still showed a marked reduction of accessory shoots (Fig. 13A). The number of accessory shoots before and 14 days after removal of dominance of axillary shoots did not differ between that line and the Wt (Fig. 11B). Moreover, accessory shoots grew out to similar length (Fig. 13C). In conclusion, these data suggest that *TAX1* overexpression did not affect accessory shoot outgrowth, the effect of developmental delay might account for the reduced number of accessory shoots observed in these lines.

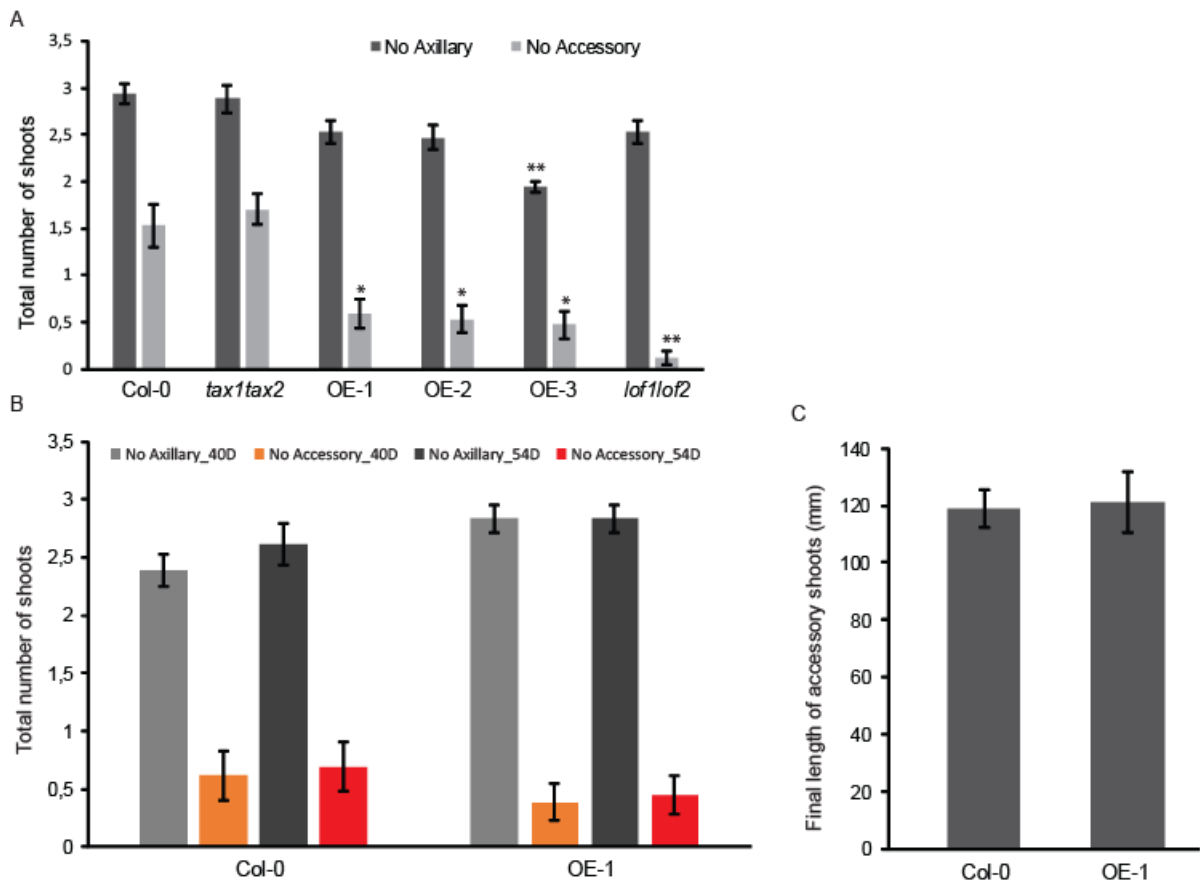


Figure 13. Reduced accessory shoot number is not due to the absence of meristem outgrowth. (A) Number of accessory and axillary shoots in 40-day-old plants. (B) The number (No) of axillary and accessory shoots were counted 40-days (40D) after sowing and again 14 days (54D) after removal of axillary stem apical dominance. (C) The length of the accessory shoots after removal of the axillary stem. Statistical analysis was performed using a Kruskal–Wallis non-parametric test followed by a post-hoc Dunn's test ($n=17$; *, $p \leq 0.05$; ** $p \leq 0.005$).

Since absence of *LOF1* expression causes the same phenotype as the *35S::TAX1*, at least three possible hypothesis to suggest how the TAX1 peptide and the MYB transcription factor functions in the plant to induce a similar phenotype can be suggested. Firstly, TAX1 can function upstream of LOF1 in the same signalling pathway and can either suppress LOF1 expression or alter its regulatory activity in the plant. Alternatively, LOF1 can function upstream of TAX1 and can (in)directly regulate its expression. It is also possible that TAX1 and LOF1 independently influence similar genes and that miss-regulation of these genes cause the bending.

To test the first hypothesis; a transient expression assay (TEA) to test if constitutive expression of *TAX1* interferes with the regulatory activity of the LOF1 alleles was performed.

Constitutive *TAX1* expression does not interfere with LOF1 regulatory activity

The *LOF1* gene has two splice variants, *LOF1.1* and *LOF1.2* (Fig. 14A) and to test their regulatory activity the full length CDS for each allele was fused to the GAL4 DNA binding domain (GAL4DBD) to generate the effector construct. The tobacco (*Nicotiana tabacum*) Bright Yellow (BY)-2 cell suspension cultures were transfected with the respective effector constructs along with a firefly luciferase (fLUC) reporter gene fused to an Upstream Activator Sequence (UAS) which can be bound by the GAL4DBD and allow the transcription factor to regulate expression of fLUC. The cells were also transfected with a construct which constitutively express *TAX1* or the *GUS* gene as a negative control to determine if *TAX1* affects the regulatory activity of the MYB transcription factors on the expression of firefly luciferase.

The two *LOF1* alleles have opposite activity with *LOF1.1* acting as an activator and *LOF1.2* as a repressor (Fig. 14B). Constitutive expression of *TAX1* caused a negligible increase (1.13-fold) in *LOF1.1* regulatory activity compared to the control *GUS* gene in this system (Fig. 14B). Overexpression of *TAX1* also caused a small reduction (16.3%) in the regulatory activity of the *LOF1.2* splice variant, but similar to the change in the *LOF1.1* regulatory activity, this value is so small it also does not have any biological significance. However, this experiment does not necessarily indicate if *TAX1* influences *LOF1* activity as some components of the signalling mechanisms in this heterologous system may be absent or not highly expressed. To determine if *TAX1* OE can result in reduced or loss of *LOF1* and other boundary gene expression, the level of these genes was quantified both in seedlings as well as the paraclade junctions of mature plants.

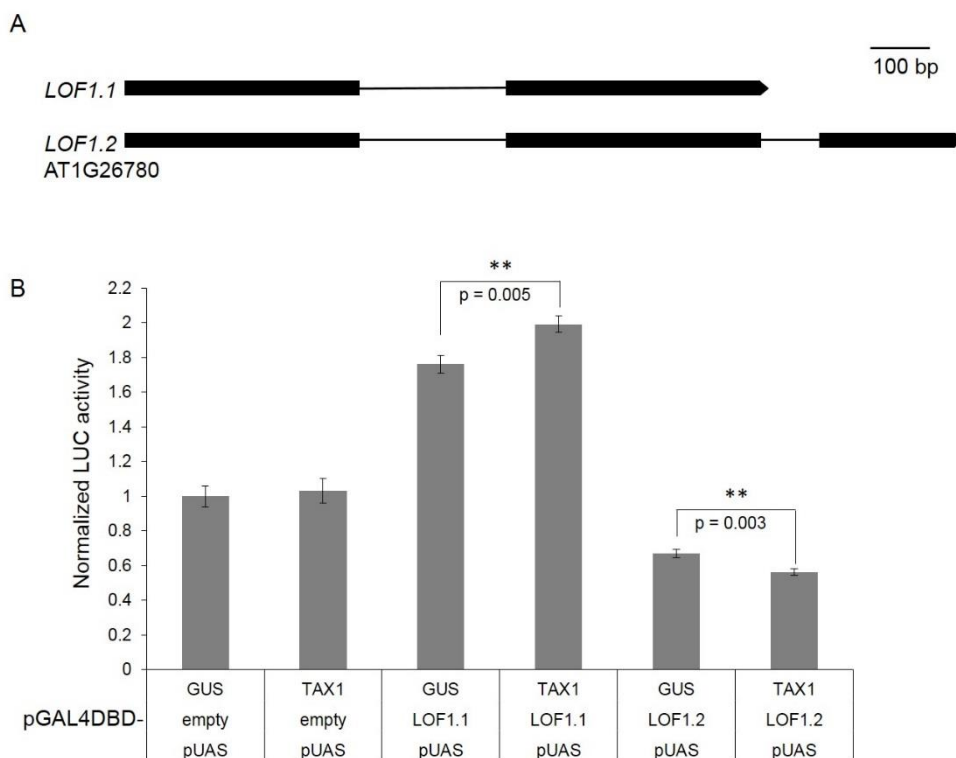


Figure 14. Transient expression assay to test if TAX1 interferes with the regulatory activity of the LOF1 splice variants. (A) Splice variants of the two LOF1 (LOF1.1 and LOF1.2). Bars represent the exons and lines represent the introns for the LATERAL ORGAN FUSION (At1g26780) transcription factor. (B) TAX1 does not interfere with the regulatory activity of the two splice variants of the MYB transcription factor LOF1. Transactivation assay in tobacco protoplasts co-transfected with a pUAS::fLUC reporter construct, effector constructs overexpressing LOF1.1 or LOF1.2 fused to GAL4DBD, 35S::TAX1 or 35S::GUS (as a control) and an rLUC construct for normalization (Vanden Bossche *et al.*, 2013). Values are fold-changes relative to protoplasts transfected only with a GUS expression construct instead of LOF1 effector constructs and are the mean (\pm SE) of eight biological repeats. Significant differences (Student's *t*-test): **, $P < 0.01$.

Expression of known boundary genes does not change in *TAX1* overexpression lines

The fusion of the cauline leaf to the stem has been reported earlier in *LOF* loss-of-function lines (Lee *et al.*, 2009) or to be associated with reduced *LOF* expression in *abcb19* (Zhao *et al.*, 2013). The expression of *LOF1* and *LOF2* in junctions of the *TAX1* overexpressing lines was therefore determined. The boundary gene *CUC3* was included, because it has been reported to be downstream of the LOF transcription factors and because loss of *CUC3* function causes fusion defects (Hibara *et al.*, 2006).

Overexpression of *TAX1* in the junctions was confirmed by RT-qPCR (Fig. 15A). Line OE-3 showed very high expression of *TAX1* at this site, corresponding to the severity of the fusion

Chapter 3

phenotypes observed in these lines associated with downward bending of axillary stems (Fig. 8). However, expression of none of the tested boundary genes was significantly altered at this site (Fig. 15B-D). Likewise, also earlier during development, *LOF* expression was unchanged in seedlings overexpressing *TAX1* (Fig. 15E-F). Finally, when the expression of the boundary genes was quantified in the paraclade junctions of mature *tax1tax2* double mutant; no changes in *LOF* expression were observed (Fig. 15G-H).

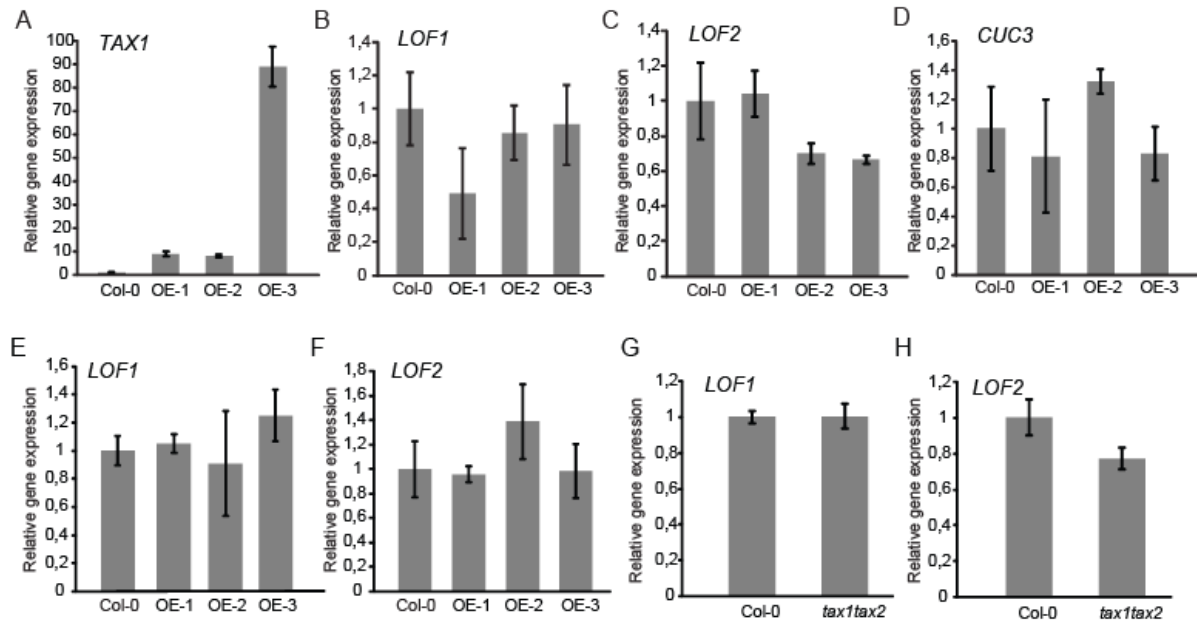


Figure 15. Expression of lateral organ boundary genes does not change in *TAX1* overexpressing lines. (A-D) Relative expression of *TAX1* and boundary genes in the paraclade junctions of 35S::*TAX1* lines (*TAX1* OE abbreviated as OE in figure A-D) cultivated in the greenhouse for 5 weeks. Expression values were normalized to those of the wild type (Col-0), set to 1. Values represent the average of three biological replicates \pm SE. (E-F) *LOF1* (E) and *LOF2* (F) expression in 19-day-old seedlings. (G-H) *LOF1* (G) and *LOF2* (H) expression in paraclade junctions of 5-week-old *tax1tax2* plants. Statistical analysis revealed no significant difference between (B-F) OE and Col-0 lines ($n=3$), or between the (G-H) *tax1tax2* ($n=4$) and Col-0.

Since expression of these genes was quantified in the paraclade junctions which were already further along in development, we generated inducible lines in which the expression of *TAX1* could be induced upon treatment with a steroid hormone dexamethasone (DEX).

Induced *TAX1* expression did not result in changes in *LOF* or *CUC* expression

An inducible line was generated by making a cross between lines expressing the UAS::*TAX1* and GAL4VP16GR constructs. Application of DEX which binds to the glucocorticoid receptor (GR) causes the GAL4VP16 protein to enter the nucleus where it binds to the UAS and drives the expression of *TAX1* resulting in overexpression of the gene. Several genes are spatiotemporally regulated, to determine if induced *TAX1* expression can result in changes in the expression of *LOF* and other boundary genes, seedlings were treated with DEX and harvested 2, 4, 6-h after treatment. Expression of *TAX1* T-DNA was visible 2-h after DEX treatment confirming that the induction worked (Fig. 16A). There was a difference in expression level between the DEX and EtOH treated samples at 2-h for *CUC3* (Fig. 16F). *CUC1* and *LOF2* level was also reduced after 4-h of DEX treatment (Fig. 16C-D) but no effect on *LOF1* was detected (Fig. 16B).

Chapter 3

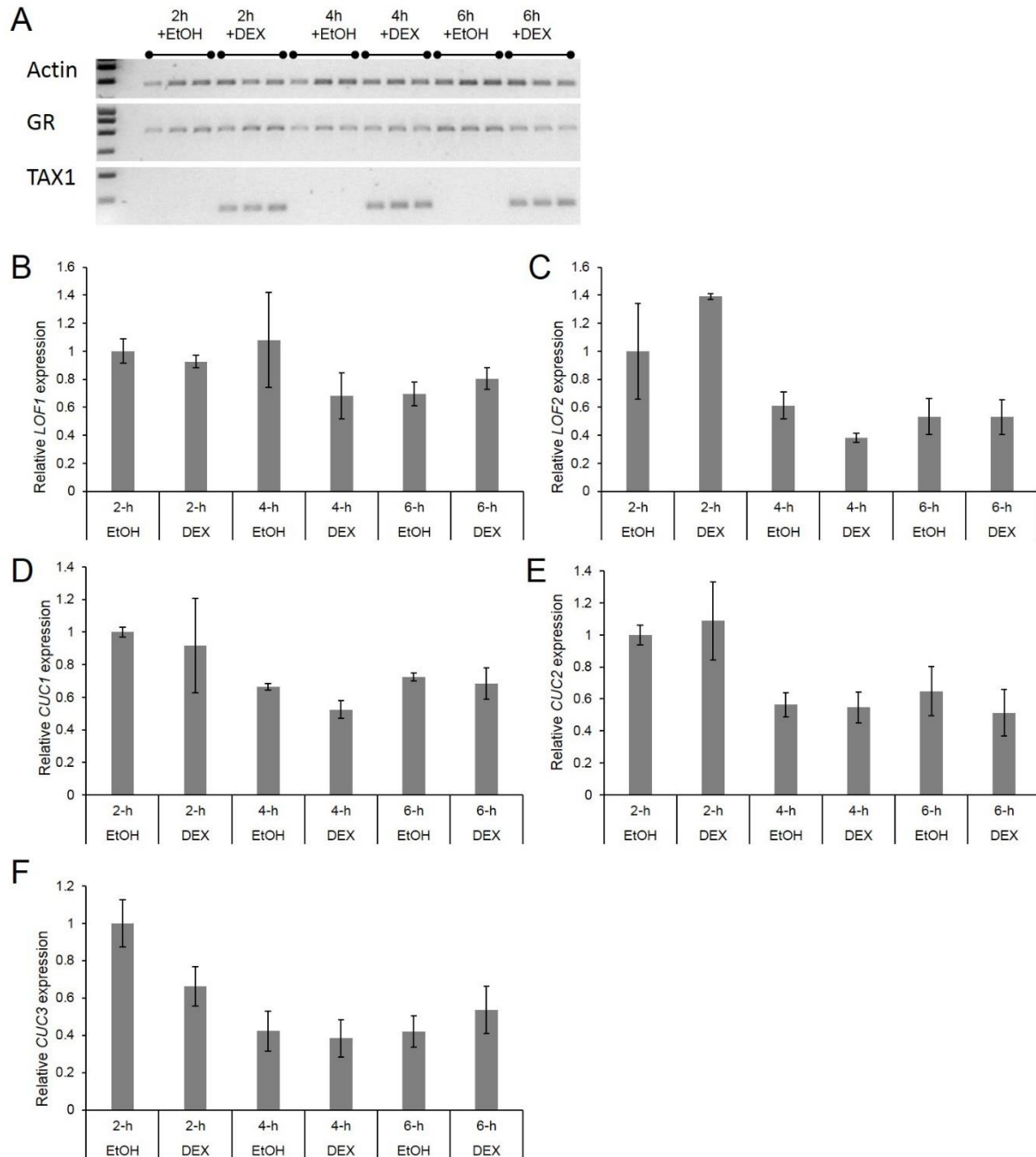


Figure 16. RT-PCR of *TAX1* expression and RT-qPCR quantification of boundary genes in Col-0 and inducible line treated with DEX or EtOH. Expression of (A) *TAX1* and *GAL4VP16GR* (in seedlings treated with 5 μ M DEX or EtOH (control) at the different time points; and (B) Relative expression levels of *LOF1* (B), *LOF2* (C), *CUC1* (D), *CUC2* (E), *CUC3* (F) in the inducible line treated with EtOH or DEX. Values represent the average of three biological replicates \pm SE (standard error).

This experiment was performed on 2-week-old seedlings and the quantification of the genes in these tissue indicated that the *LOF* and *CUC* genes were not highly expressed in seedlings. Therefore, this experiment was repeated by treating the SAM of the inducible line which were

cultivated in short day conditions with either EtOH or 5 μ M DEX. The expression of the relevant genes was quantified again and *TAX1* induction was confirmed (Fig. 17A). None of the other genes displayed a difference between the control and induced lines (Fig. 17B-F).

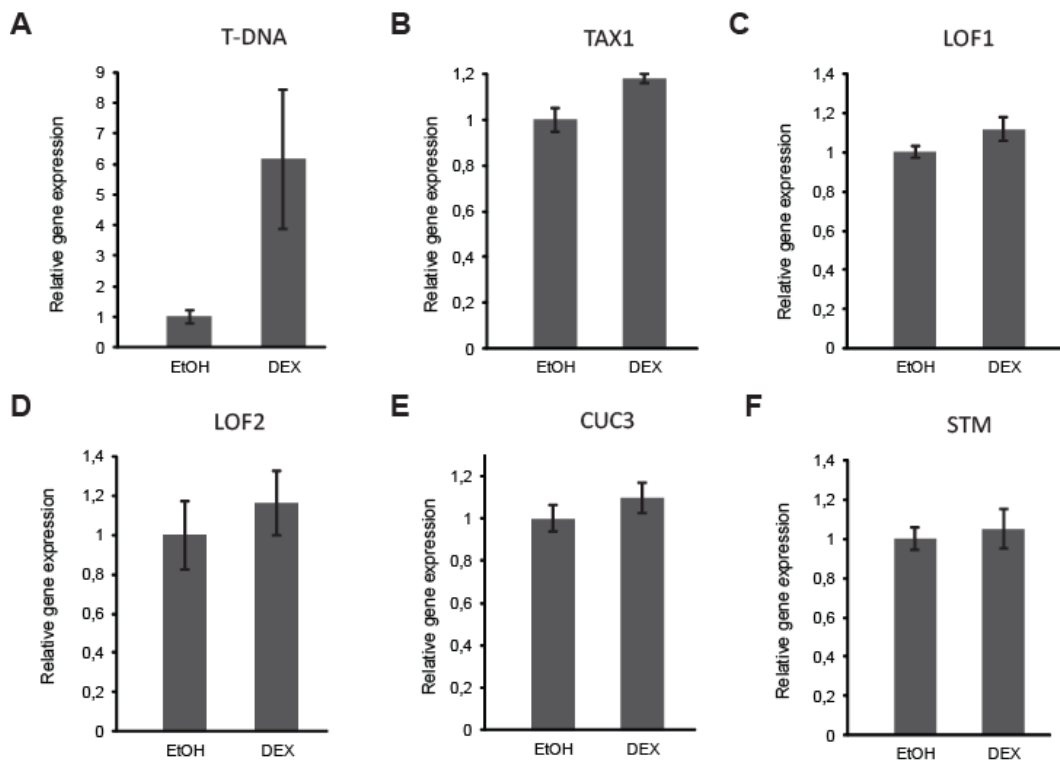


Figure 17. Quantification of the expression of boundary genes in the SAM of 6-week old DEX treated plants of the *TAX1* inducible line. Relative expression of (A) T-DNA (*TAX1*), (B) total *TAX1* (T-DNA and endogenous), (C) *LOF1*, (D) *LOF2*, (E) *CUC3* and (F) *STM* in Col-0 treated with EtOH or DEX. Expression values were normalized to those of the EtOH treated samples set to 1. Values represent the average of three biological replicates \pm SE (standard error).

Since *TAX1* OE does not appear to interfere with *LOF1* regulatory activity and also does not alter the expression of *LOF1*, it is possible that *TAX1* OE can result in miss-expression of the *LOF* genes. To determine if the expression pattern of *LOF* was altered by *TAX1* OE, crosses were made between the promoter trap (GT12154) line for *LOF1* and *TAX1* OE-2 and also between p*LOF2*::GUS and *TAX1* OE-3.

Constitutive *TAX1* expression does not alter the expression pattern in *LOF1* and *pLOF2::GUS*

In seedlings GUS expression for the promoter trap line of *LOF1* (*Ler* ecotype) was located in a band of cells on the adaxial side of rosette leaf bases and in the boundary region between the SAM and lateral organs (Lee *et al.*, 2009). This expression pattern was observed in seedlings of the promoter trap line (Fig. 18A). The expression pattern and expression intensity in this line did not change in the *35S::TAX1* background (Fig. 18B). In the *pLOF2::GUS* lines, the GUS pattern was detected in the organ boundaries (Lee *et al.*, 2009). However, no GUS expression was observed in the SAM of the *pLOF2::GUS* seedlings in the conditions used here (Fig. 18C) and this expression pattern remained unchanged after crossing with *35S::TAX1* OE-3 (Fig. 18D). In the paraclade junctions both the expression intensity and pattern of *pLOF2*-driven GUS remained unaltered under *TAX1* overexpression (Fig. 18E-F), confirming the RT-qPCR results.

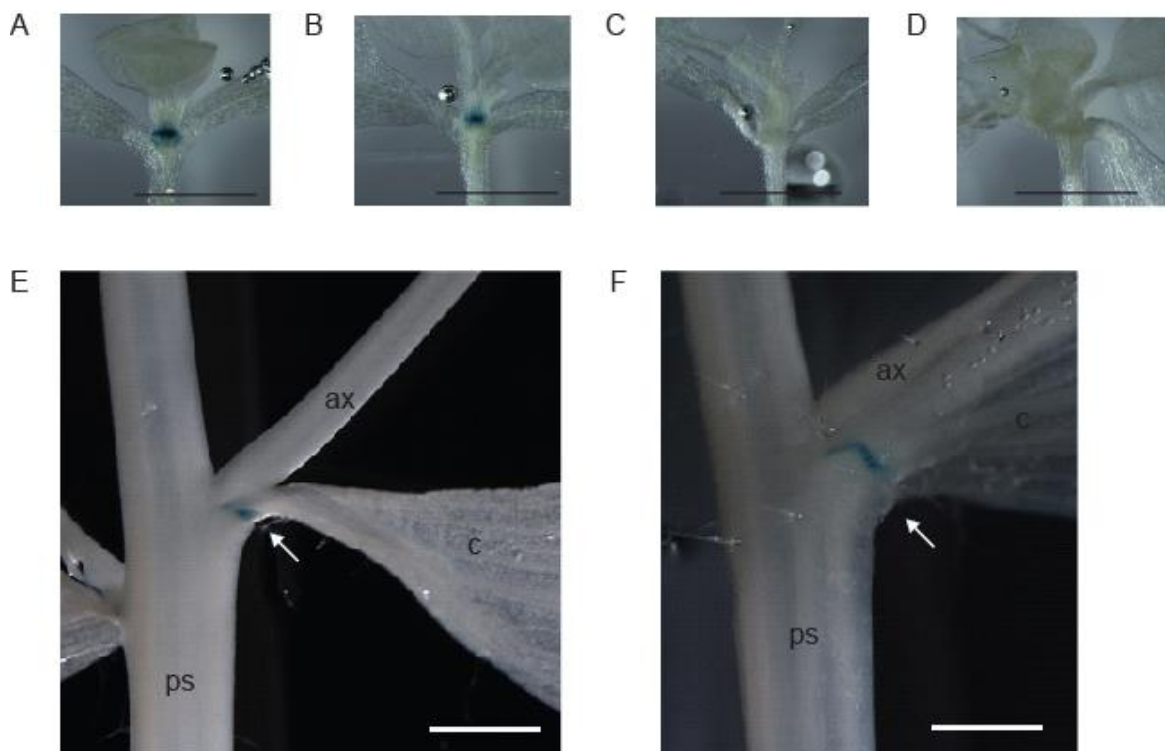


Figure 18. GUS staining of 10-day old *in vitro* germinated seeds for *LOF1* (gene trap) and *pLOF2::GUS* and the cross with *35S::TAX1*. GUS expression pattern in (A) *LOF1::GUS* (GT), (B) cross between *LOF1::GUS* (GT) and *35S::TAX1* OE-2, (C) *pLOF2::GUS* and (D) cross between *pLOF2::GUS* and *35S::TAX1* OE-3, in 10 day old seedlings. GUS expression for (E) *LOF2* was located at the base of the cauline leaf; and a similar expression was observed in the (F) cross between *pLOF2::GUS* and *35S::TAX1* OE-3 in mature 28-day old plants cultivated in the greenhouse. The scale bar in A-F is 1 mm. Arrows indicate the *LOF2* expression domain. Abbreviations are, ps, primary stem; ax, axillary stem; c, cauline leaf.

Collectively, these results indicate that TAX1 does not function upstream of LOF1. Next, whether the LOF1 transcription factor functions upstream of *TAX1* was investigated, first by testing if the LOF1 alleles can regulate *TAX1* expression using a TEA.

The two alleles of the MYB transcription factor LOF1 do not regulate *TAX1* expression

In silico analysis using the Athena promoter platform revealed that the promoter of *TAX1* has several MYB binding sites (Fig. 19A). To test if LOF1.1 and LOF1.2 can bind to the promoter of *TAX1* and regulate its expression, a TEA was performed in which the fLUC reporter gene was fused to the promoter of *TAX1* and co-transfected in tobacco protoplasts with a construct which overexpresses the LOF1.1 or LOF1.2 alleles. Changes in fLUC expression levels were quantified and only a negligible increase in fLUC expression with no biological significance was observed in this *in vitro* assay (Fig. 19B). These results suggest that *LOF1* might not directly regulate *TAX1* expression, but it is possible that other genes which regulate or are regulated by *LOF1* and/or *TAX1* may connect them *in vivo*.

Chapter 3

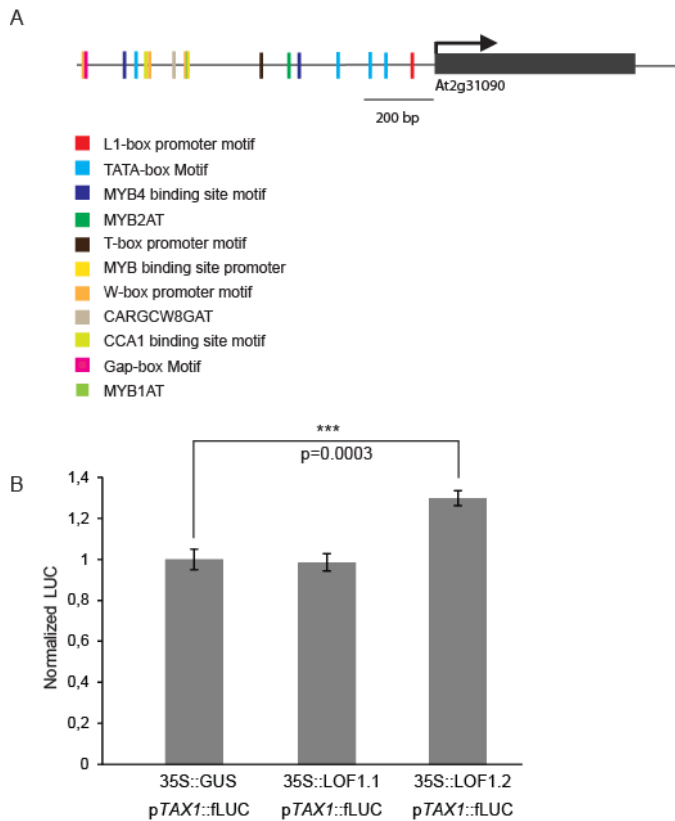


Figure 19. Transient expression assay testing if LOF1 can regulate *TAX1* expression.

(A) Promoter region of *TAX1* 989 bp upstream of the start codon for *TAX1* (adapted from Athena promoter platform (<http://www.bioinformatics2.wsu.edu/cgi-bin/Athena/cgi/visualize.pl>)). (B) *LOF1* variants do not transactivate p*TAX1*. Transactivation assay in tobacco protoplasts co-transfected with a p*TAX1*::fLUC reporter construct, effector constructs overexpressing LOF1.1 or LOF1.2 and an rLUC construct for normalization (Van den Bossche *et al.*, 2013). Values are fold-changes relative to protoplasts transfected only with a GUS expression construct instead of LOF1 effector constructs and are the mean (\pm SE) of eight biological repeats. Significant differences (Student's *t*-test): ***, $p < 0.001$.

If LOF1 does function upstream of *TAX1*, the loss of *LOF1* could result in increased *TAX1* expression. To test this, *TAX* expression in the paraclade junctions of the *lof1/lof2* line was quantified.

The expression of *TAX* genes in nodes of 6 week old *lof1/lof2* mutants remains unchanged

Quantification of the expression levels in the nodes of the *lof1/lof2* mutant indicated that *LOF1* expression was reduced, but not completely absent in this tissue in contrast to previous findings (Fig. 20A). The *STM* and *CUC3* genes were significantly reduced as reported

previously (Fig. 20B, G). No significant change in expression of the *TAX* genes were observed in the mutant (Fig. 20C-D) and the fusion phenotype in this line is therefore not correlated by the overexpression of *TAX1* in the paraclade junctions.

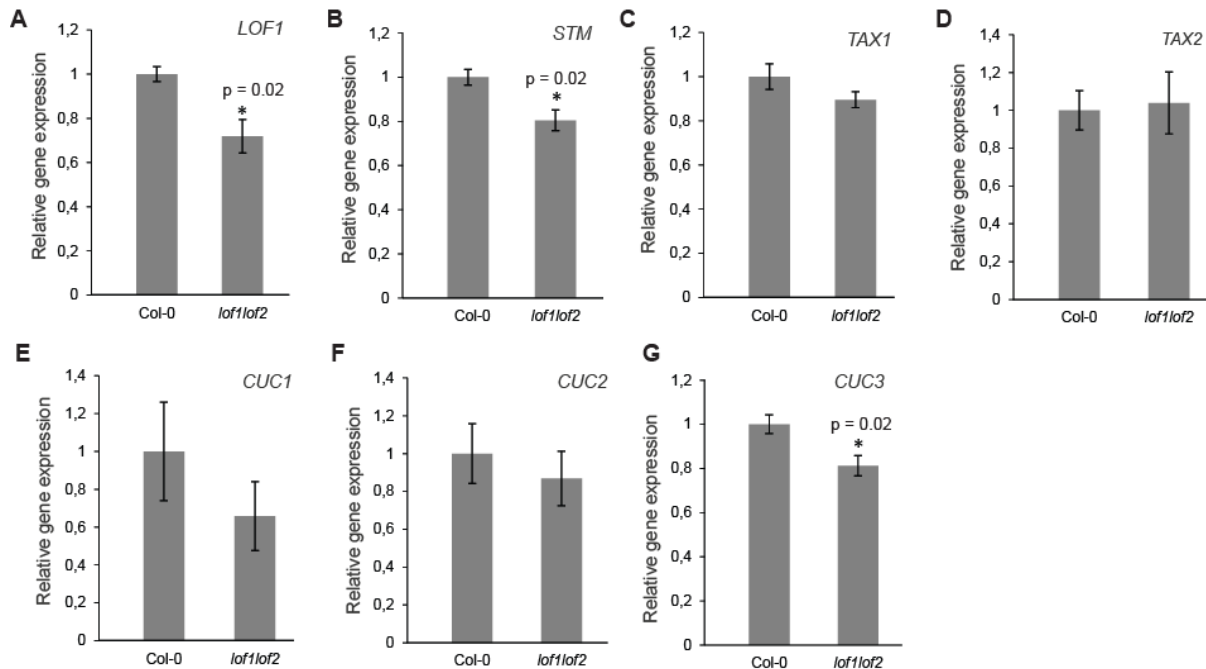


Figure 20. Quantification of *TAX* and other boundary genes in nodes of 5 week old *lof1lof2* mutants. Relative expression levels of *TAX1*, *TAX2*, *LOF1*, *CUC1-3* and *STM* were quantified in the nodes of 6 week old plants cultivated in the greenhouse. Expression values were normalized to those of the wild type (Col-0), set to 1. Values represent the average of 4 replicates \pm SE. Asterisks represent significant differences (*, $p < 0.05$; T-test)

Transformation of *TAX1* OE with *LOF1* OE construct did not rescue the fruit or paraclade junction phenotypes

Previously, transformation of the *lof* mutant with a functional copy of *LOF1* restored the bending phenotype observed in the *lof1* mutant. Therefore, transformation of the *TAX1* OE lines with a construct which constitutive express *LOF1* was used to determine if this could rescue the bending phenotype. All *TAX1* OE lines, *lof1lof2* mutant and Col-0 lines were transformed with a construct which constitutively expresses either the *LOF1.1* or *LOF1.2* allele. Preliminary observation of F1 lines indicated that the *LOF1.2* allele could rescue the bending phenotype in the *lof1lof2* mutant, but not *LOF1.1*. Neither *LOF1* alleles could rescue the phenotypes observed in the *TAX1* OE line (data not shown). This finding suggests that *TAX1* independently activates a signalling cascade for boundary formation and that

Chapter 3

overexpression of *LOF1* could not directly alter or restore the developmental program for separating organs in the paraclade junctions of these *TAX1* OE lines. However, observations from *LOF1* OE lines suggests that there may still be some links between these two signalling pathways which remains to be elucidated.

***TAX1* expression is reduced in *LOF1* OE lines**

Three lines which constitutive express the *LOF1* gene in different backgrounds were obtained. One *LOF1* OE line in the *Ler* background was generated with an activation tagging method and the 35S enhancers were inserted in the promoter region of *LOF1* (Gomez *et al.*, 2011). These plants displayed specific phenotypes in the siliques which were small and wrinkled, therefore being called CONSTRICTED FRUIT (*ctf*) phenotype. The other two *LOF1* OE (OE-1 and OE-2) lines were generated after transformation of Col-0 plants with the *LOF1.2* allele.

The expression of *LOF* and *TAX1* genes were quantified in 17-day-old *in vitro* plants. *LOF1* expression was increased in both *LOF1* OE lines (Col-0 background) with line OE-2 displaying the highest *LOF1* expression (Fig. 21B). At the same time, *LOF2* expression was reduced in both *LOF1* OE lines (Fig. 21C). Interestingly, *TAX1* expression was also reduced in both *LOF1* OE lines (Fig. 21A). Additionally, in the the *ctf* line in the *Ler* background, *TAX1* expression was also very low, with expression only being detected in two out of the four samples (Fig. 21D). However, overexpression of *LOF1* could not be confirmed in the *ctf* line, in contrast, expression of this gene appeared to be significantly reduced in this line (Fig. 21E). Previously, overexpression of *LOF1* in this line was determined by RT-qPCR in plants and also by using *in situ* hybridization to detect expression patterns in floral organs (Gomez *et al.*, 2011). Since insertion of the 35S enhancers lead to increase of the endogenous expression patterns of a gene, the phenotypes observed is representative of the increased expression rather than ectopic expression of the gene (Gomez *et al.*, 2011). Therefore, since our earlier findings indicated that *LOF1* expression in seedlings is very low, this reduced *LOF1* expression in *ctf* seedlings may be representative of the low expression in this tissue or developmental stage. *LOF2* expression was also slightly, but not statistically significantly reduced in the *ctf* line (Fig. 21F).

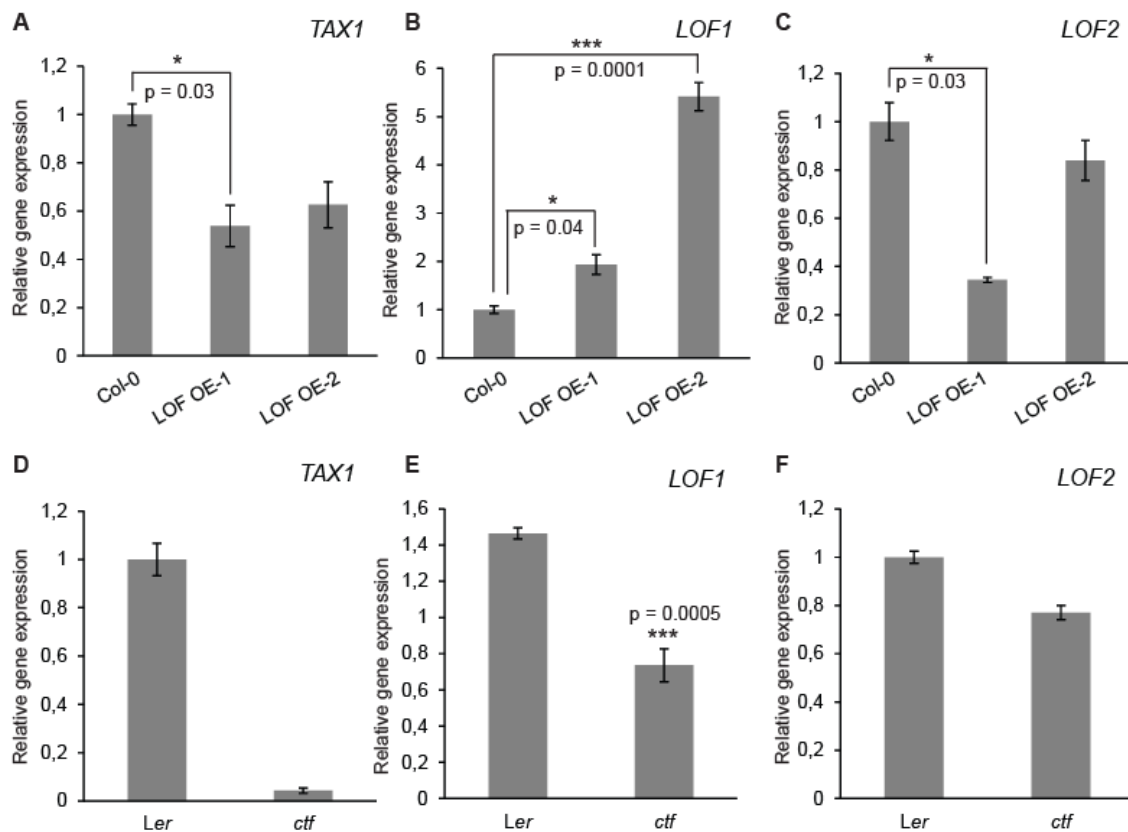


Figure 21. Quantification of the expression of boundary genes in Col-0, Ler, *ctf* and 35S::LOF1 lines. Relative expression of (A and D) *TAX1*, (B and E) *LOF1*, (C and F) *LOF2* was quantified in 17-day-old plants germinated *in vitro* which overexpress LOF1 in the Col-0 (A-C) or Ler (D-F) background. The expression values were normalized to those of the wild-type (set to 1). Values represent the average of four biological replicates \pm SE (standard error). *TAX1* in (D) represent the average of two samples. Asterisks represent significant differences (*, $p < 0.05$; **, $p < 0.001$; one way ANOVA, Tukeys HSD post hoc test for LOF1 OE lines (Col-0) and T-test for *ctf* line).

TAX1 overexpression has only minor effects on the leaf and root metabolome

Having documented developmental phenotypes for the *TAX1* overexpressors, and given the link of the *T. baccata* homolog *TAXIMIN* with plant metabolism (Onrubia *et al.*, 2014), an established GC-MS protocol was used to assess whether *TAX1* overexpressing seedlings contained changes in the levels of primary metabolites in their leaves (Annex, Table S3) and roots (Annex, Table S4). The results of these analysis are presented in the heatmap of Fig. 22. Four, eight, and 22 of 61 measured metabolites were significantly different in the leaves of weak (OE-1), intermediate (OE-2), and strong (OE-3) *TAX1* overexpressing lines, respectively, with only phosphate and serine being altered (enhanced in both instances) in all three lines. That said, sucrose and glucose 6-phosphate were increased in both line OE-2

Chapter 3

and line OE-3, whilst threonine was significantly decreased in both lines. Line OE-3 was additionally characterized by increased levels of histidine, putrescine, glucose, 4-hydroxyproline, ribulose 5-phosphate, asparagine, pyroglutamate, glutamine, glycerate, β -alanine, proline, malate, glutamate, and arginine. In contrast, this line displayed decreased levels of dehydroascorbate, threonate, and threitol. In roots, the changes were even less marked, with two, six, and 10 of 61 metabolites significantly different in the weak, intermediate, and strong overexpressing lines, respectively, and only serine being altered (again enhanced) in all three lines. That said, glycolate, succinate, sucrose, and β -alanine were increased in both line OE-2 and line OE-3, whilst hydroxyproline, pyroglutamate, glutamine, proline, aspartate, and fumarate were increased and histidine decreased only in line OE-3.

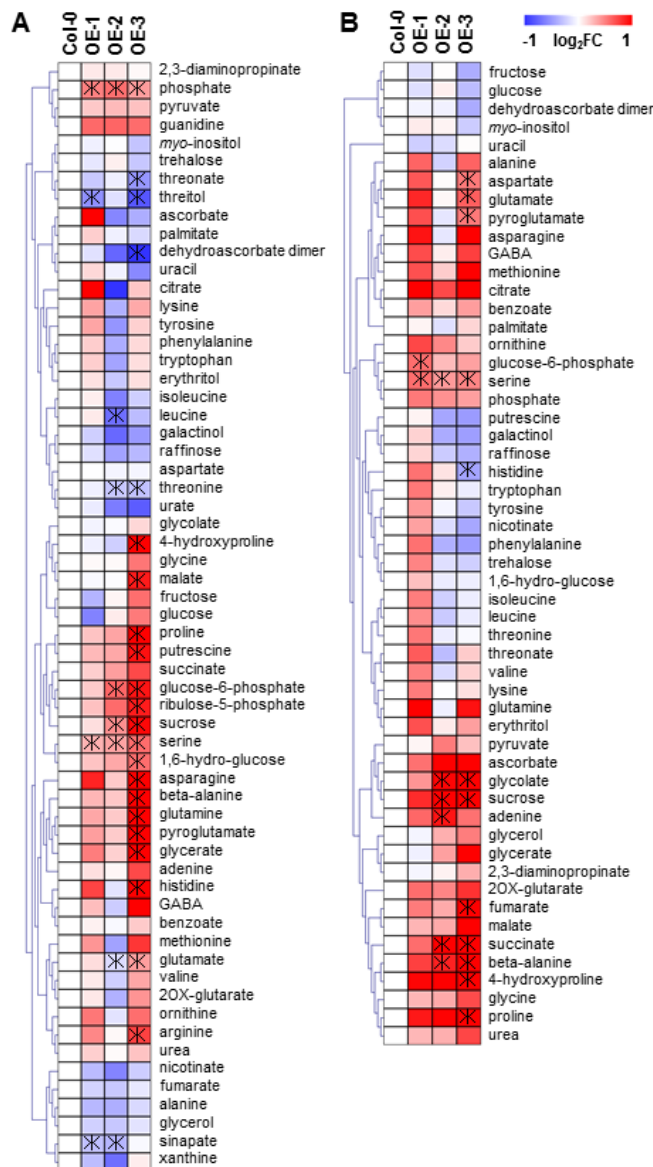


Figure 22. *TAX1* overexpression results in minor alterations of primary metabolites in leaf and root. Metabolic changes in *TAX1* overexpressing (OE) lines in (A) leaf and (B) root were visualized by heat-map. Analysis was performed with four independent biological replicates. Relative peak area was normalized by internal standard and fresh weight. Fold change against Col-0 is shown with a logarithmic scale. Fold change is visualized by colour codes, with red and blue indicating higher and lower, respectively. Hierarchical clustering by Pearson correlation was conducted using MeV software (<http://www.tm4.org/mev.html>). Asterisk represents statistical significance ($P < 0.05$).

DISCUSSION

More than 1,000 signalling peptides, most of them still uncharacterized, are encoded in the *Arabidopsis* genome (Czyzewicz *et al.*, 2013). A first characterization of a family of two

Chapter 3

Arabidopsis peptides, TAX1 and TAX2, the homologues of the TbTAX (Onrubia *et al.*, 2014), has been presented here. TbTAX was shown to localize to the plasma membrane through the secretory system and ectopically activate specialized metabolite pathways in yew and tobacco cells (Onrubia *et al.*, 2014).

Regulatory neofunctionalization of the *Arabidopsis* TAX genes

Because of the relative sequence similarity between *Arabidopsis* TAX1 and TAX2, the possible functional redundancy was investigated. During evolution, a paralogue may have lost all functionality or gained a new function. Other catalogues shared the ancestral function or remained redundant in *Arabidopsis* (De Smet and Van de Peer, 2012). The promoters of the *Arabidopsis* TAX genes have very distinct expression patterns, with TAX2 being expressed mainly in the vasculature and TAX1 rather at specific sites such as anthers and nectaries in flowers, the paraclade junction on the primary stem and the L1 layers of the SAM, implying at least regulatory neofunctionalization of the two *Arabidopsis* TAX genes. Furthermore, overexpression of TAX1, but not of TAX2 or TbTAX led to severe developmental phenotypes, suggesting functional specialization of the *Arabidopsis* TAX peptides, with roles in diverging target pathways. The pronounced effects caused by TAX1 overexpression on the *Arabidopsis* developmental programs that we report here, raise the possibility that the effect of TbTAX on metabolism might be indirect and caused by preceding developmental rewiring. Accordingly, the biosynthesis of paclitaxel in *Taxus* spp. is tissue-dependent (Vidensek *et al.*) and overexpression of TbTAX in tobacco hairy roots led to morphological changes (Onrubia *et al.*, 2014).

TAX1 overexpression mimics loss of LOF function

Several developmental phenotypes are apparent in TAX1 overexpressing lines at the paraclade junction: (i) cauline leaves are partially fused to the axillary stem, (ii) the leaf base forms a decurrent strand extending down along the primary stem and (iii) axillary stems bend downwards before growing upwards again, probably due to phototropism. The severity of these phenotypes was associated with the TAX1 expression levels in the paraclade junctions. Similar phenotypes have been described for the *lof1-1* and *lof1-1lof2-1* mutants (Lee *et al.*, 2009). The latter lines are defective in the closely related MYB-domain transcription factors LOF1 and LOF2, which are expressed in *Arabidopsis* organ boundaries. In *lof1-1*, the cauline leaves are also fused to the axillary branch at the base, which bends down and completely

lacks accessory shoots (Lee *et al.*, 2009). Only in the *lof1-1lof2-1* double mutant, additional phenotypes that are also presented in *TAX1* overexpressing lines, such as the decurrent leaf attachment, were observed.

Nonetheless, *TAX1* expression did not interfere with LOF1 regulatory activity *in vitro* (Fig. 14) and no reduction in *LOF1* and *LOF2* expression levels was detected in *TAX1* OE paraclade junctions or seedlings (Fig. 15B-C, E-F). Therefore, down-regulation of *LOF1* and *LOF2* is not causal for the phenotype. Conversely, *TAX1* expression was not de-regulated in *lof1-1lof2-1* paraclade junctions (Fig. 20C), suggesting that high *TAX1* expression was not causal for fusion defects in this line. Additionally, LOF1 did not alter *TAX1* expression in the *in vitro* expression assay (Fig. 19B). Another boundary gene that has been linked to fusion of cauline leaves to the primary stem is *CUC3* (Hibara *et al.*, 2006). *CUC3* expression was also down-regulated in *lof1-1* and *lof1-1lof2-1* paraclade junctions (Lee *et al.*, 2009) and *LOF1* expression was down-regulated in the *cuc3-105* mutant (Gendron *et al.*, 2012). The *cuc3-105* allele also enhanced paraclade fusions in the *lof1-1* background (Lee *et al.*, 2009). However, *CUC3* expression did not change in paraclade junctions of the *TAX1* overexpression lines (Fig. 15D). Fusion phenotypes are often observed in loss-of-function mutants for genes expressed in the boundary (Žádníková and Simon, 2014). However, promoter activity in the SAM shows that *TAX1* is not a boundary gene itself. The fact that the most well-known boundary genes affecting fusion of cauline leaves to neighbouring organs do not show a change in expression in *TAX1* overexpressing lines suggests that *TAX1* might work in a converging, yet unknown, signalling pathway.

Another *TAX1* overexpression phenotype linked with the paraclade junction is the reduced capability to form accessory shoots (Fig. 13). Removal of apical dominance of the axillary branch did not increase the number of accessory shoots, but the ones that did grow out had Wt length. Interestingly, all *TAX1* overexpressing lines, including those with modest *TAX1* overexpression showing no obvious fusion defect, have reduced numbers of accessory shoots. This result corresponds to the hypothesis that organ fusion and lack of accessory shoot formation could be independent processes (Lee *et al.*, 2009) and the effect on accessory shoots could be related to the developmental lag observed in the *TAX1* OE lines.

***TAX1* overexpression also affects fruit development**

TAX1 overexpression also resulted in shorter siliques with outwards protrusions at the tip of both valve tissue and the replum resulting in seed crowding (Fig. 5D). Basal parts of the fruit were however normal. In contrast to lateral organ separation, a role for plant peptides in

Chapter 3

Arabidopsis fruit development is known. For instance, the CLE peptide family was discovered due to the club-shaped fruit of the *clv3* mutant, resulting from an enlarged flower meristem and extra floral whorls (Clark *et al.*, 1996). Overexpression of members of the *DEVIL/ROTUNDIFOLIA4 (DVL/ROT)* family resulted in an alteration of silique morphology with different members causing different phenotypes, including protrusions at the tip in *DVL1* overexpressors (Wen *et al.*, 2004). Although the exact cellular and molecular bases of these phenotypes are currently not well understood, *DVL1* expression was associated with down-regulation of the valve identity regulator *AGL8/FRUITFUL (FUL)* (Wen *et al.*, 2004). Several organ-meristem boundary genes also influence fruit development. Gain-of-function lines of *CUC1* and *CUC2* prevent congenital fusion of carpels (Larue *et al.*, 2009; Nikovics *et al.*, 2006; Sieber *et al.*, 2007) and the *LOF1* gain-of-function line *constricted fruit 1 (ctf1)* displays small misshapen fruits with increased replum size and enhanced expression of the valve margin identity markers *SHATTERPROOF1 (SHP1/AGL1)* and *SHP2/AGL5* (Gomez *et al.*, 2011). The effect of *TAX1* overexpression on fruit development could therefore be linked to its influence on lateral organ separation.

LOF1 overexpression influences TAX1 expression

Quantification of *TAX1* expression in *LOF1* OE lines showed that overexpression of *LOF1* can result in a reduction in *TAX1* expression. Although we could not show increased *LOF1* expression in the *ctf* line, this result may be due to the low expression level of *LOF1* in the seedlings and may be caused by gene silencing in this tissue. However, *TAX1* expression was significantly reduced in these *ctf* lines. This suppression may be indirect through one of the target genes of *LOF1*. It is possible that in the *lof1* mutant, the loss of *LOF1* regulation may result in (directly) in *TAX1* expression in a stage or in tissue where it should be repressed (ectopic expression). This would explain the observed phenotypes when *TAX1* is constitutively expressed with a 35S promoter and could be further investigated by crossing the promoter lines for *TAX1* (p*TAX1*::GUS) in the *lof1* mutant background.

TAX1 overexpression mildly affects the primary metabolome

The primary metabolome of *TAX1* overexpressing seedlings was profiled to determine if *TAX1* influences metabolism since TbTAX signalling appeared to influence plant metabolism (Onrubia *et al.*, 2014). The changes observed in the primary metabolites were comparatively mild in the overexpressors with only two of the changes conserved across the genotype in

leaves, namely phosphate and serine, and only one (again serine) in the roots. However, the extent of metabolic change was consistent with the degree of overexpression and the severity of the developmental phenotypes in the lines. When assessed at a pathway level, the leaf data clearly suggest an elevated rate of photosynthesis on a per gram fresh weight basis, with increases in pentose- and hexose phosphates as well as in sucrose. In addition, the intimately connected pathway of photorespiration appears to be upregulated as indicated by the above-mentioned increases in serine and also in glycerate. The enhanced levels of phosphate would also be anticipated to facilitate the operation of photosynthesis, which can be phosphate-limited *in vivo*, suggesting that the increase in sucrose was not due to an inhibition of sucrose export driven by the lower sink strength, but rather indicative of an increased rate of sucrose synthesis. Of note, but only in the strongest line, was a general increase in the levels of the amino acids intimately associated with the TCA cycle. Such changes have previously been observed following increases in leaf sucrose (see for example Purdy *et al.*, 2013) and have been noted to invoke changes in the levels of some phytohormones, such as gibberellic acid (Araújo *et al.*, 2012). However, these metabolic changes were only seen in line OE-3 and not in line OE-2, which has a very similar, albeit less severe, developmental phenotype, and as such it is difficult to envisage them being causal of these phenotypes. Similar arguments preclude a strong case for a role of putrescine in the determination of the phenotype, despite considerable evidence being presented that this metabolite can exhibit bioactivity (Handa and Mattoo, 2010). The root data presented fewer metabolic differences; however, two were highly notable. First, consistent with recent reports on the functionality of the enzymatic reactions of photorespiration in roots (Nunes-Nesi *et al.*, 2014), considerable changes were seen not only in serine but also in glycolate within this tissue. However, given that the exact function of these reactions in root tissue is currently not established, the significance of this observation remains unclear. Second, a much clearer up-regulation of the TCA cycle intermediates and closely associated metabolites were observed, albeit only significantly in the strongest overexpressing line. Previous work on tomato lines exhibiting reduced expression of any of the TCA cycle enzymes revealed that this resulted in decreased root growth, most likely as a compound result of decreases in cell wall biosynthesis and an alteration in the balance of phytohormone levels (van der Merwe *et al.*, 2009).

Peptide signalling in lateral organ separation

Additional phenotypes were caused by *TAX1* overexpression in the *Ler* background compared to *Col-0*, such as bending at a tertiary branch point and twisting of the stem. It has been reported that the *Ler* ecotype influences lateral organ phenotypes. For example, the *Ler*

Chapter 3

background possibly increases organ fusion between cauline leaf and axillary stem in *lob* mutants defective in the transcription factor LATERAL ORGAN BOUNDARIES (LOB) (Bell *et al.*, 2012). LOB negatively regulates brassinolide (BR) biosynthesis in organ boundaries by activating the expression of the *BAS1* gene encoding a BR-inactivating enzyme. Consequently, loss of *LOB* leads to hyperaccumulation of BR in the boundary (Bell *et al.*, 2012). Similarly, hyperactivation of BR signalling in the *bzr1-D* mutant or BR treatment also leads to fusion of the cauline leaf to the axillary stem and is associated with bending of the primary stem (Gendron *et al.*, 2012). The *bzr1-D* mutation constitutively activates the BZR1 transcription factor, capable of targeting the promoters of a plethora of genes, including *CUC3* (Gendron *et al.*, 2012; Guo *et al.*, 2013). Accordingly, not only *CUC3* expression, but also *LOF1* expression was reduced in *bzr1-D* paraclade junctions by BR treatment (Gendron *et al.*, 2012). Further work will be required to determine the relationship between *TAX1* overexpressing phenotypes and hormone signalling.

The lack of any obvious phenotype for a *tax1* loss-of-function mutant raises the possibility of functional redundancy or that overexpression of *TAX1* leads to ectopic receptor activation (Rowe and Bergmann, 2010; Torii, 2012). Notwithstanding, the presented work implicates the existence of a peptide signal cascade regulating lateral organ separation in *Arabidopsis*.

ACKNOWLEDGEMENTS

We thank Patricia Springer for providing seeds of *lof1-1lof2-1*, p*LOF2*::GUS, GT12154 (*LOF1* gene trap) and ET4016 (*LOF1* enhancer trap) and Juann Carbonell for providing seeds for *ctf*. Paul Wintermans, Amparo Cuéllar Pérez, Astrid Nagels Durand and Robin Vanden Bossche are thanked for excellent technical assistance, and Annick Bleys for help in preparing the manuscript. This work has been supported by funding from the Research Foundation-Flanders through the project G005312 and the Special Research funds from Ghent University and the National Research Foundation (NRF) from South-Africa for a North-South “Sandwich”-type predoctoral scholarship to J.C. L.P. is a postdoctoral fellow of the Research Foundation-Flanders.

REFERENCES

Aida M, Tasaka M (2006). Genetic control of shoot organ boundaries. *Current Opinion in Plant Biology* **9**: 72 – 77.

Alonso JM, Stepanova AN, Leisse TJ, Kim CJ, Chen H, Shinn P, Stevenson DK, Zimmerman J, Barajas P, Cheuk R, Gadrinab C, Heller C, Jeske A, Koesema E, Meyers

CC, Parker H, Prednis L, Ansari Y, Choy N, Deen H, Geralt M, Hazari N, Hom E, Karnes M, Mulholland C, Ndubaku R, Schmidt I, Guzman P, Aguilar-Henonin L, Schmid M, Weigel D, Carter DE, Marchand T, Risseuw E, Brogden D, Zeko A, Crosby WL, Berry CC, Ecker JR (2003). Genome-wide insertional mutagenesis of *Arabidopsis thaliana*. *Science* **301**: 653 – 657.

Araújo WL, Tohge T, Osorio S, Lohse M, Balbo I, Krahnert I, Sienkiewicz-Porzucek A, Usadel B, Nunes-Nesi A, Fernie AR (2012). Antisense inhibition of the 2-oxoglutarate dehydrogenase complex in tomato demonstrates its importance for plant respiration and during leaf senescence and fruit maturation. *Plant Cell* **24**: 2328 – 2351.

Bell EM, Lin W-C, Husbands AY, Yu L, Jaganatha V, Jablonska B, Mangeon A, Neff MM, Girke T, Springer PS (2012). *Arabidopsis* lateral organ boundaries negatively regulates brassinosteroid accumulation to limit growth in organ boundaries. *Proceedings of the National Academy of Sciences of the United States of America* **109**: 21146 – 21151.

Borghi L, Bureau M, Simon R (2007). *Arabidopsis* JAGGED LATERAL ORGANS is expressed in boundaries and coordinates KNOX and PIN activity. *The Plant Cell* **19**: 1795 – 1808.

Clark SE, Jacobsen SE, Levin JZ, Meyerowitz EM (1996). The CLAVATA and SHOOT MERISTEMLESS loci competitively regulate meristem activity in *Arabidopsis*. *Development* **122**: 1567 – 1575.

Clough SJ, Bent AF (1998). Floral dip: A simplified method for *Agrobacterium*-mediated transformation of *Arabidopsis thaliana*. *Plant Journal* **16**: 735 – 743.

Czyzewicz N, Yue K, Beeckman T, De Smet I (2013). Message in a bottle: Small signalling peptide outputs during growth and development. *Journal of Experimental Botany* **64**: 5281 – 5296.

De Smet R, Van de Peer Y (2012). Redundancy and rewiring of genetic networks following genome-wide duplication events. *Current Opinion in Plant Biology* **15**: 168 – 176.

Fernie AR, Aharoni A, Willmitzer L, Stitt M, Tohge T, Kopka J, Carroll AJ, Saito K, Fraser PD, DeLuca V (2011). Recommendations for reporting metabolite data. *The Plant Cell* **23**: 2477 – 2482.

Gaillochet C, Daum G, Lohmann JU (2015). O Cell , Where Art Thou? The mechanisms of shoot meristem patterning. *Current Opinion in Plant Biology* **23**: 91 – 97.

Gendron JM, Liu J-S, Fan M, Bai M-Y, Wenkel S, Springer PS (2012). Brassinosteroids regulate organ boundary formation in the shoot apical meristem of *Arabidopsis*. *Proceedings of the National Academy of Sciences of the United States of America* **109**: 21152 – 21157.

Gomez MD, Urbez C, Perez-Amador MA, Carbonell J (2011). Characterization of constricted fruit (*ctf*) mutant uncovers a role for AtMYB117/LOF1 in ovule and fruit development in *Arabidopsis thaliana*. *PLoS One* **6**: e18760.

Guo H, Li L, Aluru M, Aluru S, Yin Y (2013). Mechanisms and networks for brassinosteroid regulated gene expression. *Current Opinion in Plant Biology* **16**: 545 – 553.

Ha CM, Jun JH, Nam HG, Fletcher JC (2007). BLADE-ON-PETIOLE 1 and 2 control *Arabidopsis* lateral organ fate through regulation of LOB domain and adaxial-abaxial polarity genes. *The Plant Cell* **19**: 1809 – 1825.

- Handa AK, Mattoo AK** (2010). Differential and functional interactions emphasize the multiple roles of polyamines in plants. *Plant Physiology and Biochemistry* **48**: 540 – 546.
- Hara K, Kajita R, Torii KU, Bergmann DC, Kakimoto T** (2007). The secretory peptide gene EPF1 enforces the stomatal one-cell-spacing rule. *Genes and Development* **21**: 1720-1725.
- Hara K, Yokoo T, Kajita R, Onishi T, Yahata S, Peterson KM, Torii KU, Kakimoto T** (2009). Epidermal cell density is autoregulated via a secretory peptide, EPIDERMAL PATTERNING FACTOR 2 in *Arabidopsis* leaves. *Plant and Cell Physiology* **50**: 1019 – 1031.
- Heisler MG, Ohno C, Das P, Sieber P, Reddy GV, Long Ja, Meyerowitz EM** (2005). Patterns of auxin transport and gene expression during primordium development revealed by live imaging of the *Arabidopsis* inflorescence meristem. *Current Biology* **15**: 1899 – 1911.
- Hibara K-i, Karim MR, Takada S, Taoka K-i, Furutani M, Aida M, Tasaka M** (2006). *Arabidopsis* CUP-SHAPED COTYLEDON3 regulates postembryonic shoot meristem and organ boundary formation. *The Plant Cell* **18**: 2946 – 2957.
- Indriolo E, Tharmapalan P, Wright SI, Goring DR** (2012). The ARC1 E3 ligase gene is frequently deleted in self-compatible *Brassicaceae* species and has a conserved role in *Arabidopsis lyrata* self-pollen rejection. *The Plant Cell* **24**: 4607 – 4620.
- Joshi V, Laubengayer KM, Schauer N, Fernie AR, Jander G** (2006). Two *Arabidopsis* threonine aldolases are nonredundant and compete with threonine deaminase for a common substrate pool. *The Plant Cell* **18**: 3564 – 3575.
- Karimi M, Inzé D, Depicker A** (2002). Gateway vectors for *Agrobacterium*-mediated plant transformation. *Trends in Plant Science* **7**: 193 – 195.
- Karimi M, Bleys A, Vanderhaeghen R, Hilson P** (2007). Building blocks for plant gene assembly. *Plant Physiology* **145**: 1183 – 1191.
- Karimi M, De Meyer B, Hilson P** (2005). Modular cloning in plant cells. *Trends in Plant Science* **10**: 103 – 105.
- Khan M, Xu H, Hepworth SR** (2014). BLADE-ON-PETIOLE genes: Setting boundaries in development and defense. *Plant Science* **215-216**: 157 – 171.
- Khan M, Xu M, Murmu J, Tabb P, Liu Y, Storey K, McKim SM, Douglas CJ, Hepworth SR** (2012). Antagonistic Interaction of BLADE-ON-PETIOLE1 and 2 with BREVIPEDICELLUS and PENNYWISE regulates *Arabidopsis* Inflorescence architecture. *Plant Physiology* **158**: 946 – 960.
- Kopka J, Schauer N, Krueger S, Birkemeyer C, Usadel B, Bergmuller E, Dormann P, Weckwerth W, Gibon Y, Stitt M, Willmitzer L, Fernie AR, Steinhauser D** (2005). GMD@CSB.DB: the Golm Metabolome Database. *Bioinformatics* **21**: 1635 – 1638.
- Larue CT, Wen J, Walker JC** (2009). A microRNA-transcription factor module regulates lateral organ size and patterning in *Arabidopsis*. *Plant Journal* **58**: 450 – 463.
- Laufs P, Peaucelle A, Morin H, Traas J** (2004). MicroRNA regulation of the CUC genes is required for boundary size control in *Arabidopsis* meristems. *Development* **131**: 4311 – 4322.
- Lee D-K, Geisler M, Springer PS** (2009). LATERAL ORGAN FUSION1 and LATERAL ORGAN FUSION2 function in lateral organ separation and axillary meristem formation in *Arabidopsis*. *Development* **136**: 2423 – 2432.

Lisec J, Schauer N, Kopka J, Willmitzer L, Fernie AR (2006). Gas chromatography mass spectrometry-based metabolite profiling in plants. *Nature Protocols* **1**: 387 – 389.

Long Y, Scheres B, Blilou I (2015). The logic of communication: roles for mobile transcription factors in plants. *Journal of Experimental Botany* **66**: 1133 – 1144.

Mandel T, Moreau F, Kutsher Y, Fletcher JC, Carles CC, Eshed Williams L (2014). The ERECTA receptor kinase regulates Arabidopsis shoot apical meristem size, phyllotaxy and floral meristem identity. *Development* **141**: 830 – 841.

Murashige T, Skoog F (1962). A revised medium for rapid growth and bio assays with tobacco tissue cultures. *Physiologia Plantarum* **15**: 473 – 497.

Murphy E, Smith S, De Smet I (2012). Small signaling peptides in *Arabidopsis* development: how cells communicate over a short distance. *The Plant Cell* **24**: 3198 – 3217.

Nikovics K, Blein T, Peaucelle A, Ishida T, Morin H, Aida M, Laufs P (2006). The balance between the MIR164A and CUC2 genes controls leaf margin serration in *Arabidopsis*. *The Plant Cell* **18**: 2929 – 2945.

Noh B, Murphy AS, Spalding EP (2001). Multidrug resistance-like genes of *Arabidopsis* required for auxin transport and auxin-mediated development. *Plant Cell* **13**: 2441 – 2454.

Nunes-Nesi A, Florian A, Howden A, Jahnke K, Timm S, Bauwe H, Sweetlove L, Fernie AR (2014). Is there a metabolic requirement for photorespiratory enzyme activities in heterotrophic tissues? *Molecular Plant* **7**: 248 – 251.

Onrubia M, Pollier J, Vanden Bossche R, Goethals M, Gevaert K, Moyano E, Vidal-Limon H, Cusidó RM, Palazón J, Goossens A (2014). Taximin, a conserved plant-specific peptide is involved in the modulation of plant-specialized metabolism. *Plant Biotechnology Journal* **12**: 971 – 983.

Proost S, Van Bel M, Vanechoutte D, Van de Peer Y, Inze D, Mueller-Roeber B, Vandepoele K (2014). PLAZA 3.0: an access point for plant comparative genomics. *Nucleic Acids Research* **43**: D974 – D981.

Purdy SJ, Bussell JD, Nunn CP, Smith SM (2013). Leaves of the *Arabidopsis* maltose exporter1 mutant exhibit a metabolic profile with features of cold acclimation in the warm. *PLoS One* **8**: e79412.

Rast MI, Simon R (2008). The meristem-to-organ boundary: more than an extremity of anything. *Current Opinion in Genetics & Development* **18**: 287 – 294.

Rowe MH, Bergmann DC (2010). Complex signals for simple cells: the expanding ranks of signals and receptors guiding stomatal development. *Current Opinion in Plant Biology* **13**: 548 – 555.

Schauer N, Steinhauser D, Strelkov S, Schomburg D, Allison G, Moritz T, Lundgren K, Roessner-Tunali U, Forbes MG, Willmitzer L, Fernie AR, Kopka J (2005). GC-MS libraries for the rapid identification of metabolites in complex biological samples. *FEBS Letters* **579**: 1332 - 1337.

Shimada TL, Shimada T, Hara-Nishimura I (2010). A rapid and non-destructive screenable marker, FAST, for identifying transformed seeds of *Arabidopsis thaliana*. *Plant Journal* **61**: 519 – 528.

Chapter 3

Sieber P, Wellmer F, Gheyselincx J, Riechmann JL, Meyerowitz EM (2007). Redundancy and specialization among plant microRNAs: role of the MIR164 family in developmental robustness. *Development* **134**: 1051 – 1060.

Skopelitis DS, Husbands AY, Timmermans MCP (2012). Plant small RNAs as morphogens. *Current Opinion in Cell Biology* **24**: 217 – 224.

Takeuchi H, Higashiyama T (2012). A species-specific cluster of defensin-like genes encodes diffusible pollen tube attractants in *Arabidopsis*. *PLoS Biology* **10**: e1001449.

Torii KU (2012). Mix-and-match: Ligand-receptor pairs in stomatal development and beyond. *Trends in Plant Science* **17**: 711 – 719.

Uchida N, Lee JS, Horst RJ, Lai H-H, Kajita R, Kakimoto T, Tasaka M, Torii KU (2012). Regulation of inflorescence architecture by intertissue layer ligand-receptor communication between endodermis and phloem. *Proceedings of the National Academy of Sciences* **109**: 6337 – 6342.

Van den Bossche R, Demedts B, Vanderhaeghen R, Goossens A (2013). Transient expression assays in tobacco protoplasts. In: Jasmonate signaling. Goossens A, Pauwels L (eds.). *Methods in Molecular Biology* 1011, pg. 227 – 239.

Van der Merwe MJ, Osorio S, Moritz T, Nunes-Nesi A, Fernie AR (2009). Decreased mitochondrial activities of malate dehydrogenase and fumarase in tomato lead to altered root growth and architecture via diverse mechanisms. *Plant Physiology* **149**: 653 – 669.

Van Norman JM, Breakfield NW, Benfey PN (2011). Intercellular communication during plant development. *The Plant Cell* **23**: 855 – 864.

Vernoux T, Besnard F, Traas J (2010). Auxin at the Shoot Apical Meristem. *Cold Spring Harbor Perspectives in Biology* **2**: a001487 – a001487.

Vidensek N, Lim P, Campbell A, Carlson C (1990). Taxol content in bark, wood, root, leaf, twig, and seedling from several *Taxus* species. *Journal of Natural Products* **53**: 1609 – 1610.

Wen J, Lease Ka, Walker JC (2004). DVL, a novel class of small polypeptides: Overexpression alters *Arabidopsis* development. *Plant Journal* **37**: 668 – 677.

Žádníková P, Simon R (2014). How boundaries control plant development. *Current Opinion in Plant Biology* **17**: 116 – 125.

Zhao H, Liu L, Mo H, Qian L, Cao Y, Cui S, Li X, Ma L (2013). The ATP-Binding Cassette Transporter ABCB19 regulates postembryonic organ separation in *Arabidopsis*. *PLoS ONE* **8**: e60809.

Chapter 4

TAXIMIN results in changes in light response in *Arabidopsis thaliana*

INTRODUCTION

Organ development is tightly regulated by a network of transcription factors (TF), hormones and sRNA molecules. Co-ordination of these pathways is necessary to ensure optimal growth and development and allow for adequate response to a changing environment. Although several environmental factors regulate development, light plays an essential role. Light is important for plants as it drives photosynthesis. Changes in day length also regulate key processes such as inducing seed germination and flowering (Lepistö and Rintamäki, 2012). The quality and quantity of light is an important factor, too much or too little light can cause stress or changes in growth responses in plants resulting in photoinhibition (inhibition of photosynthesis by too much light) or etiolation (Taiz and Zeiger, 2010). *Arabidopsis thaliana* is a facultative long day plant, exposure to photoperiods longer than 12-h stimulates flowering (Lepistö and Rintamäki, 2012). Cultivation in short day conditions (less than 12-h light) prolongs the vegetative phase and delays the onset of senescence (Lepistö and Rintamäki, 2012). Certain conditions such as high light can also stimulate the production of secondary metabolites such as the phenylpropanoids and anthocyanins (Ramakrishna and Ravishankar, 2011).

To co-ordinate the responses to changes in the environment, plants also make use of small signaling peptides. Growth and development in the shoot apical meristem is regulated by transcription factors (WUSCHEL) and signalling peptides (CLAVATA3) and also involves interaction with plant hormones such as auxin (Griffiths and Halliday, 2011). Characterization of the signalling peptide TAX1 (At2g31090) indicated a possible role in organ-boundary formation in paraclade junctions of lateral organs in *Arabidopsis thaliana* (Chapter 3, Colling *et al.*, 2015). Additionally, TAX1 functions independently of known boundary regulating transcription factors such as LATERAL ORGAN FUSION (LOF) or the CUP SHAPED COTYLEDONS 3 (CUC3) (Lee *et al.*, 2009; Colling *et al.*, 2015). Mutants of *LOF* also displayed fusion in lateral organs (Lee *et al.*, 2009) similar to *TAX1* overexpression lines and additionally, the fusion phenotype in the *lof* mutant was more severe in short day conditions (Lee *et al.*, 2009).

To determine if light also results in changes in *TAX1* OE lines, these plants were cultivated in growth rooms with different photoperiods. The effect on the metabolism and on the growth and development of these lines was investigated.

MATERIALS AND METHODS

In vitro cultivation

Seeds for four lines which constitutively express *TAX1* (*TAX1* OE1-4), wild type (Col-0), *lof1lof2* and the *tax1tax2* mutant were gas sterilized and transferred to MS (Murashige and Skoog, 1962) basal medium supplemented with 250 μ M cefotaxime and stratified at 4°C for 2 days. Petri dishes were transferred to either a growth room with continuous (24-h) or 16-h light/ 8-h dark photoperiod. Seedlings (10-days) for all lines were transferred to jiffy soil and covered with plastic film for two days and kept in the 12-h light growth room. Plants were watered weekly.

Metabolite extraction and analysis

Samples were collected, rapidly frozen in liquid nitrogen and finely ground. Powdered sample (100 mg) was extracted in 100 μ l MeOH at room temperature on a rotary stand for 10 min. Samples were centrifuged at 14 000 rpm for 10 min. The clear supernatant was transferred to a new 2 ml eppendorf and the methanol was evaporated overnight using a vacuum dryer. The dried residue was resuspended in 400 μ l H₂O/cyclohexane (1:1; v/v) and centrifuged at 13000 rpm for 10 min. The aqueous layer (200 μ l) was transferred to an HPLC vial and used for analysis on the Ultra Performance Liquid Chromatography Electron Spray Ionization Ion Trap Mass Spectrometry (UPLC-ESI-ITMS). Peaks were integrated and aligned with XC-MS for preliminary identification of compounds (Smith *et al.*, 2006).

RESULTS AND DISCUSSION

The role of signalling peptides in development have been demonstrated several times and their interaction with other regulators in the pathway are known. To determine if a reduced light period affects the fusion phenotypes observed in *TAX1* OE lines, we cultivated these plants in a growth room with a 12-h light photoperiod. After 2 months of growth, the *lof1lof2* mutant displayed more severe fusion with the cauline leaf stretching from the paraclade junction at the primary stem to the first paraclade junction on the axillary stem (similar to the decurrent strand) resulting in severe bending (Fig. 1A-C). Growth of the *TAX1* OE in these conditions did not result in similar phenotypes (results not shown). However, since the *TAX1* OE lines display a developmental lag, we can not conclusively exclude that this phenotype is absent in the *TAX1* OE lines.

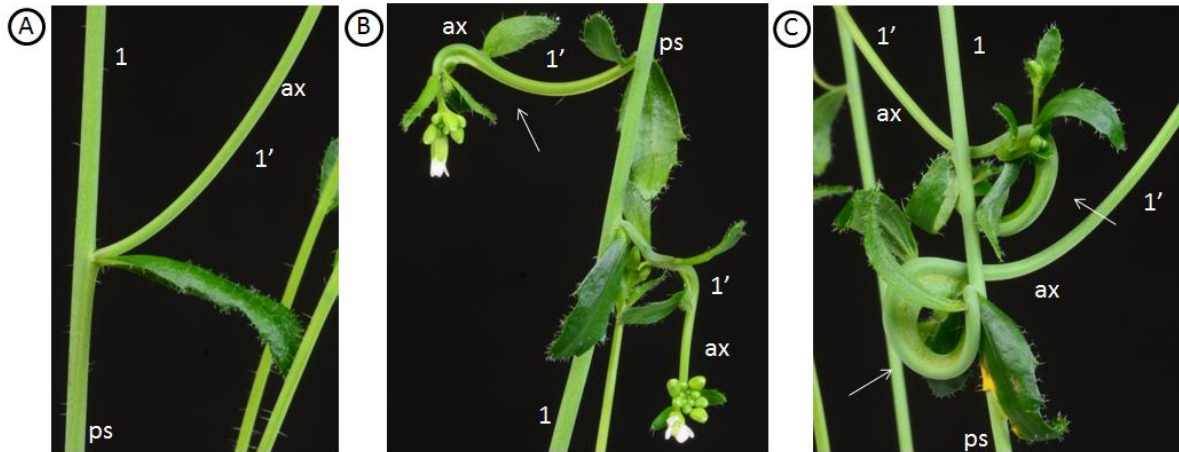


Figure 1. Fusion phenotypes induced by short day conditions in the *lof1lof2* mutant. (A) A paraclade junction of a wild type Col-0 plant displaying clear boundaries between organs. (B) A 'decurent' strand resulting due to fusion of the leaf from the paraclade junction on the primary stem (1) down the axillary stem (1') as indicated by the arrows. (C) The fusion resulted in bending of the axillary stems. Abbreviations are ax axillary stem; ps primary stem.

Cefotaxime reduces light stress response of *TAX1* OE lines

Interestingly, germination of *TAX1* OE seeds in growth rooms with different photoperiod resulted in growth phenotypes. Seeds for the wild type (Wt) and four *TAX1* OE lines which displayed variation in *TAX1* expression level were cultivated on MS medium in a growth room with continuous (24-h) or long day (16-h light/ 8-h dark) photoperiod. Wild type seedlings growing in continuous light appeared larger and greener than those growing in the long day conditions (Fig. 2). The *TAX1* OE plants in continuous light were smaller than Wt seedlings and turned yellow (Fig. 2). In contrast the stress phenotype was less severe for seedlings germinated in the long day growth room (Fig. 2). Cultivation of the *tax1tax2* and *lof1lof2* mutant in continuous or long day conditions did not result in obvious morphological differences compared to the Wt (Fig. 3)

An interesting observation was that cultivation of *TAX1* OE seedlings on medium containing the antibiotic cefotaxime rescued this *TAX1* OE stress phenotype observed in continuous light (Fig. 2). Cefotaxime is one of the antibiotics (eg carbenicillin, timentin) which are regularly used to remove *Agrobacterium* growth after transformation and they are mainly selected for their reduced toxicity to plant cultures (Mathias and Boyd, 1986). Cefotaxime, a cephalosporin, belongs to the *b*-lactam group and functions to bind to penicillin binding proteins and interferes with peptidoglycan synthesis in bacteria (Mathias and Boyd, 1986). Depending on the concentration of the antibiotic added some antibiotics may influence

development of the plant. For example addition of low concentrations of cefotaxime stimulated the growth, regeneration and organogenesis of wheat callus in culture (Mathias and Boyd, 1986). In *Arabidopsis* cultures, cefotaxime inhibited regeneration from *Arabidopsis* root explants after *Agrobacterium* transformation (Valvekens *et al.*, 1988).

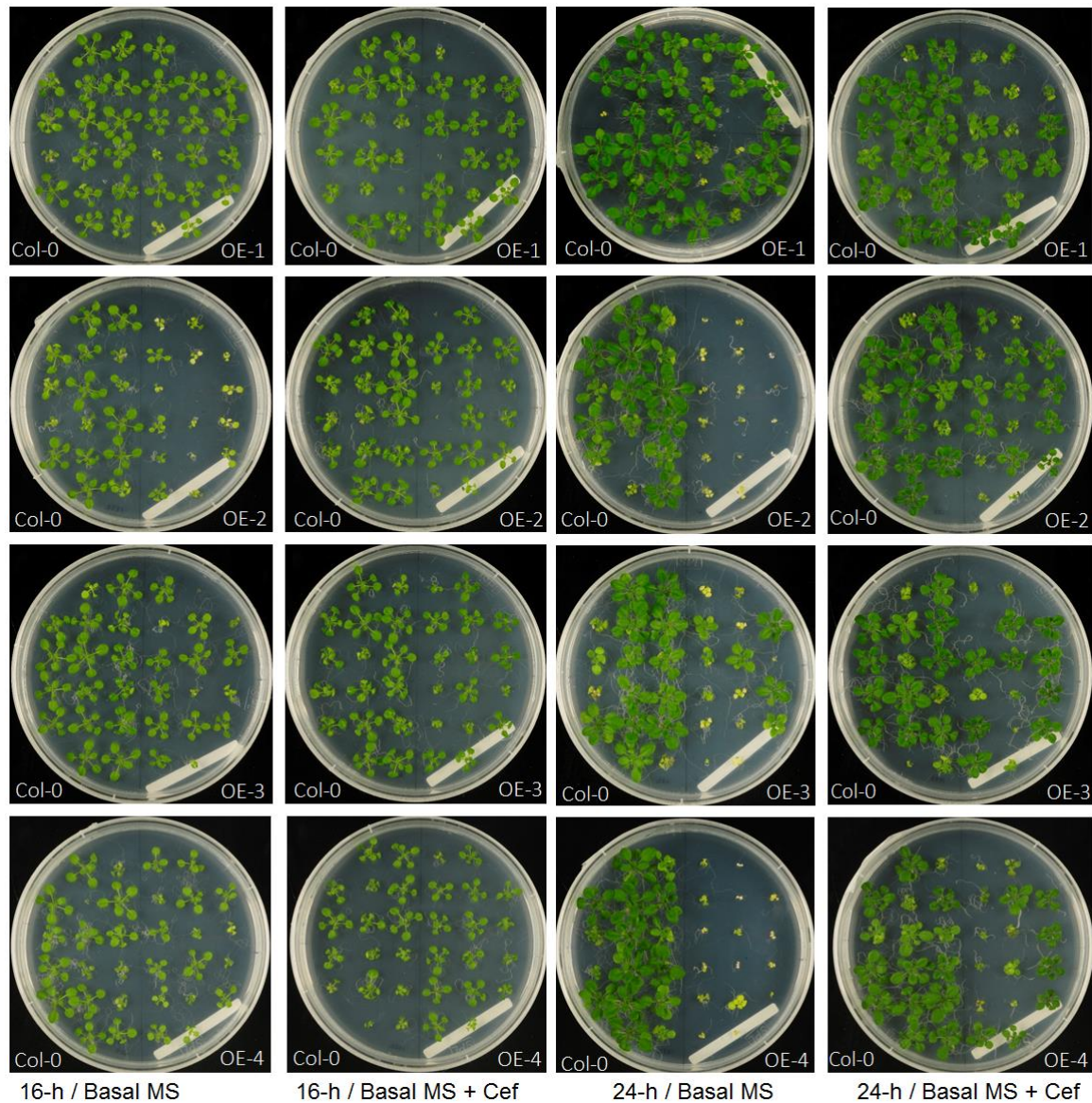


Figure 2. Cefotaxime alters the light stress response of *Arabidopsis thaliana* TAX1 OE lines. *Arabidopsis* plants cultivated in long day (16-h) or continuous (24-h) light on Basal MS or MS supplemented with cefotaxime (Cef) for 21 days. The left panel represents plants cultivated on Basal MS and the panel on the right represent plants cultivated on cefotaxime medium. Each plate contains wild type Columbia (Col-0) plants (left) and four TAX1 overexpression (TAX1 OE) lines on the right. Wild type seedlings appear larger and greener in 24-h light conditions whilst TAX1 OE seedlings appear smaller and more stressed. Additions of Cefotaxime alleviated this stress response observed in the TAX1 OE seedlings.

Chapter 4

Although no experimental evidence for their reported effect has been found, some suggestions for this observed effect include the involvement of plant esterases which could degrade cefotaxime to products which could influence development (Mathias and Boyd, 1986). Alternatively, antibiotics may display plant hormone like properties at low concentrations (Lin *et al.*, 1995). Some antibiotics might also be sensitive to light and higher temperature and the degradation products of these compounds may also influence plant growth and development.

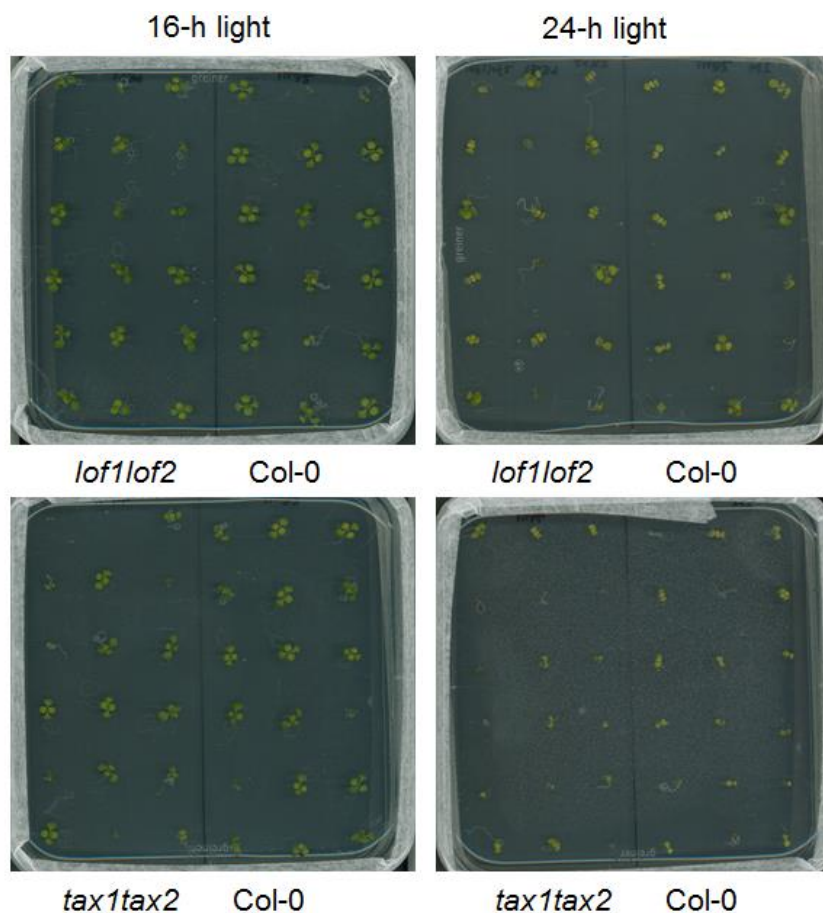


Figure 3. *TAX* and *LOF* double mutants cultivated in continuous (24-h) or long day (16-h light/8-h dark) conditions. Mutants for *lof1lof2* and *tax1tax2* along with wild type (Col-0) were germinated on basal MS medium and cultivated in 24-h or 16-h light conditions and phenotypes were compared after 10-days.

To determine if the observed changes in the morphology of these plants and the effect of cefotaxime are the result of metabolic changes, extracts of Wt (24- vs 16-h light) and *TAX1*-OE seedlings growing in long day conditions were analyzed with UPLC-ESI-ITMS.

Continuous light stimulates secondary metabolite production

In total 4234 m/z peaks were detected. An unsupervised PCA analysis of the metabolites separated samples into two clusters; those cultivated in 24-h light vs 16-h light photoperiod and this separation was independent of the genotype (Fig. 4A). PLS-DA analysis was used to discriminate compounds which cause the separation between the two clusters in the different light regimes (Fig. 4B). Tentative identification of the compounds responsible for the separation indicated that they belonged to the flavonoids (3-Rha-7-Rha-Kaempferol, 3-Glc-7-Rha-Kaempferol), glucosinolate (4-methoxy- glucobrassicin) and phenylpropanoid (sinapoyl malate) pathway (Fig. 4C). Comparison of the level of these compounds in different samples revealed an increase in their abundance in the 24-h light growth room compared to 16-h light growth conditions (Fig. 5A-E).

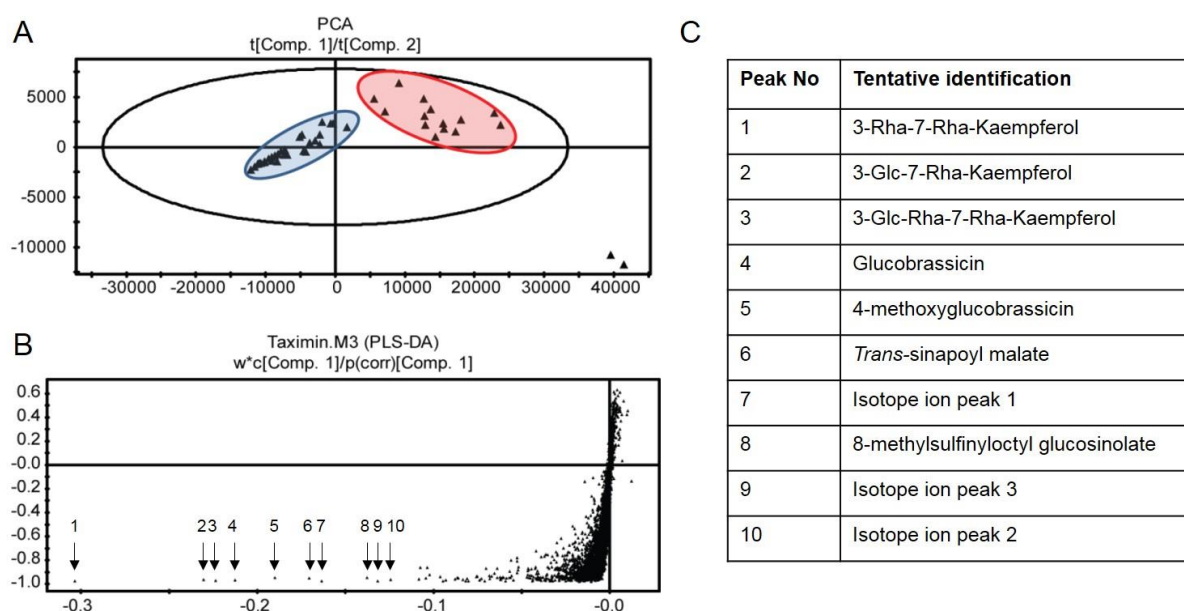


Figure 4. Analysis of the metabolic differences induced by different light photoperiods in seedlings of Wt and *TAX1* OE line. (A) Principal component analysis displaying cluster analysis of samples from 16-h light versus 24-h light. (B) S-plot displaying compounds which were responsible for the separation of the two clusters. (C) Tentative identification of the metabolites which are responsible for the separation into different clusters. Red circle indicates samples from 24-h light conditions and the samples in the blue cluster represent the 16-h light conditions.

Additionally, the abundance of some of the compounds such as 3-glc-7-rha-kaempferol, 3-glc-rha-7-rha-kaempferol and 3-rha-7-rha-kaempferol in the *TAX1* OE lines appeared to be below wild type levels in long day conditions (Fig. 5B-D). When cultivated on cefotaxime, the levels of these compounds in the *TAX1* OE lines were similar to wild type levels and were also increased to similar levels when cultivated in continuous light (Fig. 5B-D).

Chapter 4

An interesting observation was that extracts from transgenic lines growing in long day conditions had reduced abundance of trans-sinapoyl malate compared to Wt, regardless of the medium it was cultivated on (Fig. 5F). Sinapoyl malate is one of the sinapic acid esters and plays a role in UV-B protection in leaves (Landry *et al.*, 1995). Reduced levels of this compound may partly indicate why *TAX1* OE plants are less tolerant to high light conditions. Sinapoyl malate synthesis occurs from precursors of the phenylpropanoid pathway and these precursors are also used for lignin biosynthesis (Lim *et al.*, 2001). Sinapoyl malate is synthesized from 1-O-sinapoyl- β -glucose and L-malate by the enzyme 1-O-sinapoyl β -glucose: L-malate sinapoyltransferase (Santos-Filho *et al.*, 2012). From the metabolite analysis of root and leaf extracts (Fig. 22, Chapter 3) an increase in malate level was only observed in leaves of *TAX1* OE-3. Malate accumulation in this line could be an indication of reduced sinapoyl malate synthesis in this line. In seedlings, sinapate (or sinapic acid) can also be converted to sinapoyl malate through a series of enzymatic reactions (Ruegger *et al.*, 1999). Interestingly, the level of sinapate was significantly reduced in *TAX1* OE lines OE-1 and OE-2, but not OE-3 (Fig. 22; Chapter 3). In these lines a reduction in precursor levels could result in reduced sinapoyl malate synthesis. These results indicate a possible link between *TAX1* OE light stress phenotype and the phenylpropanoid metabolism which is also responsible for the synthesis of flavonoids. However, no link between reduced sinapoyl malate content and bending phenotype observed in these lines could be found. Additionally no significant changes in the level of phenylalanine the precursor for the phenylpropanoid pathway which could explain reduced flavonoid content in the *TAX1* OE, was observed. The effect of cefotaxime on secondary metabolism also requires further investigation to determine if this antibiotic can enhance metabolite production perhaps through activity on the cell wall synthesis enzymes or if other mechanisms may be involved in the observed stress alleviating response.

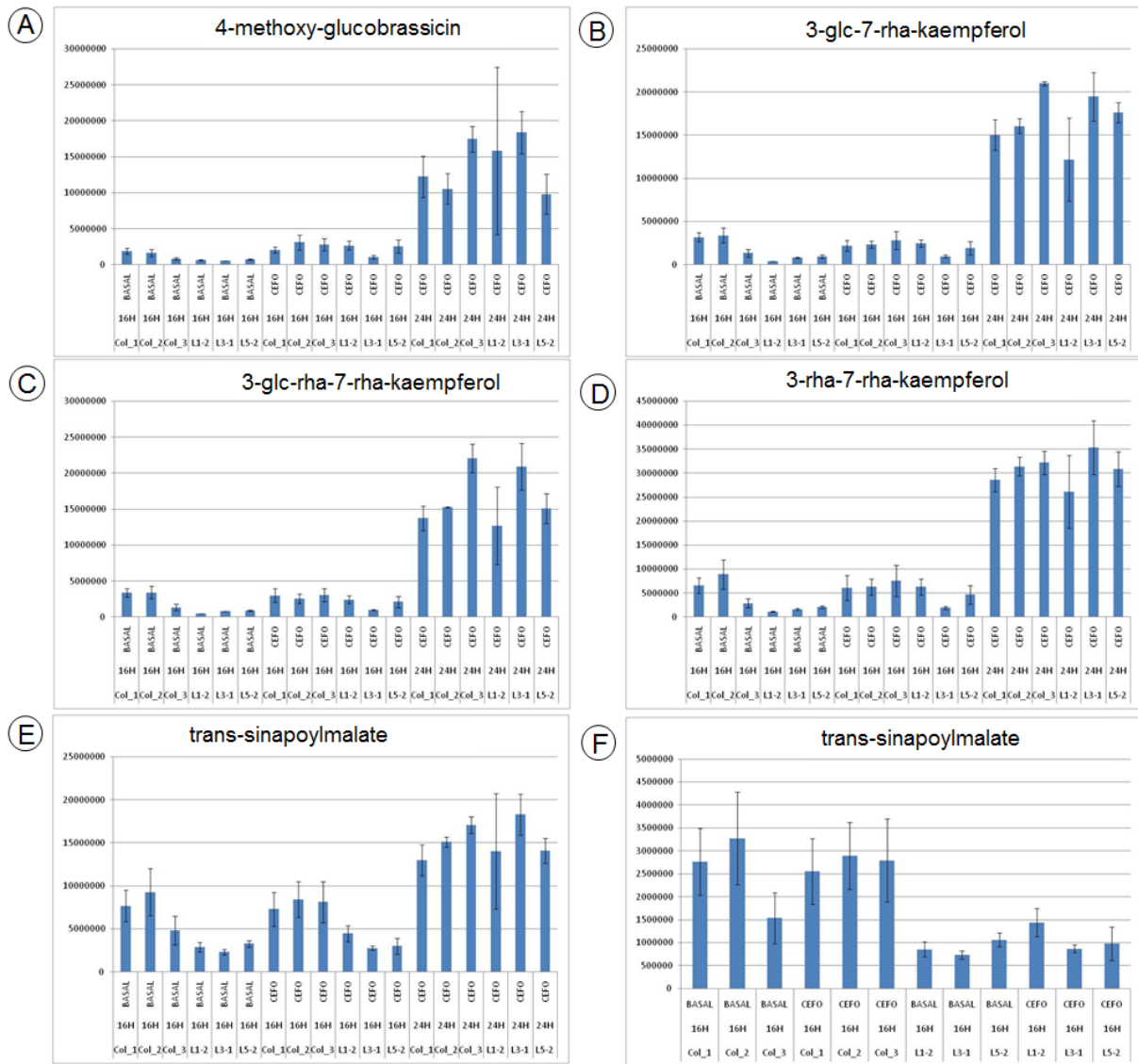
Light responses in *Arabidopsis* TAX1 overexpressors

Figure 5. IT-MS analysis of *Arabidopsis* wild type (Col-0) and *TAX1* overexpression lines on Basal MS or MS supplemented with cefotaxime in continuous or 16-h light growth room. Relative abundance of (A) 4-methoxy-glucobrassicin; (B) 3-glc-7-rha-kaempferol; (C) 3-glc-rha-7-rha-kaempferol; (D) 3-rha-7-rha-kaempferol; (E) trans-sinapoyl malate in Col-0 and three *TAX1* OE lines cultivated in 16-h or 24-h light on basal MS (BASAL) or MS supplemented with cefotaxime (CEFO). *TAX1* OE-1 which looks similar to the Wt was excluded from this analysis and only OE-2 (L1-2); OE-3; (L5-2) and OE-4 (L3-1) which displayed the most severe stress response were analyzed. (F) Relative abundance of trans-sinapoyl malate in Wt and *TAX1* OE lines cultivated in 16-h light on either Basal MS or MS supplemented with Cefotaxime showed significant differences.

CONCLUSIONS

Light is an important factor for regulating development in plants. The regulatory network mediating these responses may involve interaction between signalling peptides and plant growth regulators. These peptides could assist with both biotic and abiotic stress responses.

Chapter 4

In this study we describe the effects of overexpression of the *TAX1* gene and the growth response observed in seedlings cultivated in continuous light. The difference in fusion of paracade junctions between the *lof1lof2* mutant and the *TAX1* OE in 12-h light conditions emphasizes our previous findings that they may function in independent converging pathways to regulate organ boundary formation. This is also emphasized by the observation that seedlings of the *TAX1* OE lines show a severe stress response to continuous light, whilst the *lof1lof2* seedlings look similar to the Wt. The lack of an observable morphological response in the *tax1tax2* mutant in the different light photoperiods, raises the possibility that the effect detected in the *TAX1* OE lines might be due to ectopic expression of the signaling peptide. Transfer to continuous light activates certain secondary metabolite pathways which can assist with the stress response related to excess light on the photosystem for example scavenging of ROS. The reduction in production of certain metabolites such as sinapoyl malate in the *TAX1* OE lines could account for the reduced tolerance of these plants in continuous light conditions. Additionally, supplementation with the antibiotic cefotaxime to the growth medium appeared to alleviate the stress response in *TAX1* OE lines and elucidating of this mechanism may assist with discovery of the impact of antibiotics on the metabolism of plants.

ACKNOWLEDGEMENTS

We thank Patricia Springer for providing seeds of *lof1-1lof2-1* and Jacob Pollier for metabolite analysis and data processing with the UPLC ESI-ITMS. Karel Spruyt is thanked for assistance with recording the observed phenotypes graphically.

REFERENCES

Clough SJ, Bent AF (1998). Floral dip: a simplified method for *Agrobacterium*-mediated transformation of *Arabidopsis thaliana*. *Plant Journal* **16**: 735 – 743.

Colling J, Tohge T, De Clercq R, Brunoud G, Vernoux T, Fernie AR, Makunga NP, Goossens A, Pauwels L (2015). Overexpression of the *Arabidopsis thaliana* signalling peptide TAXIMIN1 affects lateral organ development. *Journal of Experimental Botany* **66**: 5337 – 5349.

Gomez MD, Urbez C, Perez-Amador MA, Carbonell J (2011). Characterization of constricted fruit (*ctf*) mutant uncovers a role for AtMYB117/LOF1 in ovule and fruit development in *Arabidopsis thaliana*. *PloS One* **6**: e18760.

Griffiths J, Halliday K (2011). Plant development: Light exposure directs meristem fate. *Current Biology* **21**: R817 – R819.

- Landry GL, Chapple CCS, Last RL** (1995). *Arabidopsis* mutants lacking phenolic sunscreens exhibit enhanced ultraviolet-B injury and oxidative damage. *Plant Physiology* **109**: 1159 – 1166.
- Lee D-K, Geisler M, Springer PS** (2009). LATERAL ORGAN FUSION1 and LATERAL ORGAN FUSION2 function in lateral organ separation and axillary meristem formation in *Arabidopsis*. *Development* **136**: 2423 – 2432.
- Lepistö A, Rintamäki E** (2012). Coordination of plastid and light signalling pathways upon development of *Arabidopsis* leaves under various photoperiods. *Molecular Plant* **5**: 799 – 816.
- Lim E-K, Li Y, Parr A, Jackson R, Ashford DA, Bowles DJ** (2001). Identification of glucosyltransferase genes involved in sinapate metabolism and lignin synthesis in *Arabidopsis*. *The Journal of Biological Chemistry* **276**: 4344 – 4349.
- Lin J-J, Assad-Garcia N, Kuo J** (1995). Plant hormone effects of antibiotics on the transformation efficiency of plant tissues by *Agrobacterium tumefaciens* cells. *Plant Science* **109**: 171 – 177.
- Mathias RJ, Boyd LA** (1986). Cefotaxime stimulates callus growth, embryogenesis and regeneration in hexaploid bread wheat (*Triticum aestivum* L em. thell). *Plant Science* **46**: 217 – 223.
- Murashige T, Skoog F** (1962). A revised medium for rapid growth and bioassays with tobacco tissue cultures. *Physiologia Plantarum* **15**: 473 – 497.
- Ramakrishna A, Ravishankar GA** (2011). Influence of abiotic stress signals on secondary metabolites in plants. *Plant Signaling & Behavior* **6**: 1720 – 1731.
- Ruegger M, Meyer K, Cusumano JC, Chapple C** (1999). Regulation of ferulate-5-hydroxylase expression in *Arabidopsis* in the context of sinapate ester biosynthesis. *Plant Physiology* **119**: 101 – 110.
- Santos-Filho PR, Vitor SC, Frungillo L, Saviani EE, Oliveira HC, Salgado I** (2012). Nitrate reductase- and nitric oxide-dependent activation of sinapoylglucose: malate sinapoyltransferase in leaves of *Arabidopsis thaliana*. *Plant Cell Physiology* **53**: 1607 – 1616.
- Smith CA, Want EJ, O'Maille G, Abaqvan R, Siuzdak G** (2006). XCMS: processing mass spectrometry data for metabolite profiling using nonlinear peak alignment, matching, and identification. *Analytical Chemistry* **78**: 779 – 787.
- Taiz L, Zeiger E** (2010). *Plant physiology* 5th edition. Sinauer Associates Inc. Massachusetts, USA.
- Valvekens K, Van Montagu M, Van Lijsebettens M** (1988). *Agrobacterium tumefaciens*-mediated transformation of *Arabidopsis thaliana* root explants by using kanamycin selection. *Proceedings of the National Academy of Science of the USA* **85**: 5536 – 5540.

Chapter 5

Engineering of *Sutherlandia frutescens* L. R. Br. metabolism

***author contributions:** writing of the manuscript, cDNA-AFLP, LC-MS quantification of SUB

INTRODUCTION

Sutherlandia frutescens L. R. Br is a medicinal plant indigenous to southern Africa and belongs to the family Fabaceae (Van Wyk and Albrecht, 2008). Extracts prepared from these plants are traditionally used in South Africa to treat a range of health-related problems such as cancer and diabetes (Van Wyk and Albrecht, 2008). These biological activities (eg. anti-oxidant, immune-modulating) can be linked to the complex chemistry of this plant. The presence of triterpene saponins (sutherlandiosides A-D) and flavonoids (sutherlandins A-D) is of great interest for its health promoting properties. Since the environment has been shown to influence metabolite production and pharmaceutical products of *Sutherlandia* are manufactured from cultivated plants or from plants growing wild, these herbal supplements have to be standardized to ensure they contain high quantities of the metabolites of interest. To assess the impact of various stress conditions, focus was placed on establishing a system in which plants could be exposed to a uniform growth environment which can be manipulated towards production of high levels of desired metabolites. Studies on these *in vitro* cultivated *S. frutescens* plants showed that under standard conditions, *in vitro* plants contained lower sutherlandioside B (SUB) levels than wild growing plants and could therefore benefit from methods to increase the yield (Albrecht *et al.*, 2012). Metabolite production of *in vitro* plants can be manipulated by changing the growth conditions for example changes in temperature, light, nutrient manipulations, and through the addition of elicitors (Ramakrishna and Ravishankar, 2011).

Since extracts from *Sutherlandia* plants growing in the coastal regions displayed higher anti-proliferating activity (Chinkwo, 2005), we were interested if growth conditions in this area result in alterations to metabolism. Plants were cultivated *in vitro* in limited or increased nitrogen content or exposed to salt and water stress (Colling *et al.*, 2010). Results indicated that canavanine synthesis was correlated to nitrogen availability, but that salt and water stress had no impact on canavanine production (Colling *et al.*, 2010). Here, we follow up on the experiments that were conducted to gain more insight in the response to the stress conditions described in that study. Since salt stress results in both ionic stress and reduced water content in plant organs (Amjad *et al.*, 2014), water stress was replaced with Methyl Jasmonate (MeJA) elicitation.

Except for abiotic stress, plants are also exposed to biotic stress either through the feeding of herbivores or predators on the leaves or through growth of other organisms such

as fungi or bacteria (Aharoni and Galili, 2011). This type of stress can be applied to *in vitro* plants through the addition of elicitors such as MeJA. These abiotic and biotic stresses can be used to study expression on a genomic level towards identification of key regulators of specific responses. These target genes can be altered through genetic engineering to generate plants which are more tolerant to specific stresses. It can also be used to engineer secondary metabolism towards increased production of metabolites of interest.

In one such an experiment, studies indicated that the TAXIMIN peptide in *Taxus baccata* cell suspension cultures could be a potential regulator of secondary metabolism and might be involved in the pathogenesis response (Onrubia, 2012). We were therefore interested what effect overexpression of this peptide would have on the metabolism of *S. frutescens*. Although cell suspension cultures provide a useful platform to study secondary metabolism, this system also has several limitations. Cultures may be genetically unstable (Giri and Narasu, 2000), slow growing, produce low metabolite levels and upscale to bioreactors may not always be successful (Rao and Ravishankar, 2002). Therefore to study the effect of TAXIMIN overexpression, hairy roots were generated using transformation with the gram negative soil bacterium *Agrobacterium rhizogenes* (Giri and Narasu, 2000). The benefits of working with hairy roots are that they grow fast, they do not require addition of plant growth hormones to the medium, whole plants can be regenerate from the roots and they are genetically and biochemically stable over several subcultures (Giri and Narasu, 2000). These roots are also capable of producing secondary metabolites which are normally produced in root tissue (Giri and Narasu, 2000).

The aim of this chapter was firstly to investigate if the *in vitro* application of two abiotic and one biotic stress could induce the expression of genes regulating various stress related metabolic pathways and how certain physiological parameters responded to the stress. This was achieved by 1) applying salinity or MeJA treatments or to alter the level of available nitrogen. Next, preliminary identification of the changes on the transcriptome level towards the identification of potential genes which may allow for engineering of metabolism was studied. 2) The impact of stress conditions on the physiology of the plants were assessed. The effect of salinity stress on production of 3) free amino-acids which can function as osmolytes and 4) the effect on secondary metabolism was investigated by analysis on SUB production. Secondly, the impact of transformation with the TAXIMIN peptide on the biosynthesis of secondary metabolites was investigated towards upregulation of metabolite production.

MATERIALS AND METHODS

1. Plant material

Sutherlandia frutescens seeds were obtained from Silverhill seeds (Kenilworth, South Africa). Prior to germination seeds were scarified with sand paper and incubated in 100% (v/v) ethanol for 5 min. Next, seeds were incubated in a bleach solution (3% (v/v) NaOCl) for 22 min and washed three times in sterile dH₂O for 15 min. Surface decontaminated seeds were transferred to ¼ strength MS (Murashige and Skoog, 1962) medium solidified with 8 g/L agar agar and the pH adjusted to 5.8 using 0.1 M NaOH or 0.1 M HCl. Seeds were kept in the light growth room with a 16-h light and 8-h dark photoperiod at 25±5°C to germinate. Cultures were established from the germinated shoots and subcultured on a monthly basis by transferring the nodes containing the axillary buds or the tip of the shoot with the shoot apical meristem to fresh medium.

2. Stress treatments

To induce stress, the conditions previously described by Colling *et al.*, (2010) were used. Briefly, three shoots (2 cm) were transferred to a glass bottle containing 30 ml MS medium supplemented with (50 or 100 mM) NaCl for salt stress using basal MS medium as the control treatment. For nitrogen treatments MS medium was prepared and the amount of KNO₃ (1.9 g L⁻¹) and NH₄NO₃ (1.65 g L⁻¹) in the basic MS medium was either halved or doubled to establish low or high nitrogen conditions, respectively. Plants were cultivated on this medium for a month and harvested in liquid N₂ for molecular analysis or freeze dried for amino-acid analysis or dried in the oven at 60°C for three days for SUB analysis. MeJA (50 µM) treatment was applied to 26-day old shoots cultivated *in vitro*, an equal volume of ethanol was added as control treatment. All cultures were kept for 48-h in the light growth room prior to harvesting for analysis.

3. RNA isolation and cDNA synthesis

RNA was isolated from shoots using the method described by White *et al.*, (2008). Briefly, 0.1 g of finely ground material was transferred to a tube containing 1.2 µl CTAB buffer containing 3% (v/v) β-mercapto-ethanol, vortexed for 15 s and incubated at 60°C for 30 min. After centrifuging (13 000 rpm), an equal volume of chloroform: iso-amylalcohol (24:1) was transferred to the supernatant and vortexed for 30 s. The sample was centrifuge at 13 000

rpm for 15 min. The chloroform: iso-amylalcohol (24:1) step was repeated and 10 M Lithium chloride was added to the supernatant to a final concentration of 2 M. Samples were incubated overnight at -20°C and the RNA pelleted the following day by centrifuging at 13 000 rpm for 20 min at 4°C. The RNA pellet was washed in 1 ml 70% (v/v) molecular grade EtOH and resuspended in 50 µl DEPC water and kept at -80°C. First strand cDNA was synthesized from 2 µg RNA using Superscript II reverse transcriptase (Invitrogen). Second strand cDNA synthesis was performed by DNA Polymerase I, *E. coli* ligase and RNase H. The cDNA was purified using the nucleospin extraction kit (Macherey-Nagel) following the manufacturers' instructions.

4. cDNA-AFLP

The method described in Chapter 2 was followed (Colling *et al.*, 2014). The templates were first digested with the rare cutting restriction enzyme *Bst*YI, followed by a second digestion using the frequent cutting enzyme *Mse*I (New England Biolabs, USA). The *Bst*YI and *Mse*I adapters were ligated on the products and pre-amplification using *Bst*YI-(T/C)+0 and *Mse*I+0 was performed using Silverstar Taq polymerase (Eurogentec). The product was diluted (600x) and selective transcript profiling was performed using all 128 possible combinations of *Bst*YI(T/C)+1/*Mse*I+2 primer combinations. PCR products were separated on a 5% polyacrylamide gel and TDF selected based on their absence or differential intensity. The tags were cut from the gel using a razor blade and resuspended in 100 µl milliQ water and re-amplified and send for sequencing. Sequences of tags were analyzed using BLASTX searches for homologous sequences against the non-redundant public sequence database of the National Center for Biotechnology Information database (<http://www.ncbi.nlm.nih.gov/BLAST>).

5. Physiological analysis – Gas exchange

The net CO₂ assimilation rate (P_n) as well as the transpiration rate were measured. Shoots were extracted from the glass vessel and a part of the youngest fully expanded leaf was inserted in the leaf chamber. Analysis was performed using the LI-COR LI-6400 portable photosynthesis system (Li-Cor Inc, Lincoln, Nebraska, USA) for five randomly selected plants. A constant photosynthetic photon flux density (PPFD) of 1500 µmol m⁻² s⁻¹ was applied by a LED light at a constant temperature of 17°C and humidity of 60 – 70%.

6. Foliar ^{13}C and N^{15} analysis

Analysis of $\delta^{13}\text{C}$ was performed at the Archeometry Department (University of Cape Town, South Africa). *Sutherlandia frutescens* shoots were dried in the oven and finely ground using a mortar and pestle. Samples (± 2 mg) were weighed into tin capsules prior to Dumas combustion in a Fisons NA 1500 (Series 2) CHN analyzer (Fisons Instruments SpA, Milan, Italy). The isotope ratios were measured with a Delta XP mass spectrometer (Finnigan MAT GmbH, Bremen, Germany). Analysis of $\delta^{15}\text{N}$ was also carried out at the Archeometry Department (University of Cape Town, South Africa). The method described by Vardien *et al.*, (2014) was used. Briefly the $\delta^{15}\text{N}$ isotopic ratio was calculated as $\delta = 1000 \ln [R_{\text{sample}}/R_{\text{standard}}]$, where R is the molar ratio of the heavier to the lighter isotope ($^{15}\text{N}:^{14}\text{N}$) of the sample and standards as defined by Farquhar *et al.*, (1989). The dried plant sample (± 2 mg) was weighed off in 8 x 5 mm capsules (Elemental Microanalysis Ltd., Devon, U.K.) on a Sartorius microbalance (Goettingen, Germany). The samples were combusted and a Finnigan Matt 252 mass spectrometer (Finnigan MAT GmbH, Bremen, Germany), which was connected to a CHN analyzer by a Finnigan MAT Conflo control unit was used to quantify the $\delta^{15}\text{N}$ values for the nitrogen gases.

7. Amino-acid and sutherlandioside B isolation

The total free amino acids were determined as described by Grobbelaar *et al.*, (2014). Finely ground freeze dried material (0.05 g) was extracted in 0.1%: 50% (v/v) formic acid: acetonitrile and sonicated for 1-h. For amino acid analysis, the undiluted extracts (10 μl) were derivitized with Waters AccQ Tag Ultra Derivatization kit (Waters, Milford, MA, USA), following the instructions of the manufacturers (Cohen and Michaud, 1993) and placed in the heating block at 55°C for 10 min prior to injection. Extraction of SUB was performed by incubating 0.05 g material (dried in the oven) in 2 ml 0.1%: 50% (v/v) formic acid: acetonitrile solution for 1-h. Samples were centrifuged to remove plant material and the supernatant was used for LC-MS analysis.

8. Amino-acid quantification and SUB analysis

Amino acid and SUB analysis of samples was performed as described by Grobbelaar *et al.*, (2014). Briefly a Waters API Quattro Micro triple quadrupole mass spectrometer (Milford, MA, USA) which was linked to a Waters Acquity UPLC and Acquity photo diode array (PDA) detector was used for quantification of amino acids relative to internal free amino acid

standards. The cone voltage was set to 15 V and the capillary voltage was 3.5 kV and electrospray ionization was in the positive mode. Nitrogen was used as the desolvation gas and was applied at a rate of 350 L/h at a desolvation temperature of 350°C. The sample (1 µl) was injected and separated on a Waters AccQ Tag C18 column (2.1 x 100 mm, 1.7 µm particle size). Dilutions of Waters AccQ Tag Ultra Eluent A and Waters AccQ Tag Ultra Eluent B was used to elute the derivatives, followed by their quantification using a UV detector set at 255 nm. The mass spectrometer scanned peaks with a m/z of 200 – 600. The total run time of 9.5 min was set up using a solvent gradient system consisting of 99.9% eluent A and 0.1% eluent B (held for 0.54 min), followed by a linear gradient to 21.2% (B) for 7.2 min, adjusted to 90% eluent B over 0.31 min and finally to 100% eluent B for 0.45 min was set up. Next the column was maintained at 100% eluent B for 1 min. The flow rate for the solvent was kept at 0.7 ml/min.

Analysis of SUB was performed on a Waters Synapt G2 quadrupole time of flight mass spectrometer (Waters, Milford MA, USA) which was connect to a Waters Acquity ultraperformance liquid chromatograph (UPLC) and Acquity PDA detector. Samples were filtered prior to injection and diluted ten times. Samples (3 µl) were separate on a Waters UPLC BEH C18 column (2.1 x 50 mm; 1.7 µm particle size) and electrospray ionization in the positive mode was applied. The cone voltage was 15 V and a capillary voltage of 2.5 kV was applied. The desolvation gas (650 L/h) was nitrogen and the temperature was set to 275°C. Formic acid (solvent A; 0.1%) and acetonitrile (solvent B) was used to create a gradient starting with 100% formic acid kept for 0.5 min, followed by a linear gradient to 22% solvent B over 2.5 min, increasing to 44% solvent B over 4 min and ending with solvent B (100%) for 5 min. Solvent B was maintained for another 2 min before the column was re-equilibrated for 1 min. The flow rate was adjusted to 0.4 ml/min and the total run lasted for 15 min. A low energy of 6 V was used to acquire the MS data and a collision energy of 15 to 60 V was used to generate fragmentation data (MS^E).

9. Cloning of TbTAX and Medicago homologs

The two homologs in *Medicago truncatula* (Mt163920 and Mt7260335) with closest homology to *TbTAX* was PCR amplified into the pDONR221 GatewayTM vector from *Medicago* as described by Gholami (2013). The *TbTAX* gene was obtained as described in chapter 3. An LR reaction was performed to clone the CDS for each gene into the pK7WG2D (Karimi *et al.*, 2002) destination vector. For hairy root induction the *Agrobacterium rhizogenes* strain LBA9402 was transformed with the various vectors containing the genes of interest.

10. Induction of *Sutherlandia frutescens* hairy roots which overexpress two *Medicago TAXIMIN* orthologs

Seedlings (14 days old) were used for transformation experiments. The hypocotyls and cotyledons were separated and incubated in a bacterial suspension for each of the three genes *TbTAX*, *Mt163920* (*MtTAX2*), *Mt7260335* (*MtTAX1*) and empty LBA9402 strain for 45 min. Explants were blot dried on sterile tissue paper and transferred to ½ MS medium (2.2 g/L MS with vitamins, supplemented with 0.1 g/L myo-inositol, 30 g/L sucrose, pH adjusted to 5.8 and solidified with 8 g/L agar agar powder) and containing 250 µM acetosyringone. After two days of co-cultivation in the dark (25°C), the explants were washed four times for 15 min in sterile dH₂O containing 250 µM cefotaxime and transferred to ½ MS medium supplemented with 250 µM cefotaxime and kept in the dark growth room. Developing roots were examined with a fluorescence microscope to select GFP positive roots and single root tips representing individual clones were excised after 30 days and transferred to ½ strength MS (Murashige and Skoog, 1962) medium (2.2 g/L MS, 30 g/L sucrose, 0.1 g/L myo-inositol, pH adjusted to 5.8 and solidified with 8 g/L agar agar) to establish new lines which overexpress the respective genes. The presence of the T-DNA genes was confirmed by PCR using the 35S forward and T35S reverse primer (Annex, Table S1) to amplify respective genes. Bands for *TbTAX* (394 bp), *MtTAX2* (TC163920; 412 bp) and *MtTAX1* (NP7260335; 409 bp) were used to confirm transgenesis. Amplification of *rolB* was used to confirm hairy root status. Absence of residual *A. rhizogenes* which can create false positives was confirmed by PCR amplification of the *virCD* genes which should be absent from hairy roots cultures. Hairy root lines were cultivated on ½ MS medium for 30 days and subcultured onto fresh medium on a monthly basis.

11. Metabolite isolation of transgenic hairy root extracts and FT-MS analysis

Root tips (10) were transferred to 15 ml ½ strength MS medium in 50 ml Falcon tubes and cultivated on a shaker (120 rpm) in the dark for 2 weeks prior to the addition of 20 ml fresh medium. Root cultures were cultivated for an additional 2 weeks. MeJA (250 µM) was added to cultures and 5 cultures were treated per solvent and cultivated for 48-h prior to harvesting. Roots were extracted from the medium, rinsed in milliQ water and dried on tissue paper prior to freezing in liquid N₂ and kept at -80°C. Samples were finely ground and 100 mg was extracted in 100 µl MeOH at room temperature on a rotary stand for 10 min. Extracts were centrifuged at 14 000 rpm for 10 min and the clear supernatant was transferred to a new 2 ml eppendorf. The methanol was evaporated overnight using a vacuum dryer. The dried residue was resuspended in 400 µl H₂O: cyclohexane (1:1; v/v) and centrifuged at 13000 rpm for 10

min. The aqueous layer (200 μ l) was transferred to an HPLC vial and used for FT-ICR MS. The method described by Gholami (2013) was used for analysis of samples.

11. Statistical analysis

The results for Pn, Gs, E are the mean \pm SE values of five different plants. The results for the amino acid quantification and SUB content was also determined for five samples (n = 5). Statistical analysis of data was performed using Statistica v12 software package (Statsoft Inc. 2013). The Shapiro Wilk's W-statistics test was used to determine the normal distribution and homogeneity of variance of all data. A one way analysis of variance (ANOVA) was performed and the Tukey's honestly significant difference (HSD) comparison post-hoc test was used to determine statistically significant difference between normally distributed data. A Kruskal Wallis was performed to compare the means of data which was not normally distributed. Only p-values less than or equal to 0.05 were considered to be statistically significant.

RESULTS AND DISCUSSION

Various plants species respond differently to the same stress conditions and responses may depend on the tolerance of plants to the particular type of stress and on the growth stage of the plant (Abdallah *et al.*, 2013; Salem *et al.*, 2014). In this study, different types of stress were applied to *in vitro* cultivated plants towards increased production of secondary metabolites and to study the responses on a transcriptomic, physiological and metabolic level. One limitation for the identification of genes which regulate secondary metabolism may be that some genes are expressed tissue specifically. Since our previous analysis of the flavonoid and terpenoid biosynthesis of this species indicated that these metabolites were only detected in shoot tissue (Colling, 2009), all experiments were conducted using this material. As *S. frutescens* has never been sequenced before the use of cDNA-AFLP which does not require any prior sequence information was chosen to determine differences in gene expression profiles of *S. frutescens* shoots subjected to salt stress, nitrogen-availability and MeJA elicitation.

cDNA-AFLP identifies genes which are typically involved in stress responses in plants

To determine the effect of abiotic stress on gene expression, salinity stress was applied to *in vitro* growing plants by cultivating shoots in media containing different levels of

Chapter 5

sodium chloride (50, 100 mM NaCl). To assess the effect of nutrient availability the amount of nitrogen (KNO_3 and NH_4NO_3) in MS medium was modified to half (0.5x) or double (2x) the normal concentration. Shoots (three shoots were pooled to form one replicate) were cultivated in this medium for 28 days prior to harvesting. Biotic stress was induced by applying MeJA treatment for 48 hours. RNA was isolated from two biological samples for each stress treatment and cDNA-AFLP was used to study changes in gene expression. A total of 128 primer combinations were used for this experiment. Visual inspection of the gels was used to identify tags which displayed differential expression from the control treatments. The transcriptionally differentially expressed fragments (TDF) were isolated from the gel (hereafter called Sf tags), eluted in water and re-amplified. In total 63 tags displaying altered expression were identified and sent for sequencing, only 49 of these sequences had a good quality and only 37 fragments with a size larger than 100 bp were considered (listed in Table 2). The sequences of these 37 tags were analysed by BLASTx to tentatively annotate potential homologues in other species focussing especially on the legume family. Twenty nine tags resulted in putative hits, whilst 8 TDFs displayed no database matches. Differential gene expression for both the primary and secondary metabolism was discovered.

Nitrogen availability

Nitrogen is an important macronutrient required by all plants for the production of amino acids, proteins, nucleic acids, plant hormones and chlorophyll synthesis (Lian *et al.*, 2006). Limited nitrogen levels affected several genes which are involved in chloroplast or chlorophyll synthesis or metabolism. For example expression of the chloroplast photosystem (PS) II light harvesting complex protein was reduced in low nitrogen conditions (Fig. 1B-C). Photosystem II is part of the electron transport chain which captures light energy and drives photosynthesis (Grewe *et al.*, 2014). Several other tags (Sf016, Sf017, Sf020, Sf054) with a role in photosynthesis have reduced expression in low nitrogen conditions. The light harvesting chlorophyll a-b binding (LHCB) proteins are apoproteins and forms part of the Photosystem II complex (Xu *et al.*, 2011). Previously, a reduction in the expression of genes involved in photosynthesis was also observed in rice seedlings cultivated under limited nitrogen conditions (Lian *et al.*, 2006). This reduction may be directly attributed to decrease in the available nitrogen levels required for synthesis of these enzymes. In rice seedlings the reduction was attributed to a survival response which causes a reduction of those processes in the plant which consume a lot of energy and/or nutrients (Lian *et al.*, 2006). Changes in expression of these genes may affect the photosynthetic capacity of plants.

Genes that are also specific to stress responses were also induced for example expression of tag Sf006 corresponding to the enzyme ornithine aminotransferase (OAT) was reduced in 0.5x nitrogen cultivated shoots. Ornithine aminotransferase is an enzyme located in the mitochondrion, it converts ornithine to L-glutamate γ -semialdehyde and L-glutamate (Khan *et al.*, 2015). These products can be converted to Δ 1-Pyrrolidine 5-Carboxylate (P5C) which is catalysed by Δ -1-pyrroline-5-carboxylate synthetase (P5CS) to produce proline (Stránská *et al.*, 2008; Khan *et al.*, 2015).

Salinity stress

Expression of a tag (Sf021) corresponding to the enzyme S-adenosylmethionine synthetase which is responsible for the production of S-adenosylmethionine (S-AdoMet) was down-regulated in salt treated shoots. S-AdoMet functions as a precursor for polyamine (spermidine and spermine) and ethylene biosynthesis (Bouchereau *et al.*, 1999).

A reduction in expression of tag Sf023 which had homology to an abscisic acid receptor PYL4-like with increasing salt concentration was observed (Fig. 1D). PYL receptors encode functional abscisic acid (ABA) receptors which inhibits the type-2C protein phosphatases (PP2C) which are negative regulators of ABA signaling (Coello *et al.*, 2011). ABA plays an important role in regulating plants' responses to drought and salinity stress.

An increase in expression of tag Sf026 with homology to a glyceraldehyde-3-phosphate dehydrogenase (GPD) which functions in the glycolytic pathway to break down glucose and is located both in the cytosol and in the plastids was observed (Muñoz-Bertomeu *et al.*, 2010). This enzyme converts glyceraldehyde-3-phosphate to glycerate-1,3-bisphosphate which produces energy for the cell (Muñoz-Bertomeu *et al.*, 2010). GPD deficiency can affect both amino acid (specifically serine levels in the roots) and sugar metabolism (Muñoz-Bertomeu *et al.*, 2010). The role of this gene in environmental stress has been shown (Khan *et al.*, 2015) for example potato plants were transformed with the GPD from oyster mushroom. These transgenic plants which overexpressed GPD displayed increased salt tolerance (Jeong *et al.*, 2001).

A tag (Sf055) with homology to the S-Adenosyl-L-Methionine: 2,7,4-Trihydroxyisoflavanone 4-O-Methyltransferase of *Glycyrrhiza echinata* (GeHI4'OMT) was also identified in this screen. This enzyme catalysis an intermediary step to convert a flavonone precursor to formononetin and has homology to other SAM-dependent OMT in other species (Akashi *et al.*, 2003).

Chapter 5

Other examples include Tag Sf034 corresponding to the FKBP12-like peptidyl-prolyl isomerase which is involved in ensuring correct protein folding (Kurek *et al.*, 1999) was increased by salt stress (Fig. 1E). Tag Sf051 which correlates to a E2 ubiquitin conjugating enzyme which is involved in adding ubiquitin groups to lysine residues of proteins which are targeted for protein degradation (Zhang *et al.*, 2015) was reduced by high nitrogen conditions (Fig. 1F). Expansin (Tag Sf063) which plays a role in cell wall loosening (Geilfus *et al.*, 2010) was decreased by higher salt concentrations (Fig. 1G).

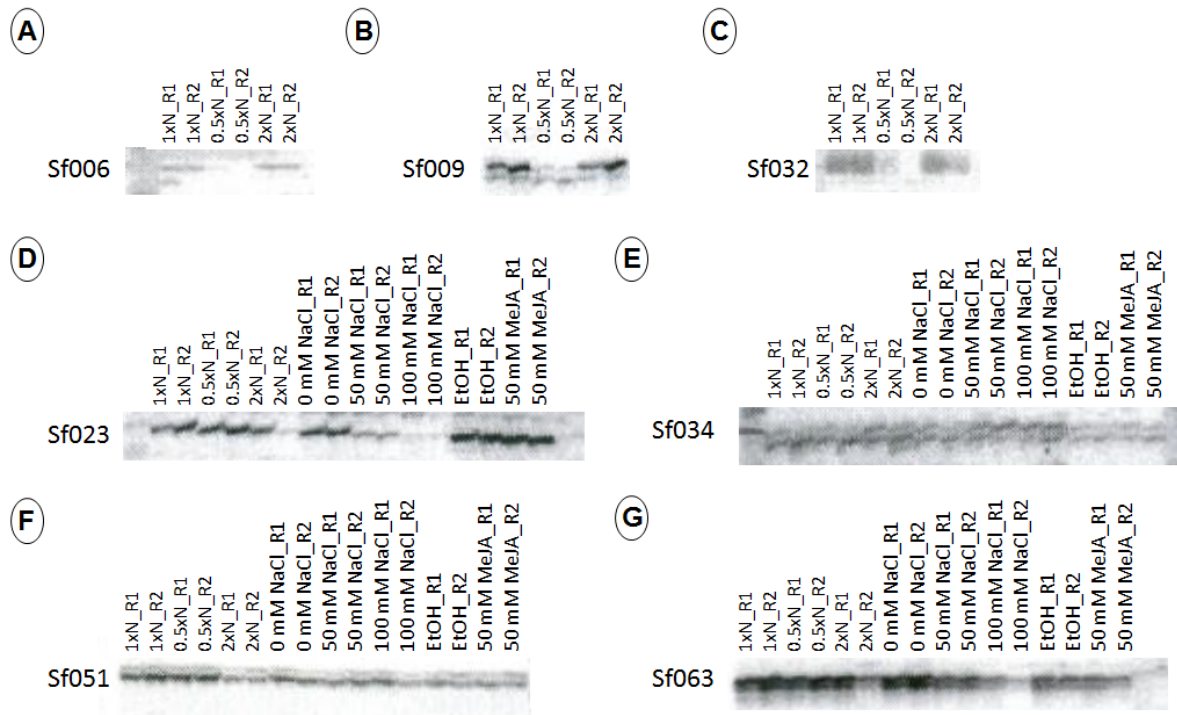


Figure 1. Examples of Transcriptionally differentially expressed fragments (TDF) of *in vitro* stressed *Sutherlandia frutescens* shoots identified with cDNA-AFLP. Shoots were cultivated in medium containing 1x nitrogen (N) which is the control conditions or half (0.5xN) or double (2xN) the nitrogen content to determine the effect of nitrogen availability on gene expression. Shoots were also cultivated in 0 mM NaCl (control), 50 and 100 mM NaCl to induce salt stress. Finally shoots were treated for 48-h with 50 mM Methyl jasmonate (MeJA) or ethanol (EtOH) as a control. Two replicates were used per stress treatment. (A) Tag Sf006 corresponding to Ornithine amino transferase (OAT) and (B and C) Sf009 and Sf032 corresponding to a chloroplast photosystem II light harvesting complex protein type I was reduced in 0.5xN treatment. (D) A tag identified as an abscisic acid (ABA) PYL4 like receptor was reduced by increasing salt concentration. (E) Tag Sf034 corresponding to peptidyl-prolyl cis-trans isomerase FKBP12-like was increased by higher salt levels. (F) Sf051 identified as an E2 ubiquitin conjugating enzyme was reduced in 2xN conditions. (G) Tag Sf063 identified as Expansin was decreased by higher salt levels.

Most of the transcriptomic responses observed were general stress responses observed for plants subjected to stress, therefore we decided to focus only on the salt treated plants for further experimentation. Salinity stress causes osmotic stress, whilst accumulating ions cause ion toxicity and nutrient deficiency. Since these factors have been shown to affect photosynthesis and nitrogen uptake, we first quantified various physiological parameters to determine how these processes respond.

Photosynthesis remain unaltered, but nitrogen uptake decreased in salt treated shoots

Previously, mild salt stress (50 mM) resulted in shoots with a higher fresh mass, however salt-stressed plants appeared shorter and displayed chlorosis (Colling *et al.*, 2010). *In vitro* cultivation and application of stress may affect several physiological mechanisms in plants. Photosynthesis for example can be directly or indirectly inhibited by the uptake of the sodium ions which can be transported in the transpiration stream to the leaves where they accumulate (Dinneny, 2015) and can interfere with photosynthetic enzyme activities such as Rubisco (Silva *et al.*, 2010; Salem *et al.*, 2014). Additionally, salt stressed plants may close their stomata to limit water loss and this can also result in changes to photosynthesis (Stepien and Johnson, 2009).

Since *in vitro* plants grow in a non-ventilated system that restricts photosynthesis and can result in non-functional photosynthetic machinery, plants are supplemented with a carbon source (sucrose) to provide an energy source for the growing plants (Arigita *et al.*, 2002). To perform physiological experiments, the plants were extracted from the glass vessel and the net photosynthesis rate (P_n), stomatal conductance (G_s), transpiration rate (E) and water use efficiency (WUE) of the plants was quantified. Although the P_n in salt treated plants was slightly reduced, there was no statistically significant difference in net photosynthesis rate (Fig. 2A) between salt treated and control plants. This suggests that the salt treated plants had the same photosynthetic capacity as control plants and that the rate of photosynthesis was maintained in salt treated plants. A substantial reduction in the stomatal conductance (G_s) was observed in 50 mM and 100 mM treated plants which coincide with a reduction in transpiration (E), however these results were not statistically significant (Fig. 2B and C). The stomatal conductance and transpiration rate of the control untreated samples displayed a lot of biological variation. Previously, it has been shown that the stomata of *in vitro* cultivated plants are not able to close when extracted from the culture (Hazarika, 2006). Additionally the cuticular wax layer of *in vitro* cultivated plants is under-developed which may result in increased water loss (Hazarika, 2006). These features may have contributed to the large variation observed in the control shoots. It would be interesting to determine if cultivation of plants in salt-containing medium positively influences these characteristics. This pre-exposure to abiotic stress may prime the plant to better adapt to *ex vitro* acclimatization. Adjustments in stomatal conductance/transpiration parameters of salt treated plants can result in an increase in WUE (Barbieri *et al.*, 2012) which represents the ratio of biomass gained versus the amount of water vapor lost through transpiration (Lotter *et al.*, 2014).

Since plants discriminate against the use of ^{13}C during photosynthesis (Lotter *et al.*, 2014), due to preferential binding of Rubisco to $^{12}\text{CO}_2$, the quantification of the carbon isotope

composition ($\delta^{13}\text{C}$) of plant material can be used as an indication of a plants' transpiration efficiency for the period of time during which the plants grow and can therefore also be used as an indicator of the *WUE* (Wang *et al.*, 2013). These levels (Fig. 3A) also indicated that there was no statistically significant difference between salt treated and control plants confirming the results obtained earlier (Fig. 2D).

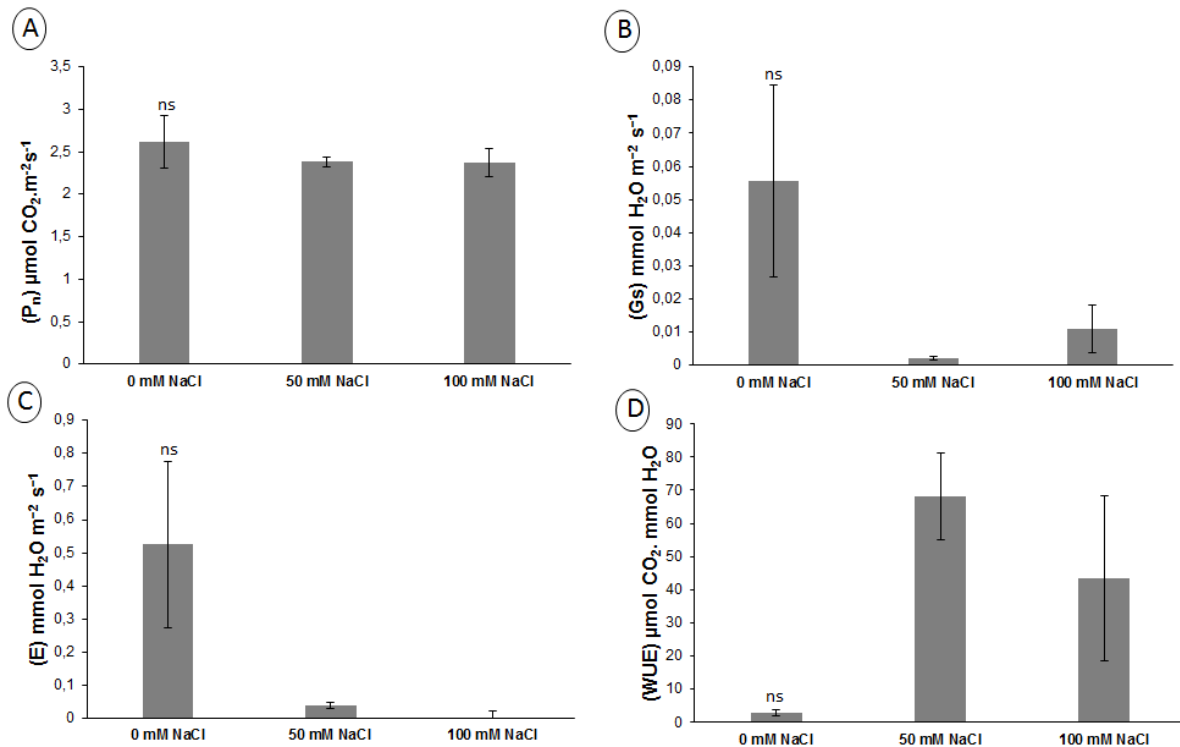


Figure 2. Effect of salt stress on the physiological parameters of *in vitro* *S. frutescens* shoots. (A) The net photosynthetic rate (P_n); (B) stomatal conductance (G_s); (C) transpiration rate (E) and (D) water use efficiency (WUE) of *in vitro* *Sutherlandia frutescens* shoots cultivate on control or salt (50 or 100 mM NaCl) medium for 28-days. ($n = 5$). Values represent the mean \pm SE of five independent samples ($n=5$). ns is the abbreviation for no significant difference. Statistical significant difference for P_n and WUE was determine with an ANOVA; followed by a post hoc Tukeys' HSD test and a Kruskal Wallis test was used for G_s and E . ($P < 0.05$ was considered to be statistically significant).

A link between the amount of carbon fixed and the nitrogen taken up by plants exists since photosynthesis provides the energy and carbon skeletons necessary for nitrogen assimilation (Ncube *et al.*, 2014). Therefore the amount of nitrogen in shoots was quantified as salt stress can also interfere with nitrogen uptake. A statistically significant increase in the $^{15}\text{N}/^{14}\text{N}$ ratio was observed in the 100 mM salt treated shoots (Fig. 3B). Since the ^{15}N in the atmosphere remains the same and all plants were cultivated in the basal MS medium containing the same NO_3^- and NH_4^+ content, a reduction in biological nitrogen fixation occurred. Nitrogen uptake by plants may be affected by high salinity in the soil, since high levels of salt ions cause a

Chapter 5

competition with nutrient uptake. No significant change in the C:N ratio was observed (Fig. 3C). The ability of the shoots to maintain their physiological processes suggests that the plants have mechanisms in place to reduce the effect of salt stress.

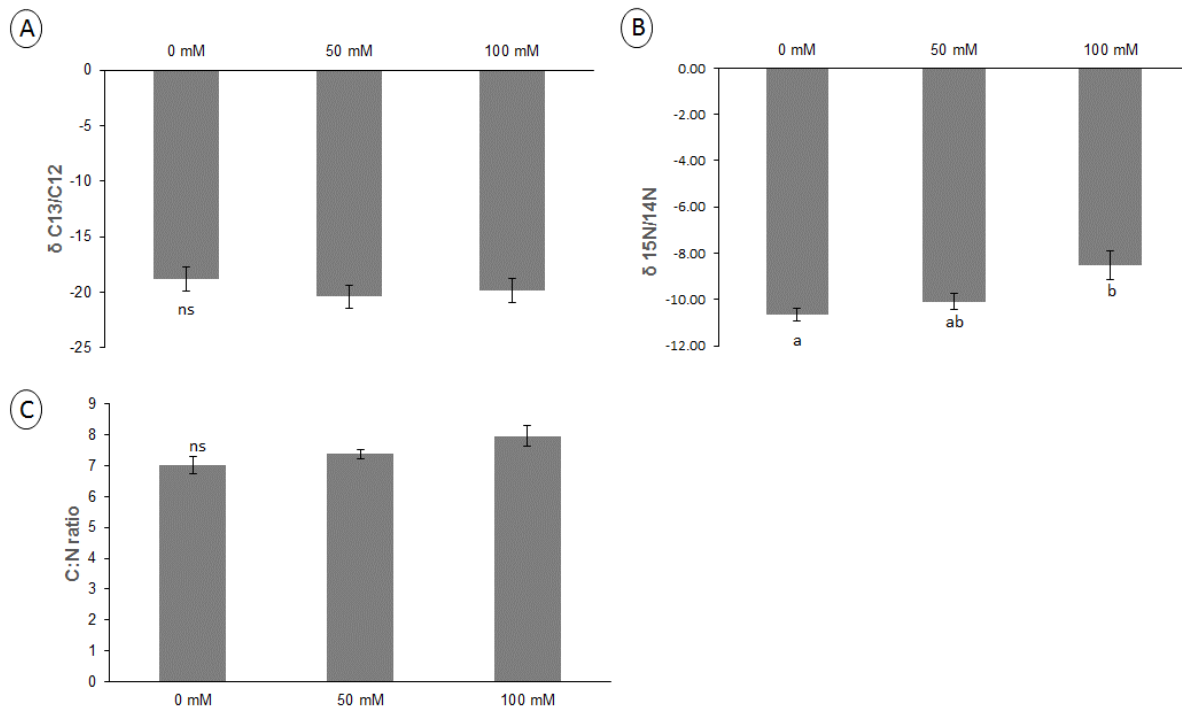


Figure 3. $^{15}\text{N}/^{14}\text{N}$ and $^{13}\text{C}/^{12}\text{C}$ abundance and carbon:nitrogen (C:N) ratio in salt treated *Sutherlandia frutescens* shoots. (A) The $^{15}\text{N}/^{14}\text{N}$ ratio; (B) $^{13}\text{C}/^{12}\text{C}$ ratio and (C) C:N ratio was quantified in 28-day-old *in vitro* plants cultivated in basal MS medium supplemented with either 50 or 100 mM NaCl. Five biological replicates ($n=5$) were used for each treatment. Statistical significant difference for N15/N14 and C:N ratio was determined using an one-way ANOVA, followed by Post hoc Tukeys' HSD test. For the C13/C12 a Kruskal Wallis test was applied. ($P < 0.05$ was considered to be statistically significant).

Salt treatment affected free amino acid levels but had no effect on SUB content

As indicated by the cDNA-AFLP, the expression of enzymes involved in the production of osmotic regulators was altered and to study if salt stress impacted production of these osmo-regulatory metabolites, we quantified various free amino acids in the plants. Detection of the amino acids may be of commercial significance as this can be used as a quality control measure (Mncwangi and Viljoen, 2012). The percentage of each amino acid out of the total amino acids quantified was determined (Fig. 4A). Asparagine was the most abundant amino acid in the control samples, followed by arginine and then canavanine (Fig. 4A).

Application of salt cause a statistically significant reduction in the threonine, tyrosine and asparagine content in salt treated shoots were observed (Table 1). There was a significant reduction in threonine in 50 mM (1.8-fold) and 100 mM (2.5-fold), whilst tyrosine was reduced 5.2-fold (50 mM) and 6.9-fold (100 mM) in salt treated plants (Table 1). The asparagine level was also reduced 1.4-fold (50 mM) and 2.1-fold (100 mM). Furthermore, lysine was not detected in the 100 mM salt treated plants, whilst methionine was absent in more than 50% of the samples and cysteine was not detected in any of the samples with the technique described in this study. Previously, cysteine was detected in samples collected from wild growing plants, but methionine was only detected in two populations and very low or absent in the rest (Mncwangi and Viljoen, 2012). Cysteine and methionine was also previously detected in the *in vitro* cultures (Grobbelaar *et al.*, 2014). These findings show that *S. frutescens* can synthesize these amino acids both in the *in vitro* and *ex vitro* plants, but the variation in detection of some amino acids could be related to changes in experimental or growth conditions. Additionally, certain amino acids such as methionine are very unstable and may rapidly degrade (Mncwangi and Viljoen, 2012).

Conversely, a statistically significant increase in the arginine and proline levels was induced by the salt treatment (Table 1). Salt stress increased proline content four (50 mM) and eight fold (100 mM) in salt treated shoots. Arginine (which can be converted to proline (Dunn *et al.*, 1998) was significantly increased (1.7-1.8 fold) in salt treated shoots, similar as found previously (Colling, 2009). There was also an increase (1.5-fold) in aspartic acid at 50 mM NaCl (Table 1). Increased levels of free amino-acids such as proline and arginine can be due to reduced amino acid degradation, inhibition of protein synthesis, increased protein degradation, or the *de novo* synthesis of amino acids (Azevedo Neto *et al.*, 2009). During salt stress there is a reduction in the growth rate which can result in increased ammonia accumulation (Azevedo Neto *et al.*, 2009). Increased arginine and proline biosynthesis is also a mechanism by which plants can bind excess ammonia in tissue to detoxify the ammonia (Azevedo Neto *et al.*, 2009; Kováčik and Klejdus, 2014).

Unexpectedly the polyamines, putrescine and spermidine levels decreased under salt stress. Spermine could only be detected in three of the control samples, and only in one of the 100 mM treated shoots (results not shown). The reduction in polyamine levels can suggest decreased biosynthesis which could also be linked to a reduction in precursors such as S-AdoMet. Observation of cDNA-AFLP results indicated a reduction in the expression of S-AdoMet synthetase which is responsible for S-AdoMet synthesis from methionine. The reduction in polyamine (spermidine and putrescine) synthesis could partly indicate that the precursors are preferentially sequestered towards other pathways for example arginine and proline synthesis.

Table 1: Amino acid concentrations (mg/ μ l) in control and salt treated *in vitro* *Sutherlandia frutescens* shoots

Amino acid	0 mM	50 mM	100 mM
Serine	9.51 \pm 1.82	8.20 \pm 1.34	6.99 \pm 0.91
Arginine	162.52 \pm 27.22 a	282.35 \pm 14.29 b	297.62 \pm 39.51 b
Glycine	0.21 \pm 0.07	0.17 \pm 0.02	0.29 \pm 0.05
Aspartic acid	4.27 \pm 0.61 a	6.28 \pm 0.43 b	5.36 \pm 0.4 ab
Glutamic acid	14.99 \pm 2.54	12.56 \pm 1.13	12.86 \pm 1.37
Threonine	11.83 \pm 1.78 a	6.43 \pm 0.5 b	4.82 \pm 0.52 b
Alanine	1.42 \pm 0.25	1.37 \pm 0.12	1.68 \pm 0.18
Proline	9.15 \pm 1.57 a	42.92 \pm 5.12 b	74.89 \pm 14.44 b
Lysine	0.44 \pm 0.08	0.38 \pm 0.02	ND
Tyrosine	1.60 \pm 0.3 a	0.31 \pm 0.07 b	0.23 \pm 0.03 b
Valine	1.00 \pm 0.18	0.60 \pm 0.06	0.79 \pm 0.12
Isoleucine	2.50 \pm 0.54	2.69 \pm 0.28	2.20 \pm 0.04
Leucine	0.540 \pm 0.08 a	0.19 \pm 0.02 b	0.26 \pm 0.04 ab
Phenyl alanine	0.45 \pm 0.11	0.29 \pm 0.03	0.39 \pm 0.05
Asparagine	244.68 \pm 28.67 a	173.99 \pm 10.49 b	117.63 \pm 15.75 b
GABA	3.68 \pm 0.58	3.16 \pm 0.53	2.30 \pm 0.4
Canavanine	111.24 \pm 24.56	95.98 \pm 9.31	79.69 \pm 7.49
Putrescine	12.89 \pm 2.31 a	4.59 \pm 1.35 b	3.62 \pm 0.34 b
Spermidine	10.51 \pm 2.26 a	8.08 \pm 1.05 a	3.93 \pm 0.26 b

ND – not detected

A biplot analysis of the samples was performed, and the ellipses represent a significance level of 0.5 (Fig. 4B). In the first analysis we included lysine values and the first principal component (PC1; 52%) separated the control samples from the salt treated samples based on the presence of 5 amino-acids (tyrosine, spermidine, putrescine, threonine and aspartic acid) which was higher in control samples (Fig. 4B). The second principal component (PC2; 19%) separated the salt treated samples from the control samples based on three amino acids (alanine, arginine and proline) which was more abundant in the stressed plants (Fig. 4B). In the second biplot analysis we excluded lysine samples and only continued with 0 mM and 50 mM salt treated shoots. In this biplot the first principal component (PC1; 60%) separated the control samples from the 50 mM salt treated shoots based on proline which was higher in the 50 mM sample, whilst PC2 (21%) was based on 7 amino-acids (phenylalanine, valine, asparagine, leucine, putrescine, threonine and tyrosine) which was higher in the control samples (Fig. 4C). The increased production of proline, show that the salt stress response of *Sutherlandia* plants may favour the production of proline to counteract salt stress above the other osmolytes (putrescine and spermidine). Since salt stress impacted production of certain

amino acids and as some of these are also used for the secondary metabolites production we investigated the effect on the metabolism of salt treated shoots to determine if changes occurred.

Due to lack of available standards, only Sutherlandioside B (SUB) content was investigated. SUB eluted at 5.65 min and the relative abundance of the peaks for the different treatments was determined. Although there was a reduction in the SUB content for the salt treated shoots there was no statistical significant difference in SUB abundance (Fig. 4D). Lack of changes in SUB content hints that the production of these metabolites are not involved in the 'salt stress-relief' response of this plant, but that its synthesis may be involved in other pathways. For example an increase in SUB content was detected in the *in vitro* *S. frutescens* shoots treated with the synthetic strigolactone Nijmegen-1 and the auxin NAA (1-naphthalene acetic acid) suggesting a response to plant growth regulators (Grobbelaar *et al.*, 2014).

Chapter 5

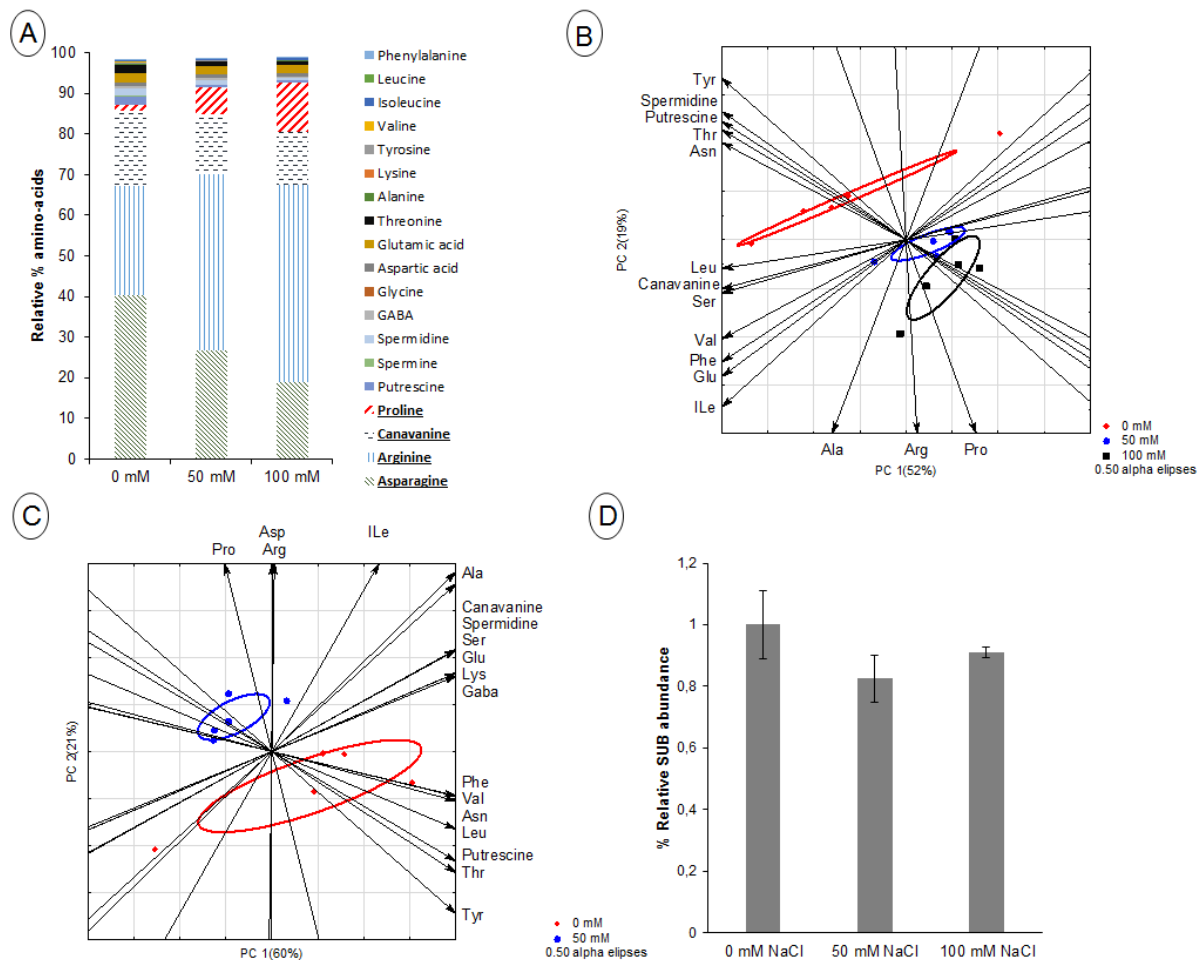


Figure 4. Amino-acid and polyamine levels represented as relative percentage (%) or as biplots and SUB content of salt treated shoots. *In vitro* shoots were cultivated in 50 or 100 mM NaCl medium to induce salt stress for 1 month. (A) Presence of each amino acid calculated as a percentage of the total amino-acids; (B) Unscored biplot of principal component analysis (PCA) for the principal components PC1 (52% of variation) and PC2 (19% of variation) and (C) for principal components PC1 (60% of variation) and PC2 (21% of variation) for amino acids found in control and salt treated *Sutherlandia frutescens* shoots. Samples labelled according to Table 1. Data are from five shoot replicates representative for each treatment (n=5). Amino acids were omitted when R^2 was < 0.5 corresponding to GABA, Glycine and aspartic acid in plot (B) and glycine in plot (C). Ellipses represent a significance level of 0.5. (D) Relative abundance of sutherlandioside B measured in salt treated shoots. SUB values represent the average \pm SE for 5 biological repeats (n=5).

Collectively, these results indicated that *S. frutescens* was tolerant to the NaCl treatment and that salinity stress did not result in a pronounced reprogramming of the expression of genes involved in secondary metabolism. Due to the limited effect of salt stress, another

strategy to alter *S. frutescens* secondary metabolism was launched. A previous report suggested that the TAXIMIN (TAX) peptide might promote secondary metabolism (Onrubia *et al.*, 2014), therefore the effect of TAX overexpression (TAX OE) in hairy roots of *S. frutescens* was investigated.

Genetic engineering of *Sutherlandia frutescens* using TAXIMIN homologs from *Medicago truncatula*

Gholami (2013) described five *TbTAX* homologs (*MtTAX1-5*) which were identified in *Medicago truncatula*. Phylogenetic analysis indicated that these five genes could be divided into two subclades with *MtTAX1* and *MtTAX2* displaying closest homology to *TbTAX*. The influence of gain- or loss-of-function of these genes on the secondary metabolism of *M. truncatula* hairy roots was investigated. Preliminary studies showed that *MtTAX2* OE and *MtTAX2* knock down did not alter the metabolic profile compared to control roots. However, overexpression of the *TbTAX* peptide in hairy roots increased production of triglycosylated saponins in *M. truncatula* (Gholami, 2013). Overexpression of the *MtTAX* genes did not affect the expression of saponin genes, but silencing of these genes negatively impacted expression of saponin biosynthesis genes (Gholami, 2013). A protoplast assay testing the effect of *TbTAX* OE on the promoters of taxol biosynthesis genes showed that TAXIMIN could induce their expression with MeJA elicitation enhancing this activity emphasizing the synergistic relationship (Onrubia, 2012). Constitutive expression of TAXIMIN in tobacco hairy roots did not cause significant changes in alkaloid levels. However, application of MeJA to *TbTAX* OE hairy root lines induced higher alkaloid (nicotine, anabasine, anatabine) production than observed in control lines (Onrubia, 2012; Onrubia *et al.*, 2014).

To investigate constitutive expression of *TbTAX* on *S. frutescens* metabolism, plants were transformed with *A. rhizogenes* strain LBA9402 carrying the plasmid pK7WG2D. Hairy roots which overexpress *TbTAX* or two of the *M. truncatula* TAXIMIN homologues (*MtTAX1* and *MtTAX2*) with closest homology to the *TbTAX* gene were regenerated (Gholami, 2013). The hairy roots appeared after a couple of days and single root tips which emerged, representing individual clones (Giri and Narasu, 2000), were transferred to media. At least four lines which overexpress the TAXIMIN gene and *M. truncatula* orthologs were established. Hairy roots transformed with unmodified *A. rhizogenes* bacteria were generated as a control to monitor the effect of *rol* genes on secondary metabolism. PCR amplification was used to confirm that the various genes of interest (*TbTAX*, *MtTAX1* and *MtTAX2*) were present in the

Chapter 5

genome of each hairy root line (Fig. 5A). The hairy roots displayed typical characteristics associated with the presence of *rol* genes which include agravitropical growth on media free of plant growth regulators (Giri and Narasu, 2000). This type of growth is beneficial as it enhances aeration of the roots which improves growth (Giri and Narasu, 2000). The transgenic status was confirmed by PCR amplification of a (780 bp) band for *roB* in all lines (Fig. 5B). At the same time absence of residual *Agrobacterium rhizogenes* was confirmed by PCR amplification of the *virulence* genes (*Vir CD*) which was detected in the plasmid DNA, but was absent from hairy root samples (data not shown).

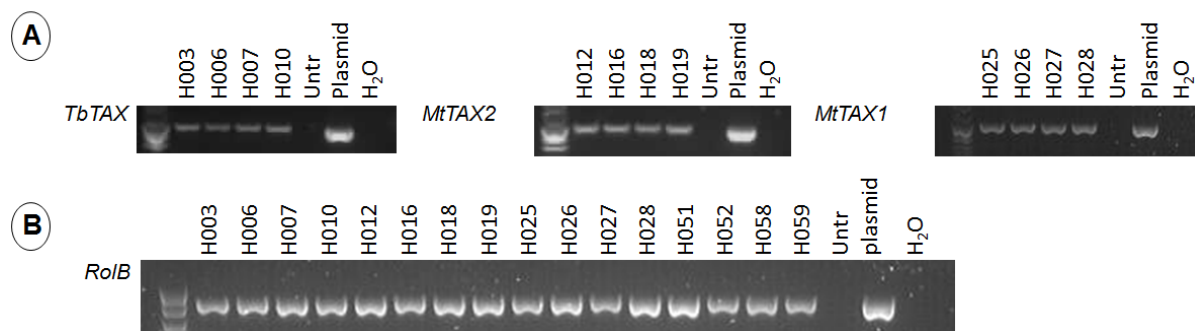


Figure 5. PCR amplification of T-DNA in hairy roots of *Sutherlandia frutescens*. Confirmation of the presence of (A) T-DNA (*TbTAX* and Medicago orthologs *MtTAX1* and *MtTAX2*) insertion and (B) the *roB* gene which is responsible for hairy root phenotype. Molecular marker VIII (Roche) was used to confirm the sizes of the amplified PCR products. Plasmid DNA from *A. rhizogenes* strain LBA9402 was used as a positive control and DNA from untransformed (untr) plants was used as a negative control.

To determine if *TAX* OE resulted in changes in the secondary metabolite chemical profiles, hairy roots were treated with MeJA and an untargeted metabolite profiling was performed using liquid chromatography electron spray ionization Fourier transform ion cyclotron resonance mass spectrometry (LC-ESI FT-ICR MS). Previously, the presence of the sutherlandins and sutherlandiosides in hairy roots could not be detected using Liquid Chromatography Mass Spectrometry (LC-MS) (Colling, 2009). Use of the FT-ICR MS resulted in the tentative identification of these compounds in hairy root extracts (Fig. 6). This instrument can be used to provide an accurate measurement of the mass, which enables the prediction of the molecular formula of detected ions (Pollier *et al.*, 2011). Although sutherlandiosides and sutherlandins could be detected, the differences between the control lines or lines transformed with the *TbTAX* (*TB595*) or *M. truncatula* homologs were insignificant (Fig. 6). This corroborates the previous report, in which overexpression of some *MtTAX* homologs in *M. truncatula* hairy roots did not affect secondary metabolism, i.e. of triterpene saponins and flavonoids either (Onrubia *et al.*, 2014).

A comparison of mock- versus MeJA treated hairy root samples revealed that accumulation of soyasaponin but not sutherlandioside or flavonoid compounds were stimulated by MeJA elicitation. Soyasaponin and saponin biosynthesis is known to be jasmonate-inducible (Lambert *et al.*, 2011; Gholami *et al.*, 2014), but here we show that the different branches of the *S. frutescens* triterpenoid pathway are distinctly regulated by MeJA elicitation. Finally, interclonal differences were visible with some lines (H027, H028, H051, H052) displaying absence of sutherlandioside A and C (Fig. 6C-D). Thereby, this transformed *S. frutescens* root culture set represents an interesting source for a gene discovery program that will be launched in the near future and may allow identification of genes encoding enzymes in the biosynthesis pathway of *S. frutescens* sutherlandiosides.

Chapter 5

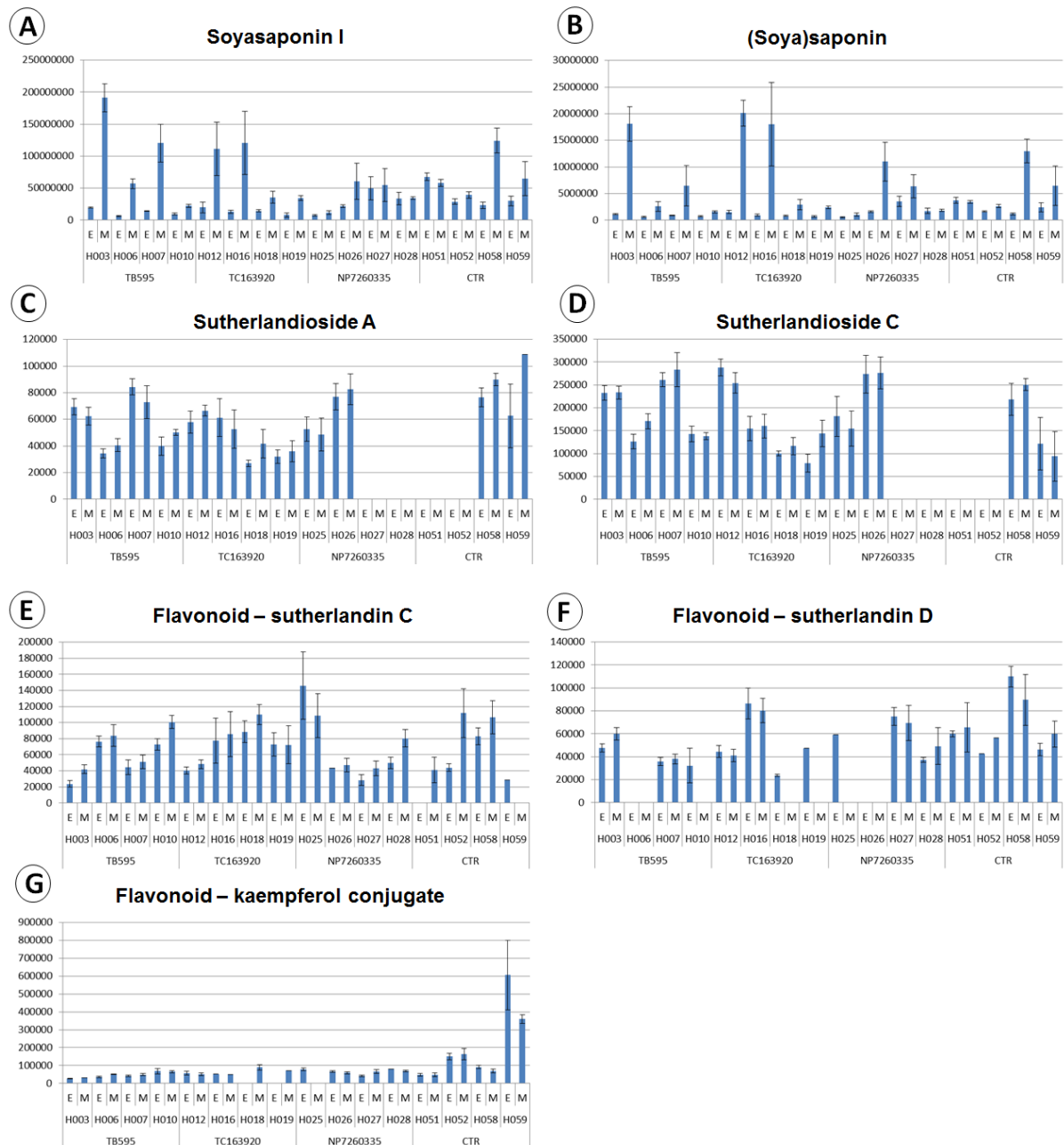


Figure 6. FT-MS analysis of MeJA (M) or EtOH (E) treated *S. frutescens* hairy roots. Four independent hairy root lines which overexpress TB595 (*TbTAX*; H003, H006, H007, H010), TC163920 (*MtTAX2*; H012, H016, H018, H019), NP7260335 (*MtTAX1*; H025, H026, H027, H028) were generated. Four lines (H051, H052, H058, H059) transformed with *A. rhizogenes* strain LBA9402 alone was used as control (CTR) for transformation and to investigate the effect of the insertion of *rol* genes on the metabolism of this plant. Roots (10 root tips) were cultured in ½ strength MS medium for one month prior to application of MeJA or EtOH treatment for 48-h. The effect of MeJA treatment on the production of soyasaponin (Fig. 6A-B) were determined for all lines. The relative abundance of the triterpenoid sutherlandioside A and C (Fig. 6C-D respectively) and the flavonoids sutherlandin C and D (Fig. 6E-F respectively) and a tentatively identified flavonoid kaempferol conjugate (Fig. 6G) were monitored in the different lines.

CONCLUSION

In this study we report for the first time the use of cDNA-AFLP towards understanding the effect of stress on the transcriptome of the medicinal plant *S. frutescens*. With cDNA-AFLP we found several genes identified in other studies which respond to abiotic and biotic stress responses. These candidates could represent targets which could be manipulated to generate plants which are more tolerant to specific stress conditions. Since different types of stress result in similar effects in plants, there is overlap between the responses. In this study, the results indicated that *S. frutescens* was tolerant to mild and higher levels of salinity stress and maintained net photosynthesis although a significant reduction in nitrogen fixation occurred. The production of osmolytes was involved in this response possibly to offset the negative effects of accumulating ions in the plant cells. Secondly, we also report on the successful transformation of this species to induce overexpression of a heterologous gene(s) from *Taxus baccata* or *M. truncatula*. Although overexpression of the *TAXIMIN* genes did not result in changes in secondary metabolism, we identified lines with differences in their chemical profiles which will be useful towards the identification of genes involved in the production of flavonoids and terpenoids in this species.

ACKNOWLEDGEMENTS

Mr L Ingelbrecht is thanked for assistance with cDNA-AFLP analysis of *S. frutescens*. Miss H Witbooi is thanked for assistance with analysis of physiological parameters. Jan Mertens and Robin van den Boscche are thanked for assistance with maintenance of *Sutherlandia* cultures. Dr M Stander and Mr F Hiten at Central Analytical Facility (CAF) are thanked for metabolite analysis. Carbon and nitrogen isotope analysis was performed at the Archeometry Department (University of Cape Town, South Africa).

REFERENCES

- Abdallah SB, Rabhi M, Harbaoui F, Zar-Kalai F, Lachaâl M, Karray-Bouraoui N** (2013). Distribution of phenolic compounds and antioxidant activity between young and old leaves of *Carthamus tinctorius* L. and their induction by salt stress. *Acta Physiologiae Plantarum* **35**:1161–1169.
- Aharoni A, Galili G** (2011). Metabolic engineering of the plant primary-secondary metabolism interface. *Current Opinion in Biotechnology* **22**: 239 – 244.
- Akashi T, Sawada Y, Shimada N, Sakurai N, Aoki T, Ayabe S** (2003). cDNA cloning and biochemical characterization of S-Adenosyl-L-Methionine: 2,7,4'-Trihydroisoflavanone 4'-O-

Chapter 5

Methyltransferase, a critical enzyme of Legume isoflavonoid phytoalexin pathway. *Plant Cell Physiology* **44**: 103 – 112.

Albrecht CF, Stander MA, Grobbelaar MC, Colling J, Kossmann J, Hills PN, Makunga NP (2012). LC-MS-based metabolomics assists with quality assessment and traceability of wild and cultivated plants of *Sutherlandia frutescens* (Fabaceae). *South African Journal of Botany* **82**: 33 – 45.

Amjad M, Akhtar J, Anwar-ul-Haq M, Yang A, Akhtar SS, Jacobsen S-E (2014). Integrating role of ethylene and ABA in tomato plants adaptation to salt stress. *Scientia Horticulturae* **172**: 109 – 116.

Arigita L, González A, Sánchez TR (2002). Influence of CO₂ and sucrose on photosynthesis and transpiration of *Actinidia deliciosa* explants cultured *in vitro*. *Physiologia Plantarum* **115**: 166 – 173.

Ashraf M, Bashir A (2003). Salt stress induced changes in some organic metabolites and ionic reactions in nodules and other plant parts of two crop legumes differing in salt tolerance. *Flora* **198**: 486 – 498.

Azevedo Neto AD, Prisco JT, Gomes-Filho E (2009). Changes in soluble amino-N, soluble proteins and free amino acids in leaves and roots of salt-stressed maize genotypes. *Journal of Plant Interactions* **4**: 137 – 144.

Barbieri G, Vallone S, Orsini F, Paradiso R, De Pascale S, Negre-Zakharov F, Maggio A (2012). Stomatal density and metabolic determinants mediate salt stress adaptation and water use efficiency in basil (*Ocimum basilicum* L.). *Journal of Plant Physiology* **169**: 1737 – 1746.

Bassard J-E, Ullmann P, Bernier F, Werck-Reichhart W (2010). Phenolamides: Bridging polyamines to the phenolic metabolism. *Phytochemistry* **71**: 1808 – 1824.

Bouchereau A, Aziz A, Larher F, Martin-Tanguy J (1999). Polyamines and environmental challenges: recent development. *Plant Science* **140**: 130 – 125.

Chinkwo KA (2005). *Sutherlandia frutescens* extracts can induce apoptosis in cultured carcinoma cells. *Journal of Ethnopharmacology* **98**: 163 – 170.

Coello P, Hey SJ, Halford NG (2011). The sucrose non-fermenting-1-related (SnRK) family of protein kinases: potential for manipulation to improve stress tolerance and increase yield. *Journal of Experimental Botany* **62**: 883 – 893.

Colling J (2009). Towards understanding the metabolism of *in vitro* *Sutherlandia frutescens* (L.) R. Br. cultures. Stellenbosch University. Faculty of Sciences. <http://scholar.sun.ac.za/handle/10019.1/4601>

Colling J, Stander MA, Makunga NP (2010). Nitrogen supply and abiotic stress influence canavanine synthesis and the productivity of *in vitro* regenerated *Sutherlandia frutescens* microshoots. *Journal of Plant Physiology* **167**: 1521 – 1524.

Colling J, Pollier J, Makunga NP, Goossens A (2014) cDNA-AFLP-based transcript profiling for genome-wide expression analysis of jasmonate-treated plants and plant cultures. In: *Jasmonate Signaling*. Goossens A, Pauwels L (eds.). *Methods in Molecular Biology* **1011**: 287 – 303.

Dinneny JR (2015). Traversing organizational scales in plant salt-stress responses. *Current Opinion in Plant Biology* **23**: 70 – 75.

Dunn DC, Duncan LW, Romeo JT (1998). Changes in arginine, PAL activity and nematode behaviour in salinity-stressed citrus. *Phytochemistry* **49**: 413 – 417.

Farquhar GD, Ehleringer JR, Hubick KT (1989). Carbon isotope discrimination and photosynthesis. *Annual Review of Plant Physiology and Plant Molecular Biology* **40**: 503 – 537.

Geilfus C-M, Zörb C, Mühling KH (2010). Salt stress differentially affects growth-mediating β -expansins in resistant and sensitive maize (*Zea mays* L.). *Plant Physiology and Biochemistry* **48**: 993 – 998.

Gengmao Z, Yu H, Xing S, Shihui L, Quanmei S, Changhai W (2015). Salinity stress increases secondary metabolites and enzyme activity in safflower. *Industrial crops and products* **64**: 175 – 181.

Gholami, A (2013). Identification of potential regulators of Jasmonate-modulated secondary metabolism in *Medicago truncatula*. Ghent University. Faculty of Sciences.

Gholami A, De Geyter N, Pollier J, Goormachtig S, Goossens A (2014). Natural product biosynthesis in *Medicago* species. *Natural Products Report* **31**: 356 – 380.

Giri A, Narasu ML (2000). Transgenic hairy roots: recent trends and applications. *Biotechnology Advances* **18**: 1 – 22.

Grewe S, Ballottari M, Alcocer M, D'Andrea C, Blifernez-Klassen O, Hankamer B, Musgnug JH, Bassi R, Kruse O (2014). Light-harvesting complex protein LHCBM9 is critical for photosystem II activity and hydrogen production in *Chlamydomonas reinhardtii*. *The Plant Cell* **26**: 1598 – 1611.

Grobbelaar MC, Makunga NP, Stander MA, Kossmann J, Hills PN (2014). Effect of strigolactones and auxins on growth and metabolite content of *Sutherlandia frutescens* (L.) R. Br. microplants *in vitro*. *Plant Cell Tissue Organ Culture* **117**: 401 – 409.

Hazarika BN (2006). Morpho-physiological disorders in *in vitro* culture of plants. *Scientia Horticulturae* **108**: 105 – 120.

Jeong J-M, Park S-C, Byun M-O (2001). Improvement of salt tolerance in transgenic potato plant by glyceraldehyde-3 phosphate dehydrogenase gene transfer. *Molecules and Cells* **12**: 185 – 189.

Karimi M, Inzé D, Depicker A (2002). Gateway vectors for *Agrobacterium*-mediated plant transformation. *Trends in Plant Science* **7**: 193 – 195.

Khan MS, Ahmad D, Khan MA (2015). Utilization of genes encoding osmoprotectants in transgenic plants for enhanced abiotic stress tolerance. *Electronic Journal of Biotechnology* **18**: 257 – 266.

Kováčik J, Klejdus B (2014). Induction of phenolic metabolites and physiological changes in chamomile plants in relation to nitrogen nutrition. *Food Chemistry* **142**: 334 – 341.

Kurek I, Aviezer K, Erel N, Herman E, Breiman A (1999). The wheat peptidyl prolyl *cis-trans*-isomerase FKBP77 is heat induced and developmentally regulated. *Plant Physiology* **119**: 693 – 704.

Lambert E, Faizal A, Geelen D (2011). Modulation of triterpene saponin production: *In vitro* cultures, elicitation and metabolic engineering. *Applied Biochemistry and Biotechnology* **164**: 220 – 237.

- Lian X, Wang S, Zhang J, Feng Q, Zhang L, Fan D, Li X, Yuan D, Han B, Zhang Q** (2006). Expression profiles of 10,422 genes at early stage of low nitrogen stress in rice assayed using a cDNA microarray. *Plant Molecular Biology* **60**: 617 – 631.
- López-Gómez M, Cobos-Porras L, Hidalgo-Castellanos J, Lluch C** (2014). Occurrence of polyamines in root nodules of *Phaseolus vulgaris* in symbiosis with *Rhizobium tropici* in response to salt stress. *Phytochemistry* **107**: 32 – 41.
- Lotter D, Valentine AJ, Archer Van Garderen E, Tadross M** (2014). Physiological responses of a fynbos legume, *Aspalathus linearis* to drought stress. *South African Journal of Botany* **94**: 218 – 223.
- Mncwangi NP, Viljoen AM** (2012). Qualitative variation of amino acids in *Sutherlandia frutescens* (Cancer bush) – towards setting parameters for quality control. *South African Journal of Botany* **82**: 46 – 52.
- Muñoz-Bertiney J, Cascales-Miñana B, Alaiz M, Segura J, Ros R** (2010). A critical role of plastidical glycolytic glyceraldehyde-3-phosphate dehydrogenase in the control of plant metabolism and development. *Plant Signaling & Behavior* **5**: 67 – 39.
- Ncube B, Finnie JF, Van Staden J** (2014). Carbon-nitrogen ratio and *in vitro* assimilate partitioning patterns in *Cyrtanthus guthrieae* L. *Plant Physiology and Biochemistry* **74**: 246 – 254.
- Onrubia Ibáñez, M** (2012). A molecular approach to Taxol biosynthesis. Universitat Pompeu Fabra. Department of experimental and health sciences. <http://www.tesisenred.net/bitstream/handle/10803/83344/tmoi.pdf?sequence=1>
- Onrubia M, Pollier J, Vanden Bossche R, Goethals M, Gevaert K, Moyano E, Vidal-Limon H, Cusidó RM, Palazón J, Goossens A** (2014). Taximin, a conserved plant-specific peptide is involved in the modulation of plant-specialized metabolism. *Plant Biotechnology Journal* **12**: 971 – 983.
- Pollier J, Morreel K, Geelen D, Goossens A** (2011). Metabolite profiling of triterpene saponins in *Medicago truncatula* hairy roots by liquid chromatography Fourier Transform ion cyclotron resonance Mass Spectrometry. *Journal of Natural Products* **74**: 1462 – 1476.
- Ramakrishna A, Ravishankar GA** (2011). Influence of abiotic stress signals on secondary metabolites in plants. *Plant Signaling & Behavior* **6**: 1720 – 1731.
- Rao SR, Ravishankar GA** (2002). Plant cell cultures: Chemical factories in secondary metabolites. *Biotechnology Advances* **20**: 101 – 153.
- Salem N, Msaada K, Dhifi W, Limam F, Marzouk B** (2014). Effect of salinity on plant growth and biological activities of *Carthamus tinctorius* L. extracts at two flowering stages. *Acta Physiologiae Plantarum* **36**: 433 – 445.
- Silva EN, Ribeiro RV, Ferreira-Silva SL, Viégas RA, Silveira JAG** (2010). Comparative effects of salinity and water stress on photosynthesis, water relations and growth of *Jatropha curcas* plants. *Journal of Arid Environments* **74**: 1130 – 1137.
- Statsoft Inc.,** (2013). STATISTICA (Data Analysis Software System) version 12. (<http://www.statsoft.com>).
- Stepien P, Johnson GN** (2009). Contrasting responses of photosynthesis to salt stress in the glycophyte *Arabidopsis* and the halophyte *Thellungiella*: Role of the plastid terminal oxidase as an alternative electron sink. *Plant Physiology* **149**: 1154 – 1165.

Strànskà J, Kopečný D, Tylichová M, Snégaroff J, Šebela M (2008). Ornithine δ -aminotransferase. *Plant Signaling & Behavior* **3**: 929 – 935.

Syvvertsen JP, Garcia-Sanchez F (2014). Multiple abiotic stresses occurring with salinity stress in citrus. *Environmental and Experimental Botany* **103**: 128 – 137.

Van Wyk B-E, Albrecht C (2008). A review of the taxonomy, ethnobotany, chemistry and pharmacology of *Sutherlandia frutescens* (Fabaceae). *Journal of Ethnopharmacology* **119**: 620 – 629.

Vardien W, Jolanta Mesjasz-Przybylowicz J, Przybylowicz W, Steenkamp ET, Valentine AJ (2014). Nodules from fynbos legume *Virgilia divaricata* have high functional plasticity under variable P supply levels. *Journal of Plant Physiology* **171**: 1732 – 1739.

Wang Y, Zhang X, Liu X, Zhang X, Shao L, Sun H, Chen S (2013). The effects of nitrogen supply and water regime on instantaneous WUE, time-integrated WUE and carbon isotope discrimination in winter wheat. *Field Crops Research* **144**: 236 – 244.

White EJ, Venter M, Hiten NF, Burger JT (2008). Modified cetyltrimethylammonium bromide method improves robustness and versatility: the benchmark for plant RNA extraction. *Biotechnology Journal* **3**: 1424 – 1428.

Xu Y-H, Liu R, Yan L, Liu Z-Q, Jiang S-C, Shen Y-Y, Wang X-F, Zhang D-P (2011). Light-harvesting chlorophyll a/b-binding proteins are required for stomatal response to abscisic acid in *Arabidopsis*. *Journal of Experimental Botany* **63**: 1095 – 1106.

Zhang Z, Li J, Liu H, Chong K, Xu Y (2015). Roles of ubiquitination-mediated protein degradation in plant responses to abiotic stresses. *Environmental and Experimental Botany* **114**: 92 – 103.

Chapter 5

Table 2: Sequences and BLASTx results of transcriptionally differentially expressed fragments (TDF) of *in vitro* stress treated *Sutherlandia frutescens* shoots

Tag no	Size (bp)	sequence	Blast	Blast score (E)	Accession
Sf001	501	5'- GAATAGGGCAACCTTTTGAAGTGCCTGCTCCACGGGCAGGCAAGAGACAACCTGGCGA ACTGAAACATCTTAGTAGCCAGAGGAAAAGAAAAGCAAAAGCGATTCCCTTAGTAGCGGC GAGCGAAATGGGAGCAGCCTAAACCGTGAAAACGGGGTTGTGGGAGAGCAATACAAG CGTCGTGCTGCTAGGCGAAGCACTCGAATGATGCACCCTAGATGGTAAAAGTCCAGTA GTCGAAAGCATCACTAGCTTATGCTCTGACCCGAGTAGCATGGGGCACGTGGAATCCC GTGTGAATCAGCAAGGACCACCTTGAAGGCTAAATACTCCTGGGTGACCGATAGTGA AGTAGTACCGTGAGGGAAAAGGTAAAAGAACCCCGTCGGGGAGTAAAATAGAACATG AAACCGTAAGCTCCCAAGCAGTGGGAGGAGTAAGGGCTGACCCGCTGCCTGTTGAA GAATGAGCCGGCGACTCATAGGCAGTGGCTTAGTTAA-3'	ref XP_003637074.1 Cell wall-associated hydrolase, partial [<i>Medicago truncatula</i>]	9e-42	XP_003637074.1
Sf006	112	5'- GAAGCCAAAAGATGCTGCTCCTCCAGCTGGCCCTAGTGCATGTGATCGTTGTGGTCTGA GTGGTATATGGTTAACCAGATAATGGTTGAATGGTTTTGAATGTGCAACTTAA-3'	emb CAC82185.1 ornithine aminotransferase [<i>Medicago truncatula</i>]	4e-06	CAC82185.1
Sf007	295	5'- GAAGCTTTTTTATGACAAATTAGATTCTGCTTATTCTACTGATGATGACGACTCTGAGGT GGAGGATTGATGATGGAGATGAAGCATATCTTGAGAGCTACAATAGTAAAATGATAGT GAAGTTGAAAGTGATAATGTTTATTCTTCAGCCTAAAGAATTTTCTCAATAAGTTGAAG GTCAAGGGTCATGTAATCTTGGTGATTCTGATGCCTATGTGATTCATTAGTGGCACCTA TTACATTGAAACACGGGCTGATTGAGGAAGAATGTACAGTAGCTCGTTTCAGATTAA-3'	No hit		
Sf009	413	5'- TGGGCTTGATTACTTGGGTAACCCAAGTTTGATCCATGCTCAAAGTATCCTTGCAATTTG GGCCGTTCAAGTTATCTTGATGGGTGCTGTTGAAGGTTACCGTATTGCTGGTGGGCCTC TTGGTGAGGTTGTTGACCCACTTTACCCAGGTGGTAGCTTTGACCCATTGGCCTTGCT GACGACCCAGAGGCATTTGCTGAGCTTAAGGTGAAGGAACTTAAGAATGGTAGGTTAG CTATGTTCTCCATGTTTGGATTCTTTGTTGAGGCTATTGTTACTGGAAGGGTCTTTGG AGAACCTTGCTGATCACCTTGCTGACCCAGTCAACAACAACGCTTGGGCTTTTGCCACC AACTTCGTCCCCGAAAGTAAAAGAAGAGTGTCAAGTGGGTTTGGGTTTGGGTTTTAA- 3'	gb AEV59645.1 chloroplast photosystem II light harvesting complex protein type I [<i>Oxytropis lambertii</i>]	1e-80	AEV59645.1
Sf012	156	5'- GATCCAAAAGCTTGGTGCTCCTATTTCCCTCAAGAATTCTTGCACATATGATTGATCATT ATACATGTCAGAGGAAAACAGCAAAAAGTTGAAAGCACATGTAAAATAATTGTTGAAAGA ACAAATGATTATTTTATGATTGATGGATTCTTTAA-3'	No hit		

Sf013	193	5'- TTATGGACTATGTTTTTGGGATAGTTTTTCATCCTTCAGAAAATGTTTACAGAAAATTGGT TGATCCTCTTCTTCAAAAATATGTGCACCAATTCTTCTAGCTTCTATTAGTTAGTTTTGTA CAACTTACTGACATGTGATGCTTACCCTTTTTTCTGTAAAGACGAGATTACTATTATTAT TTGCATTTAA-3'	gb KHN45937.1 GDSL esterase/lipase EXL3 [<i>Glycine soja</i>]	6e-09	KHN45937.1
Sf016	423	5'- GACCGGAGAAGTCCCCGGCGACTATGGTTATGACCCATTTGGTCTTGGCAAGAAGCCT GAAGACTTTGCCAAATATCAGGCATTTGAGTTGATTCATGCAAGATGGGCAATGCTTGG TGCTGCTGGATTCATCATTCTGAAGCCTTGAACAAATTTGGAGCCAATTGGTCTCTG AGGCTGTTTGGTTCAAGACAGGAGCTCTGCTTCTCGATGGGAACACATTGAACTACTTT GGAAAATCTATTCCCATCAACCTTGTGTTGCTGTCATTGCTGAGGTTGTTCTTTTGGGA GGTGCTGAGTACTACAGAATTACCAATGGACTGGAATTTGAGGACAAGCTACATCCAGG AGGTCCTTTTGTATCCACTAGGACTAGCAATGATCCAGACCAAGCAGCAATTCTAAAAG TGAAGGAAAT-3'	gb AGV54683.1 chlorophyll A/B binding protein CP26 chloroplastic-like protein [<i>Phaseolus vulgaris</i>]	2e-76	AGV54683.1
Sf017	264	5'- TGCTGTCAGTTGCTTCTTTGGTTCCATTGTTCCAAGGTGTCAGCGTGGAGTCTAAGTCC AAAGGGGTGTTTTCTCCGATGCAGAGTTGTGAATGGAAGGTTTCCATGTTGGGTTT GATTGCTCTGGCTTTTACTGAGTATGTCAAGGGAAGTACCTTGTATAAATAATAGCATA TAGTTTTGAAGGCTCATGCTTTAGGAATTGTTCTTAGAACCTAGAAGGTTTCATTGTATG GTTTCTATTGTATATATAAATTA-3'	gb KHN15724.1 Early light-induced protein, chloroplastic [<i>Glycine soja</i>]	2e-24	KHN15724.1
Sf018	118	5'- TACCAGTTGTTTGAACCTGTATCTAATGCTCTTTTTCTATGTCTTATATATCAAAGTTTCC TTCTTGAAAGACTTAAGTAAAATGGATGTGTTTAGATCAGCCAATAGTTGAATTA-3'	No hit		
Sf020	269	5'- GATACAAAGTCAAAGAAGTTAAGAATGGTCGCTTGGCTTTTGGCTTTTGGTATCT GTGTTCAACAATCAGCTTACCCTGGCACTGGTCCTTTGGAGAAGTGGCTACTCACTTG GCTGATCCATGGCACAACAACATTGGAAATGTCTCATTCCACCACAATAATTCATCAAT CATTATGTAAACTTCATCAATCATTCACTTCATGTTCTAAGTTCCTATCCGATCATCGTC TTGTAATTACTTTCAATCCTATCTTAA-3'	ref XP_004515998.1 PREDICTED: chlorophyll a-b binding protein 6, chloroplastic-like isoform X2 [<i>Cicer arietinum</i>]	3e-29	XP_004515998.1
Sf021	140	5'- GAGGACAGCTTTGATTTTAGGCCAGGCATGATCTCTATCAACCTTGATCTCAAGAGGGG TGGCAATAGCAGGTTCTTAAAGACTGCTGCATATGGACATTTTGAAGGGATGACACTG ACTTCACATGGGAAGTGTTAA-3'	ref XP_006379697.1 S-adenosylmethionine synthase family protein [<i>Populus trichocarpa</i>]	6e-23	XP_006379697.1
Sf022	153	5'- TGCTCCTAGACTTTTTAGATGTGTTTGAAGAGATAGAGCAAATTTGGATTGTTCAAATA TGGAGGGTTGCCTCACTGGGGAAAAAATAGAACTTGGCATTTGAAGGAGCCATCAAG AAATATGATAATGCAGGTAAGTTTTTGAAGGTTAA-3'	ref XP_003548406.2 PREDICTED: L-gulonolactone oxidase-like [<i>Glycine max</i>]	7e-20	XP_003548406.2
Sf023	369	5'- TGAACGCCACGTCATCAGTTTCAGTGTGTTGGCGGTGATCACCGGCTTAGAACTACC GGTCGGTGACGACGCTTACGGTGACGGTGTGGTGGGACGGTTGTCATTGAATCGTA	ref XP_004491006.1	1e-39	XP_004491006.1

		CAAGGACAGTAAAAATGTTGGATGTCCAGCAACATACACTGCTCAGGTTCAAATCCA AATGGAGTCACCGTTTCTGTGAAGCCAAAGAAGTTGAAGTTCAAAAAATGGCGAAGA AAAGAGGTTAA-3'	[<i>Cicer arietinum</i>]		
Sf034	191	5'- GCAACCCCTTTCACATTCAAATCGGTCAAGGTTCAAGTAAATCAAAGGATGGGATGAAGG TGTGCATTGGCATGCAAGTTGGGGAAATTGCTCGTCTCAGGTGTTCTCCTGATTATGCT TATGGAGCTGGTGGATTTCTGCTTGGGGAATACAGCCCACTCCATATTGGAATTTGA AATCGAGGTCTTAA-3'	ref XP_004485605.1 PREDICTED: peptidyl-prolyl cis- trans isomerase FKBP12-like [<i>Cicer arietinum</i>]	1e-21	XP_004485605.1
Sf035	124	5'- atgcatttGGTGTCTCCAGTGTGCCGCGATATGGTGCCAGTCTCAGCTTGCCACAAGCACTT ACCAACACAAGAAGTATGCACCTGGAGCACTCTACAGAGAAGGGGCGGCTTCTTATCT TAA-3'	ref XP_003518516.1 PREDICTED: leucine-rich repeat extensin-like protein 5-like isoform X1 [<i>Glycine max</i>]	8e-12	XP_003518516.1
Sf036	117	5'- TGGTGTCTCCAGTGTGCCGCGATATGGTGCCAGTCTCAGCTTGCCACCAGCACTTACC AACACAAGAAGTATGCACCTGGAGCACTCTACACAGAAGGGGCGGCTTCTTATCTTAA -3'	ref XP_006575665.1 PREDICTED: leucine-rich repeat extensin-like protein 5-like isoform X2 [<i>Glycine max</i>]	2e-7	XP_006575665.1
Sf039	150	5'- tggttGGACTCATTATGAAAAAATTGATCAGATGGCTCAAATCGCGTGATTGTGTTGACT GAAGAGAATCCAAAACATAAAgCGAATGCTTCTATTCCCAACCAACAACCTcgAAAGCA AAATGCAAATGTAAACAGGTTCAATTTAA-3'	No hit		
Sf042	179	5'- CAATAATGTAAGTGAAcATAATTTTAGCAACTTGTCAGCTTCTCCAGTGCATCAATAATT GATTCCAAGGAATCAACCTAATCTCATTACTTCTCCAATTAGTAAGTCAATATTTTAC TTAGTTTGATGGTTTGTAAATATTGCTATATTTCTCATTGACTCTCGTTTTTTGTTAACTTGT ACAAAGTGGTCCCA-3'	No hit		
Sf043	341	5'- AGCTGTAATTTCAAGGGTTGGCACACGACATTATTACAGAAAACCTGGGATATGAGCTTG AGGGCCCTTACATGGTGAAATATCTAATGTAATAATAGTAGTTATTGTCATGTAATTTTAT AGCATGTGATAGGTGTGGGTTTTATATGCCGAGGCATTCAATTTATGCTCAAAGATTTTC CTACGTCCAATTCTCTGTTTTTATAGTTCACTAATTTGCGTCCAAGATTCAATAGACCG GATGTGATTAGTTTCATTAGAAGTCGTGTCAACAATTGCACTAATCTATCGCTGACCATA CCTTGCATTTCTTTTGAATACAACCTTGCTTGCATGGTTAA-3'	ref XP_003526977.1 PREDICTED: elongator complex protein 3-like [<i>Glycine max</i>]	5e-08	XP_003526977.1

Chapter 5

Sf047	383	5'-GTGTGCGGAGCAGCTGAATAAAAACGTGAAGGCGCATGATAACACTATGGTGAGGAAGTTCGTAGAGGATTGGGAAAGTAACCCGAGGTGTTCCCGTTGGGGAACCCTGATGGTGCATCGATAACTATGGGAAGTTCTCCGAGGTTTCCAATGTACGATAATGATTTTGGATGGGGAGACCATTGGCGGTTAGGAGTGGAAAGGCAAATAAATTTGACGGTAAGATTTCCGCGTTTCCAGGTAGAGATGGAAGCGGAACCGTTGATTTGGAGGTTGTTTTGGCGCCAGAAACCATGGCGGGGCTTGAGTCTGATCCTGAGTTTATGCAATACGCTTCGAGACAGTTATGACAGGTGTCGAATTGTGGTGTGGTCAAATTA-3'	ref XP_004490956.1 PREDICTED: uncharacterized acetyltransferase At3g50280-like [<i>Cicer arietinum</i>]	1e-71	XP_004490956.1
Sf048	120	5'-TCATCCATCAGAAAGAAGCAAATAGACTCATTGTTGATAAATCTGGACTGGAACAACCGAATATATGCACCCAATGAACCTTAGTACCATTATTGCTTTAGATTCTAAGACCTAATTA-3'	ref XP_004513280.1 PREDICTED: GDSL esterase/lipase At5g33370-like [<i>Cicer arietinum</i>]	2e-11	XP_004513280.1
Sf049	180	5'-GATGGGAGCTGGTCTGGAGATGCCAATCACTACTTCAAGTTTGGTGTGTTATGTGCAGATGATCCTTCCAATTACATGGAATCTCGTTGGAGAGATATCAAAATATTTAGAAAATAGTTGCTTTCAAATGATTTGAATAAATAAGACAAGTGGAGAAGTTGTTGGATATGCTCTTAA-3'	ref XP_003602526.1 Citrate binding protein [<i>Medicago truncatula</i>]	7e-11	XP_003602526.1
Sf050	153	5'-AGAAATCTATTTTGACAAAACCTGGGTTTCATTGAGTAATATTGTTTGGCTGGATGTTGTGATTACCATCTCATTTTGGAGTCTTGCAATAGAGCGAAAAAATAAAGCTCCTCCTTTTCGTTTCTGTTGTTTTGTATCTTGTCTTAA-3'	No hit		
Sf051	177	5'-ACTTTTCTGGTGGGCTACGAcCAAATCCTAATTTGTACGAGTCGGGGAAAgTTTGTGTTGAGCCCTCTAAATACTTGGACTGGCACTGGAAGTGTGGAATCCTATAGCTTCCACTGTTCTTCAAGTCTTCTCTCTGCAAGGCTCTTGCTTACTCAGGACTCATCACCC-3'	ref XP_003528454.1 PREDICTED: probable ubiquitin-conjugating enzyme E2 24-like [<i>Glycine max</i>]	6e-08	XP_003528454.1
Sf052	119	5'-ACcGATGAgtCTGATCGCCTCCTCACCATGAAtaAGACCTTACCCAAcActAATTATTGGTCAtGATGAaGCaGGTTTAGCCATTAGCCGGGTGGATGCTTCAGCTCGTGTGGACTTAA-3'	No hit		
Sf053	134	5'-AGCAGAAGGAAGCTATCTGCTCCCAATCATTGATGATGGTCCATCCACACTTGACAAGGAGGATGGATTCAACAATCTTCAAGATTTGGAGAGTTCACTTGCTTCAATTTCCGACTAAACCTCTTCAAGCACTTAA-3'	ref XP_003618262.1 Serine/threonine protein kinase [<i>Medicago truncatula</i>]	2e-13	XP_003618262.1
Sf054	101	5'-GATCTCAAGGcaCAGAtATCAGTCATcgCGAAAAAGGCAAGGAGATGAGCaAGGCAGAGAGTGAGGcagGGAGACGAGGTGCACTGGTGAGGTAGTTGAC-3'	ref XP_004503801.1 PREDICTED: chaperone protein ClpC, chloroplastic-like isoform X1 [<i>Cicer arietinum</i>]	7e-05	XP_004503801.1

Sf055	138	5'- ATCAACAAACATGAAAAACCAATCACAGCTTCTGAACTAAGCCTCAGCTTTGAAACTCGG CCCTTCAAAAATTTGAACTCCTAAACCGTTTCATGCGGTTGCTAACACACAATGGATTCTT TGCCAAAAACAACAGTTAA-3'	sp Q84KK6.1 I4OMT_GLYEC S-adenosyl-L- methionine: 2,7,4'- trihydroxyisoflavanone 4'-O-methyl transferase [<i>Glycyrrhiza echinata</i>]	1e-06	Q84KK6.1
Sf058	255	5'- TGAAGATTGACCTTAAGACTGAAGCTGGTGTCCACCCTGCAACCTACCAAGAA GAAGGTTATCTATTGTTTCATGCTTGAAGTGGAGTGCAGATGGAAGCACCTTGTTTAGTG GATATACTGACGGCTTGGTCAGAGTTTGGGGAATTGGGCGTTATTAGTAATGCTTCTGT TGTTTCATCTGGCAATCTGTTTTGATCTTTGTTTTGATTTGTGAGACAAAATTAGTTTACG GTTTCATCGTAGAATTAA-3'	gb KHN00175.1 Guanine nucleotide-binding protein subunit beta-like protein [<i>Glycine soja</i>]	3e-20	KHN00175.1
Sf063	226	5'- TGCTATGAATGAGATGTGATGATGATCCAAGATGGTGTAAACCTACCTCTATTATTGTTA CTGCTACAAAATTTTGTCCACCAAACCCATCTTTGCCAATAACAATGGCGGTTGGTGTA ATCCTCCTTTACAGCACTTTGATATGGCTGAACCTGCTTTCCTGCAAATTGCTGAATATA GAGCTGGAATTGTGCCTGTGGCTTTTGAAGGGTGCCTTGCCTTAA-3'	gb AEC46865.1 Expansin [<i>Glycine max</i>]	2e-38	AEC46865.1

** *Cicer arietinum* common name chickpea

Table 3: Full length gene sequences for *TbTAX* gene and homologs in *Medicago truncatula*

Gene	Sequence	bp
<i>TbTAX</i>	5'- ATGGGGGAGTGCAGACCATTGGGATTTCTTTTGGGCCTGCCCTTGC ATTGTTATCTCTCGTTTTTGGCTGCTGTGGGTGCAGTCGTCTGGATCTT AGGGACATTGTTGAGCTGCATATGTCCGTGTTGTATATGCTTTTCTGG CCTGGCAAACATGGCGGTGGGCCTCATGAAGCTTCCTCTCAAAATCA TGCGATGGTCCATTCATCAAATACCCTGCTGA-3'	222
TC163920 (<i>MtTAX2</i>)	5'- ATGGCAGATGATGAAGGTTGTGAATGCAGGCCATTGGGTTTTTTGCT TGGATTACCTTTTGGCTCTCTTGGCTTTGATTTTATCTCTTGTGGTGCA GTTATCTGGATTTTTGGATCTATATTGAGTTGTTTGTGCCCATGTTGCA TTTGCTGCGCTGGATTGGCAAATTTGGCTGTGGGTCTTGTAAGCTT CCAGTTCGTGTTCTAAAGTGGTTTACTCGACAAATTCCTTGTTAG-3'	237
NP7260335 (<i>MtTAX1</i>)	5'- ATGGCAAGTGACCAAGACTTTTGTGAATGTAGACCTTTGGGTTTCTTC ATTGGATTACCCTTTGCTCTATTATCATTAAATTTATCTCTTATAGGAG CAATTATTTGGATTATCGGGTCAATATTGAGTTGCTGCTGTCCTTGTT GCATATGCTGCACAGGATTGCTCAATGTTGCTGTATGTTTGATAAAGC TTCCAGTTCGAATTCCTTAGATGGTTTGTAAACAAAATTCCTTGTTAG-3'	240

Chapter 6

Conclusion and future prospects

Chapter 6

The aim of this project was to describe several steps involved in the establishment of a platform for discovery of novel regulators of secondary metabolism or other metabolic responses in non-model species in response to the application of specific elicitors. It also describes the use of a model species (*Arabidopsis thaliana*) to elucidate the function of homologous genes identified in a screen and the use of non-model species (*Sutherlandia frutescens*) to test the predicted function of the discovered gene (*TbTAX*).

The discovery of novel regulators of secondary metabolism was initially conducted with cDNA-AFLP (**Chapter 2**) which can be used to study differential gene expression. The advantage of cDNA-AFLP is that it provides a genome wide analysis of changes in gene expression in response to a specific 'stress' and no prior knowledge of the genome sequence is required. This technique was successfully applied to study changes in MeJA elicited *Taxus baccata* cell suspension cultures and led to the discovery of a novel signalling peptide (TAXIMIN) with a potential role in regulation of secondary metabolite production.

The function of TAXIMIN homologs was studied using the model plant (*Arabidopsis thaliana*) (**Chapter 3**) which provides access to several tools to functionally characterize genes. These tools include the use of GUS:GFP reporter lines to study the expression pattern of the two *TAX* homologs *in situ* at seedling stage as well as in mature plants. The GUS expression revealed that the two *TAX* genes in *Arabidopsis* are differentially expressed in plant tissues and may be indicative that their expression is differentially regulated in plants. *TAX2* expression was mostly restricted to vascular tissue whereas *TAX1* expression was observed in anthers, nectaries, the base of the axillary shoot and cauline leaf and in the roots. Confocal microscopy indicated that *TAX1* is mainly expressed in the L1 layer in the shoot apical meristem and the L1 and L2 layers in the floral meristems. GUS expression was also observed on wounded tissue of the p*TAX2*:GUS reporter line. This response indicates that *TAX2* may be induced by this type of damage which could typically occur for example when insects feed on plants. Since plants often respond to mechanical damage or wounding by insects by increasing secondary metabolism, this finding agrees with the role of *TbTAX* in regulating these biosynthetic pathways. Available T-DNA insertion lines with the T-DNA inserted in the intron for both genes were used to study if loss of function in *Arabidopsis* plants resulted in growth or developmental phenotypes. Absence of gene expression was verified by RT-PCR in seedlings and by RT-qPCR in the paraclade junctions of mature plants. Neither the single nor double *TAX* mutants displayed any visible phenotypes, but this could be attributed to the presence of additional functional redundant genes which mask the effects or due to the requirement of specific growth conditions prior to becoming visible. Additionally, T-DNA inserted in the intron can be spliced out, however the use of specific primers designed to span the intron can be used to test for gene expression. Furthermore, the use of primers

to quantify expression of each exon can indicate if a part of the functional peptide is being expressed which may result in absence of a phenotype. To assess if the TAX peptides affect growth and development, additional experiments in different growth conditions can be applied to study loss of function phenotypes. Simultaneous study of changes in GUS expression in the reporter lines in the different growth conditions may assist with identifying which of these conditions influence expression of the genes. Constitutive expression of the TAX1 peptide resulted in fusion of paraclade junctions. The availability of lines such as the *LATERAL ORGAN FUSION (LOF)* mutant which displayed similar fusion phenotypes can be useful to determine if the peptide and transcription factor functions in the same signaling pathway. However, the TAX1 peptide did not directly influence *LOF* expression or activity and *LOF1* did not regulate *TAX1* expression. Since quantification of these boundary genes in mature paraclade junctions did not display changes in boundary gene expression, DEX inducible lines were generated. Increased *TAX1* expression could be induced upon treatment with DEX and changes in *LOF* and *CUC* expression could be monitored. However, DEX induced overexpression of *TAX1* did not result in a reduction in expression of the known boundary genes in the shoot apical meristem. This result contributed to our findings that *TAX1* and *LOF1* independently regulate boundary formation. However these DEX inducible lines will be useful for future experiments to assess changes in gene expression using eg. cDNA-AFLP or RNAseq to determine which genes alter expression upon induced *TAX1* overexpression. This may assist with elucidating which pathways are activated by *TAX1* signalling.

An interesting finding was that the constitutive expression of *LOF1* appeared to down regulate *TAX1* expression, but this may be an indirect effect and may require further study. Seedlings overexpressing *TAX1* also displayed a developmental lag and an increased sensitivity to longer photoperiod (described in **Chapter 4**). This light response may be linked to changes on the metabolic level for example changes in the abundance of sinapoyl malate was observed in the overexpression lines. Application of the antibiotic cefotaxime, appeared to reduce the light induced stress response in the *TAX1* OE lines. This effect has not been reported previously and it might be interesting to investigate how cefotaxime induced this response. The function of the *TbTAX* orthologue *TAX2* still remains to be elucidated.

To display the application of cDNA-AFLP this technique was used to study transcriptional changes involved in stress responses of the non-model plant *Sutherlandia frutescens* subjected to various types of stress (nitrogen availability, salinity stress and MeJA elicitation) (**Chapter 5**). The expression data indicated that there was overlap between the responses. Genes typically involved in polyamine synthesis and/or genes regulated by plant hormones showed differential expression. Few changes in expression of genes related to secondary metabolic responses were identified except for one tag which is involved in

Chapter 6

formononetin biosynthesis. This result may be attributed to the level or type of stress response which was 'too low'. Since seeds were collected from plants growing in coastal regions, these plants may have developed tolerance to these stresses. Alternatively; a time course experiment may be more informative as long term cultivation may only display transcriptome changes related to long term responses to adapt to the stress (salinity and nutrient availability).

Finally, transformation of *S. frutescens* to regenerate hairy roots which constitutively express a heterologous gene (*TbTAX*, *MtTAX1* or *MtTAX2*) from *Taxus baccata* or *Medicago truncatula* was used to determine if this peptide can regulate secondary metabolism. Neither of the heterologous genes resulted in observable changes in the abundance of flavonoid (sutherlandin) or terpenoid (sutherlandioside and soyasaponin) compounds of interest suggesting that they do not regulate these pathways. However, MeJA elicitation did result in induced soyasaponin levels. Differences in the abundance of the other secondary metabolites of interest were observed in various control hairy root lines containing only *rol* genes from *Agrobacterium rhizogenes*. These lines will provide a useful platform towards elucidating the genes involved in their biosynthesis and may allow for reconstruction of these pathways in heterologous systems such as *Saccharomyces cerevisiae*. This would allow production of these compounds in a more ecologically sustainable method which does not affect the natural populations in the wild or lead to the destruction of the habitat.

This study therefore describes methods which can be applied for the identification of new genes involved in modifications of secondary metabolites through the application of stress conditions. These genes can be used in combinatorial biosynthesis to generate novel secondary metabolites for the pharmaceutical industry. Additionally, using this approach the mechanisms involved in certain stress responses can be elucidated and may advance our understanding of tolerance or survival responses in plants which may facilitate 'transfer' of these mechanisms to other plants to make them more resistant in the future.

Acknowledgements

Firstly, I would like to extend my gratitude to my supervisors Prof Nox Makunga and Prof Alain Goossens for giving me the opportunity to do my PhD. The Joint PhD was new to all of us, thank you for your patience, support and guidance through this process. I will always be grateful to you both.

I would also like to thank Dr Laurens Pauwels for everything he did to assist me with this project, for being willing to share his knowledge, for his guidance and for making me a part of the Arabidopsis team. A special thank you also to Dr Jacob Pollier for his guidance, time, effort and metabolite analysis of large sample sets, I really appreciated your help.

I would also like to thank the following institutions for the funding which I received for this PhD, firstly the National Research Foundation (NRF) of South Africa for granting me the Abroad PhD scholarship and Ghent University for granting me the BOF scholarship for the Joint PhD. I would also like to thank the Post Graduate and International Office of Stellenbosch University especially Ms Rozelle Pieters, Ms Rhodene Amos for their kind assistance.

I would like to express my gratitude to Robin van den Bossche, Rebecca de Clercq, Maria Njo, Davy Opdenacker, Saskia Lippens, Wilson Ardiles and Karel Spruyt for their wonderful technical assistance and patience to help me with experiments, teaching me new skills and assisting me to take numerous photos of my funny phenotypes.

I would also like to thank Mr Fletcher Hiten and Dr Marietjie Stander from the Central Analytical Facility (CAF) at Stellenbosch University for their assistance with all metabolic analysis experiments. To Dr Christell van der Vyver and Prof Alex Valentine thank you for always being willing to answer technical and scientific questions, I really appreciate your kind assistance. I would also like to thank Zuki, Jan and Robin for assistance with maintenance of tissue cultured plants.

Thank you to Dr. Hannibal Musarurwa and Prof M Kidd for their excellent help with statistical analysis.

I would also like to thank Aleysia Kleinert, Janine Basson and Marí Sauerma, Moses Siebrits for their assistance at the department with technical, financial and administrative matters and for assistance in the laboratory.

Arranging this joint PhD would not have been possible without the help of several people from both Ghent and Stellenbosch University. A special thank you to Ms Dorothy Stevens for being willing to assist me with the arrangements for this Joint PhD. Thank you also to Ms Sophie Maebe for making the necessary administrative arrangements which allowed me to adjust into Ghent life a little faster.

To my amazing friends of the metabol group from way back in 2010 until now; Robin, Amparo, Astrid, Marie-Laure, Piti, Gwen, Sabrina, Tessa, Rebecca, Laurens, Andres, Jonas, Karel, Jacob, Phillip, Jennifer, Bianca, Alex, Jan, Gabriella, Azra, Michele, Michiel, Nathan, Sandra and Yue-Chen. I have been fortunate to be part of this wonderful group, you always made me feel welcome, I can't thank you enough for your wonderful friendship.

To all the other great friends that I have made at the VIB, thank you so much for creating a wonderful atmosphere to work in at the VIB.

To my lab colleagues at Stellenbosch, thank you for your friendship and support Farida, Ebs, Lana, Hannibal, Mpumi, Anathi, Samkele, Tk, Andrea, Waafeka, Rochelle, Lida.

Aan my familie en vriende insluitende Mev Honing, Marko, Jo-Marie, Leandra, Danelle, Marna en veral my ouers vreeslik baie dankie vir julle ondersteuning waarop ek nog altyd kon staat maak deur die jare, ek is baie bevoorreg om sulke wonderlike mense in my lewe te he.

Annex

Supplementary Table S1. Sequences of primers used in this study

ID		Sequence	Use
TAX1	Fw	GGGGACAAGTTTGTACAAAAAAGCAGGCTCC ATGT GCGACGGAGATTGCCG	Cloning
TAX1	Rv	GGGGACCACTTTGTACAAGAAAGCTGGGTCT CMACA AGGGATCTTGGACATG	Cloning
TAX2	Fw	GGGGACAAGTTTGTACAAAAAAGCAGGCTCC ATG GGGAGATTGTAGACCTC	Cloning
TAX2	Rv	GGGGACCACTTTGTACAAGAAAGCTGGGTCT CMACA AGGAATGGAGTGGGTAAAC	Cloning
TAX1 Δ SP	Fw	GGGGACAAGTTTGTACAAAAAAGCAGGCTCC ATG ATTATCTGGATCGTCGGATTG	Cloning
TbTAX-His	Fw	GGGGACAAGTTTGTACAAAAAAGCAGGCTT AATG GGGGAGTGCAGACCATTGGG	Cloning
TbTAX-His	Rv	GGGGACCACTTTGTACAAGAAAGCTGGGTATCAGTGGTGATGGTGATGATGGCAGGGTATTTGATGAATGG	Cloning
TAX1-Venus	Fw	GCTCCTCGCCCTTGCTCACCATAACAAGGGATCTTGGAC ATG	Fusion PCR
TAX1-Venus	Rv	CATGTCCAAGATCCCTTGTATGGTGAGCAAGGGCGAGGAGC	Fusion PCR
TAX1-Venus	Rv	GGGGACCACTTTGTACAAGAAAGCTGGGTATTACTTGTACAGCTCGTCCATGCC	Fusion PCR
pTAX1	Fw	GGGGACAACCTTTGTATAGAAAAGTTGTCTATGTTTTCTTGTGTCTCCAATGAGT	Cloning
pTAX1	Rv	GGGGACTGCTTTTTTGTACAAACTTGGGTGGCTCCGGCGGCGAGT	Cloning
pTAX2	Fw	GGGGACAACCTTTGTATAGAAAAGTTGCCCAAATTAAGGCCAAA	Cloning
pTAX2	Rv	GGGGACTGCTTTTTTGTACAAACTTGTGTGAAGACAAAAGACTAAG	Cloning
LBb1.3		ATTTTGCCGATTTCCGGAAC	Genotyping
tax1		TGTCCAAGATCCCTTGTGTA	Genotyping
tax1		TCCAATACAAGTTATGTACATGGAAGA	Genotyping
tax2		CTCTCCACAAGCCACAAGAG	Genotyping
tax2		AAAAACGACGGATTCATGATG	Genotyping
ACTIN	Fw	GTTGCACCACCTGAAAGGAAG	RT-PCR
ACTIN	Rv	CAATGGGACTAAAACGCAAAA	RT-PCR
TAX1	Fw	TGTTGTTATCATGCATATGT	qPCR
TAX1	Rv	CATGAACCACTCCATAACAT	qPCR
TAX2	Fw	ATCATTGGGACGGTATTGAGTTGTT	qPCR
TAX2	Rv	GGAGTGGGTAAACCAACGGAGG	qPCR
LOF1	Fw	CCCACAAAAGTGGAACTCA	qPCR
LOF1	Rv	CTCGGGTCCAATTGGTTAAA	qPCR
LOF2	Fw	TGTTACCAGTTCCTTGCTTCC	qPCR
LOF2	Rv	CATGCAATGTAATCGCCAAC	qPCR
CUC1	Fw	CCTTGGGAGCTTCTGAGA	qPCR
CUC1	Rv	GGGTATTTACGGTCTCTTAGTGTGA	qPCR

<i>CUC2</i>	Fw	TCGTCTTGAAGGCAAATTCTC	qPCR
<i>CUC2</i>	Rv	AAAACCCTAGAGATCACCCATTC	qPCR
<i>CUC3</i>	Fw	TCGAAAACGACCATTACAC	qPCR
<i>CUC3</i>	Rv	AAGGTAGCTGATTTGGTTATGGA	qPCR
UBC	Fw	CTGCGACTCAGGGAATCTTCTAA	qPCR
UBC	Rv	TTGTGCCATTGAATTGAACCC	qPCR
PP2A	Fw	TAACGTGGCCAAAATGATGC	qPCR
PP2A	Rv	GTTCTCCACAACCGCTTGGT	qPCR
LOF1.1	Fw	GGGGACAAGTTTGTACAAAAAAGCAGGCTCC ATG TTTATAACGGAAAAACAAG	cloning
LOF1.1	Rv	GGGGACCACTTTGTACAAGAAAGCTGGGT CTCM TAGGCTACCTTGAAAGCAATG	cloning
LOF1.2	Fw	GGGGACAAGTTTGTACAAAAAAGCAGGCTCC ATG TTTATAACGGAAAAACAAGTG	cloning
LOF1.2	Rv	GGGGACCACTTTGTACAAGAAAGCTGGGT TCM CGCCGTCCCAAGCCAAG	cloning
GAL41VP16GR	Fw	TACCACAGCTCACCCCTACC	RT-PCR
GAL41VP16GR	Rv	TCATGCATGGAGTCCAGAAG	RT-PCR
TAX1 3' UTR	Fw	TGGAGTGGTTCATGTCCAAG	qPCR
tG7 terminator	Rv	TCAGCTGGTACATTGCCGTA	qPCR
35S promoter	Fw	CGCACAATCCCACTATCCTT	genotyping
T35S terminator	Rev	ACTGGTGATTTTTGCGGACT	genotyping
<i>Rol B</i>	Fw	ATGGATCCCAAATTGCTATTC	PCR
<i>Rol B</i>	Rev	TTAGGCTTCTTTCTTCAGGTTT	PCR
Vir CD	Fw	ATGTCGCAAGGCAGTAAGCCC	PCR
Vir CD	Rev	GGAGTCTTTCAGCATGGAGCAA	PCR
TCM: reverse primers were ambiguity coded to obtain both clones with stop codon (TGA) and without (GGA).			

Supplementary Table 2. Reporting metabolite data presented in this studyReporting metabolite data was presented according to the recommendation by Fernie *et al.*, (2011)

Level	Aspect	Information	Fill in
general aspect	Type of metabolome analysis	targeted metabolite analysis	TRUE
		non-targeted metabolite class scale profiling	FALSE
		non-targeted metabolome scale profiling	FALSE
		non-targeted finger printing of mass features	FALSE
	Type of quantification	absolute or quantification	Relative quantification standard reference compounds acquired in chemical companies
	Type of reference samples	chemically defined	-
		biologically defined	-
	Type of replication	analytical (same analytical sample preparation)	1
		technological (same biological preparation)	2 (in different amount of plant material)
		biological (same experimental condition)	4
full experiment		64	
Type of technology Sample preparation	reference publication	Lisec <i>et al.</i> , (2006)	
	chemical derivatized	Lisec <i>et al.</i> , (2006)	
	method of chromatography/separation	- 70 MeV hard ionization	
	method of ionization	electron impact ionization	
metabolite/mass feature	Metabolite	metabolite name	see below
		metabolite sum formula	see below
	Identification	metabolite structure and public source of metabolite identifier	Metabolites were identified in comparison to database entries of authentic standards (Kopka <i>et al.</i> , 2005; Schauer <i>et al.</i> , 2005).
		identification process	manually supervised with TagFinder and Xculibar
		by authentic mass isotopomer added to one or all biological sample(s)	FALSE
		by authentic reference compound within a co-processed reference mixture	FALSE

	by authentic reference compound previously mapped to the analytical system	TRUE
	reference library	Metabolites were identified in comparison to database entries of authentic standards (Kopka <i>et al.</i> , 2005; Schauer <i>et al.</i> , 2005)
	type of mass spectrum	A minimum of 4 unique mass fragments was required
	by match of molecular mass (single mass fragment)	for the relative quantification of metabolite pool sizes
	by match of fragments	YES
	by match of fragmentation pattern	YES
	type of retention index	
	by match of retention time (index) to reference library	fatty acid methylesters (FAMES)
		relative quantification by internal standard and sample
Quantification	type of quantification	fresh weight
Validity testing	Recovery testing (chemical analog)	not performed
	Recovery testing (internally added mass isotopomer)	not performed
	Recovery testing (mixture of most divergent samples from the experiment)	not performed
	Test for linear range	not performed
	Limit of quantification (LOQ)	not performed
	Limit of detection (LOD)	not performed

Table 2 continued:

Experiment title: Metabolite profiles of *A. thaliana* leaf and root, Col-0 vs. *TAX1* overexpression lines
Organism/Plant species: *Arabidopsis thaliana*
Organ/tissue: leaf and root
Analytical tool: GC/TOF-MS

Peak/compound no.- number of compound found

Ret . Time- Time expected, Tag Time Index and Time deviation

Putative Name- putative identification of the metabolite/derivative

Corresponding metabolite name in literature

Mol. Formula- molecular formula of the metabolite or its FA adduct;

Mass to charge ratio (m/z)

(S)- identification confirmed by a standard compound

I, II, III- different isomers

Identification level (A; B; C; D)- (A) standard or NMR; (B) MS/MS; (C) MS^E; (D) MS only

Overview of the metabolite reporting list.

Peak/ Compound no.	retention time	Corresponding Metabolite in Literature	Metabolite Class	Molecular formula	Mass to charge ratio (m/z)	Species detected before	Identification level (A-D)
1	10,93	adenine	Amino acids	C5H5N5	264	Tomato, Arabidopsis	A
2	5,62	alanine	Amino acids	C3H7NO2	188	Tomato, Arabidopsis	A
3	9,74	arginine	Amino acids	C6H14N4O2	256	Tomato, Arabidopsis	A
4	10,47	ascorbate	Organic acids	C6H8O6	332	Tomato, Arabidopsis	A
5	7,44	asparagine	Amino acids	C4H8N2O3	188	Tomato, Arabidopsis	A
6	7,31	aspartate	Amino acids	C4H7NO4	232	Tomato, Arabidopsis	A
7	5,53	benzoate	Aromatic acids	C7H6O2	179	Tomato, Arabidopsis	A
8	6,27	beta-alanine	Amino acids	C3H7NO2	248	Tomato, Arabidopsis	A
9	9,53	citrate	Organic acids	C6H8O7	273	Tomato, Arabidopsis	A

10	10,04	dehydroascorbate dimer	Organic acids	C6H6O6	172	Tomato, Arabidopsis	A
11	6,51	erythritol	Sugar alcohol	C4H10O4	217	Tomato, Arabidopsis	A
12	9,31	fructose	Sugar (Hexose)	C6H12O6	217	Tomato, Arabidopsis	A
13	5,91	fumarate	Organic acids	C4H4O4	245	Tomato, Arabidopsis	A
14	7,22	GABA	Amino acids	C4H9NO2	174	Tomato, Arabidopsis	A
15	15,19	galactinol	Sugar alcohol	C12H22O11	204	Tomato, Arabidopsis	A
16	9,49	glucose	Sugar (Hexose)	C6H12O6	160	Tomato, Arabidopsis	A
17	12,46	glucose-6-phosphate	Sugar derivatives	C6H13O9P	160	Tomato, Arabidopsis	A
18	8,14	glutamate	Amino acids	C5H9NO5	246	Tomato, Arabidopsis	A
19	7,89	glutamine	Amino acids	C5H10N2O3	227	Tomato, Arabidopsis	A
20	5,46	glycerate	Hydroxy acid	C3H6O4	292	Tomato, Arabidopsis	A
21	4,61	glycerol	Polyol (triol)	C3H8O3	205	Tomato, Arabidopsis	A
22	5,14	glycine	Amino acids	C2H5NO2	174	Tomato, Arabidopsis	A
23	3,23	glycolate	Hydroxy acid	C2H4O3	177	Tomato, Arabidopsis	A
24	4,2	guanidine	Others	CH5N3	146	Tomato, Arabidopsis	A
25	10,91	histidine	Amino acids	C6H9N3O2	154	Tomato, Arabidopsis	A
26	5,04	isoleucine	Amino acids	C6H13NO2	158	Tomato, Arabidopsis	A
27	4,82	leucine	Amino acids	C6H13NO2	158	Tomato, Arabidopsis	A
28	9,89	lysine	Amino acids	C6H14N2O2	174	Tomato, Arabidopsis	A
29	7,04	malate	Organic acids	C4H6O5	233	Tomato, Arabidopsis	A
30	7,58	methionine	Amino acids	C5H11NO2S	176	Tomato, Arabidopsis	A
31	10,53	myo-inositol	Polyol (inositol)	C6H12O6	305	Tomato, Arabidopsis	A
32	6,14	nicotinate	Hydroxy acid	C6H5NO2	180	Tomato, Arabidopsis	A
33	9,16	ornithine	Amino acids	C5H12N2O2	142	Tomato, Arabidopsis	A
34	11,22	palmitate	Organic acids	C16H32O2	117	Tomato, Arabidopsis	A
35	8,51	phenylalanine	Amino acids	C9H11NO2	218	Tomato, Arabidopsis	A
36	5,32	phosphate	Others	H3PO4	299	Tomato, Arabidopsis	A

37	5,37	proline	Amino acids	C5H9NO2	142	Tomato, Arabidopsis	A
38	8,29	putrescine	Polyamine	C4H12N2	174	Tomato, Arabidopsis	A
39	8,12	pyroglutamate	Amino acids	C5H7NO3	156	Tomato, Arabidopsis	A
40	3,48	pyruvate	Organic acids	C3H4O3	174	Tomato, Arabidopsis	A
41	16,73	raffinose	Sugars	C18H32O16	361	Tomato, Arabidopsis	A
42	11,89	ribulose-5-phosphate	Sugar derivatives	C5H11O8P	357	Tomato, Arabidopsis	A
43	5,69	serine	Amino acids	C3H7NO3	204	Tomato, Arabidopsis	A
44	13,19	sinapate	Organic acids	C11H12O5	338	Tomato, Arabidopsis	A
45	5,81	succinate	Organic acids	C4H6O4	247	Tomato, Arabidopsis	A
46	13,59	sucrose	Sugar (disaccharide)	C12H22O11	361	Tomato, Arabidopsis	A
47	6,58	threitol	Sugar alcohol	C4H10O4	217	Tomato, Arabidopsis	A
48	7,32	threonate	Hydroxy acid	C4H8O5	292	Tomato, Arabidopsis	A
49	5,84	threonine	Amino acids	C4H9NO3	218	Tomato, Arabidopsis	A
50	15,64	trehalose	Sugars	C12H22O11	147	Tomato, Arabidopsis	A
51	12,74	tryptophan	Amino acids	C11H12N2O2	202	Tomato, Arabidopsis	A
52	10,58	tyrosine	Amino acids	C9H11NO3	179	Tomato, Arabidopsis	A
53	6,23	uracil	Others	C4H4N2O2	241	Tomato, Arabidopsis	A
54	11,93	urate	Organic acids	C5H4N4O3	441	Tomato, Arabidopsis	A
55	5,43	urea	Amide	CH4N2O	189	Tomato, Arabidopsis	A
56	4,28	valine	Amino acids	C5H11NO2	144	Tomato, Arabidopsis	A
57	12,13	xanthine	Others	C5H4N4O2	353	Tomato, Arabidopsis	A
58	8,93	1,6-hydro-glucose	Sugar derivatives	C6H10O5	204	Tomato, Arabidopsis	A
59	6,45	2,3-diaminopropionate	Organic acids	C3H8N2O2	174	Tomato, Arabidopsis	A
60	8,39	2OX-glutarate	Organic acids	C5H6O5	198	Tomato, Arabidopsis	A
61	7,16	4-hydroxyproline	Amino acids	C5H9NO3	230	Tomato, Arabidopsis	A

Supplementary Table S3. Primary metabolite profiling of Col-0 and *TAX1* overexpressing lines in leaf.

	Col-0	OE-1	OE-2	OE-3	Col-0	OE-1	OE-2	OE-3	OE-1	OE-2	OE-3
	FC	FC	FC	FC	SD	SD	SD	SD	TTEST	TTEST	TTEST
adenine	1,00	1,09	1,03	1,64	0,088	0,094	0,159	0,565	0,198	0,789	0,066
alanine	1,00	0,79	0,76	0,88	0,220	0,169	0,064	0,264	0,174	0,081	0,513
arginine	1,00	1,39	1,02	1,68	0,450	0,339	0,534	0,176	0,218	0,953	0,031
ascorbate	1,00	2,84	0,66	0,76	0,257	2,251	0,171	0,250	0,155	0,072	0,226
asparagine	1,00	1,82	1,16	4,99	0,372	0,652	0,359	2,256	0,071	0,562	0,013
aspartate	1,00	1,00	0,97	0,97	0,033	0,081	0,059	0,016	0,959	0,377	0,141
benzoate	1,00	1,04	0,98	1,16	0,203	0,106	0,106	0,177	0,738	0,878	0,286
beta-alanine	1,00	1,22	1,16	2,39	0,158	0,132	0,317	0,811	0,074	0,388	0,015
citrate	1,00	2,75	0,33	1,17	0,804	4,443	0,139	1,413	0,469	0,152	0,841
dehydroascorbate dimer	1,00	0,91	0,59	0,38	0,293	0,587	0,265	0,094	0,785	0,085	0,007
erythritol	1,00	1,08	0,83	1,09	0,140	0,198	0,055	0,215	0,511	0,069	0,499
fructose	1,00	0,77	1,03	1,48	0,436	0,517	0,204	0,588	0,530	0,904	0,233
fumarate	1,00	0,86	0,83	0,93	0,092	0,127	0,217	0,192	0,134	0,203	0,520
GABA	1,00	1,20	0,84	2,09	0,440	0,332	0,187	0,926	0,496	0,536	0,078
galactinol	1,00	0,85	0,60	0,71	0,622	1,094	0,175	0,279	0,819	0,260	0,422
glucose	1,00	0,65	1,06	1,44	0,498	0,479	0,250	0,613	0,356	0,841	0,308
glucose-6-phosphate	1,00	1,15	1,52	1,89	0,149	0,085	0,177	0,433	0,123	0,004	0,008
glutamate	1,00	1,10	0,89	1,30	0,044	0,134	0,052	0,129	0,210	0,018	0,004
glutamine	1,00	1,27	1,16	2,42	0,294	0,380	0,313	0,637	0,302	0,488	0,007
glycerate	1,00	1,43	1,14	3,52	0,216	0,733	0,394	1,187	0,307	0,566	0,006
glycerol	1,00	0,86	0,83	0,91	0,481	0,645	0,451	0,470	0,733	0,622	0,801
glycine	1,00	1,02	1,02	1,45	0,347	0,525	0,390	0,289	0,955	0,948	0,091
glycolate	1,00	0,96	0,99	1,12	0,202	0,181	0,095	0,108	0,780	0,906	0,344
guanidine	1,00	1,51	1,52	1,49	0,425	0,560	0,959	0,207	0,200	0,358	0,082
histidine	1,00	1,66	0,91	3,01	0,702	0,252	0,624	1,377	0,126	0,856	0,041
isoleucine	1,00	1,05	0,65	0,85	0,255	0,198	0,157	0,295	0,767	0,059	0,470
leucine	1,00	1,06	0,61	0,80	0,253	0,266	0,174	0,250	0,757	0,045	0,301
lysine	1,00	1,29	0,77	1,26	0,730	0,304	0,480	0,150	0,494	0,610	0,504
malate	1,00	0,98	0,99	1,86	0,138	0,249	0,184	0,543	0,912	0,956	0,022
methionine	1,00	1,34	0,73	1,73	0,455	0,160	0,240	0,517	0,213	0,337	0,078
myo-inositol	1,00	0,95	1,00	0,82	0,214	0,121	0,132	0,142	0,713	0,976	0,209
nicotinate	1,00	0,79	0,66	0,85	0,362	0,059	0,117	0,078	0,304	0,123	0,439

ornithine	1,00	1,45	0,91	1,49	0,436	0,219	0,301	0,146	0,115	0,744	0,079
palmitate	1,00	1,15	0,95	0,88	0,103	0,124	0,037	0,035	0,121	0,417	0,071
phenylalanine	1,00	1,15	0,76	1,11	0,406	0,187	0,222	0,182	0,533	0,334	0,639
phosphate	1,00	1,41	1,49	1,31	0,023	0,208	0,085	0,160	0,007	0,000	0,008
proline	1,00	1,18	1,28	2,77	0,396	0,509	0,386	0,430	0,602	0,349	0,001
putrescine	1,00	1,21	1,27	1,92	0,500	0,300	0,537	0,060	0,494	0,493	0,011
pyroglutamate	1,00	1,30	1,15	2,48	0,178	0,392	0,173	0,330	0,209	0,266	0,000
pyruvate	1,00	1,16	1,21	1,18	0,213	0,448	0,248	0,253	0,536	0,253	0,307
raffinose	1,00	0,90	0,73	0,79	0,639	1,147	0,175	0,161	0,887	0,446	0,540
ribulose-5-phosphate	1,00	1,19	1,50	1,86	0,388	0,337	0,352	0,395	0,498	0,107	0,021
serine	1,00	1,23	1,28	1,49	0,042	0,116	0,110	0,203	0,009	0,003	0,003
sinapate	1,00	0,81	0,78	0,98	0,130	0,070	0,094	0,196	0,042	0,036	0,889
succinate	1,00	1,14	1,30	1,64	0,496	0,260	0,547	0,426	0,628	0,444	0,097
sucrose	1,00	1,09	1,36	1,96	0,220	0,267	0,183	0,319	0,603	0,047	0,003
threitol	1,00	0,68	0,90	0,56	0,134	0,207	0,204	0,035	0,043	0,458	0,001
threonate	1,00	0,84	0,95	0,70	0,221	0,080	0,142	0,098	0,210	0,708	0,048
threonine	1,00	0,95	0,83	0,81	0,054	0,127	0,085	0,098	0,520	0,014	0,016
trehalose	1,00	0,93	1,05	0,83	0,147	0,105	0,152	0,183	0,449	0,673	0,195
tryptophan	1,00	1,14	0,74	1,10	0,766	0,546	0,462	0,257	0,768	0,576	0,819
tyrosine	1,00	1,28	0,70	1,14	0,868	0,700	0,666	0,112	0,633	0,603	0,763
uracil	1,00	1,11	0,96	0,67	0,118	0,298	0,264	0,131	0,510	0,779	0,010
urate	1,00	0,94	0,64	0,58	0,370	0,349	0,161	0,080	0,819	0,126	0,066
urea	1,00	1,14	1,02	1,18	0,538	0,202	0,387	0,331	0,637	0,964	0,589
valine	1,00	1,06	0,85	1,28	0,213	0,168	0,205	0,281	0,668	0,356	0,167
xanthine	1,00	0,80	0,61	1,05	0,287	0,131	0,044	0,336	0,252	0,037	0,820
1,6-hydro-glucose	1,00	1,18	1,27	1,49	0,100	0,221	0,248	0,170	0,191	0,091	0,002
2,3-diaminopropinate	1,00	1,06	1,06	1,02	0,173	0,215	0,194	0,051	0,658	0,638	0,837
2OX-glutarate	1,00	1,07	0,77	1,34	0,277	0,192	0,161	0,422	0,706	0,201	0,229
4-hydroxyproline	1,00	0,95	0,85	2,25	0,607	0,354	0,374	0,822	0,889	0,692	0,051

FC, fold change; SD, standard deviation; TTEST, student *t*-test.

Supplementary Table S4. Primary metabolite profiling of Col-0 and TAX1 overexpressing lines in root

	Col-0	OE-1	OE-2	OE-3	Col-0	OE-1	OE-2	OE-3	OE-1	OE-2	OE-3
	FC	FC	FC	FC	SD	SD	SD	SD	TTEST	TTEST	TTEST
adenine	1,00	1,51	1,90	1,47	0,271	0,348	0,501	0,372	0,059	0,020	0,085
alanine	1,00	1,53	0,86	1,53	0,422	0,776	0,351	0,244	0,279	0,628	0,073
ascorbate	1,00	1,47	7,31	7,89	1,509	2,307	6,931	8,225	0,742	0,126	0,151
asparagine	1,00	1,90	0,93	2,33	0,854	1,372	0,681	0,686	0,307	0,897	0,051
aspartate	1,00	1,58	1,01	1,44	0,097	0,655	0,254	0,280	0,129	0,949	0,025
benzoate	1,00	1,30	1,11	1,31	0,175	0,170	0,100	0,703	0,047	0,313	0,431
beta-alanine	1,00	1,68	1,83	2,74	0,369	0,497	0,486	1,352	0,069	0,035	0,048
citrate	1,00	3,15	1,64	3,32	0,446	3,498	0,506	2,034	0,269	0,106	0,067
dehydroascorbate dimer	1,00	0,96	0,96	0,75	0,551	0,145	0,516	0,099	0,899	0,913	0,412
erythritol	1,00	1,61	1,06	1,30	0,524	0,403	0,185	0,778	0,114	0,835	0,548
fructose	1,00	0,90	1,01	0,76	0,253	0,147	0,077	0,393	0,507	0,960	0,340
fumarate	1,00	1,43	1,26	2,78	0,288	0,383	0,331	1,220	0,120	0,277	0,030
GABA	1,00	1,63	1,05	1,69	0,065	0,626	0,458	0,745	0,093	0,828	0,115
galactinol	1,00	1,13	0,75	0,72	0,410	0,194	0,234	0,311	0,583	0,336	0,319
glucose	1,00	0,90	1,05	0,80	0,287	0,169	0,093	0,358	0,571	0,767	0,415
glucose-6-phosphate	1,00	1,48	1,21	1,29	0,360	0,071	0,221	0,281	0,039	0,367	0,247
glutamate	1,00	1,80	1,02	1,55	0,082	0,841	0,247	0,396	0,107	0,871	0,034
glutamine	1,00	3,42	0,95	1,91	0,502	2,982	0,702	0,411	0,160	0,907	0,031
glycerate	1,00	0,95	1,29	2,95	0,614	0,159	0,410	1,499	0,888	0,455	0,052
glycerol	1,00	0,97	1,25	1,43	0,831	0,836	1,310	1,190	0,961	0,762	0,579
glycine	1,00	1,22	1,26	1,63	0,365	0,478	0,673	0,613	0,489	0,516	0,126
glycolate	1,00	1,34	1,98	2,00	0,372	0,261	0,562	0,461	0,189	0,027	0,015
histidine	1,00	1,47	1,08	0,74	0,109	0,673	0,361	0,126	0,217	0,687	0,019
isoleucine	1,00	1,43	0,85	0,94	0,133	0,439	0,193	0,149	0,112	0,259	0,596
leucine	1,00	1,36	0,84	0,94	0,178	0,443	0,169	0,145	0,178	0,229	0,614
lysine	1,00	1,43	1,00	1,09	0,105	0,553	0,327	0,236	0,178	0,980	0,498
malate	1,00	1,22	1,27	2,24	0,322	0,112	0,183	1,261	0,235	0,202	0,106
methionine	1,00	1,61	1,15	2,03	0,098	0,442	0,287	0,857	0,036	0,359	0,055
myo-inositol	1,00	1,06	1,04	0,84	0,363	0,074	0,220	0,192	0,766	0,873	0,466
nicotinate	1,00	1,29	0,89	0,74	0,525	0,259	0,193	0,233	0,357	0,710	0,404
ornithine	1,00	1,65	1,38	1,15	0,837	1,195	1,638	0,572	0,408	0,691	0,772
palmitate	1,00	1,03	0,90	1,12	0,053	0,104	0,117	0,195	0,621	0,179	0,266

phenylalanine	1,00	1,47	0,77	0,72	0,136	0,538	0,407	0,244	0,138	0,319	0,089
phosphate	1,00	1,44	1,35	1,30	0,424	0,503	0,360	0,482	0,230	0,256	0,387
proline	1,00	1,88	1,99	5,90	0,329	1,180	0,857	2,915	0,201	0,073	0,016
putrescine	1,00	1,04	0,74	0,71	0,379	0,293	0,120	0,102	0,886	0,241	0,194
pyroglutamate	1,00	1,62	0,92	1,44	0,302	0,808	0,329	0,170	0,202	0,735	0,043
pyruvate	1,00	1,03	1,43	1,19	0,536	0,085	1,106	0,691	0,919	0,507	0,682
raffinose	1,00	1,12	0,84	0,76	0,330	0,142	0,255	0,344	0,521	0,473	0,360
serine	1,00	1,48	1,32	1,40	0,090	0,119	0,223	0,275	0,001	0,039	0,034
succinate	1,00	1,49	2,44	4,95	0,400	0,254	0,798	2,666	0,085	0,018	0,026
sucrose	1,00	1,78	3,16	4,18	0,487	0,844	1,328	1,261	0,159	0,023	0,003
threonate	1,00	1,56	0,80	1,15	0,340	0,529	0,272	0,454	0,123	0,391	0,607
threonine	1,00	1,45	0,94	0,98	0,052	0,385	0,319	0,210	0,060	0,740	0,877
trehalose	1,00	1,40	0,90	0,85	0,450	0,177	0,174	0,277	0,148	0,695	0,597
tryptophan	1,00	1,45	1,05	0,94	0,710	0,924	1,293	0,418	0,472	0,953	0,882
tyrosine	1,00	1,33	0,97	0,83	0,638	0,636	0,912	0,029	0,497	0,958	0,620
uracil	1,00	0,85	0,89	1,01	0,131	0,097	0,187	0,203	0,111	0,374	0,934
urea	1,00	1,22	1,24	1,66	0,263	0,209	0,583	0,858	0,246	0,476	0,193
valine	1,00	1,41	0,88	1,14	0,094	0,434	0,150	0,252	0,112	0,241	0,351
1,6-hydro-glucose	1,00	1,19	0,94	0,95	0,241	0,065	0,088	0,253	0,182	0,663	0,769
2,3-diaminopropinate	1,00	0,97	1,04	1,25	0,512	0,295	0,292	0,247	0,928	0,900	0,416
2OX-glutarate	1,00	1,49	1,40	1,75	0,207	0,227	0,260	0,785	0,019	0,054	0,115
4-hydroxyproline	1,00	1,97	2,70	5,22	0,247	1,064	1,373	3,242	0,125	0,051	0,041

FC, fold change; SD, standard deviation; TTEST, student *t*-test.

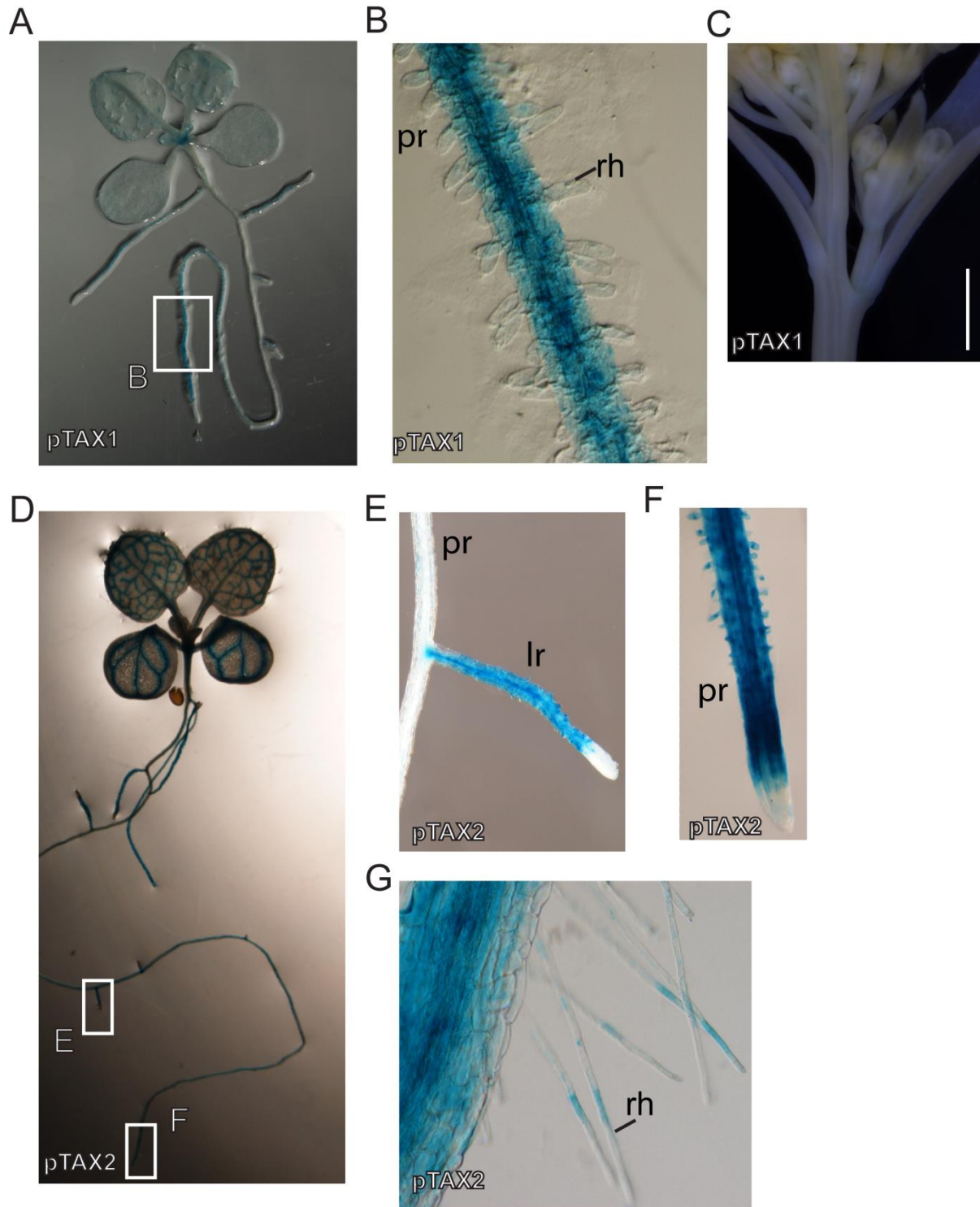


Figure S1. Gus expression patterns driven by pTAX1 and pTAX2.

Plants expressing a nuclear localized GUS-GFP fusion under control of the *TAX1* (A-C) and *TAX2* (D-G) promoter were used. (A-B) pTAX1:GUS activity in roots of 10-day-old seedlings, (C) pTAX1:GUS activity in the inflorescence of 28-day-old mature plants. (D-G) pTAX2-GUS activity in roots of 10-day-old seedlings. Abbreviations: pr, primary root; lr, lateral roots; rh, root hairs; c, cauline leaf. Scale bar, 1 mm.